

Alma Mater Studiorum – Università di Bologna

DOTTORATO DI RICERCA
IN
SCIENZE DELLA TERRA, DELLA VITA E DELL'AMBIENTE

Ciclo XXXIII

Settore Concorsuale: 04/A2 - GEOLOGIA STRUTTURALE, GEOLOGIA STRATIGRAFICA,
SEDIMENTOLOGIA E PALEONTOLOGIA

Settore Scientifico Disciplinare: GEO/02 - GEOLOGIA STRATIGRAFICA E SEDIMENTOLOGICA

Paleogeographic evolution and sequence stratigraphy
of the Upper Cretaceous Bearpaw Formation
(west-central Alberta, Canada)

Presentata da: Riccardo Zubalich

Coordinatore Dottorato

Prof. Maria Giovanna Belcastro

Supervisore

Prof. Rossella Capozzi

Correlatori

Prof. Federico Fanti
Prof. Octavian Catuneanu

Esame finale anno 2021

Abstract

This study is the first high-resolution stratigraphic analysis concerning a large and unstudied area (~97000 km²) of the west-central Alberta foreland basin. We present the first extended correlation of late Cretaceous marine deposits of the Bearpaw Fm. (southern Alberta) to the continental succession of the Wapiti Fm. in the Grande Prairie area (north-central Alberta). We provide new tools used to understand the stratigraphic patterns in correlative marine and non-marine deposits of two time-constrained transgressive-regressive (T-R) cycles. Here, we integrate gamma ray analysis (977 well logs), cross-sections, recent datings and paleontological data to determine sediment distribution, accumulation rates and paleogeographic evolution during the second-order T-R cycle of the late Campanian Western Interior Seaway, when marine waters retired from west-central Alberta for the last time. Recent chronostratigraphic data constrain the two T-R cycles of the Bearpaw Fm. with an unprecedented resolution (~200 kyr). Seven reference stratigraphic surfaces were mapped from the marine deposits into the alluvial domains and the tridimensionally modelled stratigraphic intervals resulted in isopach and cumulative thickness maps for consecutive systems tracts (ST). Data allowed a detailed interpretation of sediment distribution patterns, ST architecture and high-resolution rates of sediment accumulation mapping. This analysis led to interpret the paleogeographic evolution of west-central Alberta, focusing primarily on inferences of the paleo-coastlines and coastal environments during the two T-R cycles. Data support the interpretation that eustasy provided the main control on the evolution of the Western Interior Seaway during the deposition of the Bearpaw Fm. in late Campanian. The distribution of fine-grained, primarily marine sediments of the Bearpaw succession resulted in an effective seal for hydrocarbon accumulation within the underlying Belly River Group, preventing oil migration upsection, within the Edmonton Group.

Contents

1	Introduction	1
1.1	The Bearpaw Formation and the Western Interior Seaway	2
1.2	Research topics and goals	3
2	Geologic setting	6
2.1	Tectonic setting of west-central Alberta	6
2.2	Stratigraphic framework of the Western Canada Sedimentary Basin	10
2.3	The Cretaceous Western Interior Seaway	12
2.4	Sea level history of the Western Interior Foreland Basin	13
2.5	Stratigraphic setting of west-central Alberta	16
2.6	Previous understandings on the Bearpaw Fm.	17
2.7	Age of the Bearpaw Fm.	20
3	Data and methods	21
3.1	Well-logs database: UWI Nomenclature	21
3.2	Software	23
3.2.1	Proprietary	23
3.2.2	Open-source	24
3.3	Methods	26
3.3.1	Dataset construction	26
3.3.2	Gamma ray well logs analysis and correlation criteria	28
3.3.3	3D processing workflow and surfaces nomenclature disambiguation	31
3.3.4	Main GMT commands, scripts and workflow	32
3.3.5	Time-correlative surfaces on gamma ray well logs	35
4	Results	39
4.1	Sea level referred surfaces	39
4.2	Isopachs distribution and volumes of sediment	42
4.2.1	Belly River interval	43
4.2.2	T1 interval	44
4.2.3	R1 interval	46
4.2.4	S interval	47

CONTENTS

4.2.5	T2 interval	48
4.2.6	R2 interval	49
4.3	Cumulative thickness distribution	50
4.3.1	From datum to the top of the Belly River Group	50
4.3.2	From datum to the top of T1	51
4.3.3	From datum to the top of R1	52
4.3.4	From datum to the top of S	53
4.3.5	From datum to the top of T2	55
4.3.6	From datum to the top of R2	56
4.4	Rates of sedimentation	57
4.5	Cross sections	62
4.5.1	Cross sections with different datum	62
4.5.2	Gamma ray expression and stacking patterns on cross sections . . .	69
4.5.3	Results comparison with published data	77
4.6	Published article	84
5	Discussion and conclusions	102
5.1	Reconstructed paleogeography of the Bearpaw Fm.	102
5.1.1	MFS paleogeography of the Bearpaw Fm. tongues	102
5.1.2	Paleogeographic context of west-central Alberta during late Cam- panian	107
5.2	Paleogeographic interpretations of systems tracts	110
5.2.1	Chronostratigraphic resolutions	110
5.2.2	Geometric analysis of the Bearpaw-related systems tracts	111
5.2.3	Implications for the petroleum system analysis	116
5.3	Conclusions	118
5.4	Future developments	121
	Bibliography	123
	Appendices	
A	Format data tables, interpolate DEMs and calculate 3D models	II
B	Print maps of thickness and cumulative thickness 3D models	V
C	Calculate slope degrees and print maps	XI
D	Calculate rates of sediment accumulation and print maps	XIV
E	Calculate volumes	XX
F	Measure and print cross sections	XXIII

List of Figures

1.1	Topography of west-central Alberta. Elevations from the SRTM1s (1 arc second) dataset.	1
1.2	Stratigraphic nomenclature for the Upper Cretaceous of Alberta. Modified after Fanti and Catuneanu (2009)	4
2.1	Schematic crustal section of the collision between a continental and an oceanic plate that originated the Cordilleran Orogenic Belt. Nomenclature of the subdivision of different regions of the system is indicated along with the main vertical movements related to the compressive tectonic dynamics. Modified after Slattery et Al. (2015)	7
2.2	Calibrated geologic section crossing the main tectonic structures within the study area in the foothills of west-central Alberta. All of the sedimentary fill of the foreland basin is indicated in legend. Location in the inset map (E = Edmonton, C = Calgary). The Bearpaw Fm. depth is projected over the section trace from nearest well logs available in the dataset. Modified after Lee et Al. (2018)	8
2.3	Continental scale map of tectonic features active in the Western Interior Foreland Basin during the Late Jurassic to Paleocene. Modified after Stott (1993) ; Stelck et Al. (2007) ; Miall et Al. (2008) ; Slattery et Al. (2015)	9
2.4	Continental scale map of the large sedimentary basin of North America. Tectonic elements are indicated in legend (see also figure 2.1). Modified after Slattery et Al. (2015)	10
2.5	Geological map of west-central Alberta with evidence of major external and foothills thrust fronts. Numbered circles indicate reference exposures for the studied interval (1 = Riverbend, 2 = Grande Prairie, 3 = Blackstone River). Green dashed line bounds the study area (located in the insets, red area). Background image and vector data: topography from ETOPO1 Global Relief Model (https://www.ngdc.noaa.gov) and vectors from the Alberta Geological Survey (modified after https://ags.aer.ca).	11

LIST OF FIGURES

- 2.6 WIS shorelines of the mid Campanian (A) and early Maastrichtian (B). Shaded areas represent land. WIS shorelines are based on unpublished maps of W.A. Cobban; [Jeletzky \(1971\)](#); [Roberts and Kirschbaum \(1995\)](#); shorelines outside Western interior are modified from [Alencaster \(1984\)](#); [Owens and Gohn \(1985\)](#); [de Cserna \(1989\)](#); [Sohl et Al. \(2015\)](#); [McFarlan and Menes \(1991\)](#); [Goldhammer and Johnson \(1999\)](#); [Umhoefer and Blakey \(2006\)](#); [Blakey \(2013\)](#). Modified after [Slattery et Al. \(2015\)](#). 12
- 2.7 Summary table of worldwide recorded sea level events, from late Jurassic to early Paleogene including magnetostratigraphy, biozones, long-term and short-term sea level curves. Modified from [Haq \(2014\)](#). 15
- 2.8 Phanerozoic global sea level curves and temperature curve. The references are indicated in: (1) [Gradstein \(2012\)](#); (2) [Frakes et al. \(1992\)](#) and (3) [Miller et Al. \(2005\)](#). The shaded area represents the time interval characterized by marine flooding in the Western Interior Foreland Basin. Modified after [Slattery et Al. \(2015\)](#). 16
- 2.9 Schematic cross section of Upper Cretaceous in west-central Alberta correlating the continental formations in the Grande Prairie (Alberta) area (white) to the marine formations in southern Alberta and Saskatchewan (dark), including the Bearpaw Formations. Modified after [Fanti and Catuneanu \(2010\)](#). 17
- 2.10 Stratigraphic columns from Campanian to Maastrichtian. Columns are representative of west-central Alberta, central-southern Alberta, southern Alberta plains and north - western Montana (USA) and show correlative formations and groups. Modified after [Fanti and Catuneanu \(2010\)](#). 18
- 2.11 Cross section of the Bearpaw Fm. near the city of Edmonton (location labeled B1-B2 in the adjacent map). Reciprocal stratigraphies are represented with lighter and darker grey, hinge line dividing the reciprocal systems tracts is indicated in dark grey both in section and plan view. Modified after [Catuneanu et Al. \(1999\)](#). 19
- 3.1 IHS Markit official logo. IHS Markit developed Accumap and Acculogs, the softwares used in this study to access and correlate gamma-ray well logs. The official website is <https://ihsmarkit.com>. 23
- 3.2 Qgis official logo. Also known as *Quantum GIS* (before 2013), Qgis is widely used worldwide to visualize, organize, analyze and represent spatial data. The official website of the project is <https://www.qgis.org>. 24

3.3 GMT official logo. The *Generic Mapping Tools* is a growing collection of computer software tools for processing and displaying xy and xyz datasets. The official website of the project is <https://www.generic-mapping-tools.org> and the full documentation of the commands used in this study can be found in the **documentation section** of the official GMT website. 25

3.4 Sections (light-blue) and well logs (yellow) used in this study, projected on a Google Earth satellite image. The area in grey represents the distribution of the Bearpaw Formation (see figure 2.5). Well logs indicated with blue dots have been used to compare depth correlations from this study and literature. Reference well logs are reported in table 1 of paragraph 4.6 (crossed blue dots correspond to UWIs marked with an asterisk). Reference well logs shown in figure 4 of paragraph 4.6 are marked as orange dots. 27

3.5 The Belly River Group base (orange lines) was used as datum in this study. It was picked right above of a decametric, well-identifiable coarsening upward (CU) interval. This CU interval, not only is visually easy to spot, as there is no other similar interval in west-central Alberta, but is also unique as it always occur some tens of meters above a clear high API interval (blue squares) which was found in the entire study area and used to double-check the correlation of the datum surface. This high API interval often scores, especially in the eastern study area, well over 150 (API) and is probably related to bentonite beds or other sediments with high gamma ray emissivity. 29

3.6 Log signature shape of a low-energy fluvial system with indicated coal seams typical shape, fining-upward channel fills-like trends (CH) and coarsening-upward crevasse splays-like trends (CS). Modified after [Catuneanu \(2006\)](#). 35

3.7 Schematic representation of the diagnostic gamma ray patterns found on a typical source to sink transect (SW-NE oriented sections) in west-central Alberta within a single T-R cycle. These patterns are indicative, real-life scenario are far more complex, refer to figure 3.8 for more realistic examples. The main diagnostic features are reported above the correspondent example. In the source area, the identification of the MFS becomes very difficult and in certain cases infeasible. That's where the gamma ray correlations where stopped on the western border of the study area. 36

LIST OF FIGURES

3.8	Indicative representation of possible diagnostic gamma ray features related to the paleoenvironments of west-central Alberta within a single T-R cycle. The points represent the paleoenvironmental context in which the relative T-R cycle developed. The different signature of the MFS changes relatively to the different contexts. Note the difference between FU-CU cycles moving inland from marine settings, and how they turn into aggrading floodplain sequences, punctuated by channel-fills (see figure 3.6) and coal layers. A1: proximal fan; A2: floodplain; A3: delta; A4: marine in front of a delta; B1: swamp; B2: estuary; B3: estuary bar; B4: outer estuary; C1: floodplain; C2: lagoon; C3: barrier island; C4: marine; D1: floodplain; D2: beach; D3: open marine. See paragraph 4.5.2 for real examples of correlated well logs. .	37
4.1	Belly River Group base (datum) DEM referred to sea level.	39
4.2	Correlated surfaces DEMs referred to sea level.	40
4.3	Slope map and histograms of slope degree frequency for the datum surface and for the base and top of the Bearpaw Formation.	41
4.4	Belly River Group thickness 3D model.	43
4.5	Lower Bearpaw tongue TST and correlative deposits thickness 3D model (T1 interval).	45
4.6	Lower Bearpaw tongue RST and correlative deposits thickness 3D model (R1 interval).	46
4.7	Central Strathmore Member and correlative deposits thickness 3D model (S interval).	47
4.8	Upper Bearpaw tongue TST and correlative deposits thickness 3D model (T2 interval).	49
4.9	Upper Bearpaw tongue RST and correlative deposits thickness 3D model (R2 interval).	50
4.10	Belly River Group thickness 3D model (datum). This 3D model is equivalent to figure 4.4 but with different color palette which is the same used for every other cumulative thickness maps.	51
4.11	Cumulative thickness 3D model from the datum to the top of T1.	52
4.12	Cumulative thickness 3D model from the datum to the top of R1.	53
4.13	Cumulative thickness 3D model from the datum to the top of S.	54
4.14	Cumulative thickness 3D model from the datum to the top of T2.	55
4.15	Cumulative thickness 3D model from the datum to the top of R2.	56
4.16	Rates of sediment accumulation of the Belly River Group (from datum to the base of the lower Bearpaw tongue).	57
4.17	Rates of sediment accumulation of the Bearpaw succession (from the base of the lower to the top of the upper Bearpaw tongue).	58

LIST OF FIGURES

4.18 Rates of sediment accumulation of the T1 interval (lower Bearpaw tongue TST and correlative deposits). 60

4.19 Rates of sediment accumulation of the R1+S interval (from the lower Bearpaw tongue MFS to the base of the upper Bearpaw tongue). 61

4.20 Rates of sediment accumulation of the T2+R2 interval (referred to the entire upper Bearpaw tongue and correlative deposits). 62

4.21 Location of section traces over cumulative thickness maps described in paragraph 4.3. 63

4.22 Cross-sections 1-4 over cumulative thickness 3D models. The datum is the Belly River Group base (zero Y axis value). 64

4.23 Cross-sections 5-8 over cumulative thickness 3D models. The datum is the Belly River Group base (zero Y axis value). 65

4.24 Cross-sections 1-4 over cumulative thickness 3D models represented with MFS of the upper tongue as datum (zero Y axis value). 66

4.25 Cross-sections 5-8 over cumulative thickness 3D models represented with MFS of the upper tongue as datum (zero Y axis value). 67

4.26 Location of section traces over cumulative thickness maps described in paragraph 4.3. 69

4.27 Cross section A in northern Alberta (Grande Prairie area, location map in figure 4.26). The correlated surfaces are traced in red (base and top of the lower Bearpaw tongue), green (base and top of the upper Bearpaw tongue) and blue (MFS of the respective T-R cycle). The grey area represents the sum of regressive Highstand and Falling Stage Systems Tract deposits (R1+S interval). Well-logs traces are all gamma ray ranging between 0 and 150 API. 71

4.28 Cross section B in central northern Alberta (location map in figure 4.26). The correlated surfaces are traced in red (base and top of the lower Bearpaw tongue), green (base and top of the upper Bearpaw tongue) and blue (MFS of the respective T-R cycle). The grey area represents the sum of regressive Highstand and Falling Stage Systems Tract deposits (R1+S interval). Well-logs traces are all gamma ray ranging between 0 and 150 API. 72

4.29 Cross section C in central southern Alberta (location map in figure 4.26). The correlated surfaces are traced in red (base and top of the lower Bearpaw tongue), green (base and top of the upper Bearpaw tongue) and blue (MFS of the respective T-R cycle). The grey area represents the sum of regressive Highstand and Falling Stage Systems Tract deposits (R1+S interval). Well-logs traces are all gamma ray ranging between 0 and 150 API. 73

4.30	Cross section D in southern Alberta (location map in figure 4.26). The correlated surfaces are traced in red (base and top of the lower Bearpaw tongue), green (base and top of the upper Bearpaw tongue) and blue (MFS of the respective T-R cycle). The grey area represents the sum of regressive Highstand and Falling Stage Systems Tract deposits (R1+S interval). Well-logs traces are all gamma ray ranging between 0 and 150 API.	74
4.31	Cross section E in southern Alberta (location map in figure 4.26). The correlated surfaces are traced in red (base and top of the lower Bearpaw tongue), green (base and top of the upper Bearpaw tongue) and blue (MFS of the respective T-R cycle). The grey area represents the sum of regressive Highstand and Falling Stage Systems Tract deposits (R1+S interval). Well-logs traces are all gamma ray ranging between 0 and 150 API.	75
4.32	Section D-D' from Jerzykiewicz (1997) overlaid by surfaces from this study. The datum is sea level. Location of section trace in the inset. Modified after Jerzykiewicz (1997).	79
4.33	Section E-E' from Jerzykiewicz (1997) overlaid by surfaces from this study. The datum is sea level. Location of section trace in the inset. Modified after Jerzykiewicz (1997).	80
4.34	Section F-F' from Jerzykiewicz (1997) overlaid by surfaces from this study. The datum is sea level. Location of section trace in the inset. Modified after Jerzykiewicz (1997).	81
4.35	Section G-G' from Jerzykiewicz (1997) overlaid by surfaces from this study. The datum is sea level. Location of section trace in the inset. Modified after Jerzykiewicz (1997).	82
5.1	Paleogeography of the lower Bearpaw tongue MFS with location of the cross sections. Sediment distribution patterns indicate three adjoining areas: 1 - near the foothills, deposits are dominated by coarse, lenticular or laterally interfingered bodies; 2 - typical alluvial deposits are widespread within continental plains; 3 - distal, flat transitional areas include widespread marine signature of the lower Bearpaw tongue. Nearshore environments are likely related to a complex development of tidal embayments with vast submerged areas. Well logs indicated by red dots mark the eastward shift from subaerial to submerged deposition (in gamma ray trends). CZ = Coastal Zone.	103

5.2	Paleogeography of the upper Bearpaw tongue MFS. Sediment distribution patterns indicate three adjoining areas: 1 - near the foothills, deposits are dominated by coarse, lenticular or laterally interfingered bodies; 2 - typical alluvial deposits are widespread within continental plains; 3 - distal, flat transitional areas include nearshore environments likely related to a complex development of tidal embayments with vast submerged areas. Well logs indicated by red dots mark the eastward shift from subaerial to submerged deposition (in gamma ray trends). CZ = Coastal Zone.	104
5.3	Bearpaw Fm. shorelines inferred from paleogeographic maps of both the lower Bearpaw tongue MFS and the upper Bearpaw tongue MFS. The Bearpaw Fm. marine extension (in outcrop) is reported from the geological map of Alberta.	106
5.4	Schematic paleogeographies of the Bearpaw lower tongue MFS (A) and of the Bearpaw upper tongue top (basal Horseshoe Canyon Fm.). (B). Shorelines (black) inside the study area (red) are deducted by data from this study, lines in dark green (B) represents the shorelines reported in figure 5.3 for the upper Bearpaw tongue MFS. Shorelines next to the white background are modern shorelines of North America. Dashed lines (all colors) are indicative of the Western Interior Seaway shorelines. State boundaries and major Alberta cities are reported for geographic reference (GP = Grande Prairie, E = Edmonton, C = Calgary). Green color corresponds to land masses, light-blue corresponds to marine water.	109
5.5	Chronostratigraphic chart of the Bearpaw Formation stratigraphic interval. The TST and RST for the lower and upper Bearpaw tongues (and correlative deposits) are indicated as T1/R1 and T2/R2, respectively. Strathmore interval (S) is defined as accumulation between the top of R1 and the base of T2. Absolute dating and average thickness for each interval are indicated (Eberth and Kamo, 2020, refer to paragraph 2.7). The environmental shifts based on gamma ray logs and the depositional architecture are interpreted as products of changes in relative sea level (see discussion in the text). . . .	111
5.6	Simplified cross sections 1-4 (A, with location map on the cumulative thickness R2 interval map, see figure 4.21 for location maps over other intervals) and 5-8 (B) of the study area in west-central Alberta showing the stratigraphic distribution of intervals discussed in the text (in particular Bearpaw lower tongue, Strathmore Mbr. / Wapiti Unit 3, Bearpaw upper Tongue. Datum: upper tongue MFS). Horizontal scale in km, vertical scale in meters from the datum.	113
5.7	Paleogeographic map showing west-central Alberta during the lower and upper Bearpaw transgressive events, with section 4 plotted twice, using the MFS surfaces of both the lower and the upper Bearpaw tongues as datum. .	115

5.8 Simplified longitudinal cross sections 5 and 8 (upper tongue MFS as datum) showing the stratigraphic occurrence of the Pembina oil field and plan view of the location of section traces and exploited fields. Refer to figure 10 and relative text in paragraph 4.6 for a complete discussion about the maps under section traces. Wells are plotted on the isopach maps of (left) the Belly River Group and (right) Bearpaw lower tongue transgressive (T1) interval. Color and size of dots (productive wells) are proportional to oil exploitation (see the legend). Palette color-bars for respective thickness intervals are reported on the left in meters. Peco and Pembina East oil fields are indicated. 117

List of Abbreviations

- API** American Petroleum Institute units
- COB** Cordilleran Orogenic Belt
- CU** Coarsening Upward
- DEM** Digital Elevation Model
- FSST** Falling Stage Systems Tract
- FU** Fining Upward
- GMT** Generic Mapping Tools
- GR** Gamma Ray
- HST** Highstand Systems Tract
- MFS** Maximum Flooding Surface
- MRS** Maximum Regressive Surface
- ROI** Region Of Interest
- RST** Regressive Systems Tract
- T-R** Transgressive-Regressive (cycle)
- TS** Transgressive Surface
- TST** Transgressive Systems Tract
- UWI** Universal Well Identifier
- WCSB** Western Canada Sedimentary Basin
- WIFB** Western Interior Foreland Basin
- WIS** Western Interior Seaway

Chapter 1

Introduction

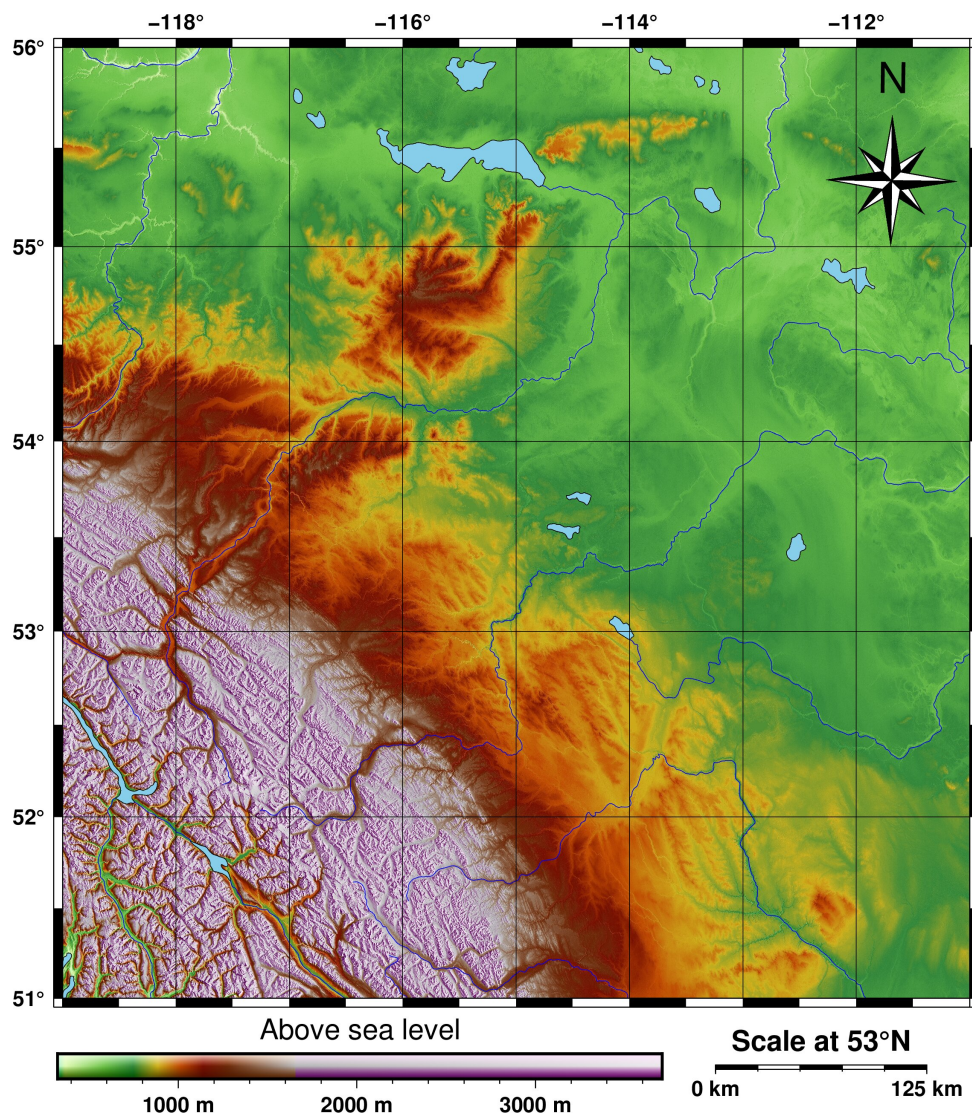


Figure 1.1: Topography of west-central Alberta. Elevations from the SRTM1s (1 arc second) dataset.

1.1 The Bearpaw Formation and the Western Interior Seaway

The Bearpaw Fm. is exposed over much of northern and eastern Montana (U.S.A.) as well as in the southern part of Alberta and Saskatchewan (Canada). The lithostratigraphic interval represented by the Bearpaw Fm. separates the two major clastic wedges named Belly River and Edmonton groups, both renowned for their remarkable fossil record (Russell and Chamney, 1967; Dodson, 1971, 1990; Currie and Koppelhus, 2016; Currie et Al., 2008; Larson, 2010; Larson et Al., 2013, 2018; Bell et Al., 2013, 2014; Eberth et Al., 2013; Freedman Fowler and Horner, 2015; Cullen and Evans, 2016; Gilbert, 2019; Gilbert et Al., 2019, and numerous others) and studies on the evolution of clastic systems, as well as for the economic significance of the hydrocarbon reserves they hosts in sand reservoirs. During the late Cretaceous, the Bearpaw Fm. deposited in the context of a north-south oriented seaway, called Western Interior Seaway (WIS), which trisected the north American continent, isolating three main landmasses called Laramidia, Appalachia and Greenland. Laramidia was the largest one, essentially constituted by the Cordilleran Orogenic Belt (COB) which spans almost 6000 km from Alaska to Mexico and reaches its maximum width of 1000 km in the western United States and southwestern Canada. The COB and its associated basins comprise approximately a seventh of the Circum-Pacific Orogenic Belt (the so-called “Ring of Fire”, 40000 km; Monger, 1993; De Celles, 2004; Slattery et Al., 2015). While Appalachia and Greenland stayed on the passive margin of North America, Laramidia was on the tectonically active margin and the processes discussed in this study are all, in different ways, related to the overall compressive tectonics affecting Laramidia or to eustatic influences on the WIS. These compressive tectonic forces were due to the subduction at a low angle of the Pacific plate under North America, which, in turn, was a consequence of the westward drift of North America relatively to Europe during the Atlantic Ocean spreading (Monger, 1993; De Celles, 2004; Miall et Al., 2008; Slattery et Al., 2015).

The palaeogeography of the WIS, from the middle Jurassic to Eocene, has always been shaped by the interplay of eustasy and physiography, the latter being influenced by all of the typical processes found in compressive continental margins such as fold and thrust-belt migration and volcanism, which induced flexural tectonics, uplift and subsidence on the basins. It can be rightfully said that the interpretation of Cretaceous strata in North America has substantially shaped our understanding of tectonics and eustasy. During the Cretaceous, tectonic forces had already developed a foreland basin, called the Western Interior Foreland Basin (WIFB), on the

east side of the COB. Its sedimentary record was structured by relative sea level oscillations, mostly due to tectonically-induced physiographic changes in the WIS but, as many studies have concluded, eustasy may have played a dominant role, at least during the Cretaceous, as important sea level oscillations have been recognized and correlated worldwide. While the scientific community is divided on the driving factors of these sea level oscillations, it is widely accepted that the interplay between tectonics and eustasy determined the paleogeographic evolution of the entire WIFB. Nonetheless, the available literature does not define in detail the reciprocal mode and tempo of eustasy and tectonics. In the WIFB of Alberta this is primarily due to difficulties in defining the magnitude of tectonic subsidence (Catuneanu et Al., 1999). This can be implemented with high-resolution data, providing chronostratigraphic data and physical horizons constraining marine incursions within the final fill-up stage of the basin. Relative sea level oscillations are recorded in the sedimentary fill of the WIFB as sand and shale interfingered deposits (Slattery et Al., 2015).

The Cretaceous North American Seaway has fascinated researchers from all over the world during the last decades. That long seaway crossing the entire continent had a terrific impact on humanity even though humanity didn't even exist at the time. Its echo on our lives is evident indeed, as the human society persistence is up to now based upon resources. These resources can impact the economies, inspire laws, motivate new technologies and knowledge production, animate human progress. Large quantities of the North American resources come from the processes that happened during the Cretaceous period thanks to the existence and evolution of this seaway that extended over the whole Northern Hemisphere, joining waters from the Arctic Ocean to the Gulf of Mexico.

1.2 Research topics and goals

In this study we investigate the deposition of the Bearpaw Formation in west-central Alberta when the seaway flooded the WIFB for the last time between 74 and 73 Myr (Rogers et Al., 2016; Eberth and Kamo, 2020). During the Campanian siliciclastic sediments deposited in the foreland basin record two clastic wedges sourced by the rising mountain range and mainly formed by alluvial and coastal units, namely Belly River Group and Edmonton Group, which in the study area are entirely represented by the deposits of the Wapiti Formation. The Bearpaw Formation intervenes between these two clastic wedges (Fanti and Catuneanu, 2009, and references therein, figure 1.2).

1.2. RESEARCH TOPICS AND GOALS

Epoch	Period	Stages	Age (Ma)	Groups, formations, and nomenclature comparison						
				CENTRAL FOOTHILLS (Jerzykiewicz and McLean, 1980)	NORTHWEST PLAINS (Allan and Carr, 1946)	NORTHWEST PLAINS (Stott, 1967)	NORTHWEST PLAINS (Dawson et al., 1994b)	NORTHWEST PLAINS (this paper)	CENTRAL PLAINS (MacEachern and Hobbs, 2004)	
CRETACEOUS	LATE	Maastrichtian	66.4	Coalspur <small>LOWER Entrance Mbr.</small>	Undefined	Not addressed	Scollard <small>UPPER Entrance Mbr.</small>	Scollard <small>UPPER Entrance Mbr.</small>	Scollard <small>UPPER LOWER</small>	
			70.6	upper	Member E	Wapiti	Wapiti	unit 5 <small>Cutbank C. Z.</small>	Edmonton Group DMT	
		Campanian	73.4	lower	Member D			Wapiti	unit 4 <small>Red Willow C. Z.</small>	Bearpaw
			79.1		Member C				unit 3	
			Member B		unit 2					
		83.5	Member A	unit 1 <small>Basal C.Z.</small>	Belly River					
Santonian	85.8	Wapiabi	Smoky Group	<small>Puskwaskau Fm.</small> Nomad Mbr. Chungo Mbr. Hanson Mbr. Thistle Mbr. Dowling Mbr.	Puskwaskau	Puskwaskau	Lea Park			
Coniacian				Bad Heart	Bad Heart	Bad Heart	Colorado Group			

Figure 1.2: Stratigraphic nomenclature for the Upper Cretaceous of Alberta. Modified after [Fanti and Catuneanu \(2009\)](#).

In the following chapters, by means of a dense subsurface (geophysical well-logs) dataset a robust framework is provided to investigate the significance of the Bearpaw marine ingressions with respect to the continental settings recorded in the Wapiti Formation.

The coastal depositional environments, being sites of very dynamic sedimentation processes, are very sensitive to the changes imposed by the highest rank natural forces (i.e. tectonics, eustasy) and host the record of shoreline shifts within the basin. Thus, coastal environments have a great potential for a high-resolution palaeogeographic reconstructions and detailed T-R cycles mapping. Data presented in this study aimed to define:

1. the geographic extent of the Bearpaw and Bearpaw-equivalent deposits in the proximal area of the foreland basin;
2. the evolution of this unit within a chronostratigraphic interval of approximately 1 Myr by integrating new radioisotopic and paleontologic constraints;
3. diagnostic tools (i.e., stratigraphic surfaces, well-log signatures and markers) for constraining the lithological transition between marine and alluvial deposits, stratigraphic stacking patterns and their mappability in the study area;
4. the sequence stratigraphic architecture resulted from multiple transgressive-regressive events;
5. if and how it is possible to weight the role of eustatic *vs* tectonic control on sediment accumulation.

Eventually, the high-resolution sequence analyses of the events recorded in this proximal section of the basin - which records variations in the foredeep-foreland setting

- aims to improve our understanding of major controlling factors on marine incursions. Therefore, this approach offers insights to refine our knowledge on the evolution of foreland systems beyond the simple eustasy-tectonic models.

As the Cretaceous foreland basin of Alberta also represents one of the most explored areas for hydrocarbon exploitation, new and three-dimensional information on the real distribution of seal units may improve the knowledge on hydrocarbon potential.

Secondary to the scientific purposes of this study, we aim to highlight that this research can be deliberately carried out preferring open source softwares over commercial ones when possible. That is a rare choice among researchers in our discipline and, likely, that is mostly due to the difficulties that the open source world community faces when dealing with the “big” public. The misunderstanding is that free software is often associated with poor quality, and open-source licenses, being free to use, are dressed by this wrong halo. We hope that this work will help more scientists to understand the advantages and possible uses of open-source tools for their research and hopefully contribute to the open-source active communities developing these tools. Technological advances in computing capabilities of personal computers made it possible to observe and manipulate exponentially greater datasets thus opening new possibilities for scientists of this century. In the 20s of the new millennium, we have enough computing capabilities to process and elaborate data on our everyday-machines and we can access professional tools to do it in a completely open-source fashion. Open-source geology-related softwares contain valuable tools for researchers, developed and evolved for the last three/four decades, and can help them save time, effort and funds. Every passage of data processing and analysis in this PhD project was obtained thanks to open-source licenses, covering the total cost of the research with the lowest budget possible (the only research-related costs were the licenses of the well-logs database access software).

Chapter 2

Geologic setting

This research has been carried out with well logs collected in west-central Alberta (Canada), within an area of almost 100000 km² between the Rocky Mountains deformation front (west), Edmonton (east), Calgary (south) and Grande Prairie (north-west).

2.1 Tectonic setting of west-central Alberta

Diachronously from south to north, tectonic forces shaped the physiography of western North America and thus the paleogeography of the Western Interior Seaway (WIS), from the Middle Jurassic to the Eocene. The Cordilleran Orogenic Belt (COB, the modern Rocky Mountains) is the most noticeable feature during this time interval, spanning roughly 6000 km from Alaska to southern Mexico and almost 1000 km in width in western United States and southwestern Canada (Monger, 1993; De Celles, 2004; Slattery et Al., 2015). The events that led to the development of the COB and its associated basins started with the westward drift of North America relative to Europe during the initial phases of expansion of the Atlantic Ocean. The drift of North America caused the subduction of the Panthalassian oceanic crust (on the Pacific Ocean side) under the North American craton. This led to regional shortening and thickening (fold and thrust-belt migration) of the continental crust. As the COB formed, an entire foreland basin (Western Interior Foreland Basin, WIFB) developed to the east of it. Accommodation space was created by induced subsidence over North America (Monger, 1993; De Celles, 2004; Catuneanu, 2004; Miall et Al., 2008; Slattery et Al., 2015, figure 2.1). In Canada, clastic wedges deposited into the WIFB since the Jurassic and their stacking patterns reflect repeated cycles of fold and thrust-belt tectonics. In most case studies these wedges were correlated to increases in sediment production due to tectonic

pulses affecting the source area (Stockmal et Al., 1992; Catuneanu, 2004; Miall et Al., 2008). After most of the Panthalassian oceanic crust got subducted, each cycle of tectonic loading on the Canadian Shield (Slattery et Al., 2015) was induced by new collisions (continental crust vs. continental crust) with terranes that were not subducted during - or resulted from - the initial stages of the subduction (Coney et Al., 1980; Ricketts, 2008; Fuentes et Al., 2009, 2011).

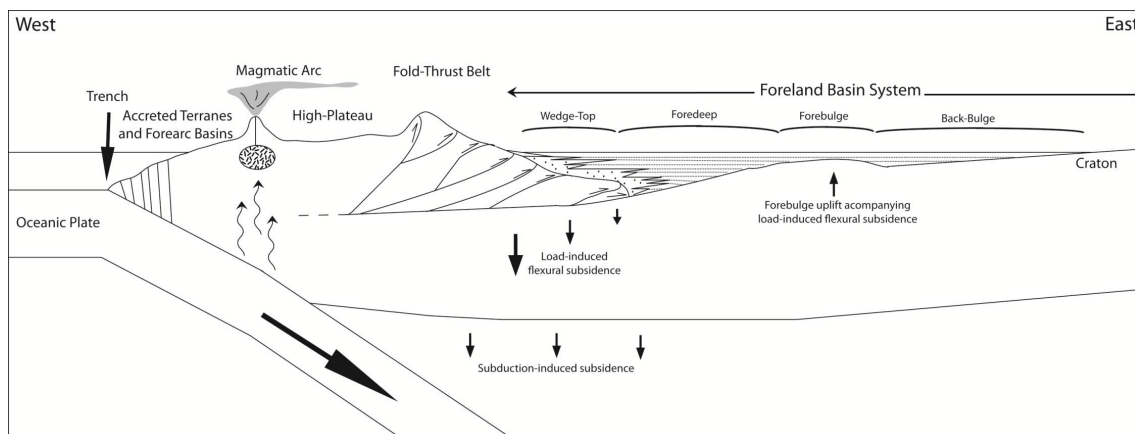


Figure 2.1: Schematic crustal section of the collision between a continental and an oceanic plate that originated the Cordilleran Orogenic Belt. Nomenclature of the subdivision of different regions of the system is indicated along with the main vertical movements related to the compressive tectonic dynamics. Modified after Slattery et Al. (2015).

The main deformation in the Alberta basin took place essentially during two orogenic periods: (1) Late Jurassic to Early Cretaceous and (2) late Cretaceous to Paleocene (Bally et Al., 1966; Jerzykiewicz, 1997). Compressive deformation from Jurassic to Paleocene transported large volumes of sediment eastward, towards the Alberta foreland basin (McMechan et Al., 1993), after the stacking of thrust sheets and detached folds which incremented erosion rates. The Alberta Foothills are mostly made of Mesozoic and Cenozoic sedimentary units (Dawson et Al., 1994, 1990). The foreland Mesozoic and Cenozoic strata dip to the SSW but in the Foothills region they are folded upward, on the east flank of structural triangle zones (Stockmal et Al., 2001) or on backthrusts (e.g. Pedley Thrust, see figure 2.2), reversing their dip to the NNE and creating the western limb of the Alberta syncline (Pană and Van Der Pluijm, 2015, figure 2.2). In the southern Alberta Foothills, the upper detachments of the structural triangle zones could have possibly developed within the Bearpaw Fm. as it represents one of the mechanically weakest Cretaceous horizons (Stockmal et Al., 2001). At its maximum expansion, the WIFB extended for over 1500 km from western Alberta to eastern Manitoba (Cross, 1986; Chamberlain et Al., 1989; Kauffman and Caldwell, 1993; De Celles and Giles, 1996; Miall et Al., 2008). That

2.1. TECTONIC SETTING OF WEST-CENTRAL ALBERTA

remarkable extension is only explainable when considering a subduction-induced subsidence component (“viscous coupling between the base of the continental plate and downward circulating mantle-wedge that is entrained by the subducting slab”; De Celles and Giles, 1996, page 115) acting in concert with a component of load-induced flexural subsidence (Kauffman and Caldwell, 1993; De Celles and Giles, 1996; Miall et Al., 2008; Slattery et Al., 2015, figure 2.1).

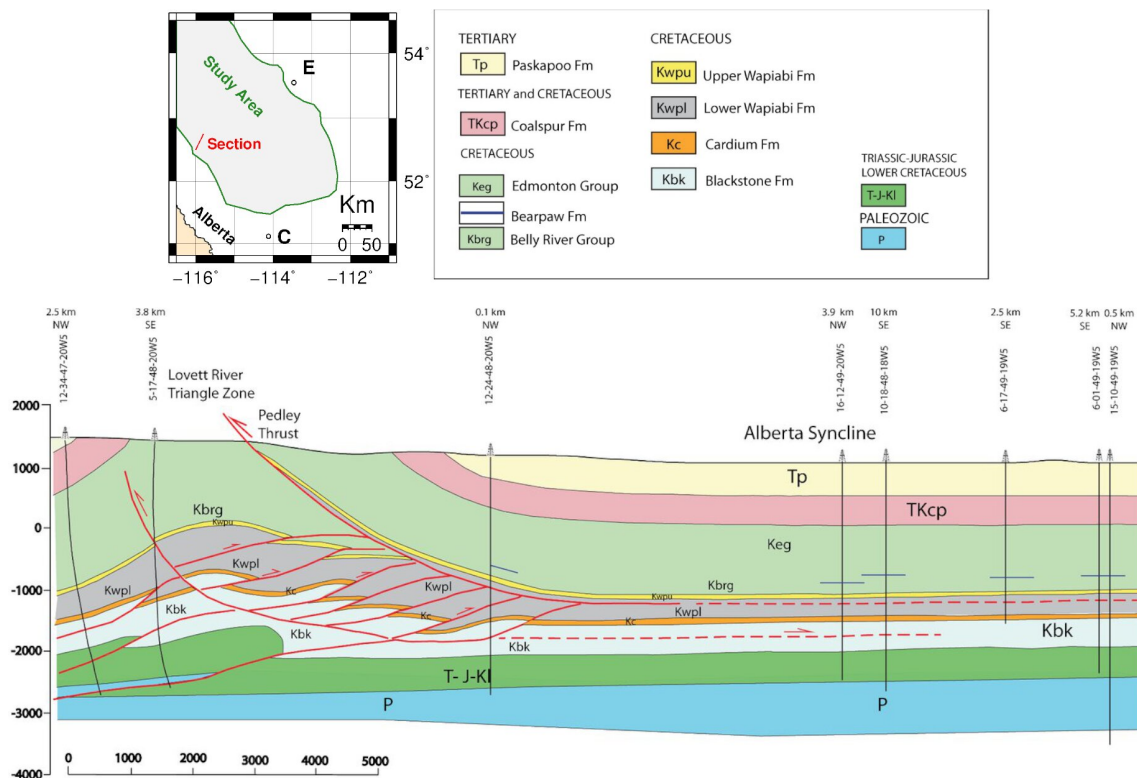


Figure 2.2: Calibrated geologic section crossing the main tectonic structures within the study area in the foothills of west-central Alberta. All of the sedimentary fill of the foreland basin is indicated in legend. Location in the inset map (E = Edmonton, C = Calgary). The Bearpaw Fm. depth is projected over the section trace from nearest well available in the dataset. Modified after Lee et Al. (2018).

The WIFB system consisted of four depositional zones, from west to east: the wedge-top, the foredeep, the forebulge and the backbulge (McMechan et Al., 1993; De Celles and Currie, 1996; De Celles and Giles, 1996, figure 2.1). The WIFB system is also affected by relatively minor, pre-existing regional tectonic elements and basement features that have influenced on different scales the basin physiography, the palaeogeographic evolution of the WIS and the lithofacies patterns within the basin. Among these, the most important consist of various arches, block-uplifts and sub-basins (Weimer, 1978; Stott, 1993; Stelck et Al., 2007; Miall et Al., 2008; Slattery et Al., 2015, figure 2.3).



Figure 2.3: Continental scale map of tectonic features active in the Western Interior Foreland Basin during the Late Jurassic to Paleocene. Modified after [Stott \(1993\)](#); [Stelck et Al. \(2007\)](#); [Miall et Al. \(2008\)](#); [Slattery et Al. \(2015\)](#).

These structural features, distributed all along the eastern side of the COB and consisting in topographic high and lows, may have acted as local sediment sources, sediment sinks (sub-basins) or even as barriers to sea level rise and reflect the probable reactivation of basement elements ([Weimer, 1978](#); [Stelck et Al., 2007](#); [Miall et Al., 2008](#); [Slattery et Al., 2015](#)). Some of these features, such as the Dave Lord-Eskimo Lake Arch (Canada), have played critical roles in the evolution of the entire seaway because of their position, acting as barriers to the marine transgressions from the Arctic Ocean or just limiting them ([Slattery et Al., 2015](#)) as happened

with the Peace River Arch in Canada or the Sweetgrass Arch on the US-Canada border (figure 2.3).

2.2 Stratigraphic framework of the Western Canada Sedimentary Basin

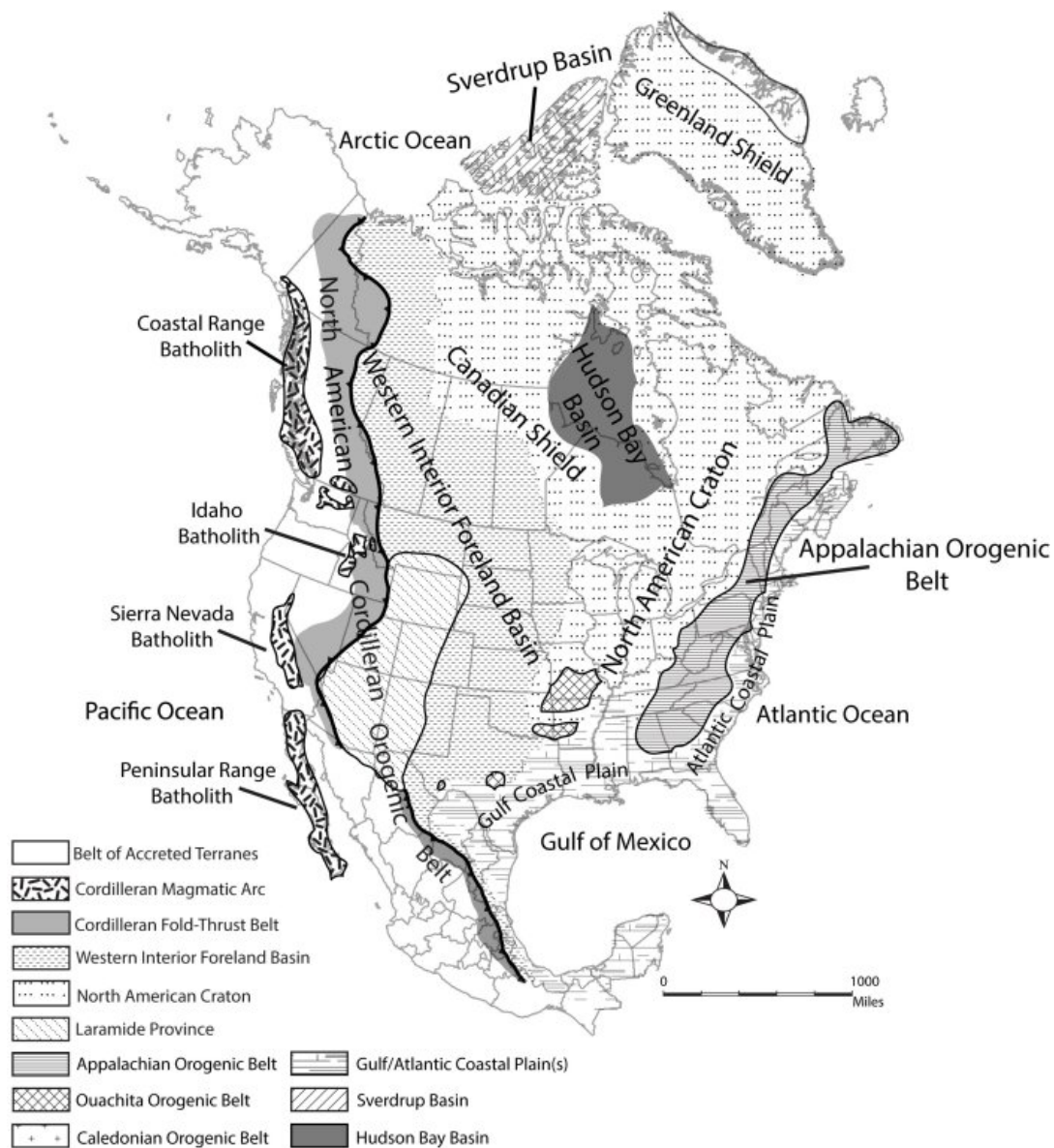


Figure 2.4: Continental scale map of the large sedimentary basin of North America. Tectonic elements are indicated in legend (see also figure 2.1). Modified after [Slattery et Al. \(2015\)](#).

The Western Canada Sedimentary Basin (WCSB, the Canadian portion of the Western Interior Foreland Basin, WIFB; figure 2.4) develops on the eastern side of the

Canadian Rocky Mountain and contains successions from the Paleozoic to the Cenozoic ages that overlie the west dipping crystalline basement (Lee et Al., 2018). The WCSB contains siliciclastics deposits with a western provenance that are linked to the uplift induced by convergent tectonics along the western margin of the North American Craton (Monger, 1989).

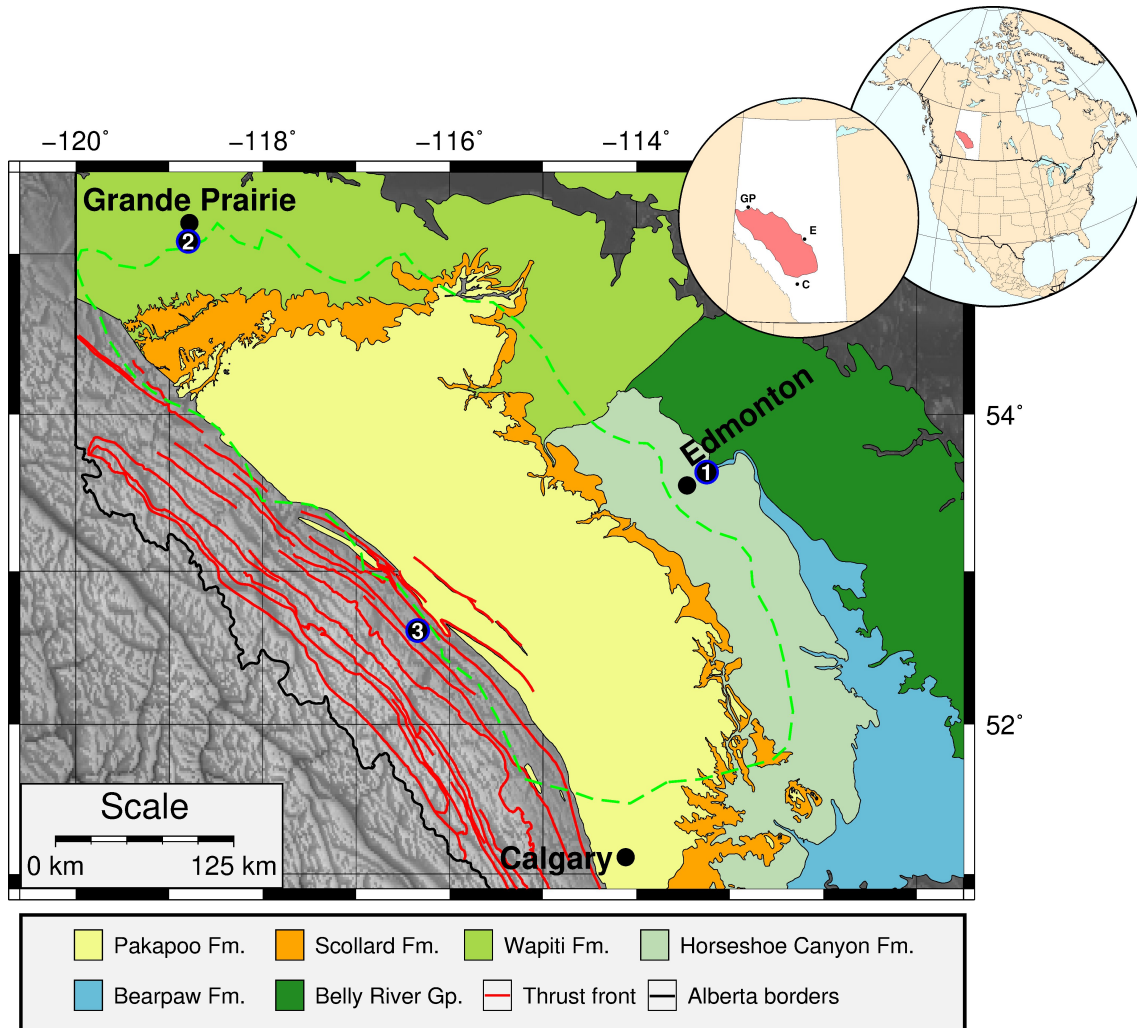


Figure 2.5: Geological map of west-central Alberta with evidence of major external and foothills thrust fronts. Numbered circles indicate reference exposures for the studied interval (1 = Riverbend, 2 = Grande Prairie, 3 = Blackstone River). Green dashed line bounds the study area (located in the insets, red area). Background image and vector data: topography from ETOPO1 Global Relief Model (<https://www.ngdc.noaa.gov>) and vectors from the Alberta Geological Survey (modified after <https://ags.aer.ca>).

Marine sedimentation related to the WIS evolution within the WIFB, dominated the earliest (Middle Jurassic - early Late Jurassic) phases of sedimentation. From late Jurassic to Eocene terrestrial sedimentation became increasingly dominant, only interrupted by phases of more pronounced marine dominance from late Early Cre-

taceous to middle Paleocene (Slattery et Al., 2015, and references therein). During late Campanian marine waters retreated for the last time from the WCSB. The Bearpaw Fm. represents the latest known marine deposits in west-central Alberta (study area, figure 2.5).

2.3 The Cretaceous Western Interior Seaway

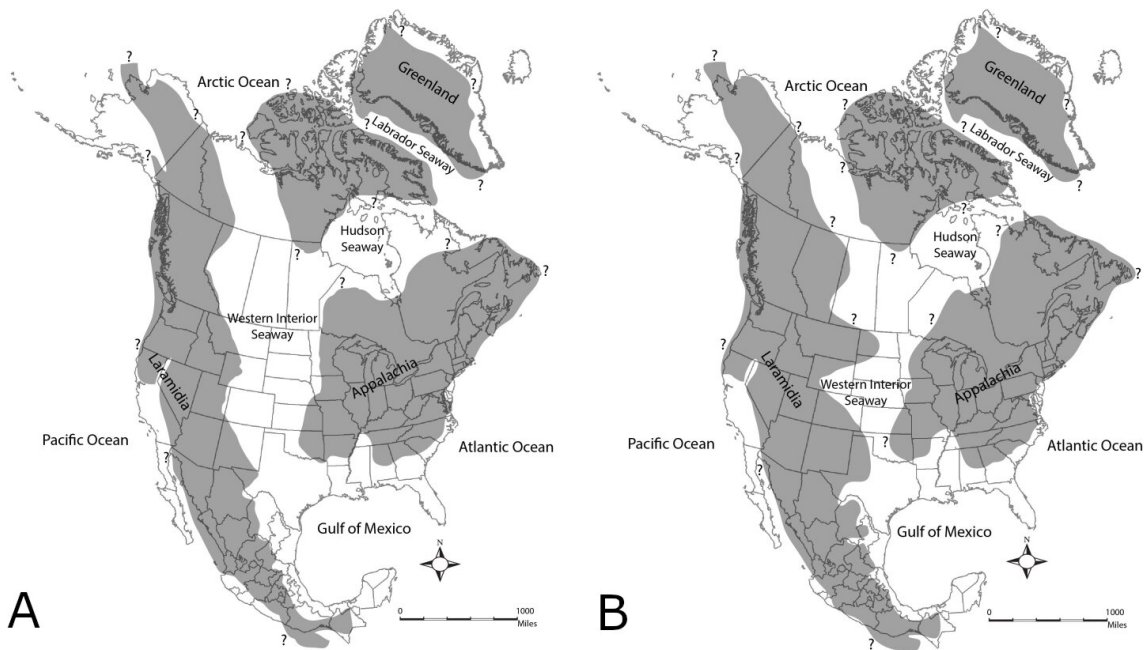


Figure 2.6: WIS shorelines of the mid Campanian (A) and early Maastrichtian (B). Shaded areas represent land. WIS shorelines are based on unpublished maps of W.A. Cobban; Jeletzky (1971); Roberts and Kirschbaum (1995); shorelines outside Western interior are modified from Alencaster (1984); Owens and Gohn (1985); de Cserna (1989); Sohl et Al. (2015); McFarlan and Menes (1991); Goldhammer and Johnson (1999); Umhoefer and Blakey (2006); Blakey (2013). Modified after Slattery et Al. (2015).

The Western Interior Seaway (WIS) was an epicontinental sea that connected the Boreal and Tethys oceans during the Cretaceous (Gill and Cobban, 1973; Cobban et Al., 1994), thanks to the isostatic downwarps that interested the crust east of the North American Cordillera (Cordilleran Orogenic Belt). The seaway started its inland propagation during Lower Cretaceous when the Sevier orogeny was thickening the crust, inducing the development of a large foreland basin to the east of the Cordillera, roughly with a north-south axis, that bisected the entire continent from Alaska to the Gulf of Mexico. The increased magmatic activity in the arc and the tectonic pulses resulted in uplifted highlands and so provided the sediment supply that filled the basin, causing more subsidence. During late Cretaceous the widest

extension of the WIS was reached (Turonian, 93 Ma), also thanks to one of the highest sea level stands in the Phanerozoic (Blakey and Ranney, 2017). That worldwide transgression peak is generally attributed to the increased volcanism in the western Pacific Ocean, which caused extensive uplift of the sea floor thus displacing large quantities of water onto all of Earth's continents (Schlanger et Al., 1981). The fore-land basins received large quantities of sediment from the uplifted Cordillera that concurrently increased the flexural effects amplifying sea ingressions. During late Campanian the southern seaway was finally closed by a major sediment influx coming from Mexico (between 75 and 72 Myr; Elder and Kirkland, 1994; Roberts and Kirschbaum, 1995; Kennedy et Al., 1998; Erickson, 1999; Blakey and Ranney, 2017). This dynamic setting, in which also eustatic sea level changes played an important role, resulted in highly dynamic shorelines recorded by a great number of paralic sequences with interfingered siliciclastic muds and sands, interrupted by numerous bentonites layers. The warm Cretaceous climate permitted the tropical vegetation to expand onto the floodplains and these organic materials were easily transported to back water swamps behind the Cretaceous shoreline, creating Alberta's richest coal and hydrocarbon reserves. The last marine deposits of the WIS in Alberta are Campanian, all paleogeographic interpretations report terrestrial sedimentation from late Campanian-early Maastrichtian onwards (Slattery et Al., 2015, see figure 2.6). Since this kind of epicontinental seas have no modern analogs, very little is known about their oceanography (Cochran et Al., 2003). Temperature and salinity estimations have been made, among others, by Hay et Al. (1993). They also suggest a wide variety of partial analogs to the WIS and discuss plausible paleocurrents scenarios. Some more recent attempts to reconstruct the WIS temperature and salinities have been carried out based on fossil shell's isotopic composition, among others, by Cochran et Al. (2003) and Petersen et Al. (2016) but a lot of uncertainties still exist about these questions and thus about the paleoceanography of the WIS.

2.4 Sea level history of the Western Interior Fore-land Basin

Haq (2014) provided the most recent review about Cretaceous sea level (figure 2.7). He reported two particular late Campanian events: the KCa7 (73.6 Myr) and the KCa6 (75.4 Myr) both recorded in Europe, Arabian platform, New Jersey margin and Tunisia (KCa6 was also recognized in New Zealand). The KCa6 was of relatively lesser amplitude than KCa7 but both are considered within the 25÷75 m medium range. The deposition of Bearpaw Fm.'s upper tongue is likely related

(dating-wise) to KCa7; KCa6 is the closer event to the Bearpaw Fm. lower tongue found in literature. Despite the overall rising trend during Cretaceous time, the long-term curve of global sea level (figure 2.7) is reported as relatively stable during the Campanian, around 220-240 m over the modern sea level, punctuated by higher rank T-R oscillations averaging roughly 40 to 90 m in cycles lasting around 1 Myr (Haq, 2014). Between the Campanian and the Maastrichtian (around 72 Myr) the global long-term curve (figure 2.7) started to record an eustatic fall, down to about 200 m over present day one (Haq, 2014), that characterizes the whole Maastrichtian and basal Paleogene (Danian). Previous studies about eustatic sea level (Unders Schultz, 1991; Frakes et al., 1992; Miller et Al., 2003, 2004, 2005, 2011; Gradstein, 2012) variations also highlighted the overall Cretaceous eustatic rise of base-levels in the WIS (Kauffman and Caldwell, 1993), between early Albian and Paleocene (figure 2.8) but differently from the curves in Haq (2014), the Maastrichtian-Danian sea level fall is way steeper, bringing sea level down to the Early Cretaceous one in a time span of about 10 Myr. The temperature curve (figure 2.8) indicate a Cretaceous period characterized by global warming. This trend inverted in coincidence with the Maastrichtian-Danian sea level fall. Most of the Authors agreed that the Cretaceous sea level rise was probably due to two main causes acting in concert and resulting in a maximum peak of about 300 m over modern sea level (Kauffman and Caldwell, 1993; Slattery et Al., 2015): (1) an acceleration of sea-floor spreading rate caused a significant increase in the volume of mid-ocean ridges and thus a global displacement of water over emerged lands to accommodate for the volume variation of the oceans (Pitman, 1978; Pitman and Golovchenko, 1983; Arthur et Al., 1985, 1991; Lillegraven and Ostresh, 1990) and (2) higher CO₂ concentrations due to the high volcanic activity increased the “greenhouse” warming effects and, therefore, caused a significant reduction of ice sheets (Arthur et Al., 1985, 1991; Miller et Al., 2003; Hay, 2008). Miller et Al. (2005) argued that CO₂ variations may have actually caused most of the Cretaceous sea level rise, thus significantly resizing estimations of oceanic crust production in mid-ocean ridges. According to Miller et Al. (2005) the rise peaked about 100 ± 50 m over present day sea level and the short-term Cretaceous oscillations (figures 2.7 and 2.8) were probably driven by changes in volume of Antarctic ice sheets. These changes, in turn, were able to modulate CO₂-related global temperature variations already happening because of the tectonically-induced increase in volcanism. Short-term sea level oscillations and, thus, shorelines evolution in the WIS, were also linked by some authors to Milankovitch cycles (Elder et Al., 1994; Sageman et Al., 1997). With a good degree of certainty, relative sea level in the WIS was controlled by the interplay of eustasy

CHAPTER 2. GEOLOGIC SETTING

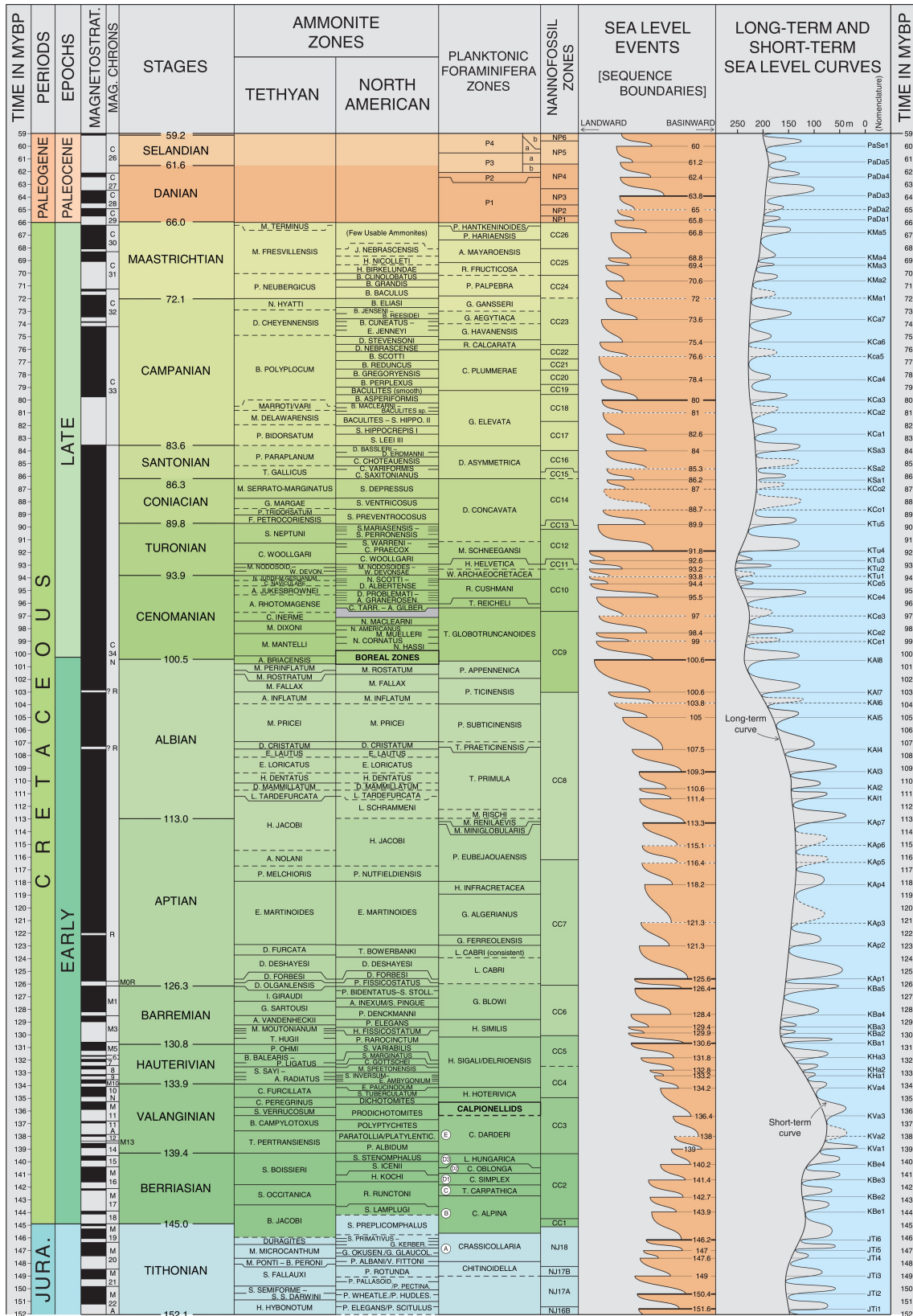


Figure 2.7: Summary table of worldwide recorded sea level events, from late Jurassic to early Paleogene including magnetostratigraphy, biozones, long-term and short-term sea level curves. Modified from Haq (2014).

and tectonics but the scientific literature is far from concordant about primary controls on Cretaceous shorelines variations in the WIFB. As reported in [Slattery et Al. \(2015\)](#), most studies have seen eustasy as the primary driver of short term sea level variations in the WIS (*e.g.* [Kauffman, 1977](#); [Weimer, 1984](#); [Kauffman, 1984](#)) but, since the early studies in the 70s, there is a trend to criticize this view recognizing the greater importance of tectonics ([Gill and Cobban, 1973](#); [Jeletzky, 1978](#)).

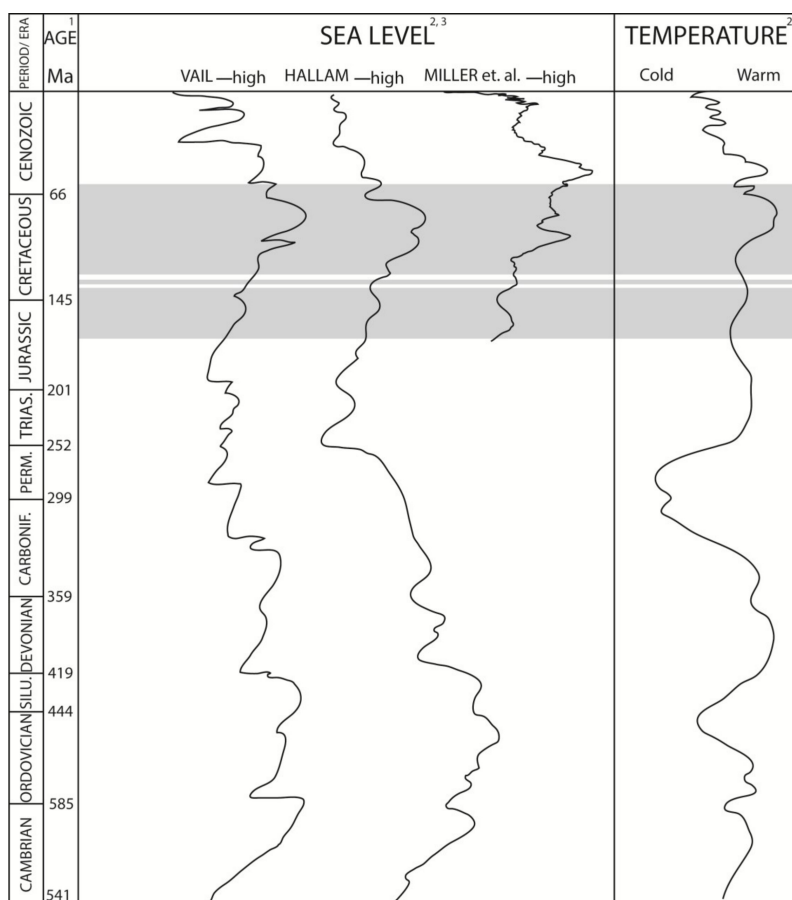


Figure 2.8: Phanerozoic global sea level curves and temperature curve. The references are indicated in: (1) [Gradstein \(2012\)](#); (2) [Frakes et al. \(1992\)](#) and (3) [Miller et Al. \(2005\)](#). The shaded area represents the time interval characterized by marine flooding in the Western Interior Foreland Basin. Modified after [Slattery et Al. \(2015\)](#).

2.5 Stratigraphic setting of west-central Alberta

In the late Campanian, during a transgressive phase, fine-grained marine shale of the Bearpaw Fm. were deposited in southern and eastern Alberta over the continental deposits of the Belly River Group. According to [Wall and Singh \(1975\)](#) the maximum limits of the transgression occurred in the southwestern Alberta Foothills, in the Edmonton area. In this work we also present how evidences of this transgression can be found further to the north and west. The Bearpaw Fm. consists of two major wedges (tongues) divided by continental coal-rich deposits belonging to the

basal member of the Horseshoe Canyon Fm. (the Strathmore Member; Edmonton Group). Hamblin (2004) introduced a third minor tongue, interposed between the two major wedges, which is not discussed in this work but was recognized also by Eberth and Braman (2012). This third tongue was likely included (as it it likely appear in a fraction of the southern study area) between the correlated surfaces, precisely within the deposits of the S interval, but its basal, MFS and top surfaces were not mapped as its deposits, compared to the mapped Bearpaw T-R cycles, represent a lower hierarchy event in the sedimentary fill of the study area. In the Grande Prairie region (west-central Alberta) alluvial successions, belonging to the Wapiti Fm., can be correlated to the entire succession from the Belly River Group up to the Bearpaw Fm. and to the Edmonton Group (Horseshoe Canyon Fm. and Battle Fm.). In particular, the Wapiti Fm. Unit 3 correlates with the Bearpaw Fm. Fanti and Catuneanu (2010). The Wapiti Fm. is overlaid by the Scollard Fm. (top of the Edmonton Group) that extends over the Battle Fm. to the south. All of the above cited formations consist of continental sediments sourced from the rising Cordillera and into the WCSB.

2.6 Previous understandings on the Bearpaw Fm.

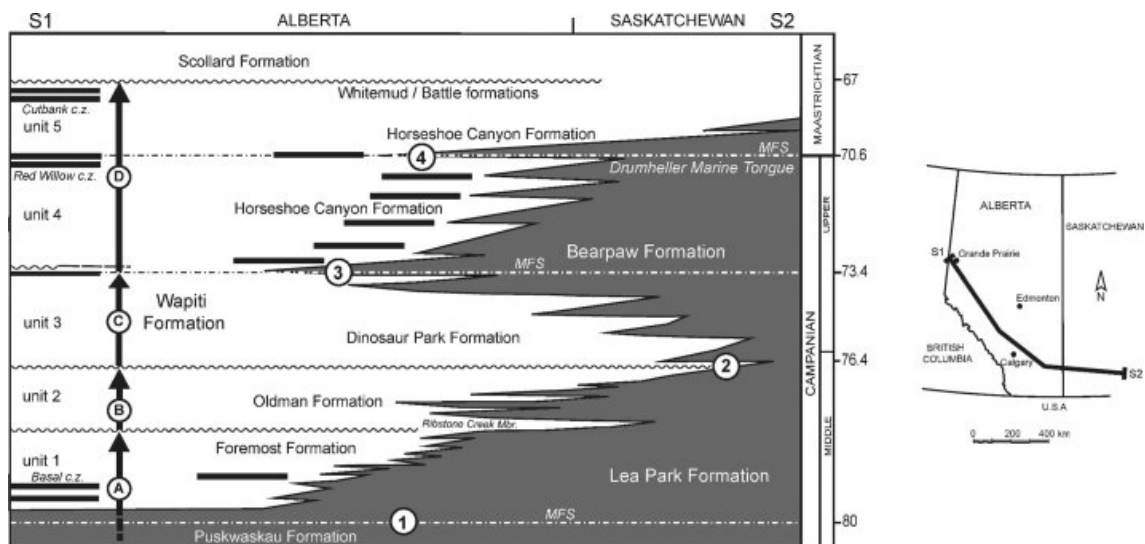


Figure 2.9: Schematic cross section of Upper Cretaceous in west-central Alberta correlating the continental formations in the Grande Prairie (Alberta) area (white) to the marine formations in southern Alberta and Saskatchewan (dark), including the Bearpaw Formations. Modified after Fanti and Catuneanu (2010).

The Bearpaw Formation was first described by Hatcher and Stanton (1903) and, since then, tens of scientific publications have dealt with its sediments, providing

2.6. PREVIOUS UNDERSTANDINGS ON THE BEARPAW FM.

valuable stratigraphic, structural and paleontological data (Price and Mountjoy, 1970; Wall and Singh, 1975; Price, 1981; Dawson et Al., 1990, 1994; Eberth and Deino, 1992; Ainsworth, 1994; Wood, 1994; Bustin and Smith, 1993; Cant, 1995; Jerzykiewicz, 1997; Catuneanu et Al., 1997, 1999, 2000, 2011; Lekie et Al., 1997; Eberth, 2002; Chen et Al., 2005; Ryan and Evans, 2005; Catuneanu, 2006; Glombick, 2010; Mallon et Al., 2012; Eberth et Al., 2013; Fanti et Al., 2015; Hathway, 2016; Bell and Currie, 2016; Gilbert et Al., 2018; Street et Al., 2019; Gilbert, 2019; Gilbert et Al., 2019, and numerous others) but many questions are still unanswered.

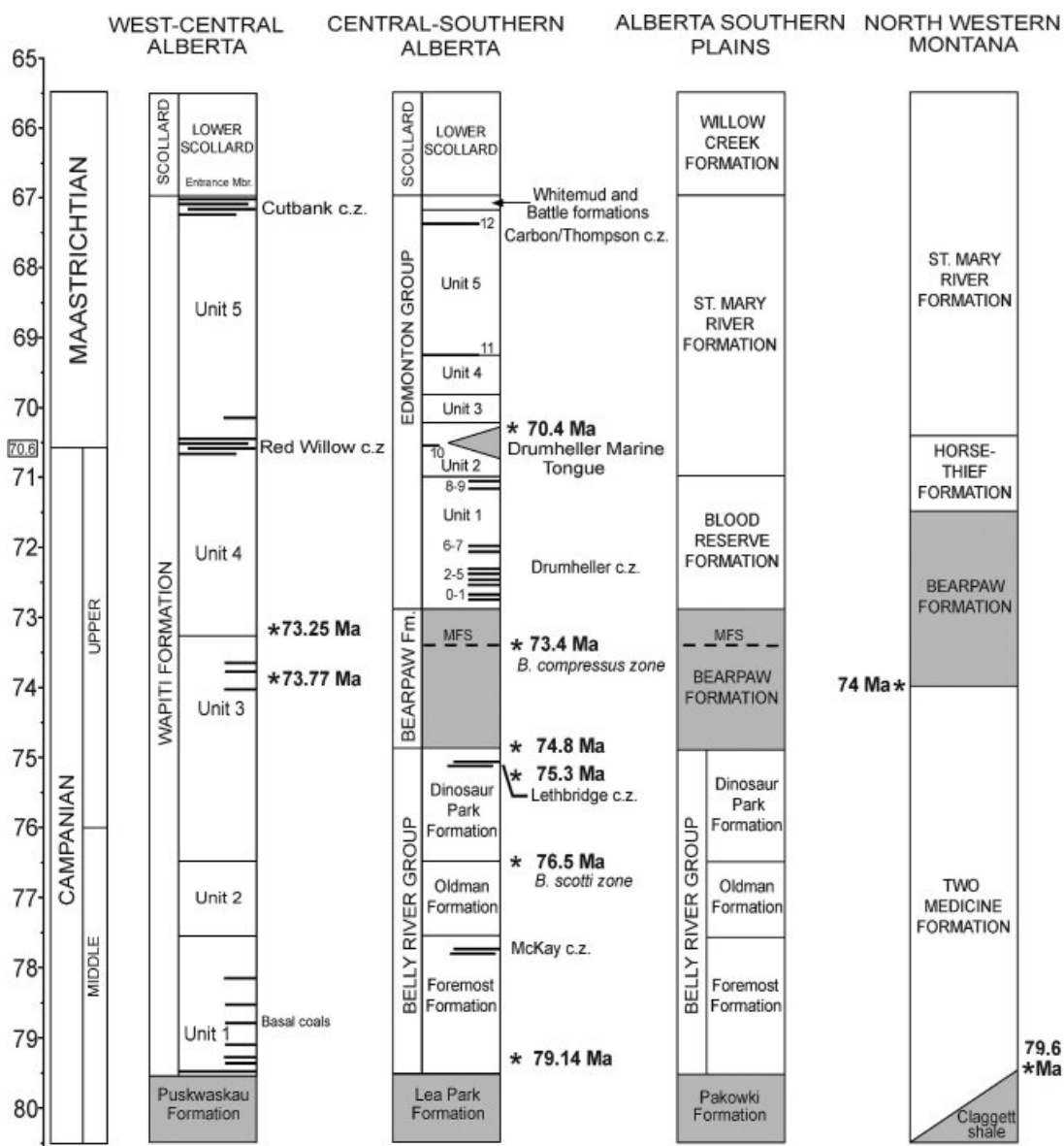


Figure 2.10: Stratigraphic columns from Campanian to Maastrichtian. Columns are representative of west-central Alberta, central-southern Alberta, southern Alberta plains and north - western Montana (USA) and show correlative formations and groups. Modified after Fanti and Catuneanu (2010).

It is an eastward and southward thickening double wedge of marine sediments that records the last T-R second-order cycle (the two wedges represent two third-order cycles, in this study we adopt the hierarchy proposed by [Catuneanu, 2006](#); [Catuneanu et Al., 2011](#); [Catuneanu, 2017, 2019a,b](#)) that interested central Alberta during the Upper Cretaceous (Campanian); that cycle was named T9-R9 by [Kauffman \(1977, 1984\)](#) and [Kauffman and Caldwell \(1993\)](#). The Bearpaw Fm. crops out in northern US and south-central Alberta. In Alberta the Bearpaw Fm. overlies the Belly River Group and is westward interfingering with the continental deposits of the basal Edmonton Group (figures 2.9 and 2.10). Eastwards, it correlates with the Riding Mountain Fm. of central Saskatchewan and Manitoba. Southwards, the Bearpaw Fm. correlates with the Pierre Shale Fm. in Montana and with the Dakotas Fm. in North Dakota. In our study area, the Strathmore Member (the basal member of

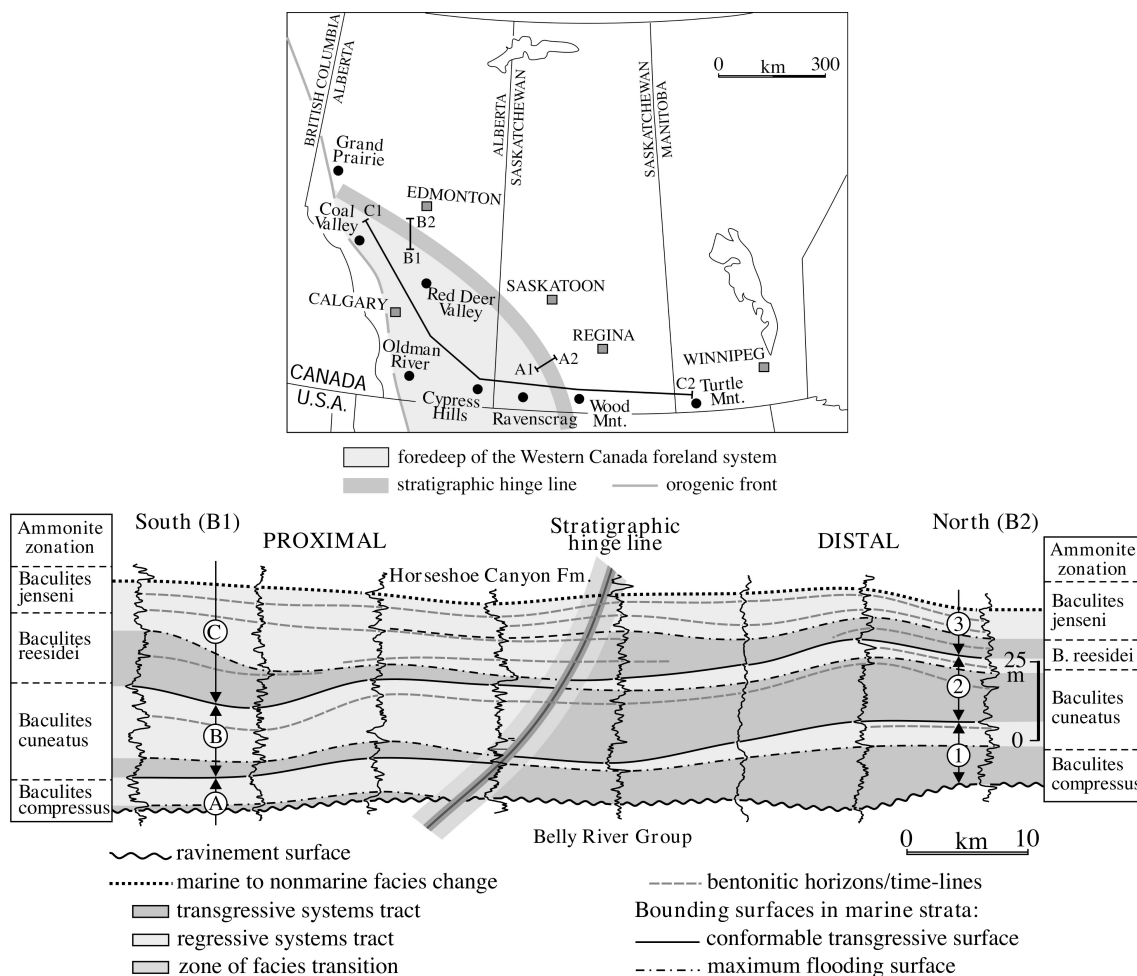


Figure 2.11: Cross section of the Bearpaw Fm. near the city of Edmonton (location labeled B1-B2 in the adjacent map). Reciprocal stratigraphies are represented with lighter and darker grey, hinge line dividing the reciprocal systems tracts is indicated in dark grey both in section and plan view. Modified after [Catuneanu et Al. \(1999\)](#).

the Horseshoe Canyon Fm.) divides the lower from the upper Bearpaw wedges (also referred to as tongues, figure 2.10). The Bearpaw Fm. consists of marine shales, siltstones and minor sandstones. Up to 22 bentonite beds have been identified within this stratigraphic interval and in several outcrops of southern Alberta also ironstone and concretionary nodules have been found (Catuneanu et Al., 1997; Chen et Al., 2005). Catuneanu et Al. (1997) and Catuneanu et Al. (1999) focused on the reciprocal architecture of the Bearpaw Fm. highlighting how the deposits are influenced by their position relative to the forebulge, and in particular to the flexural hinge line dividing the forebulge and the foredeep. They indeed traced an inferred hinge line in Alberta, west of Edmonton, through a detailed study of subsurface data, core samples and exposed intervals located in the Calgary area (figure 2.11). As they found, the deposits recorded different stacking patterns based on their position relatively to the forebulge; these patterns were related either to flexural uplift (regressive deposits near the forebulge) or to flexural subsidence (transgressive deposits towards the foredeep). The Bearpaw Fm. reciprocal stratigraphic architecture indeed consists of correlative transgressive and regressive systems tracts developed during continual base-level rise with differential rates across the flexural hinge line (Catuneanu et Al., 1999).

2.7 Age of the Bearpaw Fm.

The most recent and accurate isotope dating for the Bearpaw Fm. is provided by Eberth and Kamo (2020) who used the U-Pb CA-ID-TIMS method on bentonite beds that crop out in the Red Deer River Valley (east of Calgary, Alberta). The $^{206}\text{Pb}/^{238}\text{U}$ weighted mean age they provide is $74.308 \pm 0.031/0.050/0.130$ Myr for a bentonite layer near the base of the Bearpaw Fm. (uncertainties are in the format x/y/z; use x for comparing dates with other dates from the Jack Satterly Geochronology Laboratory where the dating was carried out; use y for comparison with the same dating method applied in other laboratories or use z to compare with other dating methods; refer to Eberth and Kamo, 2020, for full explanations) and 73.1 ± 0.1 Myr for the base of the overlying Horseshoe Canyon Fm. The MFS of the lower Bearpaw tongue was dated by (Eberth, 2005) at 74.1 Myr. The Dorothy Bentonite (DB) is an exceptionally thick (up to 13 m Lerbekmo, 2002) layer of volcanic ashes inside the Bearpaw Fm., positioned stratigraphically by Eberth and Braman (2012) within the upper tongue's regressive sequences. The dates provided by Eberth and Kamo (2020) for the DB is 73.7 ± 0.1 Myr and matches the age of 73.5 ± 0.4 Myr previously proposed by Lerbekmo (2002).

Chapter 3

Data and methods

3.1 Well-logs database: UWI Nomenclature

The Universal Well Identifier (UWI) is a standard well identification system introduced to encode into a 16-character alphanumeric sequence each significant event regarding a single well location. The same physical borehole may be associated to slightly different UWI sequences. Each number in the sequence has a precise meaning. The Canadian UWI was developed for the Petroleum Industry by the Geoscience Data Committee of the Canadian Petroleum Association ([Montgomery et Al., 1978](#)) in a computer readable format and essentially consist of four basic components. The legal survey location for one of four Canadian survey systems (Dominion Land Survey, National Topographic Series map grid subdivided by the BC Land Grid, Federal Permit, Geodetic Coordinates) and three other codes that define the approximate geographical location of a well and significant drilling or producing events at that location. The location component of the UWI codification circumscribes a small land area rather than the exact position of the well. In this study UWI names are reported in the Dominion Land Survey System (DLS), which is the one adopted in Alberta, so the first position of the UWI is a one-character code number 1, and the following description of characters refers to that particular legal survey location system; for a more detailed discussion on other legal survey location systems (codes 2 to 4) refer to [Montgomery et Al. \(1978\)](#). Characters in positions 2 and 3 (on the total 16) refers to a two-character code used for those cases when more than one well is drilled in the reference land area described by the Legal Survey System. The position 2/16 may be a letter or a number describing the actual position within the area, it is 0 (zero) for the first well located in that survey area. The second character in position 3/16 is a number defining the chronological sequence in which the wells were drilled. Characters in positions 4 to 14 describe

the Legal Survey Location. The first two numbers (positions 4-5) define the Legal Subdivision (LSD) that is a number between 1 and 16 (e.g. 01, 05, 10, 15), if LSD is unknown “00” is used. The following two numbers (positions 6-7) define the Section which is a number between 1-36, e.g. 01, 05, 10, 25, 36). The next three numbers (positions 8-9-10) define the Township and are always between 001 and 126. The following two numbers (positions 11-12) define the Range that can be between any number between 1 and 34 for Meridian 1 and between 1 and 30 for Meridians 2 to 6. Meridians are east-west coordinates origins for Ranges that are reported in position 14/16. Meridian number 1 is at longitude 97°27’28.4”W and Meridians from 2 to 6 are at 4° incrementing intervals starting from the longitude 102°W. This sequence (positions 4-14/16) is entirely made by numbers except for position 13/16 which is the direction of range numbering: a letter W defining the longitude is westward from the Meridian number (which is in position 14/16). If the Meridian number is 1 that letter may also be an E (east). Since UWI identifiers must always consist of 16 characters (for computer readability) a following 0 is added in position 15/16 (that operation is called “number padding” and is necessary in the DLS survey system here described and in all of the above cited but in the Federal Permit one). Position 16/16 is occupied by a one-character number identifying in chronological sequence, a significant drilling and/or completion operation at the well which yields a separate and unique set of geological or production data. The initial drilling and first completion are coded 0 (zero) and subsequent events 1-9. If necessary, the alphabetic series beginning with “A” (capital letter, e.g. ...8,9,A,B,C...) is used from the eleventh UWI onward, and number padding in position 15/16 is not applied. As recommended by the authors ([Montgomery et Al., 1978](#)) a typical UWI in the DLS format should be written: 1/00-16-25-123-15-W6 /04. However, a great number of publications present the most varying and personalized formats in terms of blanks spacing, special characters (the dash and the slash), number padding etc. Given the fact that the Legal Survey Location system is the same for wide areas, the leading “1” is often omitted, especially in older publications. In this study each UWI is reported exactly as exported from the IHS database used to select the dataset. The UWI was not corrected to the officially recommended format in order to ensure traceability of the data within the mother database. The exported UWI codes in the database vary in formats but most of them appear as the following: 01/00-16-25-123-15-W6/4.

3.2 Software

3.2.1 Proprietary

University of Alberta provided licenses and access to the IHS Markit (figure 3.1) software package that comprehend [Accumap](#) and [Acculogs](#), two softwares with up to date capabilities in well-logs data browsing, editing and visualization. Along with the licenses came the full access to the entire raster well-logs database of Alberta, which consist in several hundreds of thousands of well logs throughout the entire state, ranging from the end of the first half of the 20th century up to the most recent well logs of the 21st century, all scanned into raster formats by the operators starting from the paper copy. This means that some well logs may preserve absolute errors introduced by the scanning operations such as geometric distortions due to different lenses or alignment errors between different sections of the longer (reaching deeper depths) well logs that were scanned in multiple segments.



Figure 3.1: IHS Markit official logo. IHS Markit developed Accumap and Acculogs, the softwares used in this study to access and correlate gamma-ray well logs. The official website is <https://ihsmarket.com>.

Inside Accumap, well-logs data browsing and selection is user-friendly, with a GIS style graphical interface and some useful tools to filter, locate and export data. In this study, sections were traced over the study area using the best wells available near the desired section path. Thanks to well logs abundance, it was possible to select the most recent and high-quality curves in most of the study area. Where data were scarce (Foothills) it was necessary to use the available curves and that sometimes meant working with poor-quality data, produced with the outdated technologies of the 20th century. Acculogs was used to visualize the traced sections and to pick the tops (the correlated surfaces) used for correlations. The software automatically aligns the curves on a specified top (used as datum) or on sea level, greatly enhancing the possibility to interpret data horizontally.

3.2.2 Open-source

In this study professional open-source tools (publicly available on the web) were extensively used, such as **QGIS 3.10** (figure 3.2) and the **Generic Mapping Tools** (GMT 5.4.5 and partially GMT 6; [Wessel et Al., 2013, 2019](#), figure 3.3). The former is an advanced GIS software capable of every classic operation that proprietary GIS softwares do concerning vectorial or raster data formats. It is developed and updated by a worldwide community of professional users, scientists and software engineers since 2002 from an initial idea of Gary Sherman. Every four months the software is updated and known bugs are corrected into a new stable release; every year a long-term support release is published. Over the years the community was able to make it one of the most reliable and user-friendly GIS software in the world.



Figure 3.2: Qgis official logo. Also known as *Quantum GIS* (before 2013), Qgis is widely used worldwide to visualize, organize, analyze and represent spatial data. The official website of the project is <https://www.qgis.org>.

GMT was implemented in this research within scripts that were coded from scratch specifically to fulfill the needs of this study. The following texts contain a brief introduction to what GMT is, what's the potential of GMT implementation in geologic research and to what's its role in the framework of this study (a more in-depth explanation will be found in paragraph 3.3.3). GMT is an open-source collection of command-line tools developed, maintained and updated by a large community of users from an original idea Paul Wessel and Walter H.F. Smith had back in 1988 and officially released in 1991 under GNU General Public License. The tools allow to process and display xy and xyz geographic and Cartesian datasets, including rasterisation (technique of drawing 3D models), filtering and image processing operations, animations, and many more. All with high personalization capabilities that are impossible to achieve with ordinary Graphical User Interface (GUI) softwares. The command-line nature of GMT allows for scripting powerful data elaboration routines which can perform all the necessary operations on the desired dataset and display the results. The GMT commands can be integrated within

scripts that run on other programming languages to create real micro-softwares for highly personalized data processing needs and for the re-organization of the GMT input/output formats: e.g., the programming language used in this study is Bash - Bourne Again Shell -, Awk and Sed were also used (within Bash scripts) to perform various data-processing tasks in order to get the right formats (file type, order of rows and columns, headers, footers etc.) out of data tables that were exported from the IHS Markit proprietary softwares.



Figure 3.3: GMT official logo. The *Generic Mapping Tools* is a growing collection of computer software tools for processing and displaying xy and xyz datasets. The official website of the project is <https://www.generic-mapping-tools.org> and the full documentation of the commands used in this study can be found in the [documentation section](#) of the official GMT website.

The pre-processing of raw data was coded in order to fit the required input format of GMT algorithms. Every time new updates were made on the well-logs database (i.e. mistakes correction or new correlations) and consequently a new interpolation of exported results was needed, these scripts eliminated the need to manually rectify the structure of the tables in order to feed them to GMT. Without this automatic data-processing approach it would be simply too time consuming for any individual researcher to get a trustworthy correlation database based exclusively on gamma ray well-logs correlations (and that might actually extend to all types of analysis). All the code used to process data in this work is reported in Appendix 1, see paragraph [3.3.4](#) for a discussion on the most important GMT commands that were used to process data in this study and their behavior. Please note that the scripts reported in Appendix 1 (sections A to F) are “hard-coded” to work only with a very specific

architecture and content of both the starting databases (input) and the mother directory in which the script is executed on a UNIX system. All scripts were tested and debugged only for the used operative system: Linux Ubuntu 18.04LTS (properly set up with the required packages). It is worth noting that the scripts are coded with accuracy and ease-of-use in mind rather than to be efficient and fast as they were specifically designed for this study and dataset structure and will therefore need some adaptation in order to run in other situations. The use of the scripts reported in Appendix 1 is encouraged for any possible application and under the license and terms that are reported at the start of the appendix. It is nonetheless strongly suggested to use the code as reference for personalized scripts, in order to fulfill each specific need and to take advantage of the full potential of GMT implementation in data processing tasks and results visualization.

3.3 Methods

3.3.1 Dataset construction

Towards the north and north-west, the study area was cut to fit the exact extension of the selected gamma ray well logs in which the Bearpaw interval (and correlative deposits) was found, thus cutting out large interpolated areas not actually covered by high-resolution correlations. Towards the south, the study area was also cut to fit the selected well logs and extends south and southeast enough to overlay the study area of previous published works on that stratigraphic interval. After this operation, indeed, the border of the modeled area (red line in figure 3.4) coincided with correlated well logs and artifacts, due to the interpolation of data where the well logs arrangement created convex (toward the center of the study area) uncorrelated zones, were excluded from the analysis. The studied region therefore has an irregular shape and encompasses a total area of 96990 km². It was chosen mainly because of its position relative to continental successions in the north and to correlative marine outcrops in the south: it was inferred to host the transitional and coastal environments between the two. Thus we chose to limit our 3D modeling to the extension of our selected well logs, which were chosen on the base of:

1. the presence of the studied stratigraphic interval in gamma ray well logs to the east (as the late Cretaceous is mostly eroded eastwards of Edmonton) and to the north and north-west (where it crops out in the area of Grande Prairie);
2. the position of the Rocky Mountains deformation front (western border);

3. the southward and southeastward overlay with already published studies.

The studied interval is precisely defined with stratigraphic and chronostratigraphic standards from the literature. The former come from studies in the Grande Prairie area (Fanti and Catuneanu, 2009, 2010) and the latter from published analysis (particularly from Catuneanu et Al., 1997; Jerzykiewicz, 1997; Catuneanu et Al., 1999, 2000). This permitted to define a precise stratigraphic interval within which the correlated surfaces could be found. Beside that, new chronostratigraphic datings (Eberth and Kamo, 2020) permitted to reach a more accurate temporal resolution than what was previously available in the literature.

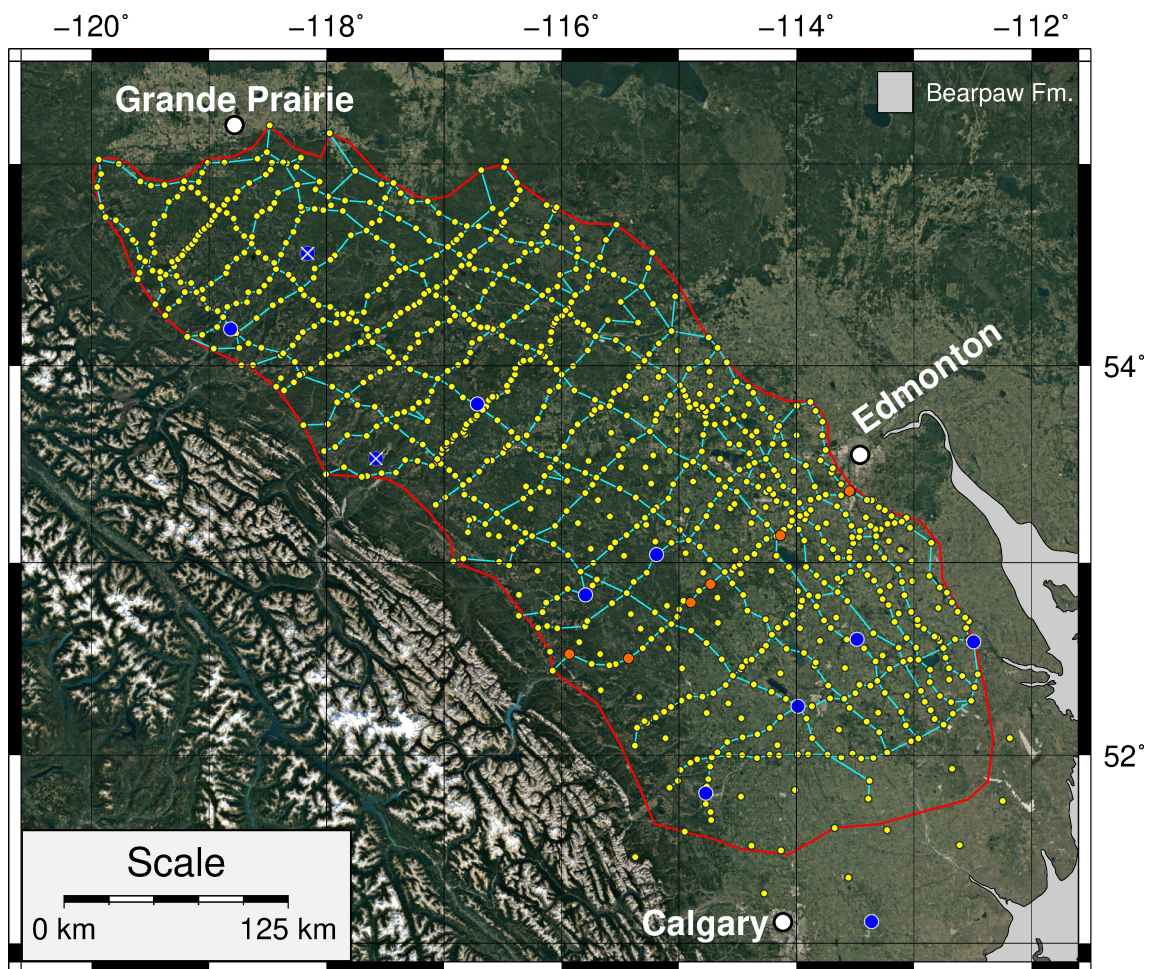


Figure 3.4: Sections (light-blue) and well logs (yellow) used in this study, projected on a Google Earth satellite image. The area in grey represents the distribution of the Bearpaw Formation (see figure 2.5). Well logs indicated with blue dots have been used to compare depth correlations from this study and literature. Reference well logs are reported in table 1 of paragraph 4.6 (crossed blue dots correspond to UWIs marked with an asterisk). Reference well logs shown in figure 4 of paragraph 4.6 are marked as orange dots.

The study area (figure 3.4) was investigated by means of gamma ray well logs, having full access to the complete database of drilled boreholes since around the

'50s up to today. Although older well logs permitted to expand the analysis in certain zones of the study area that were not drilled in recent times, younger data were always preferred over the older well logs when possible. The quality of the gamma ray emissions-counting instruments and the graphical appearance of the curves has improved dramatically over time. Along with new technologies, the vertical resolution and the accuracy of curves also improved massively. Moreover, standards for borehole depth measurements back in the 50s had not yet adapted to international metric units (imperial units were used), implying the need for a units conversion passage. With the selection of a large well-logs database, the study area was covered using 977 gamma ray well logs organized in a grid of 31 roughly 90°-crossing sections, oriented SW-NE (dip-oriented, perpendicular to the deformation front) and SE-NW (strike oriented, roughly parallel to the deformation front). The location of well logs and sections is reported in figure 3.4.

3.3.2 Gamma ray well logs analysis and correlation criteria

While the sub-planar development of the stratigraphic record in the study area combined with its flat topography (west-central Alberta topography in figure 1.1) has been an obstacle to conventional direct-data based approaches, as outcrops are not present for this very reason, the subsurface architecture is actually what permitted to base this research exclusively on subsurface observations of geophysical data and literature. This structural conformation provided the possibility to expect that coeval surfaces don't vary too rapidly in depth, thus correlations within short (few kilometers) distances could be aimed towards a narrow and predictable depths range, starting from known, published and tested well-logs tops. The dataset of this study was selected to create the first high resolution well logs based correlations of the Campanian Bearpaw Fm. and Wapiti Fm. between the cities of Grande Prairie (North) and Calgary (South), filling the gap between the published studies about northern and southern sectors of west-central Alberta. That correlation of northern continental outcrops to southern marine sequences of Alberta, has been pioneered by the works of [Fanti and Catuneanu \(2009, 2010\)](#) upon which this study is heavily based and that we extensively enlarged and detailed.

Seven surfaces were correlated on every well log in order to obtain a xyz database (longitude, latitude of the borehole and sea level-referred depth) that evenly covers the entire study area. Each depth was calibrated using a highly characteristic and recognizable datum throughout the entire dataset, which is the Belly River Group base (figure 3.5).

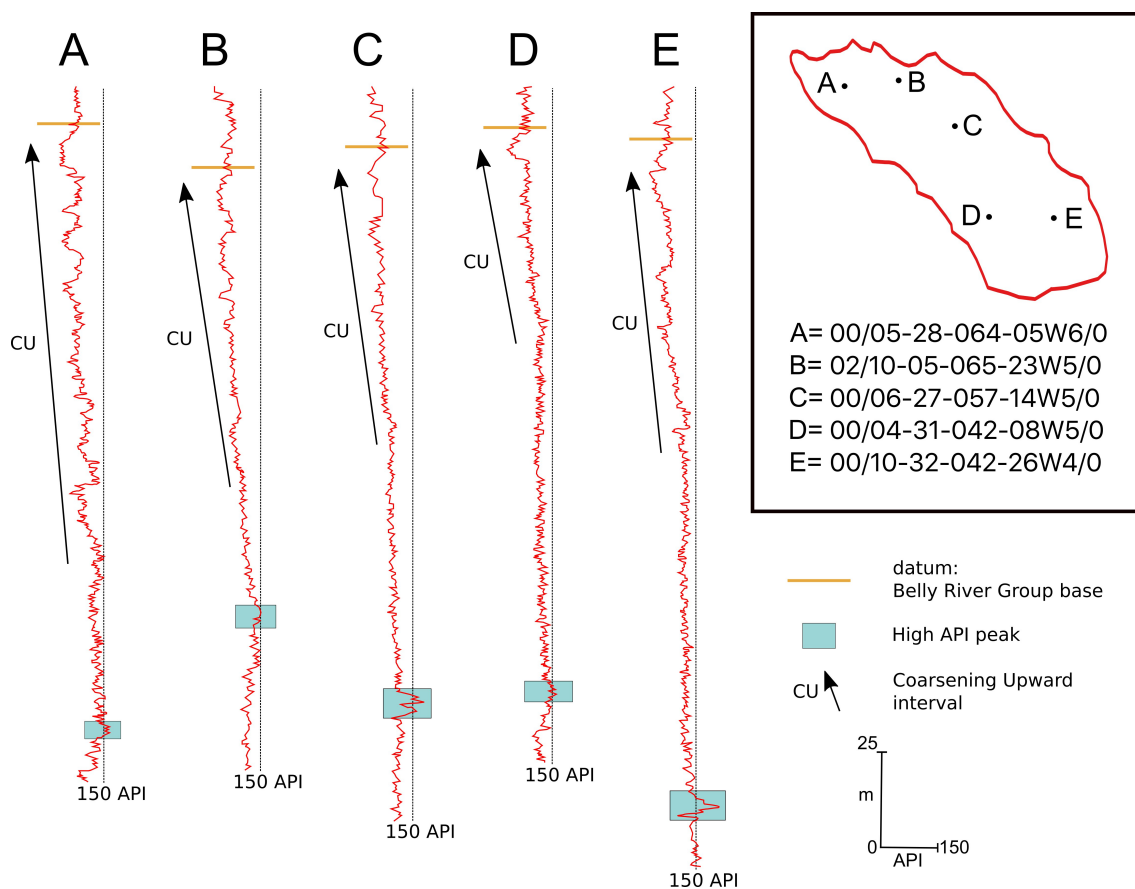


Figure 3.5: The Belly River Group base (orange lines) was used as datum in this study. It was picked right above of a decametric, well-identifiable coarsening upward (CU) interval. This CU interval, not only is visually easy to spot, as there is no other similar interval in west-central Alberta, but is also unique as it always occur some tens of meters above a clear high API interval (blue squares) which was found in the entire study area and used to double-check the correlation of the datum surface. This high API interval often scores, especially in the eastern study area, well over 150 (API) and is probably related to bentonite beds or other sediments with high gamma ray emissivity.

The datum surface can be well correlated using GR logs because there is no similar decametric coarsening upward sequence suddenly interrupted by a rapid (flat) increase in the API value (see figure 3.5). Indeed, this surface stands upon a stratigraphic interval that records the shift from the underlying marine shales of the Lea Park Formation to gradually coarser sediment near its top (CU) where the clear return to high API finer sediments (punctuated by coals) indicates the base of Belly River Group, recording the early Campanian progradation of deltaic systems over marine environments in west-central Alberta. The Belly River Group base was picked right to the depth of that rapid change in the CU trend, within fine sediments, on the first coal layer above that abrupt change. The coal is well identifiable in gamma ray logs because it generally shows low radioactivity thus resulting in a clear low API peak between fine sediments (with higher API). The next 6 surfaces

are defined as the transgressive surface (TS, see paragraph 3.3.3 for a disambiguation of the nomenclature used in this study), the maximum flooding surface (MFS) and the maximum regressive surface (MRS) for both the Bearpaw Fm. lower and upper tongues. The analysis involves some basic sedimentological concepts to recognize the main trends of fining upward (FU) and coarsening upward (CU) in GR curves, which have been used to define the lower and upper tongues thicknesses and correlative deposits. Knowing that transgressions generally shift the sedimentation towards finer grain sizes (FU) it is possible to focus on where the GR curves mark a significant inversion after an overall FU trend (transgressive) to find a maximum flooding surface and the regressive portion of the T-R cycle (CU). That correlations are easier in fully marine settings because the inversion in the trend records the condensate interval (Galloway, 1989) happening when the sea level has risen to its maximum and still stands (Highstand Systems Tract, HST) before falling again (Falling Stage Systems Tract, FSST); correlations gradually become more subject to the operator's experience moving into a fully continental depositional domain (westward in the study area). GR logs serve well for the purpose of this study because of the strict relationship between granulometric trends and radioactivity of the sediment (GR emissions): the finer the sediments the higher the average radioactive content will be and viceversa. It is due to mention that there are some known exceptions to that "rule". It should be generally applied to siliciclastic sediments/rocks only and will fail in known cases, due to masking effects that may be generated by low radioactivity layers (e.g. quartz rich sands, for more examples refer to Rider, 1990). The dataset here presented may comprehend some of these absolute errors but the consistency of the results reported by this study, in terms of thickness trends and relations between cumulative thicknesses and GR-curve's shape, suggests that those kind of errors only affect the interpolations as ground noise within a distinct and recognizable signal.

This study was carried out by means of a multidisciplinary approach (sedimentologic, geophysical, geomorphologic etc.) taking in consideration that accuracy can be highly biased by the operator of the correlation: as much as in the majority of the geologic research techniques, experience is key to succeed avoiding (or recognizing) mistakes. There is no scientific certainty (in *stricto sensu*) behind any underground correlation without the use of core samples or other directly derived data and, even in that case, the subject of Geology should never be approached as a pure science. The study area host no outcrops and no data from cores or seismic surveys was available. It was thus necessary to build the dataset using only GR well logs and published data, through a long trial and error process that went on until an accept-

able degree of coherence was reached between the geometries observed on thickness models (geomorphologic interpretation) and predictions based on GR curves (sedimentologic well-log interpretation). As an example, stacked multiple high frequency CU sequences, often found in regressive intervals, led to interpret GR shape as result of prograding bodies, so we expected to find the plan-view of a progradational coastal body on three-dimensional models. The correspondences between GR observations and 3D reconstructions had to be validated throughout the entire study area. The study area holds the requirement for testing this method: the geologic bodies in the subsurface develop almost flat and with uniform and low-intensity tectonic deformation in our depths interval of interest. Thanks to a reliable datum (Belly River Group base) a lot of possibilities to make mistakes are cut out of the process and the “signal/noise” ratio is better. Some published data were used as control points for the Bearpaw Fm. base e.g the well named 7-12-25-25-W4 (UWI) that was studied by [Catuneanu et Al. \(1997\)](#), both directly on the core and through well logs. Some control points were selected among wells forming the sections in [Eberth and Braman \(2012\)](#) that overlap the study area. The correlations were widely referred to the depths of the Bearpaw Fm. base and Belly River Group base provided by [Jerzykiewicz \(1997\)](#).

3.3.3 3D processing workflow and surfaces nomenclature disambiguation

The seven analyzed depths (Belly River Group base, lower and upper Bearpaw tongue’s TSSs, MFSs and MRSs) on each log were exported and interpolated using GMT 5.4.5 (Generic Mapping Tool) scripts to obtain 7 digital elevation models (DEM, referred to modern sea level). The interpolation between depths was based upon Green’s functions ([Wessel, 2009](#)) utilizing the built-in GMT interpolator. Sea level referred depths obtained from the interpolated DEMs were used to compare the database (paragraph 4.5.3) with the already published sections that can be found in the detailed study by [Jerzykiewicz \(1997\)](#). The published section traces D-D’, E-E’, F-F’ and G-G’ were georeferenced and digitalized using Qgis. A GMT algorithm was then developed to plot data on cartesian distance/depth axes, drawing the sections with a specified vertical exaggeration that matches the above mentioned published sections. The output sections, which count seven surfaces each (datum and Bearpaw intervals, sampled on the respective DEM surface), were superimposed to the sections from [Jerzykiewicz \(1997\)](#) and analyzed in terms of difference/similarity (see paragraph 4.5.3 for a discussion on that comparison). With simple subtractions of pairs of subsequent DEMs we obtained a thickness map for each interval: Belly

River Group, lower and upper tongues respective transgressive and regressive, S interval (mostly consisting in Strathmore Member deposits). Each thickness interval was then summed to the thickness between the top of the previous interval and the datum to obtain cumulative thickness maps. In this way, the morphology of the basin (container of the intervals) was recreated as (simplifying) we recreate a shell shape from a fossil cast. That approach would imply the focus over coeval surfaces only: MFS (which we actually discuss in this work). The correlation of each systems tract was then extended landward to make sure to include the probable shoreline and, further westwards, interpreting correlative deposits within the continental domain. In this sense, what we call “TS” (transgressive surface) and “MRS” (maximum regressive surface) are not to be considered in *stricto sensu* (i.e. as the sequence stratigraphic nomenclature defines them as “time-transgressive”), but with the amplified meaning of being comprehensive of the correlative continental deposit. Starting from southeastern study area (where the most recent literature-derived control points are located) and gradually moving north and west, the TS (s.s.) found on the border of the study area was extended landward (westward and northward) through inferred correlative continental deposits, also relying on the correlations proposed in [Fanti and Catuneanu \(2009, 2010\)](#) and on the numerous works authored or co-authored by Jerzykiewicz ([Jerzykiewicz and Sweet, 1986, 1988](#); [Jerzykiewicz and Norris, 1994](#); [Jerzykiewicz and McLean, 1980](#); [Jerzykiewicz et Al., 1996](#); [Jerzykiewicz, 1992, 1996, 1997, 2010](#)).

Cumulative thickness maps produced in this study must not be considered as accurate representations of the paleotopography. They obviously contain informations about it, as the sedimentation process is highly influenced by the topography, but they are also developing from a flattened surface (datum) upward. In that sense, the cumulative thickness maps actually show the topography that would have developed if the starting surface (Belly River Group base) was flat and if no differential compaction happened. The next step in the workflow was deducing depositional domains (the paleogeography) from the interpretation of controls over the geometry of mapped deposits. This interpretation represents an integration of literature data and observations on cumulative thickness maps, isopachs distribution in each interval and relative GR shapes-based deductions.

3.3.4 Main GMT commands, scripts and workflow

The following text contains a schematic list of the most important GMT commands with explanations about commands behavior and influence on data representation; the reader may find this useful to better understand the way raw data was processed

to get the maps shown in the following chapters.

GMT workflow to reproduce the results of this study:

1. Export *.xls* datasets from IHS Markit softwares;
2. structural conversion of data tables and assembly of the input dataset for GMT commands;
3. *greenspline*;
4. *grdmath*;
5. *grdgradients* and *grdimage*;
6. image editing and format conversions.

GMT commands:

```
gmt greenspline dataset.csv -I0.01 -Rwest/east/south/north -Gsurface.grd -D1 -Sl
```

this is the first and most important command and was used at the head of the processing workflow. It interpolates point data from *dataset.csv* (properly structured) using Green’s functions (Wessel, 2009) for splines in 3 dimensions (splines are “curves defined in the 3D space by at least two control points”; we have seven control points associated to each well log and subdivided in that many surfaces). Bilinear (interpolated in 2D) splines (*-Sl*) are then resampled in user units (*-D1*) with equidistant sampling intervals of 0.01 user units in each dimension (*-I0.01*) and within the Region Of Interest (ROI, *-Rwest/east/south/north*, the sides of the ROI are defined by latitudes and longitudes in decimal degrees). User units are set to meters. Output is a 3D model (surface) named *surface.grd* (*-Gsurface.grd*); a grid file is a matrix that, in this case, represents a spatial database of regularly spaced values sampled on the interpolation surface of multiple points in the 3D space. The greenspline tool was applied to all of the 7 mapped surfaces to obtain sea level referred Digital Elevation Models (DEM) that were then fed to the following commands:

```
gmt grdmath surface2.grd surface1.grd SUB = thickness_2-1.grd
gmt grdmath thickness_2-1.grd thickness_3-2.grd ADD = cumulative_thickness_1-3.grd
```

3.3. METHODS

The command *grdmath* applies a straightforward algorithm to mathematically combine different grid files (*.grd*) relative to the same location (the one defined by *-R* in the previous command) on a pixel-to-pixel base. With the *SUB* operator (subtraction) it is possible to obtain thickness models by subtracting sea level referred surfaces. These thickness grid files can then be summed cumulatively with the *ADD* operator (addition), to obtain cumulative thickness 3D models in *.grd* format.

The following commands relates more to data visualization than to data processing but still are worth mentioning to better understand the figures that illustrate the results of this study.

```
gmt grdgradient surface.grd -A60 -Ne0.6 -Ggradients.nc
gmt grdimage surface.grd -Rwest/east/south/north -JM15c -Cpalette.cpt -Igradients.nc
-Q > final_map.ps
```

The *grdgradient* command calculates a *gradients.nc* file (Network Common Data Form, Net-CDF) to be used as light-gradients mask for the shaded relief visualization of 3D surfaces. In all modern sea level referred images that were produced for this study light comes from ESE, 60°N (*-A60*) and the light intensity is normalized using a cumulative Laplace distribution with amplitude set to 0.6 (*-Ne0.6*); isopachs and cumulative thickness images are instead represented with two different light azimuths, to better emphasize geometric features of the surfaces; illumination comes from two different sources (it would be simply coded *-A30/150*) located 30°N (NE) and 150°N (SE). The gradients mask is fed to the *grdimage* command (*-Igradients.nc*) along with the surface to represent (*surface.grd*). The other “flags” (command settings) are the region of interest (*-Rwest/east/south/north*), the projection of the map (*-JM15c*, meaning: Mercator projection on a 15 cm image), instructions to ignore and skip NaN values (*-Q*). The output of *grdimage* is a PostScript file containing the code to get the desired images displayed.

The data represented in each image were processed with these and other basic GMT commands within a Bash framework (that’s why the letters “*gmt*” have to be re-called before the command). All of the other commands reported in Appendix 1 relate to dataset structural manipulation, graphical rendering of multi-layered images, image format conversions and operations related to technical computer-science aspects. The scripts thus assemble and process datasets directly from the *.xls* data tables (exported from the IHS Toolkit) and provide the visualization of georeferenced 3D models in a relatively short amount of time. Everything happens within

the mother directory in which the scripts are contained, the output is organized in directories and the scripts expect to find the right input files to work with in exact (pre-determined) locations, without needing any other operator action than running it onto a *UNIX* terminal.

3.3.5 Time-correlative surfaces on gamma ray well logs

As discussed in paragraph 3.3.1, gamma ray well logs can serve the purpose to carry on granulometric trends analysis of siliciclastic successions (Catuneanu, 2006). These trends basically consist in coarsening up and then fining up cycles or just intervals of the curve. On the basis of the increments or decrements of the API (American Petroleum Institute units) value and given the graphical patterns that these increments follow on the log, the succession was subdivided in different sections with similar features, that reflect different depositional architectures involved to form each interval's deposits. So doing, it's possible to apply the Walther's Law of Facies directly to our sections, given the low-grade deformation and well preserved Bearpaw Fm. continuity. Once the basal interval of the curve is interpreted (in terms of depositional environments), each overlying or adjacent facies is then predictable given the stratigraphic context, either on the vertical of the same curve and laterally between well logs (thus widely relying on the chosen datum, see figure 3.5 and paragraph 3.3.2 for a comprehensive description of correlation criteria in this study). The published literature already reports the stratigraphic context of the study area, it is known that the events we are tracing are not local to a particular area but instead interest the entire basin (or even the globe). Especially in the southeastern study area it's reliably predictable to observe shifts between coastal and marine depositional environments (Catuneanu et Al., 1997; Jerzykiewicz, 1997; Fanti and Catuneanu, 2009, 2010; Eberth and Braman, 2012; Hathway, 2016). West of the coastal zone, it is predictable to find more typically proximal deposits (that were also observed by Jerzykiewicz and Norris, 1994; Jerzykiewicz et Al., 1996; Jerzykiewicz,

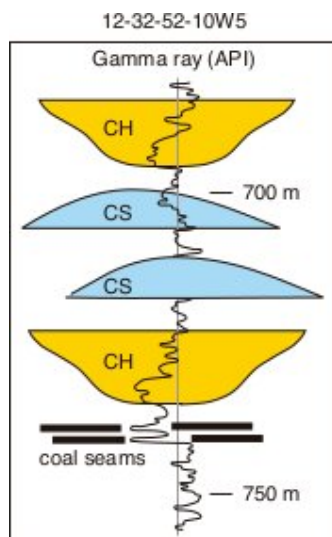


Figure 3.6: Log signature shape of a low-energy fluvial system with indicated coal seams typical shape, fining-upward channel fills-like trends (CH) and coarsening-upward crevasse splays-like trends (CS). Modified after Catuneanu (2006).

1996, 1997) since it's known that the provenance of the sediment fluxes in west-central Alberta is from the west. A number of studies about gamma ray well-logs correlations have recognized relations between some depositional environments and the shape of the radioactivity curve that the relative deposits depict (Catuneanu, 2006, and references therein). It's widely accepted, as an example, that bell-shaped bodies topped by a coal layer - with API lowest value referable to sand deposits - represent channelized deposits, or better channel-fills of a meandering drainage system within a floodplain, with the coal representing the avulsion event (figure 3.6).

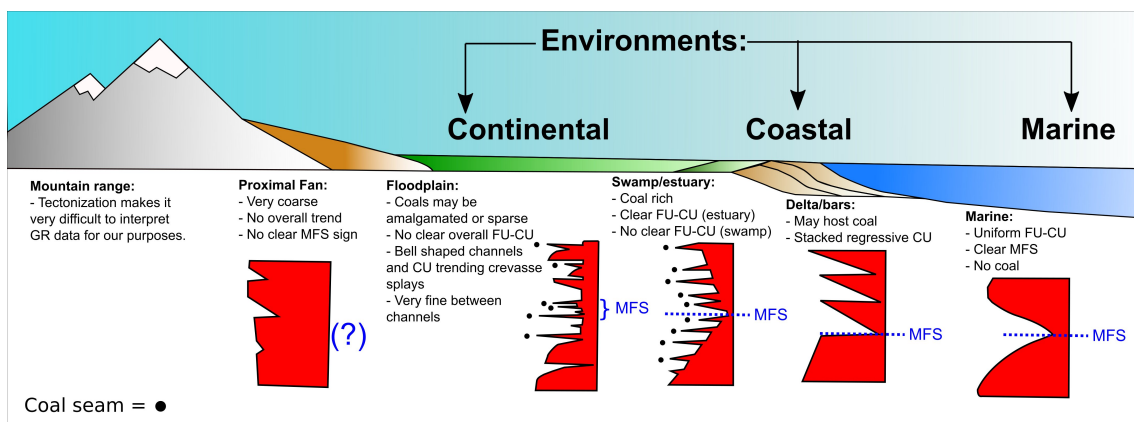


Figure 3.7: Schematic representation of the diagnostic gamma ray patterns found on a typical source to sink transect (SW-NE oriented sections) in west-central Alberta within a single T-R cycle. These patterns are indicative, real-life scenarios are far more complex, refer to figure 3.8 for more realistic examples. The main diagnostic features are reported above the correspondent example. In the source area, the identification of the MFS becomes very difficult and in certain cases infeasible. That's where the gamma ray correlations were stopped on the western border of the study area.

Another example: a series of high frequency and stacked CU shapes, in the context of the study area, represent the progradation of a fine-sediment upward-coarsening coastal body, or better the superimposition of deltaic lobes during a progradational phase (figure 3.7). Moving towards the sediment sources, from that deltaic system, the most probable environment to infer is the alluvial plain; it's easily recognized as the shapes of the well-organized FU-CU marine-dominated cycles turn into aggrading finer sequences (floodplain), interrupted by bell-shaped channelized bodies and coal (channel-fills). Moving in the same direction but coming from a beach instead of a delta (i.e. from a block-shaped, metric sandy body in the previous well log), the possible environments are alluvial plain typical ones or swamps. In case the same marine well-organized trends appear again (similarly to prior of the beach well log), the interpretation may then be concerning a promontory of the coast and

the operator then should look for a beach in the next well logs. Intuitively, basinwards (east) of the coastal environments, it's probable to find marine deposits, to note the lack of coal layers and to observe a more pronounced regularity of FU-CU trends, also between distant well logs (for schematic representations of all the environments in west-central Alberta refer to figures 3.7 and 3.8).

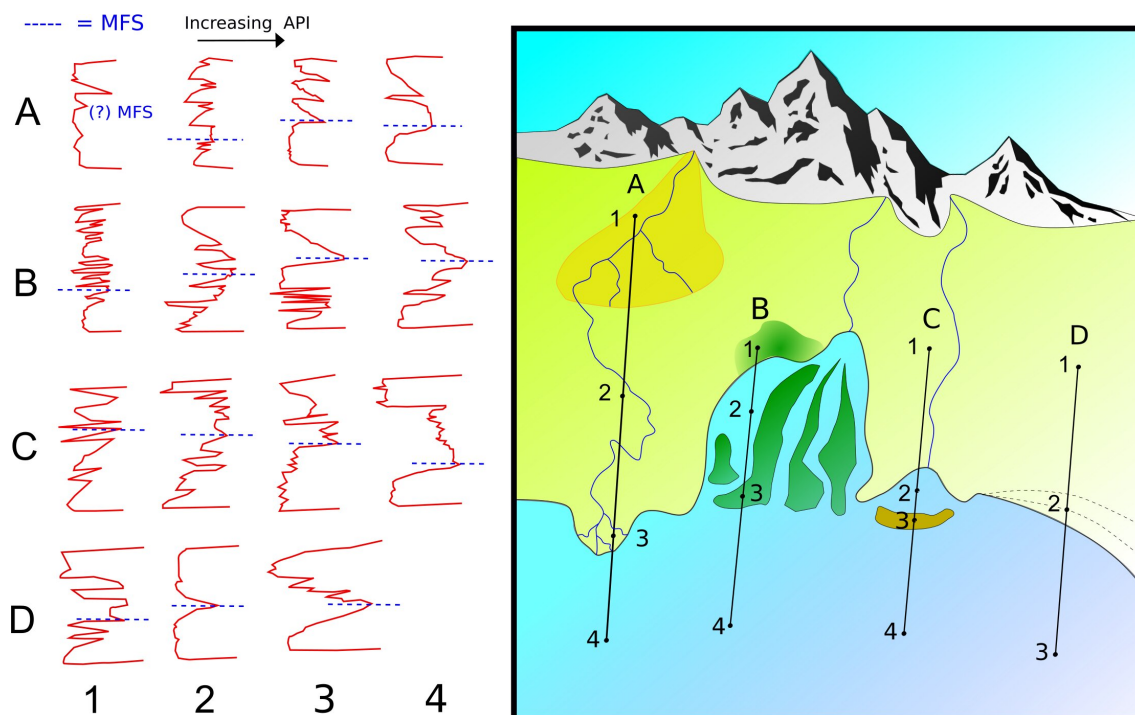


Figure 3.8: Indicative representation of possible diagnostic gamma ray features related to the paleoenvironments of west-central Alberta within a single T-R cycle. The points represent the paleoenvironmental context in which the relative T-R cycle developed. The different signature of the MFS changes relatively to the different contexts. Note the difference between FU-CU cycles moving inland from marine settings, and how they turn into aggrading floodplain sequences, punctuated by channel-fills (see figure 3.6) and coal layers. A1: proximal fan; A2: floodplain; A3: delta; A4: marine in front of a delta; B1: swamp; B2: estuary; B3: estuary bar; B4: outer estuary; C1: floodplain; C2: lagoon; C3: barrier island; C4: marine; D1: floodplain; D2: beach; D3: open marine. See paragraph 4.5.2 for real examples of correlated well logs.

The intervals traced in this study are related to T-R cycles already recognized in literature. These T-R cycles represent pivotal moments of the basin, during which environments shifted in response to higher rank events, marking changes in the balance between the sedimentation driving forces of eustasy, tectonics and climate (able to force relative sea level oscillations and variations of sediment fluxes). In this study, the bases, the MFSs and the tops of the two marine T-R cycles of Bearpaw Fm. were traced laterally into the inferred correlative continental deposits, in order to build time-correlative surfaces based on the lateral expected facies transitions.

Indeed, to trace the base of a FU (or the top of a CU) is equivalent to trace the time during which the triggering event for that granulometric shift started to be recorded by sedimentation. Thus the turning point between a FU and a CU represents another event in the T-R cycle in response of which sediment supply to that point of the basin started to become coarser, inverting the trend. When the top of the CU sequence is reached and there is an abrupt shift to finer sediments (higher API) along with a different sediment stacking style, the T-R cycle was considered closed. A different style of deposition represents a shift in the balance of the sedimentation driving factors and this major, basin-wide-spread shift can only occur because of tectonic, eustatic or climatic triggers.

Chapter 4

Results

4.1 Sea level referred surfaces

The first result of the data processing scripts described in chapter 3 are the sea level-referred Digital Elevation Models (DEMs) of each correlated surface.

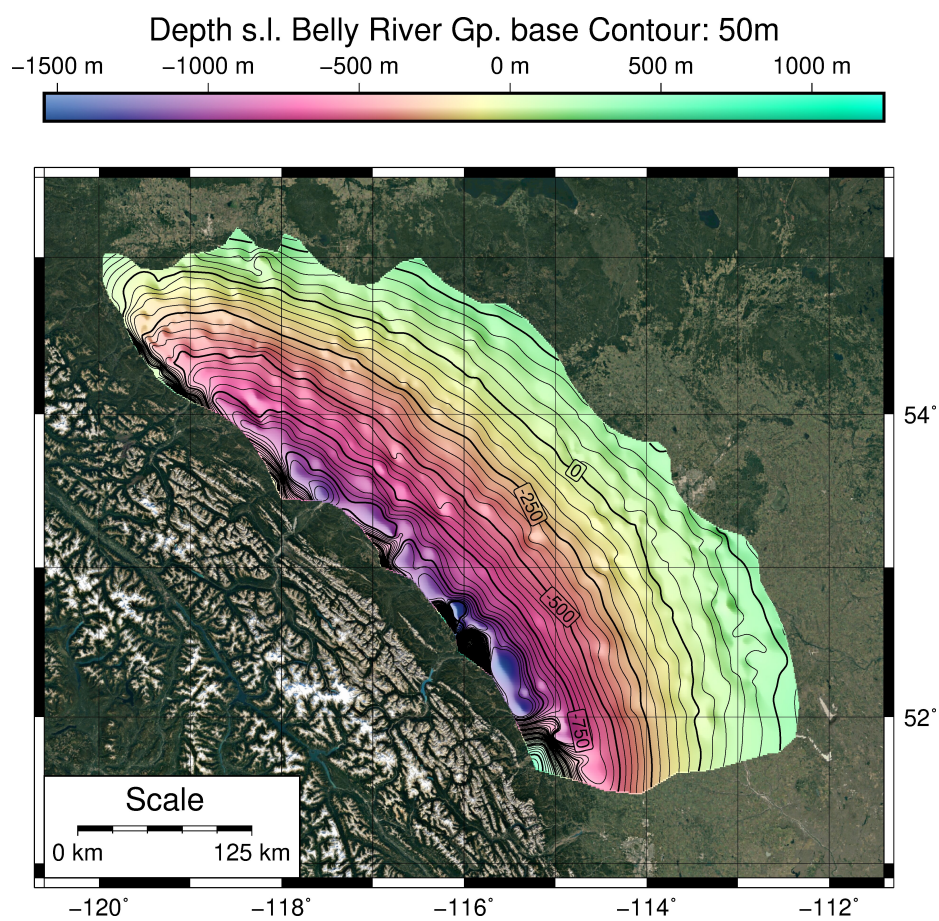


Figure 4.1: Belly River Group base (datum) DEM referred to sea level.

4.1. SEA LEVEL REFERRED SURFACES

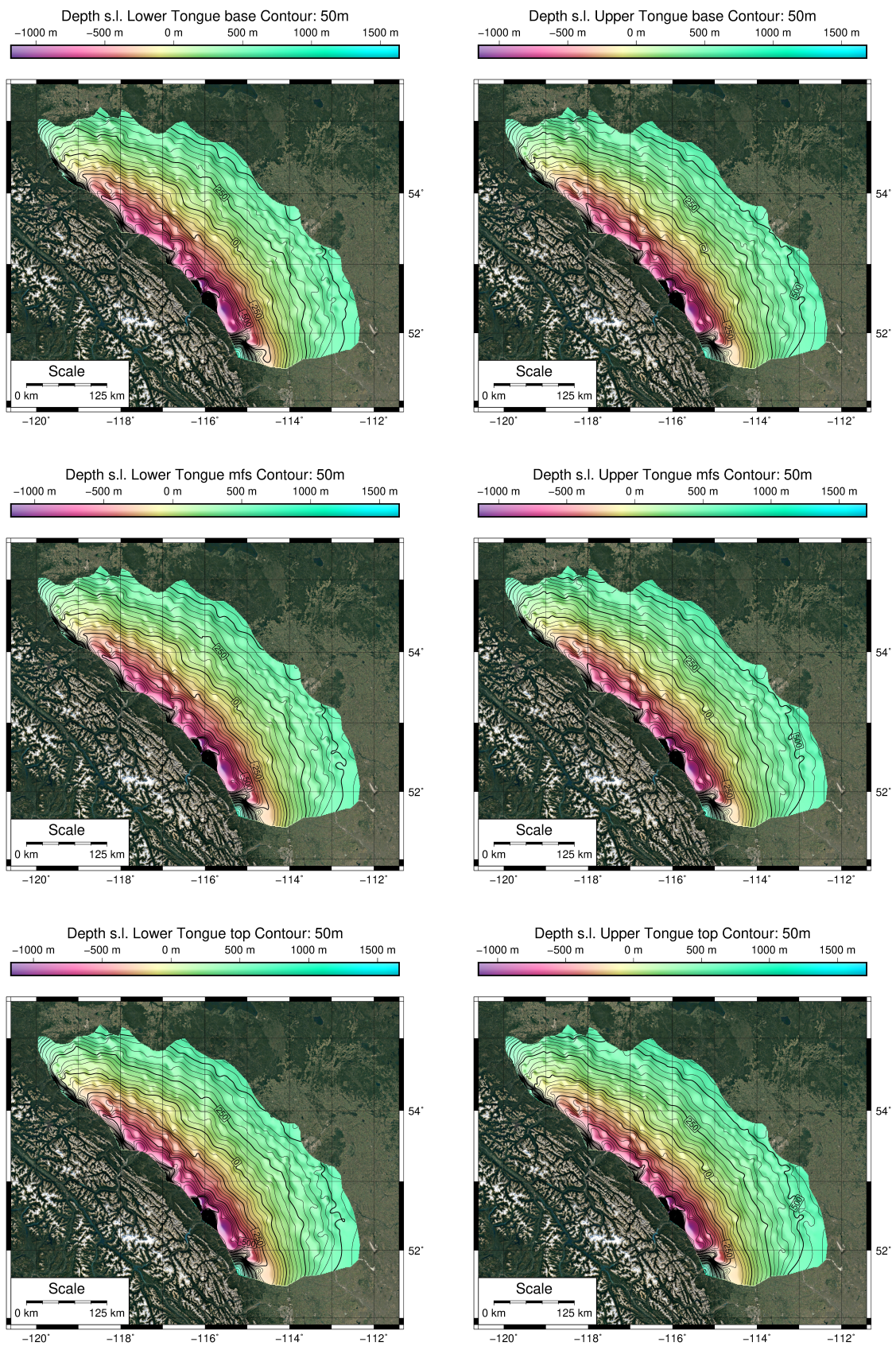


Figure 4.2: Correlated surfaces DEMs referred to sea level.

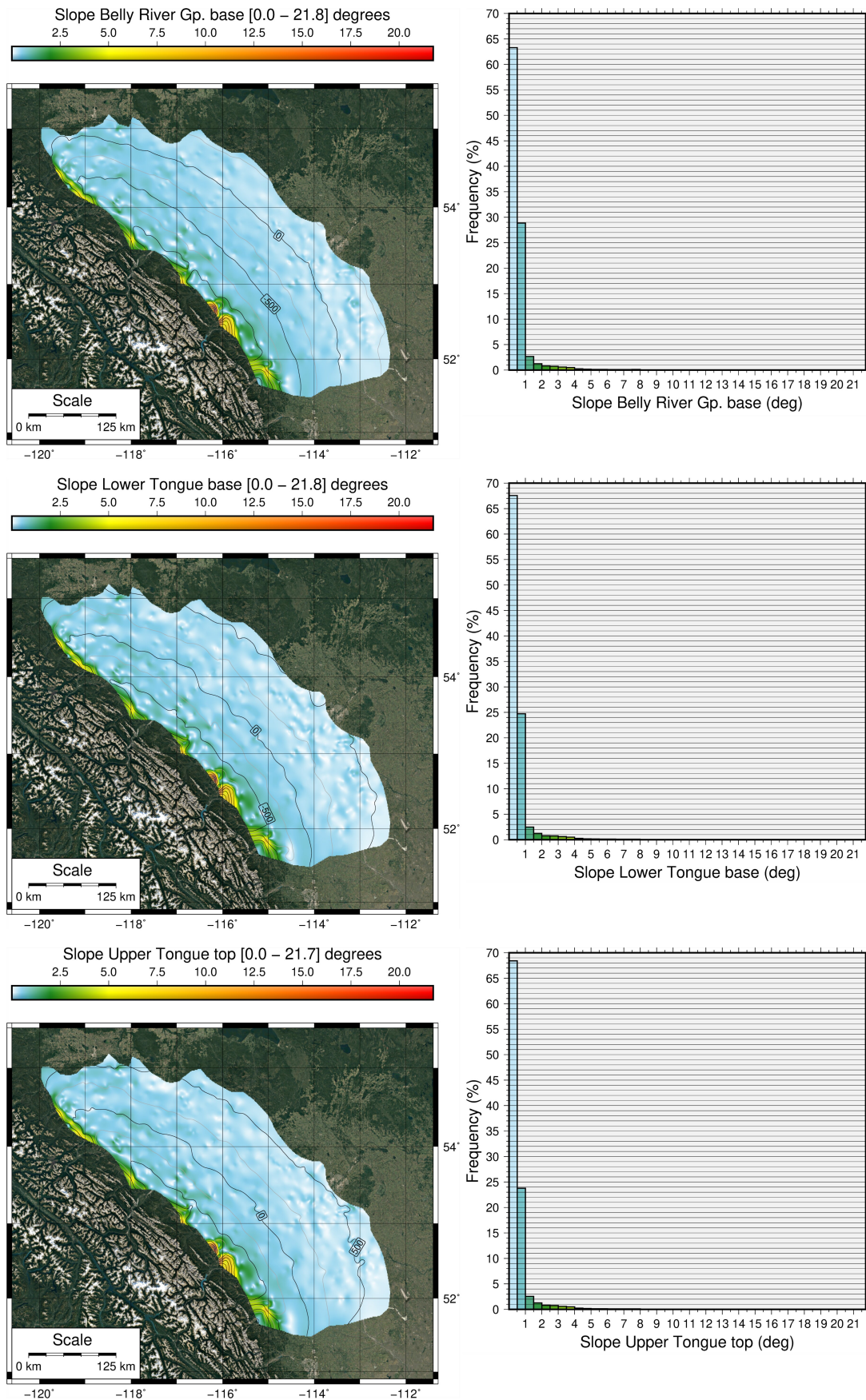


Figure 4.3: Slope map and histograms of slope degree frequency for the datum surface and for the base and top of the Bearpaw Formation.

The seven obtained DEMs (figure 4.1 and 4.2) develop parallel (or sub-parallel) in the tridimensional space. Parallelism is also highlighted by the slope degrees maps and histogram distributions (figure 4.3), that show little to no variation between surfaces. Depths generally increase westward. Lower slope values in the eastern study area steadily increase moving toward the foothills area with a bowl-like geometry. The average westward dip is between 0° and 1° (over 90% of the study area) but under the foothills the dip reverse to the east (forming a syncline geometry) on a roughly 30 km wide band that develops with a NW-SE orientation (figure 4.3) on the whole western border of the study area. The degrees of eastward dip within that band are consistently higher than values of westward dip outside it and range between 1° and 10°, with peak values over 20°. The eastward-facing slopes are not homogeneously distributed within that 30 km band. The higher values are grouped and localized in spots that geographically correspond to modern super-imposed river valleys of the Canadian Rocky Mountains in Alberta. Steeper areas on the south-western border often correspond to major tectonic lineaments of the Rocky Mountain deformation front such as the Pedley and the Ancona thrusts (Lee et Al., 2018; Pană and Van Der Pluijm, 2015, and references therein). These tectonic elements form triangle zones (cross-section geometries) right where data records the peak (steeper) slope values. The correspondence of slope degree with major faults was not observed in the northern study area.

4.2 Isopachs distribution and volumes of sediment

Given the overall flatness of the study area, thickness distribution models were derived from simple pixel-based subtractions of subsequent DEMs. In case of more pronounced inclinations of the correlated surfaces, a pixel-based subtraction will result in overestimated thicknesses and thus should be corrected with simple trigonometry in order to compensate for the dip angle:

$$THICKNESS_{true} = THICKNESS_{measured} * \sin(90 - DIP_{degrees})$$

Given the decametric sequence studied, this error accounts on average for less than millimetric overestimations. Considering a dip angle of 1° (which is only reached in about 25% of the study area), the overestimation accounts for 0.0002% and is thus negligible (0.4 mm over an interval of 20 m) being way beyond the vertical resolution of the dataset (1 m). Nonetheless, in very small portions of the foothills area, peak dip values (around 20° in the triangle zones) produced localized overestimations of roughly 6%, which imply an error of 1.2 m on an interval of 20 m. Given the very

small area interested by these dip values (less than 1% of the study area presents dip angles between 1° and 22° , see figure 4.3 and the relative discussion in the last paragraph 4.1), these overestimated thicknesses were considered negligible too.

Thickness distribution patterns and sediment volume vary considerably among the six considered intervals but all of the Bearpaw-time deposits seem to have undergone the influence of the underlying geometries of the Belly River Group. For that reason what follows comprehend a presentation of the main trends and results about the Belly River interval, as well as every studied interval concerning the Bearpaw succession.

4.2.1 Belly River interval

This interval spans from the base of the Belly River Group (datum surface) to the base of the Bearpaw Fm. (figure 4.4).

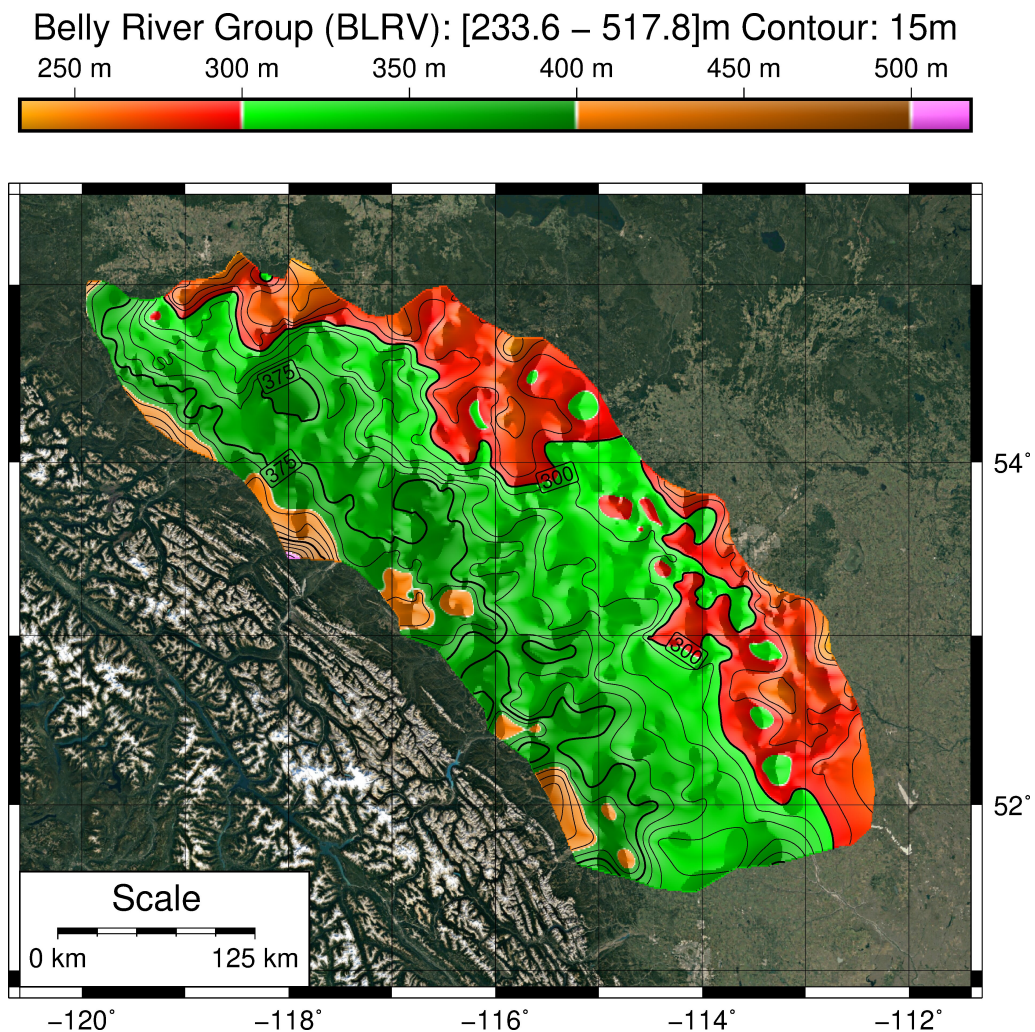


Figure 4.4: Belly River Group thickness 3D model.

The Belly River interval contains deposits accumulated between roughly 80 Myr ago up to 74.3 Myr (almost 6 Myr) and include an overall sediments volume of 32196 km³. The distribution patterns and the thicknesses of deposits highlight a clear eastward direction of sediments flows coming from the west, as deposits are thicker under the foothills and get progressively thinner toward the east. It is possible to operate a subdivision of the study area into three roughly NW-SE oriented sectors (reported in brown, green and red in figure 4.4) which correspond to proximal, middle and distal deposits of the basin and respectively to highest (>400 m), medium (300-400 m) and lowest (<300 m) sediment accumulation. The proximal deposits record the highest accumulation, conformed in steep (relatively to the rest of the study area) fan-like deposits, radially distributed from localized areas on the western border that often correspond to modern river valleys. The middle area (green in figure 4.4) records a rapid shift to almost flat deposits, highlighted by the greater distance between isopachs. The eastern border of the middle area is characterized by two large lobate (in plan view) shapes and several smaller ones which have a more pronounced cuspidate geometry than the former ones. The northern large deposit has a more regular lobate morphology, presents internal steeper geometries and is also bordered by a steeper slope. The second large body is located in the central study area (Edmonton latitude), is the largest one and shows an irregular morphology, with borders that protrude within the distal deposits area through narrow and elongated shapes. The middle area (green in figure 4.4) include the flattest internal surfaces. Every geometry found in the west corresponds to - or is aligned (and points) toward - one of the lobate or cuspidate geometries found on the border between the middle and the distal area, suggesting that the sediment flows direction was aligned from the western geometries toward the east into this lobate or cuspidate geometries. The distal area (red in figure 4.4) records thinner deposits that become gradually thicker toward to the its border with the middle area (the green area in figure 4.4). Deposits get generally thinner towards the east in the whole study area. Slopes are steeper than the slopes found within the middle area but not as steep as in the proximal area. The distal (eastern) area is punctuated by several dome-shaped or elongated deposit thicker than 300 m.

4.2.2 T1 interval

This interval spans from the base of the Bearpaw Fm. (74.3 Myr) to the MFS of the lower tongue (74.1 Myr; for a comprehensive lithostratigraphy and chronostratigraphic chart of the Bearpaw succession refer to respectively figures 2 and 5 of the published article reported in paragraph 4.6). During T1, 565 km³ of sediment accu-

culated in 200 kyr, average thickness is 6 m. The distribution of isopachs generally shows that thicker deposits occur mainly in the northern study area. Deposits are organized in patches of irregular shape, often bordered by steep slopes.

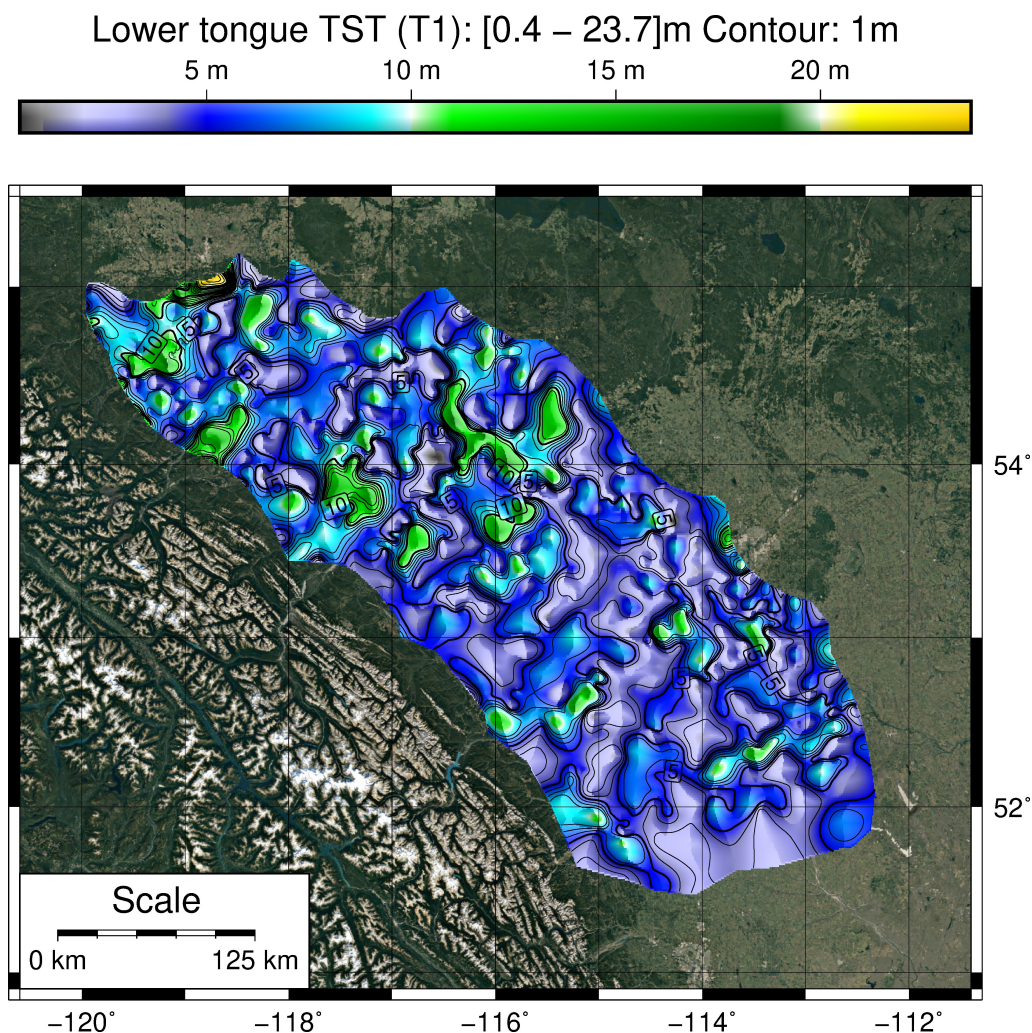


Figure 4.5: Lower Bearpaw tongue TST and correlative deposits thickness 3D model (T1 interval).

Deposits thinner than 5 m cover 41% of the study area and are mainly organized in large, widely interconnected and irregularly shaped patches, larger southwards than northwards. Deposits between 5 and 10 m cover 53% of the study area and thicker bodies are often interconnected and elongated SW-NE or NW-SE. The remaining 6% of the study area is covered by deposits thicker than 10 m; the peak accumulation is reached in the Grande Prairie region and measure up to almost 24 m. The thicker deposits on the western study area correspond to modern river valleys of the Canadian Rocky Mountains. It is also worth noting that large and interconnected areas with minimum values of sediment accumulation ($<5\text{m}$) expands

also to the north of Edmonton.

4.2.3 R1 interval

This interval spans from the MFS of the Bearpaw Fm. lower tongue to its top (including correlative deposits, figure 4.6). Sediments volume accumulated during R1 is 700 km³, average thickness is 7 m. Isopachs distribution records an increase in sediment accumulation that, compared to T1, interested the central study area more than the northern sector. The thicker deposits of T1 in the northwestern study area continued to be fed, as thick bodies are present in the same location, but new deposits of comparable thickness also occur in the central sector, especially on the western border of the study area.

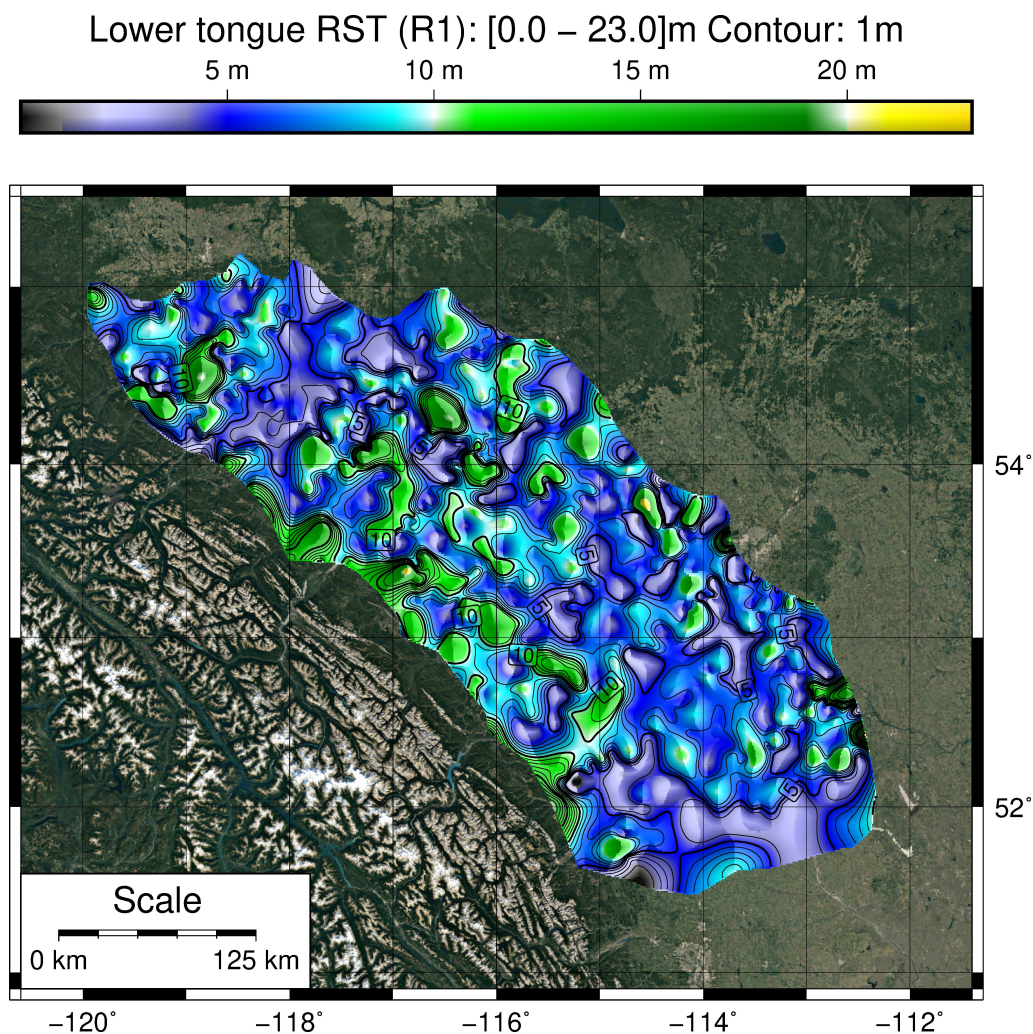


Figure 4.6: Lower Bearpaw tongue RST and correlative deposits thickness 3D model (R1 interval).

Deposits over 10 m cover 10% of the study area and are often bordered by steep

slopes (closer isopachs with respect to the surroundings) and are poorly interconnected. Thicker deposits on the western border of the study area geographically coincide with modern river valleys (figure 4.6) and show a pronounced fan-like geometry bordered by steep slopes. Deposits between 5 and 10 m interconnect all of the zones of thicker accumulation ($>5\text{m}$) and cover 68% of the study area. Deposits under 5 m cover 20% of the study area and are distributed in smaller areas with respect to T1. The low-accumulation ($<5\text{m}$) zones are also poorly interconnected and mainly localized in the northern and southern sectors. Only small and disconnected areas of low accumulation appear in the central sector.

4.2.4 S interval

The S interval spans from the top of the Bearpaw Fm. lower tongue to the base of the upper tongue and comprehends most of the Strathmore Member deposits (basal

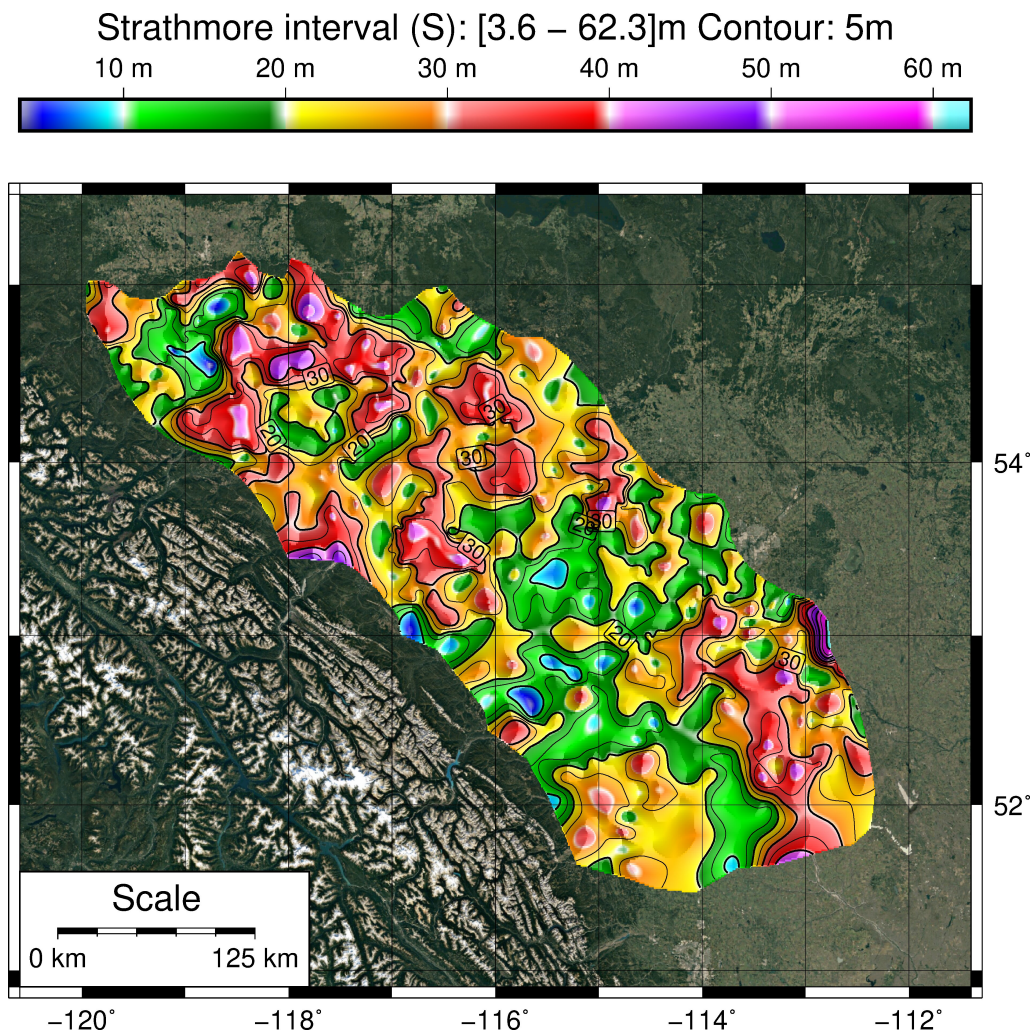


Figure 4.7: Central Strathmore Member and correlative deposits thickness 3D model (S interval).

Horseshoe Canyon Fm.). This interval includes the thicker deposits of the Bearpaw succession with peaks of accumulation well over 50 m, a total volume of 2365 km³ and an average thickness of 24 m. The sediment volume involved is almost twice the volume of the entire Bearpaw Fm. lower tongue (increment of 87% with respect to the sum T1+R1). The northern and central sectors of the study area record thick (>20 m) deposits localized in close - if not coincident - positions relative to R1. From the western border of the study area thick deposits can be followed until the eastern border. The main difference in sediment distribution patterns, relatively to the underlying intervals, is in the southern study area where thick deposits accumulated under the foothills area and even thicker deposits accumulated between the southeastern border and Edmonton. Thicker deposits over 30 m cover 22% of the study area and deposits between 20 and 30 m cover 49%. Thinner (<20m) deposits thus cover the 29% of the study area and are distributed in two main areas, the first one is located to the southwest of Grande Prairie (north-westernmost region) and the second one (the largest) interest the central-southern study area. That larger southern zone of low sediment accumulation is well interconnected to other smaller low-accumulation areas and separates the thicker southern deposits.

4.2.5 T2 interval

This interval spans from the base of the Bearpaw Fm. upper tongue to its MFS. Similarly to the T1 interval, the sediments volume involved in T2 is 579 km³ and the average thickness is 6 m. The base of this interval was dated 73.7 Myr (precise dates, uncertainties and references are reported in paragraph 2.7) and this means the upper tongue accumulation spans for 600 kyr thus roughly half of the time of deposition of the entire Bearpaw succession.

Although total sediment accumulation is comparable to T1 (only 2% higher), sediment distribution patterns changed considerably. Thicker deposits (>10m) cover 5% of the study area and accumulated mainly in the central and southern sectors toward the western border of the study area. In the northern sectors, nonetheless, small and isolated areas host deposits slightly over 10 m thick. These deposits accumulated over and in front of the northern, lobate geometry observed on the Belly River interval isopach map (4.4).

Low accumulation areas (<5 m) covered by thin deposits accounts for 34% of the surface. Large areas of thin deposits are located in the northern sector, but the largest are found in the southeastern study area, recording a remarkable decrease in sediment accumulation compared to the S interval. The remaining 61% of the study area is covered by deposits in the range 5-10 m, which are widely interconnected

and homogeneously distributed in the whole west-central Alberta, from the western to the eastern border of the studied region.

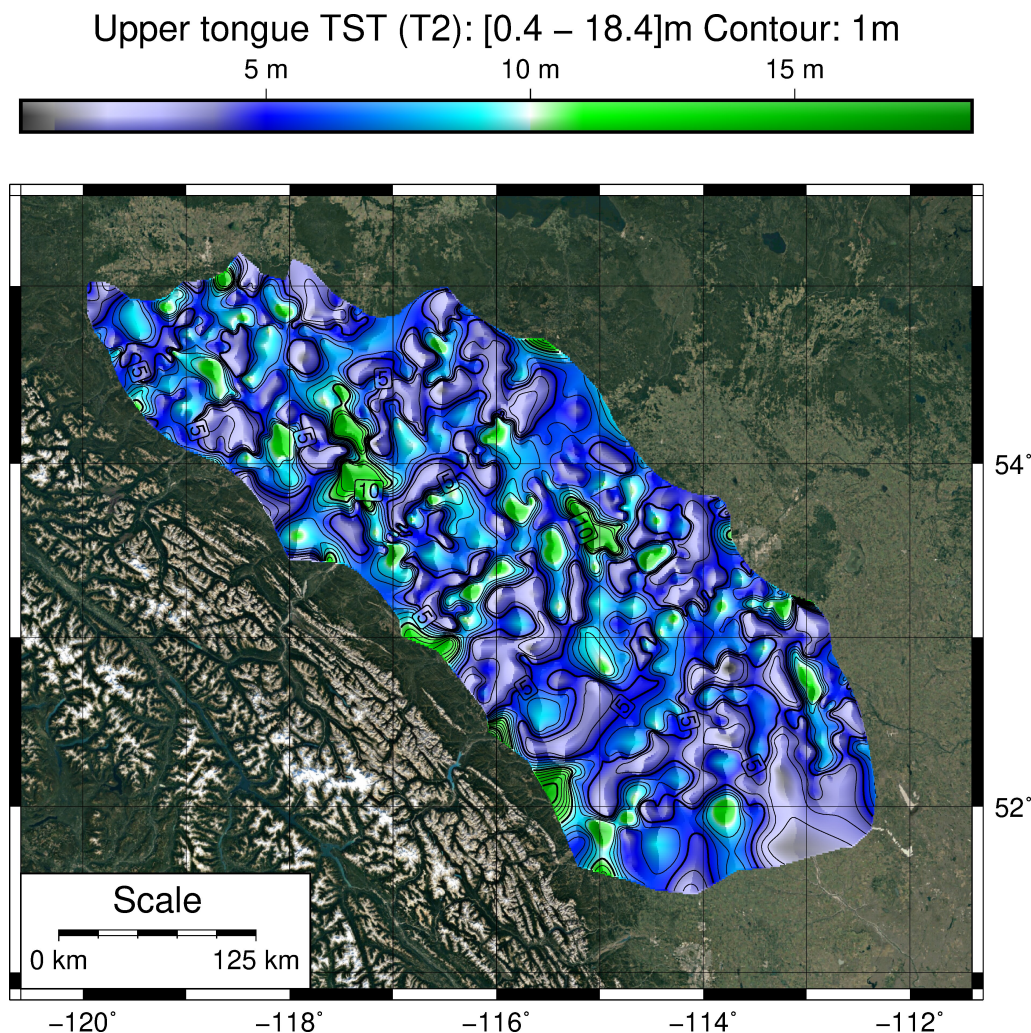


Figure 4.8: Upper Bearpaw tongue TST and correlative deposits thickness 3D model (T2 interval).

4.2.6 R2 interval

This interval spans from the MFS of the Bearpaw Fm. upper tongue to its top (the base of the Drumheller Member of the Horseshoe Canyon Fm.). The volume of sediment involved in R2 is 700 km^3 (1% higher than R1) and average thickness is 7 m. The R2 interval records a moderate increase sediment accumulation (21% more) with respect to T2 and an overall northward shift of main deposition. In fact, thicker deposits ($>10\text{m}$) accumulated mainly in the central-northern study area, focusing in the same positions as the main deposits of the S interval. The area covered by thick deposits is 12% and the patches tend to align on either SW-NE direction and, towards the east, also on a NW-SE direction.

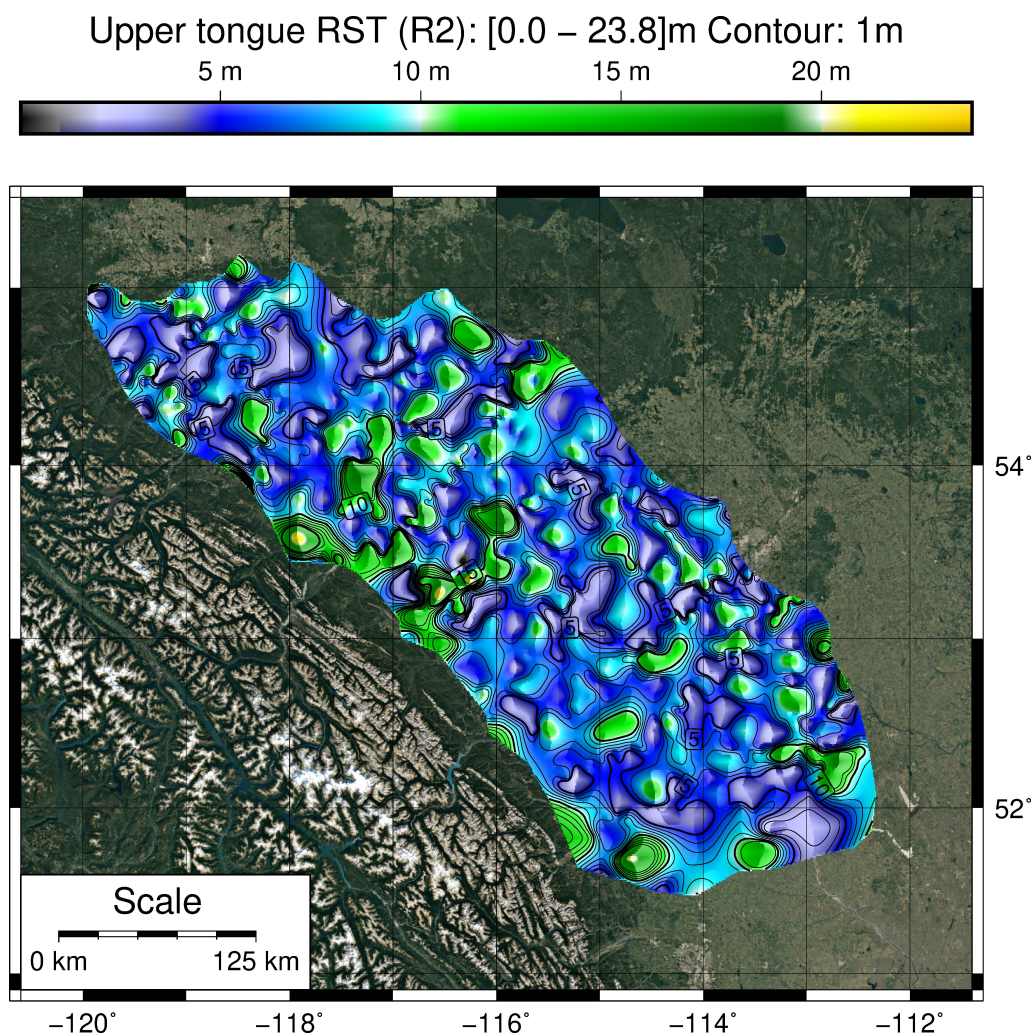


Figure 4.9: Upper Bearpaw tongue RST and correlative deposits thickness 3D model (R2 interval).

Deposits in the range 5-10 m cover 72% of the study area, patches in this range are completely interconnected and no clear alignment is found but the same one evidenced by thicker deposits (>10 m) which they surround. Thin deposits (<5m) cover 16% of the study area and, compared to the underlying intervals, the interconnection between them is lost and single, isolated patches cover smaller areas, mainly aligned and elongated on a SW-NE direction (basinwards).

4.3 Cumulative thickness distribution

4.3.1 From datum to the top of the Belly River Group

The palette used to color cumulative thickness intervals is set to assign the same color to the same thickness ranges, in order to visualize how these ranges shift

due to the accumulation of the Bearpaw succession over the starting surface, which is represented by the thickness of the Belly River Group (discussed in paragraph 4.2.1). Figure 4.10 represent the same thickness surface as 4.2.1, but with ranges represented with the cumulative thickness color palette.

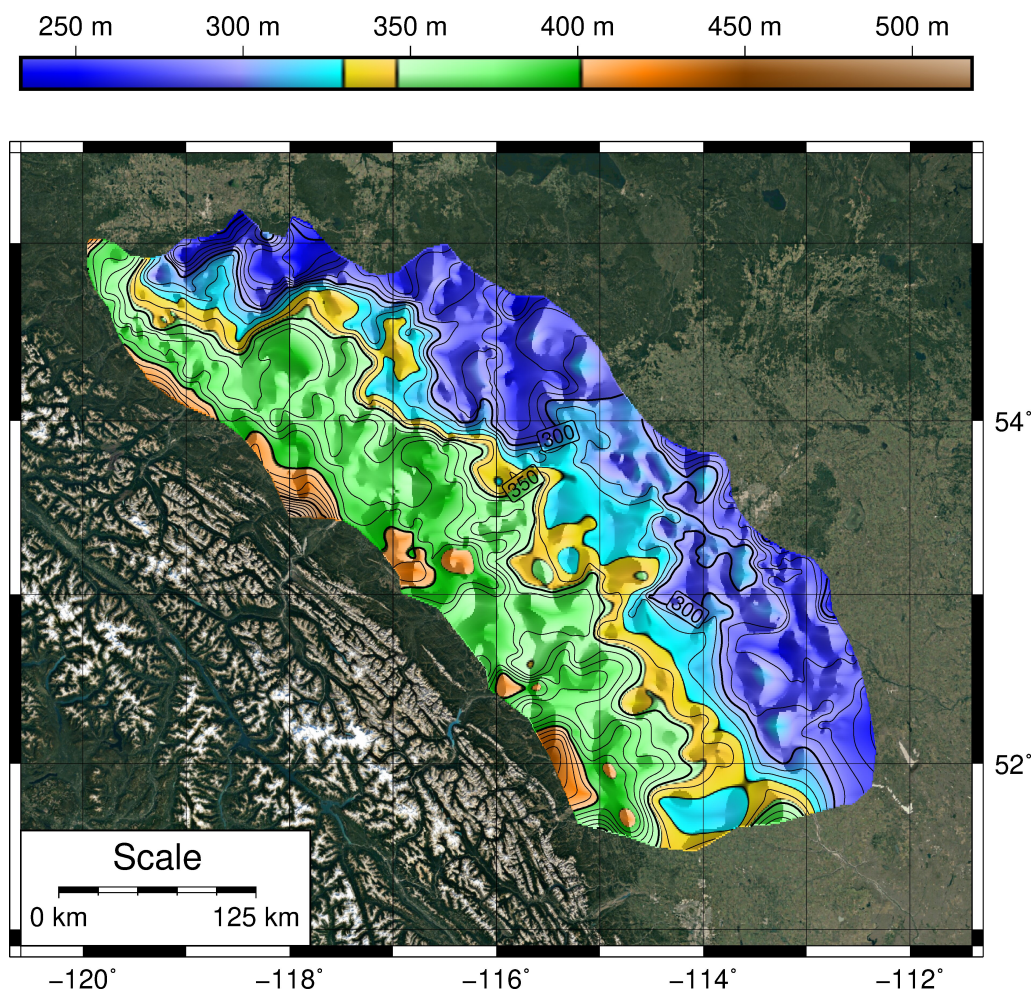


Figure 4.10: Belly River Group thickness 3D model (datum). This 3D model is equivalent to figure 4.4 but with different color palette which is the same used for every other cumulative thickness maps.

4.3.2 From datum to the top of T1

This interval represent the Transgressive Systems Tract (TST) of the lower Bearpaw tongue and equivalent deposits. The T1 interval accumulation distributed over the Belly River Group and equivalent deposits, almost draping the surface and only producing minor differences with respect to the underlying interval. The large lobe/fan-like geometries of the Belly River Group were preserved after T1 deposition and most of the accumulation in the northern sector produced slightly more

4.3. CUMULATIVE THICKNESS DISTRIBUTION

regular eastern slopes of these geometries. The number of smaller scale bays and promontories characterizing this cumulative thickness range (yellow range in figure 4.11) is reduced by T1 deposition.

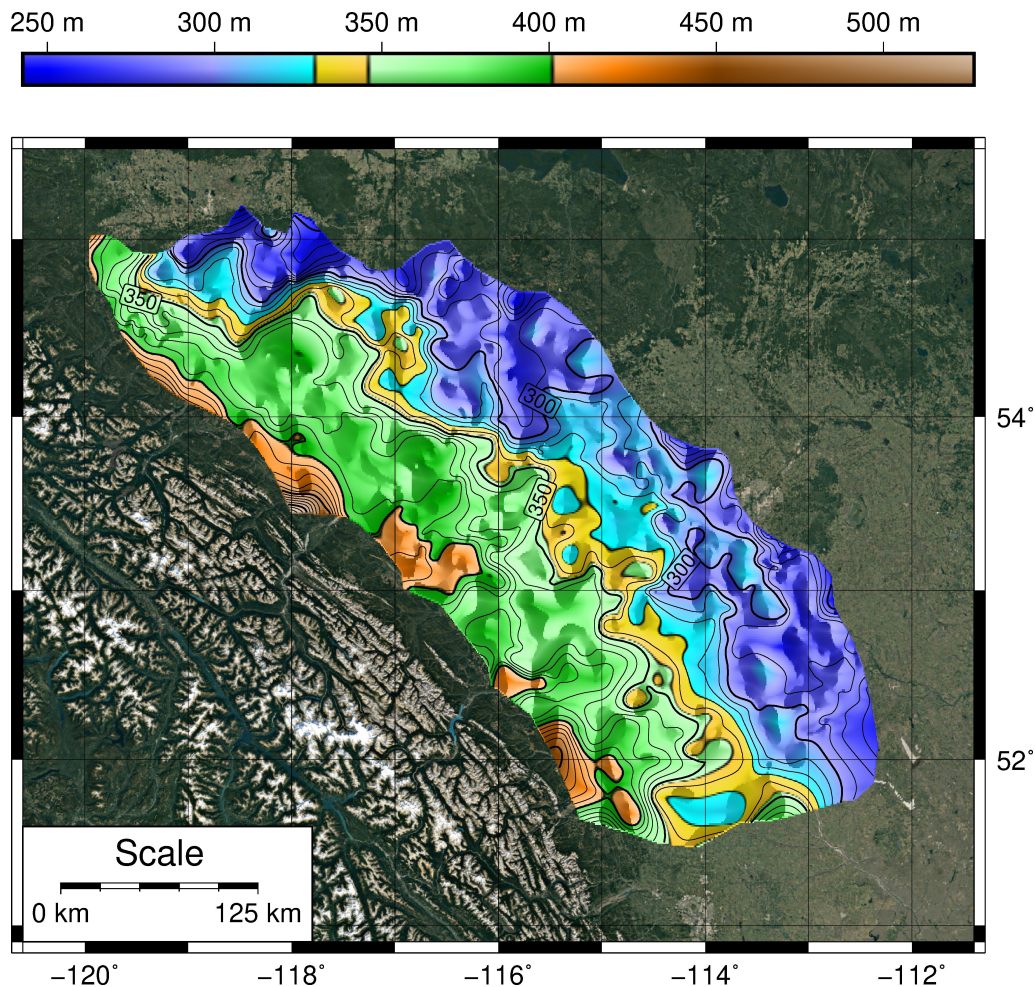


Figure 4.11: Cumulative thickness 3D model from the datum to the top of T1.

Major sedimentation of this interval happened in the foothills region, along the present day Smoky River. In the foothills region, near the present day deformation front, multiple areas of high accumulation produced an accretion of the proximal fan-like deposits located in correspondence of major modern river valleys. These areas are approximately located, from south to north, along the Tay and Panther Rivers, North Saskatchewan River and Athabasca River.

4.3.3 From datum to the top of R1

This interval represents the Regressive Systems Tract (RST) of the lower Bearpaw tongue and correlative non-marine basal beds of the Strathmore Member (Horseshoe

Canyon Fm.). The same depositional trends described in paragraph 4.3.2 continued during the deposition of R1, producing a more pronounced partitioning of the study area into southern, central and northern sectors. The cumulative thickness map of R1 (figure 4.12) shows an overall basinward shift of depositional systems, especially in the central foothills area, where proximal deposits (browns in figure 4.12) expanded significantly toward the east, maintaining their fan-like morphology and alignment with major, lobate geometries of the northern and central sectors. The northern sector records low accumulation in the distal area and thus minor, eastward progradation of the observed geometries. In the southern sector proximal deposits prograded eastward too, but less than in the central sector. An area of low accumulation is present south of Edmonton.

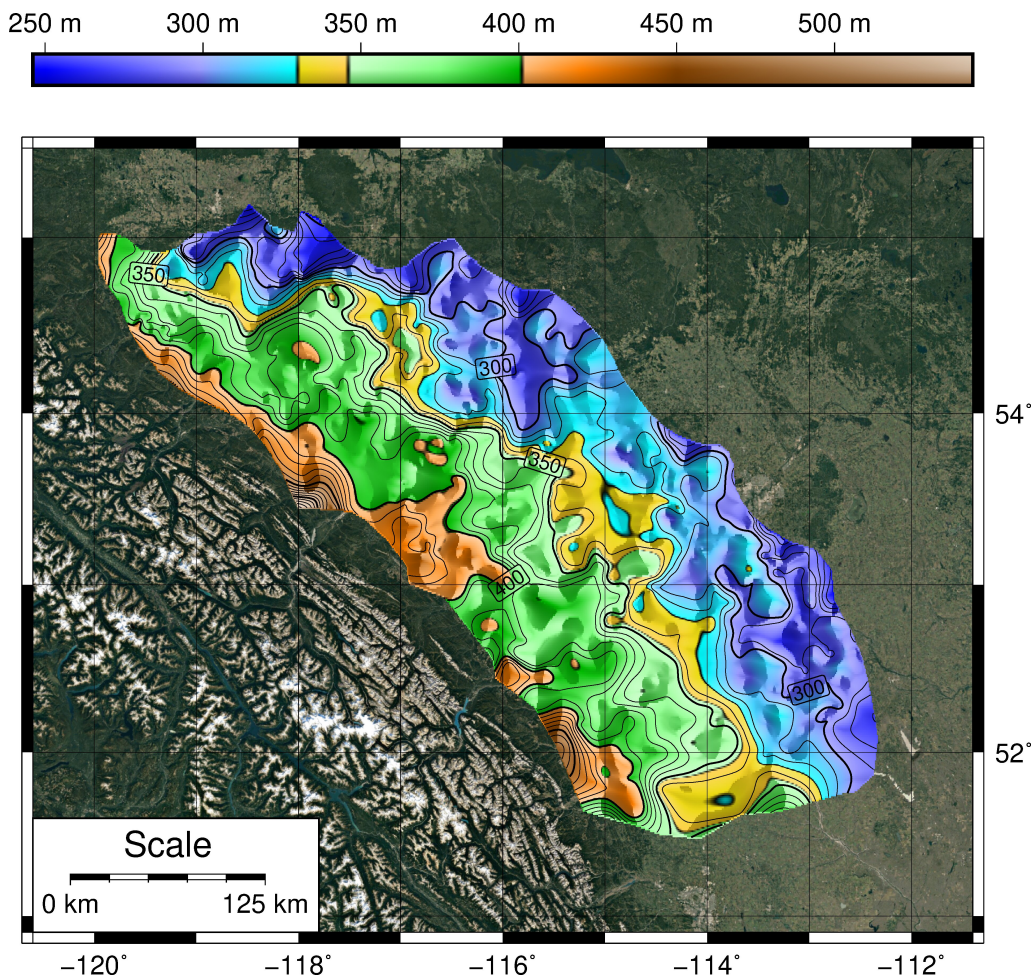


Figure 4.12: Cumulative thickness 3D model from the datum to the top of R1.

4.3.4 From datum to the top of S

The cumulative thickness maps show an overall major north-eastward progradation of depositional systems in the whole study area. The proximal deposits (browns in

4.3. CUMULATIVE THICKNESS DISTRIBUTION

figure 4.13) consistently extended eastward creating a band of high accumulation areas over the whole western border of the study area (covering up to about a third of the surface). Major accumulation is recorded in the central sector, particularly in front of the pedemontane fans of the Smoky, Athabasca and Brazeau Rivers, and south of the North Saskatchewan River. The northern sector, despite accumulation increments with respect to the previous interval, shows an area of relatively low accumulation southeast of the town of Grande Prairie.

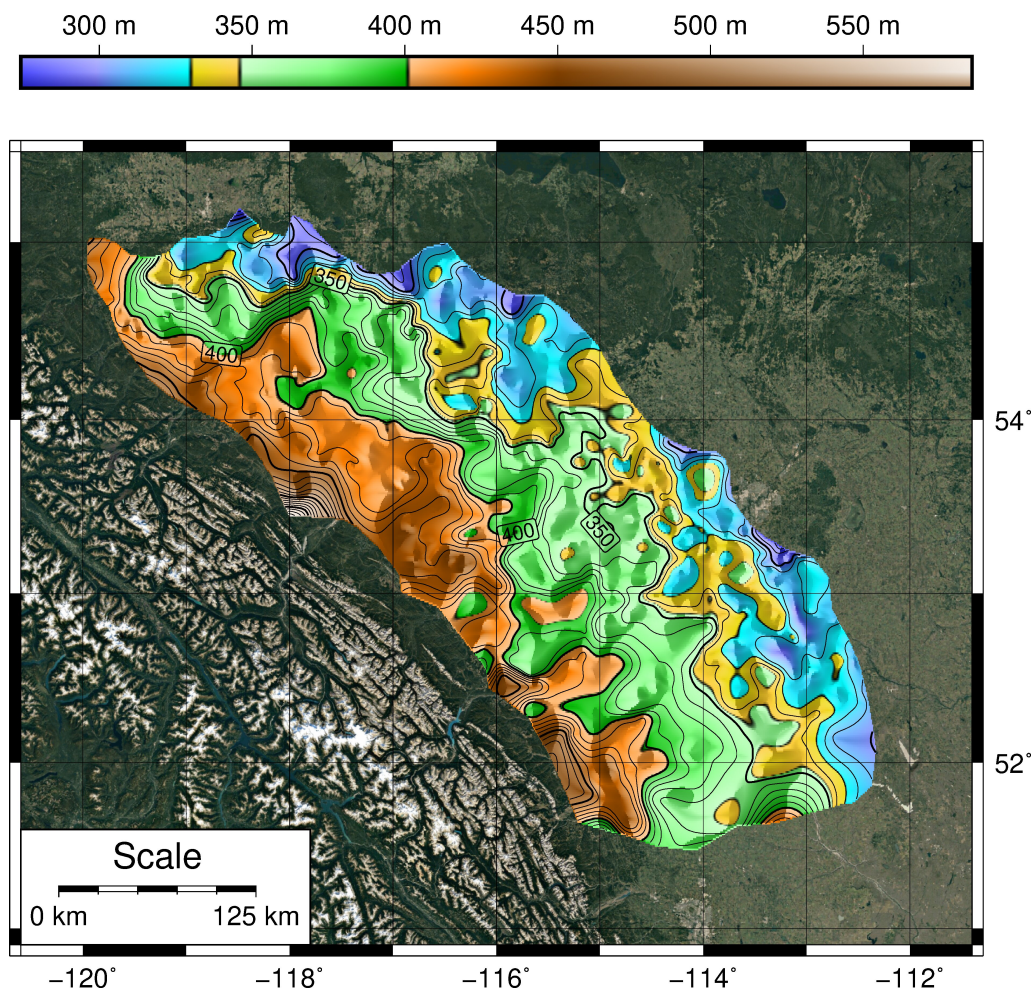


Figure 4.13: Cumulative thickness 3D model from the datum to the top of S.

The central sector recorded the major eastward expansion of high-accumulation areas, also reshaping previously discussed bays and promontories (yellows in figure 4.13) which advanced roughly 60 km east of the location reached during the R1 interval. The southern sector still records high accumulation in the western study area. To the east, around the 350 m isopach (between greens and yellows in figure 4.13) cuspidate geometries prograded eastward at longitudes where only lobate bodies were present during the previous intervals.

4.3.5 From datum to the top of T2

The T2 interval records a return to previous low depositional rate conditions. This transgressive interval likely lasted way longer than the previous one (T1, paragraph 4.3.2) as the Bearpaw upper tongue and correlative deposits accumulated between 73.1 and 73.7 Myr (totally 600 kyr, see paragraph 2.7 for a detailed report about datings of the studied succession).

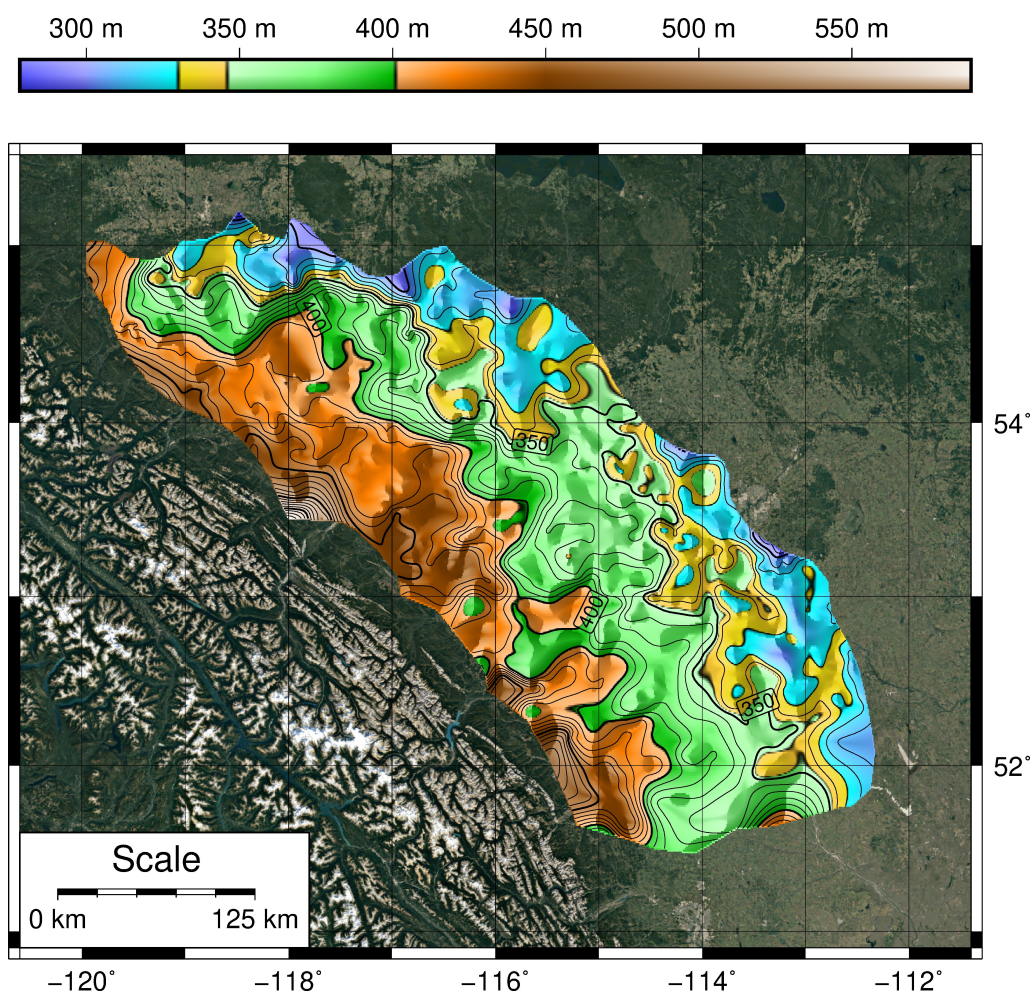


Figure 4.14: Cumulative thickness 3D model from the datum to the top of T2.

The northern area records little to no morphologic changes except for a single cuspidate system, located roughly 60 km south of Grande Prairie which advanced northward almost as much as the systems in the southern and central sectors advanced eastwards. The central portion of the map in figure 4.14, show eastward progradation predominantly occurred in the central study area although sediment fluxes continued to feed also the southern cuspidate geometries on the 350 m isopach that formed during the S interval, emphasizing their elongated shape toward E and

NE.

4.3.6 From datum to the top of R2

The R2 interval records an increase in sediment fluxes and a general continuation of the trends described in for T2.

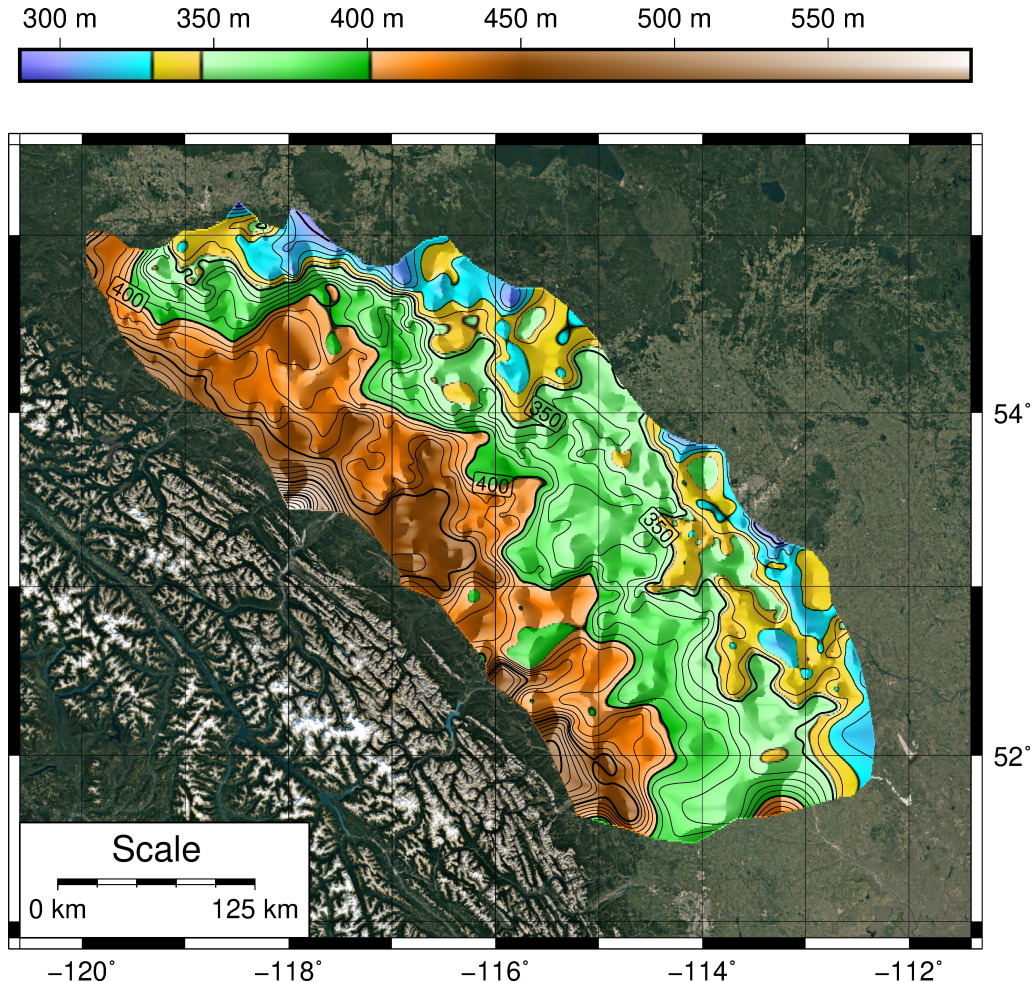


Figure 4.15: Cumulative thickness 3D model from the datum to the top of R2.

Areas of major accumulation (> 400 m, browns in figure 4.14) in the foothills region interested more than a third of the study area and in contrast, lower cumulative thicknesses (< 330 m, blues in figure 4.14) almost disappeared from the map due to eastward expansion of the central and southern geometries. Lower cumulative thicknesses in the northern sector surrounded the underfed, 100 km large, lobate geometry but a slight increase in sediment supply to that region is reported during the R2 interval. Low cumulative thickness is recorded also in the southern sector, in front of the cuspidate geometries. Generally, the arrangement in bays and promontories that was observed in previous intervals was flattened by the R2 deposition,

resulting in a more linear 330 m isopach (that divides yellow and blue in figure 4.15) although the 350 m isopach preserved the most evident promontories of the underlying interval, especially in the southern sector. In the northwestern region of the study area, the only deposit which received sediments during the R2 interval was the one located 60 km south of Grande Prairie (a northward protruding promontory drawn by the 350 m isopach). Most of this R2 sediment accumulated in front of this deposit and into the bay to the W of it (note the morphologic changes that the bay underwent during R2 with respect to the T2 cumulative thickness model in figure 4.14).

4.4 Rates of sedimentation

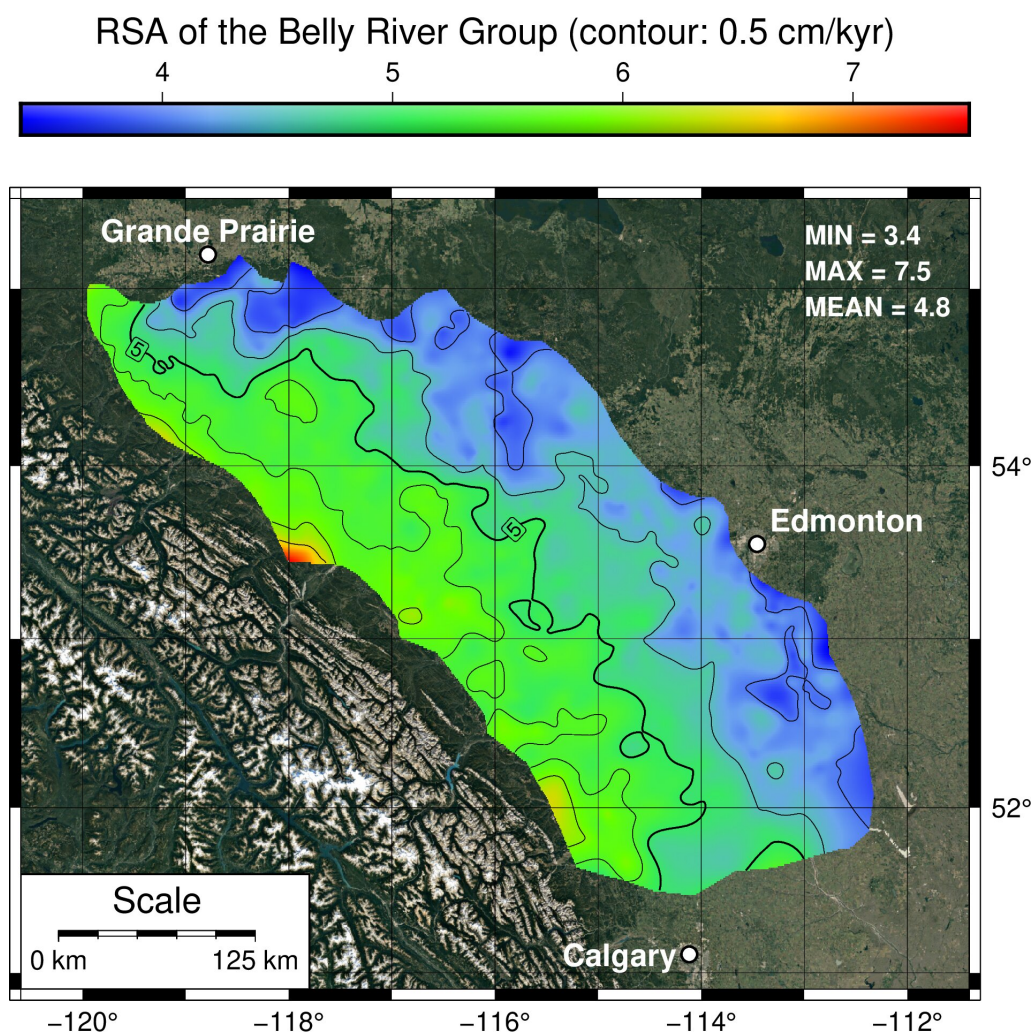


Figure 4.16: Rates of sediment accumulation of the Belly River Group (from datum to the base of the lower Bearpaw tongue).

4.4. RATES OF SEDIMENTATION

The most recent and accurate published radioisotopic datings for the studied successions are from [Eberth and Kamo \(2020\)](#). Based on their results (see paragraph [2.7](#)), the Bearpaw succession (from the base of the lower tongue to the top of the upper tongue) spans 1.2 ± 0.2 Myr. [Eberth and Kamo \(2020\)](#) also estimated rates of sediment accumulation (RSA) for the late Cretaceous of Alberta. According to their understanding, the RSA is consistent from the Dinosaur Park Fm. up to the Horseshoe Canyon Fm. (Bearpaw Fm. included) and measure 8.1 cm/kyr (196 m/2.425 Myr; [Eberth and Kamo, 2020](#)). As they pointed out in their work, 8.1 cm/kyr is a relatively high value compared to previously published estimations for southern Alberta Upper Cretaceous non-marine sequences (3.5-4.8 cm/kyr reported by [Eberth, 2005](#); [Lerbekmo et Al., 2005](#); [Lerbekmo and Braman, 2005](#)). In this study we used the published datings (provided in [2.7](#)) to estimate RSA within our stratigraphic intervals.

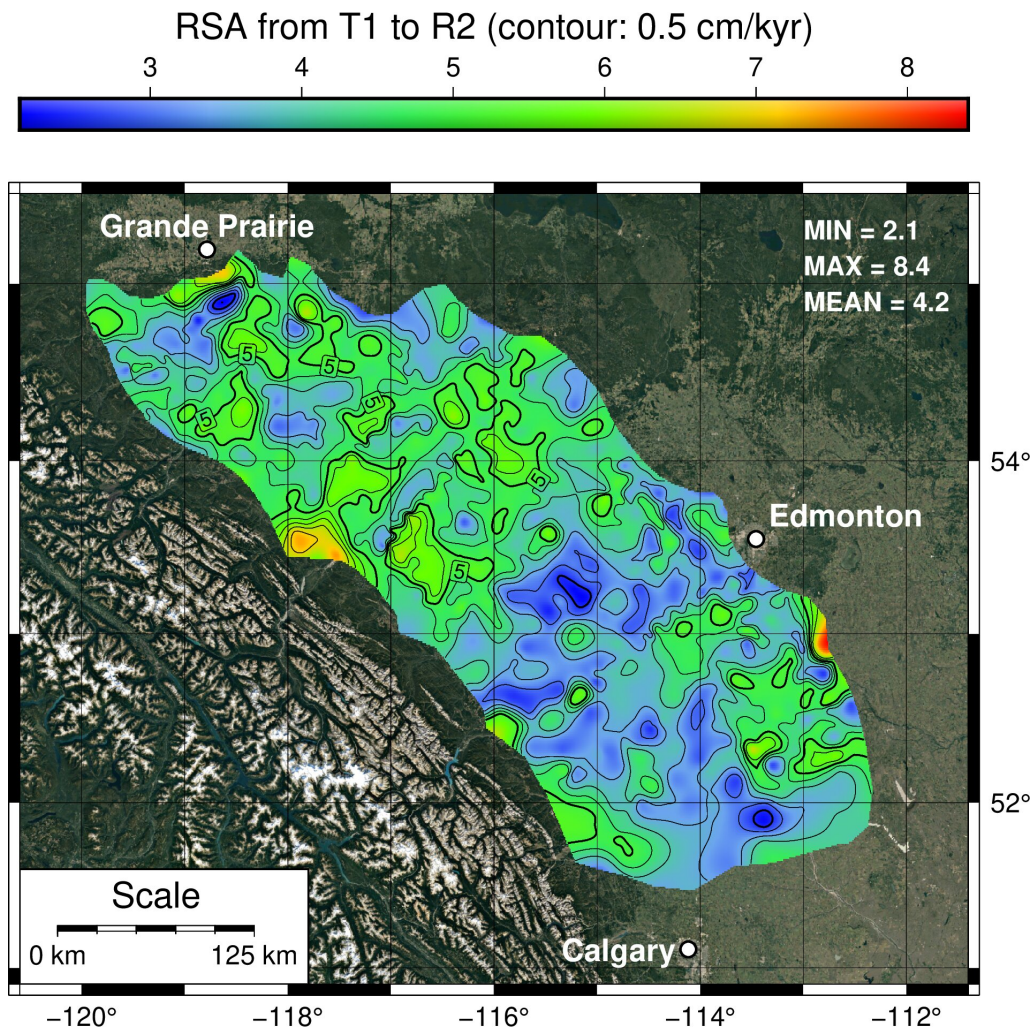


Figure 4.17: Rates of sediment accumulation of the Bearpaw succession (from the base of the lower to the top of the upper Bearpaw tongue).

By means of a simple GMT algorithm, the RSA was estimated pixel-by-pixel over the whole extension of the study area for every dated interval of the Bearpaw succession. In order to contextualize RSA variations during the Bearpaw time, the RSA was measured for the Belly River Group too (figure 4.16), between 80 Myr and 74.3 Myr (the base of the Bearpaw Fm.). The Belly River Group has a mean value of 4.8 cm/kyr, with a maximum of 7.5 cm/kyr. The minimum value is 3.4 cm/kyr and lower values are spread along the eastern study area, from the southern regions up to the Grande Prairie area. The eastward decreasing trend evidenced by RSA values distribution, was also noticed by [Jerzykiewicz \(1997\)](#) in cross sections that were used in this study as control points for well-logs correlations in the foothills area. RSA values were also measured for the entire Bearpaw succession (from T1 base to R2 top, figure 4.17) and spans from 2.1 cm/kyr to a maximum of 8.4 cm/kyr. The whole 1.2 Myr Bearpaw succession has an average thickness of 51 ± 8 m, thus the average RSA is 4.2 ± 0.7 cm/kyr. The highest depositional rates of the T1-R2 interval are recorded in the westernmost central study area (at the latitude of Edmonton) and in the southeastern study area roughly 100 km SE of Edmonton. Most of the peak values are due to the high accumulation during the S interval (>50 m thickness). The RSA records the higher values in the northern regions (between 4 and 6 cm/kyr) and the lower (under 4 cm/kyr) in the central and southwestern study area. It is worth nothing that even within the lower RSA to the SW, the foothills region still records above-average RSA located in front of modern river valleys.

Based on the datings of the lower Bearpaw tongue base (74.3 Myr; [Eberth and Kamo, 2020](#)), the lower tongue MFS (74.1 Myr; [Eberth, 2005](#)), the upper tongue base and upper tongue top (respectively 73.7 and 73.1 Myr; [Eberth and Kamo, 2020](#)), RSA values were measured for the lower tongue TST (T1 interval, figure 4.18), for the entire upper tongue (T2+R2 interval, figure 4.20), and for the interval between the lower tongue MFS and the upper tongue base (R1+S interval, figure 4.19). The T1 interval (74.3-74.1 Myr) shows the lowest RSA values of the entire Bearpaw succession, reaching a minimum of 0.2 cm/kyr; the low RSA zones cover most of the study area and are well interconnected in the central and southern regions. The mean thickness of this interval is around 6 m and thus the mean RSA value is 2.9 cm/kyr (figure 4.18). Between the T1 interval and the upper tongue, the R1+S interval (figure 4.19) records the highest RSA of the entire Bearpaw succession (and of the Belly River Group as well). During these 400kyr (between 74.1-73.7 Myr) the RSA peaked at 17.7 cm/kyr in the area southeast of Edmonton. High values around 15 cm/kyr are also present in the westernmost central study area. The whole northern region stayed well over 8 cm/yr for the entire interval, exception

4.4. RATES OF SEDIMENTATION

made for the lower values (under 3 cm/kyr) recorded only in the Grande Prairie region which changed significantly compared to the above-average RSA recorded during T1 and held this trend during the deposition of the upper tongue.

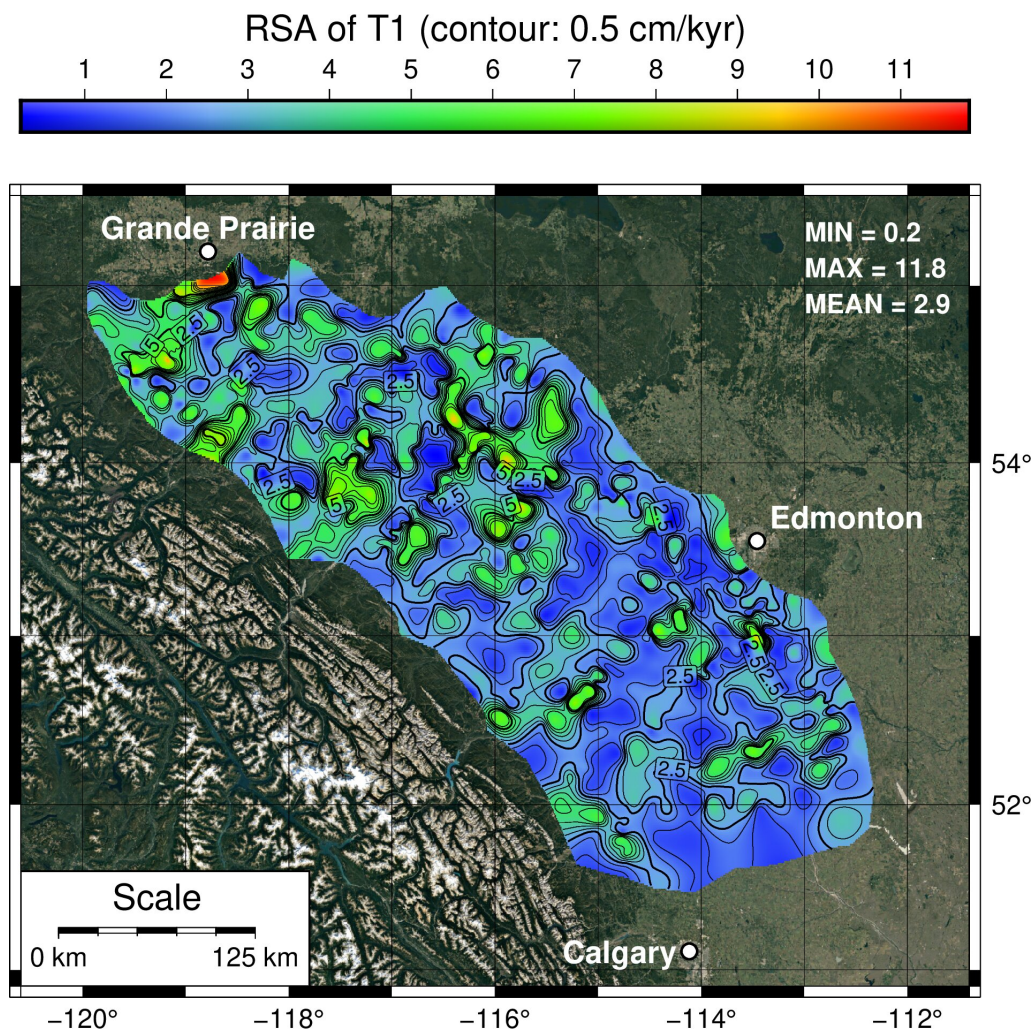


Figure 4.18: Rates of sediment accumulation of the T1 interval (lower Bearpaw tongue TST and correlative deposits).

The R1+S interval records the lowest rates (2.8 cm/kyr minimum and generally under 6 cm/kyr) in the central and south-western study area. The southeastern study area records high depositional rates (> 10 cm/kyr) comparable to those in the northern region. The mean value during this interval is 7.9 cm/kyr which is around +170% (+5 cm/ky) with respect to the other described intervals, and +65% with respect to the previous continental-deposition-dominated interval (Belly River Group). The upper Bearpaw tongue has a mean RSA value of 2.2 cm/kyr (T2+R2 intervals, figure 4.20), thus records a slight decrease with respect to the lower Bearpaw tongue. Most of the upper tongue, recorded values well over 2 cm/kyr, distributed in patches

spread over the whole study area. Higher values are aligned SW-NE in the central

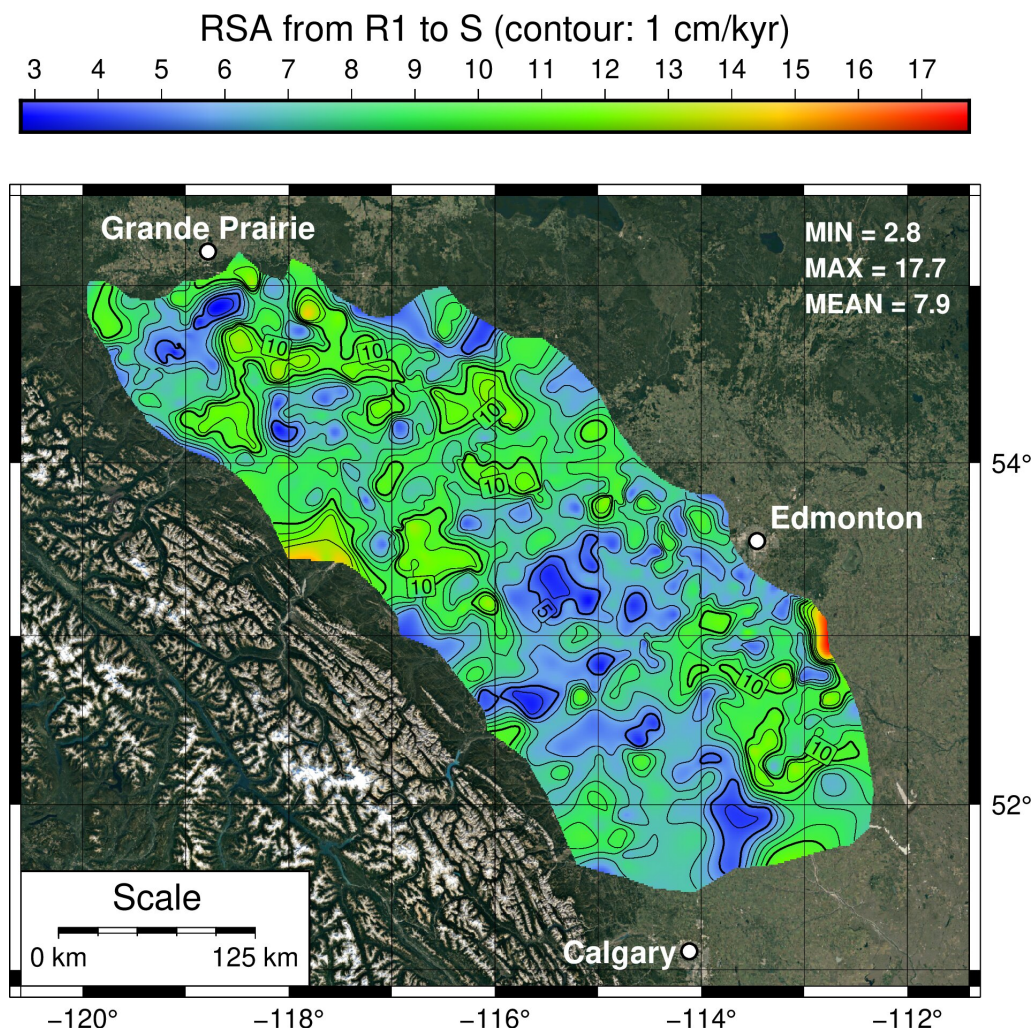


Figure 4.19: Rates of sediment accumulation of the R1+S interval (from the lower Bearpaw tongue MFS to the base of the upper Bearpaw tongue).

study area and RSA generally decreased toward the east. The RSA values distribution during the T2+R2 interval depict an overall deficiency of sediment in the study area, considering the longer timespan (600 kyr) with respect to the lower Bearpaw tongue. Most of the accumulation of the upper Bearpaw tongue happened in the central study area within river valleys.

Most of the sediment of the Bearpaw succession actually deposited rapidly during the S interval (roughly 400kyr, in figure 4.19). The S interval rapid increase in RSA is responsible for the increase of the mean depositional rates calculated from the base of the Belly River Group (80Myr) up to the top of the Bearpaw succession (73.1Myr) from 4.8 (during the Belly River interval) to 5.6 cm/kyr. The Bearpaw Fm. (thus excluding the S interval that belongs to the Horseshoe Canyon Fm.) in-

stead records the lowest value of the studied Campanian succession of west-central Alberta (under 3 cm/kyr), especially during the 600 kyr of deposition of the upper tongue (half of the Bearpaw time).

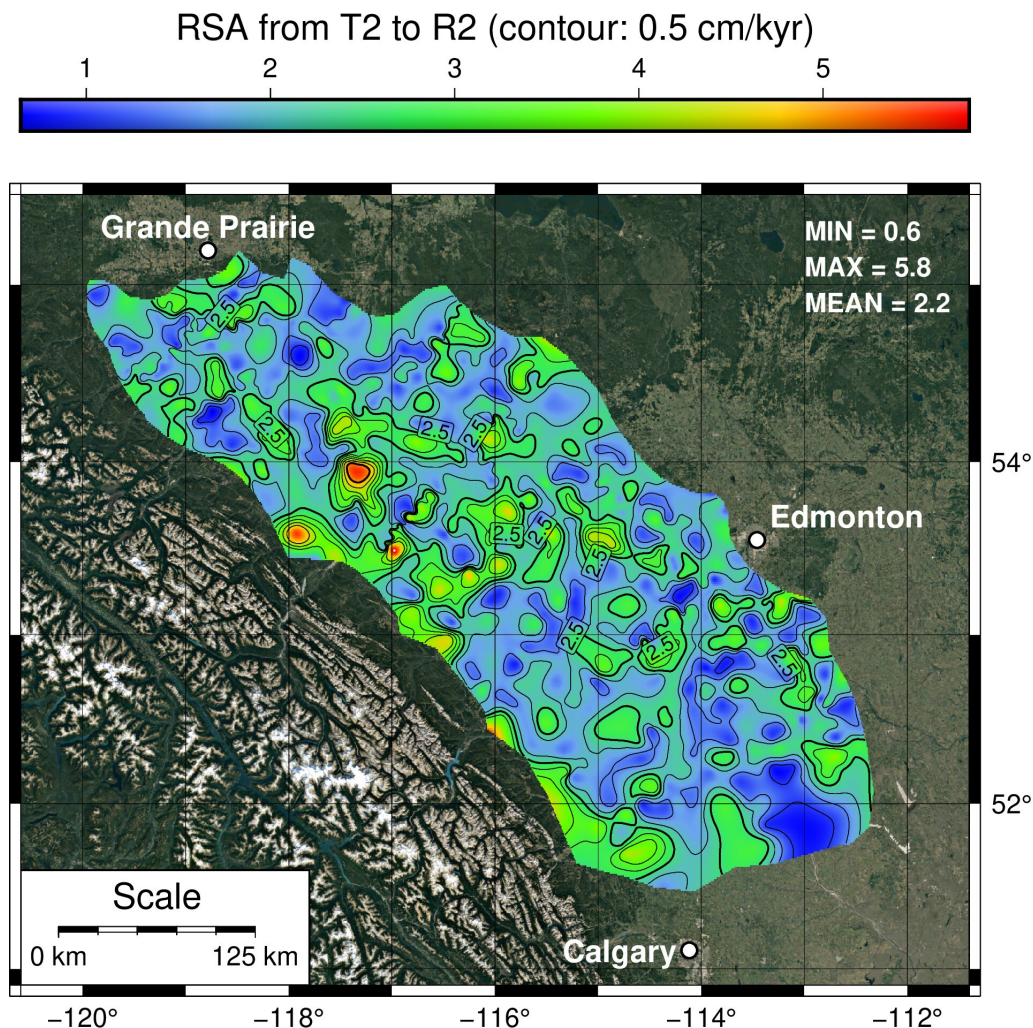


Figure 4.20: Rates of sediment accumulation of the T2+R2 interval (referred to the entire upper Bearpaw tongue and correlative deposits).

4.5 Cross sections

4.5.1 Cross sections with different datum

Eight cross sections represent the entire Bearpaw succession in the study area, six were oriented normally to the Rocky Mountains deformation front (SW-NE) and the remaining two were traced parallel to it (SE-NW). Therefore these sections do not create a regular grid of square meshes but instead shift slightly in orientation according to the curvature of the deformation front.

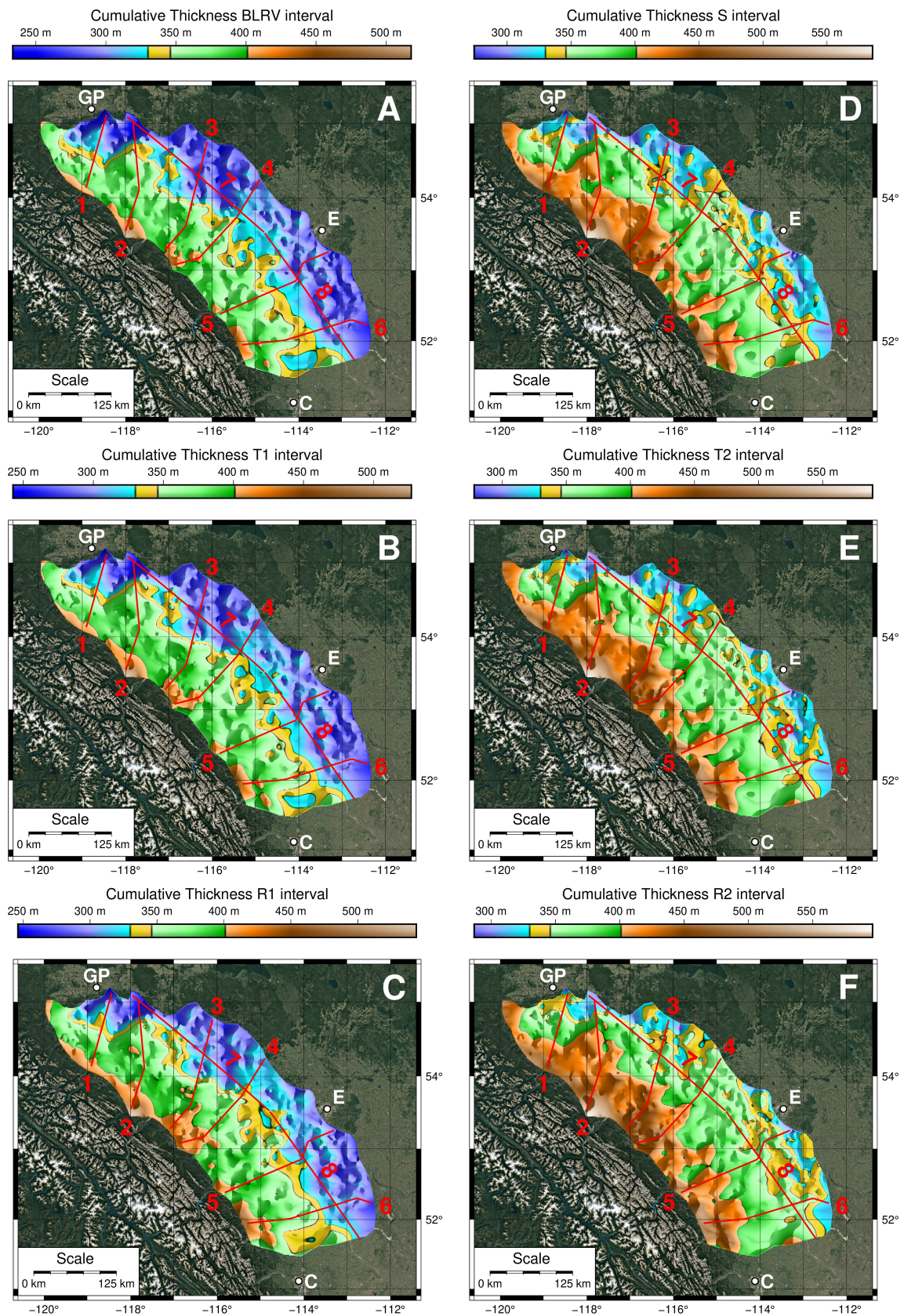


Figure 4.21: Location of section traces over cumulative thickness maps described in paragraph 4.3.

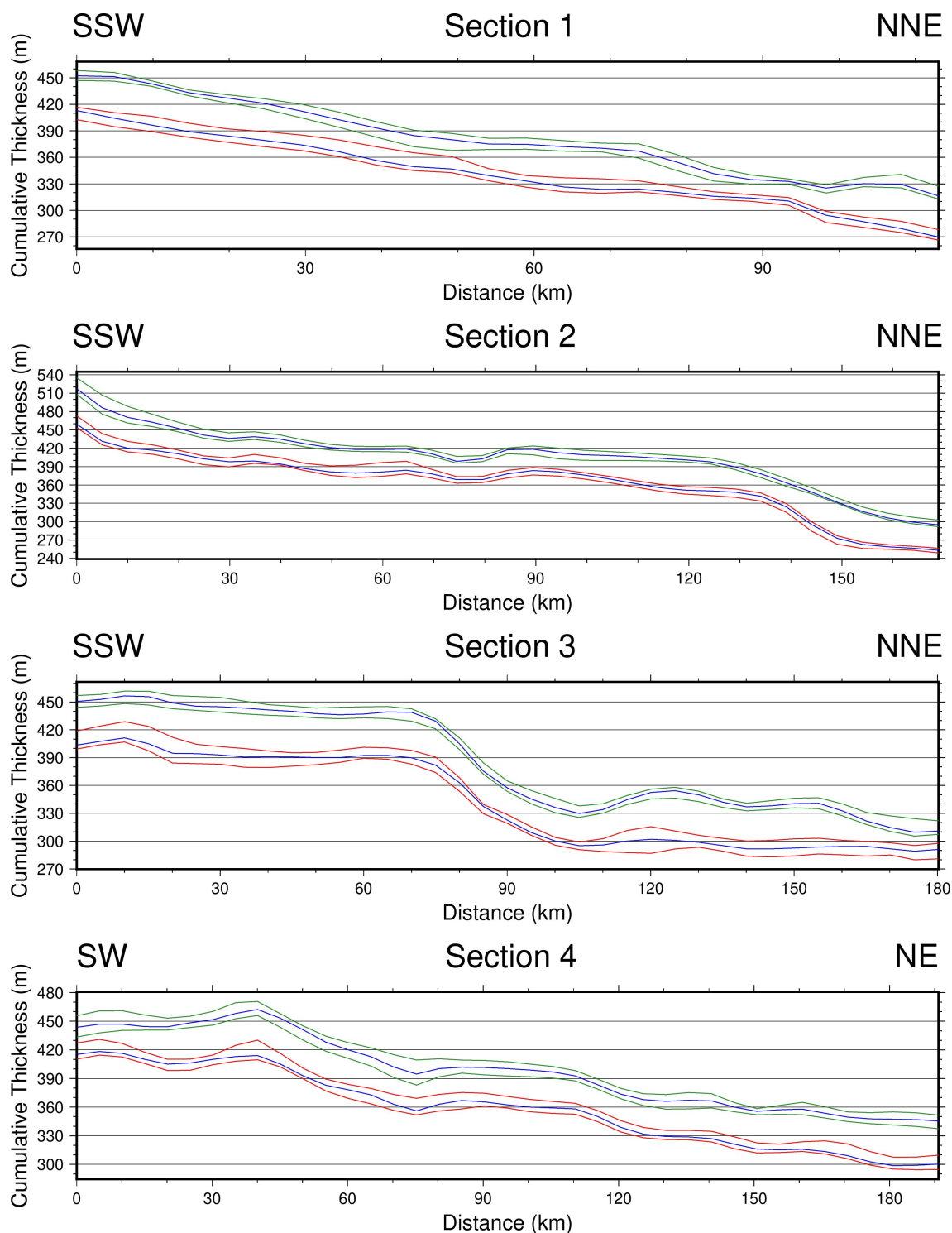


Figure 4.22: Cross-sections 1-4 over cumulative thickness 3D models. The datum is the Belly River Group base (zero Y axis value).

Some sections were not traced on a straight line in order to follow the evolution of the main geometries represented on cumulative maps. The location of all sections over cumulative thickness maps is reported in figure 4.21. The algorithm to plot cross sections over the desired tridimensional models made it possible to also change

the datum referring them to a specific user-defined surface. Each surface represented in figures 4.22 and 4.23 is referred to the main datum used in this study (the Belly River Group base value is thus the “zero” value of the Y axis).

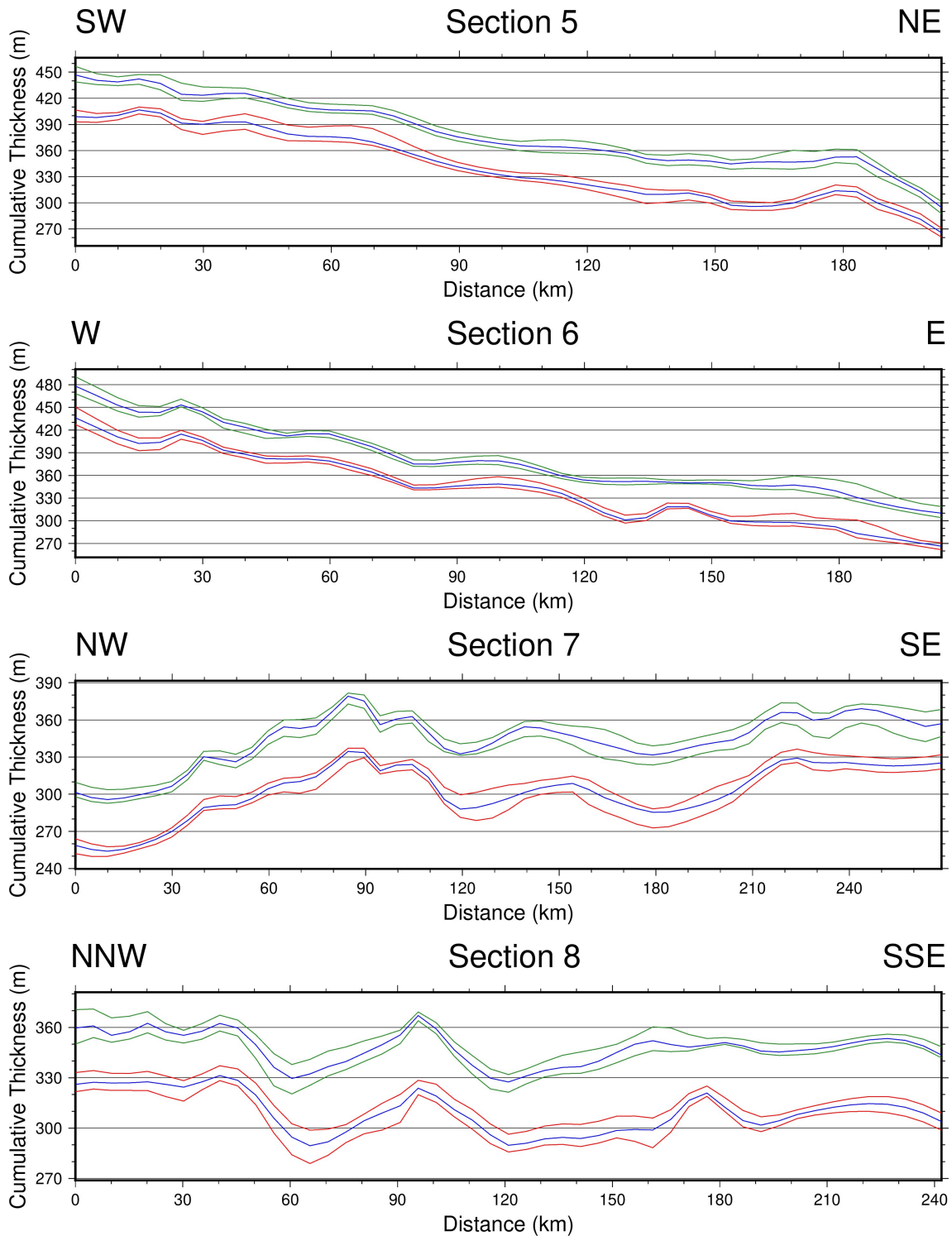


Figure 4.23: Cross-sections 5-8 over cumulative thickness 3D models. The datum is the Belly River Group base (zero Y axis value).

4.5. CROSS SECTIONS

Data in figures 4.24 and 4.25 instead represent the cumulative thickness referred to the upper tongue MFS, used as datum (“zero” Y value), negative thickness values are therefore intended under the upper MFS surface and positive values were assigned above it.

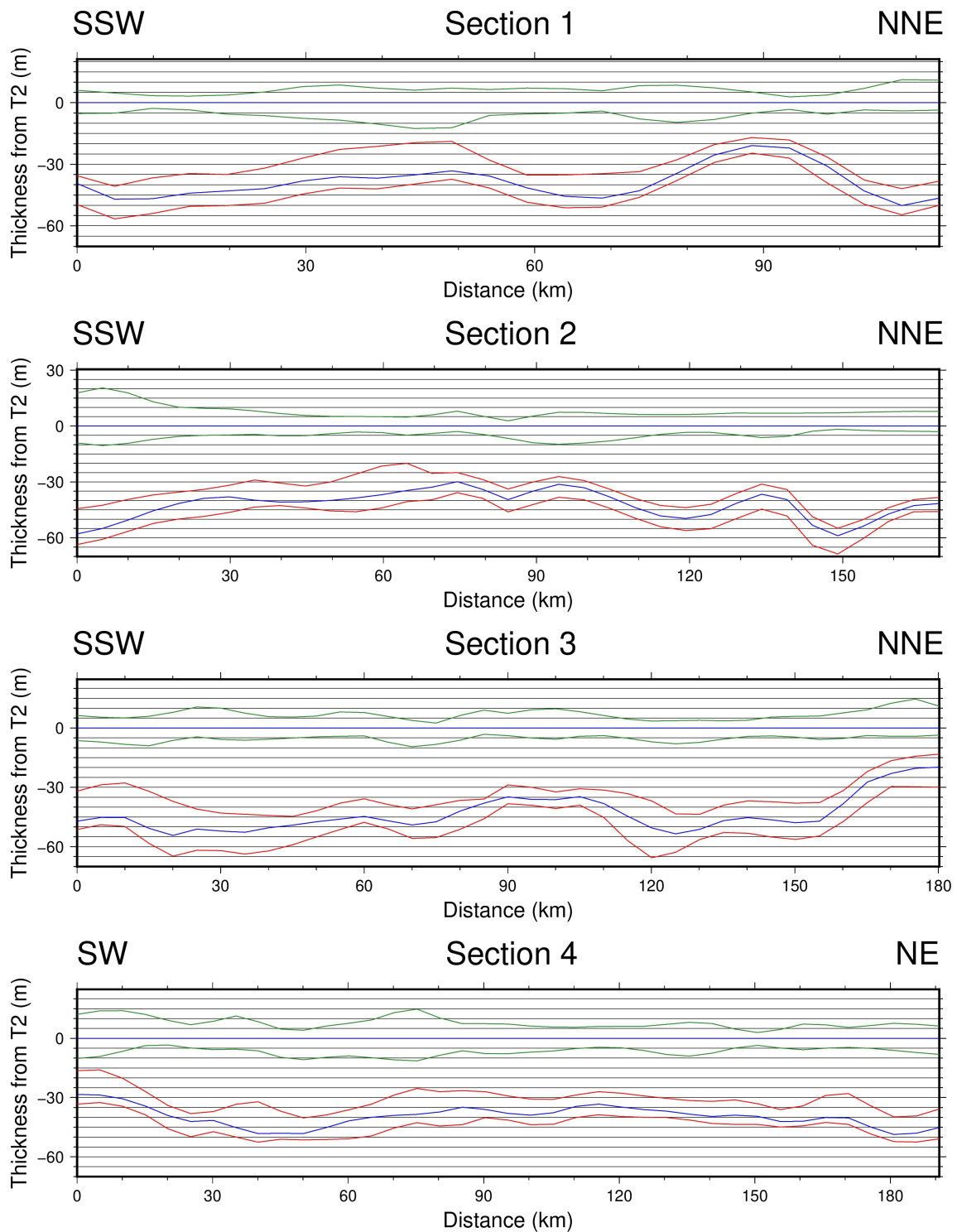


Figure 4.24: Cross-sections 1-4 over cumulative thickness 3D models represented with MFS of the upper tongue as datum (zero Y axis value).

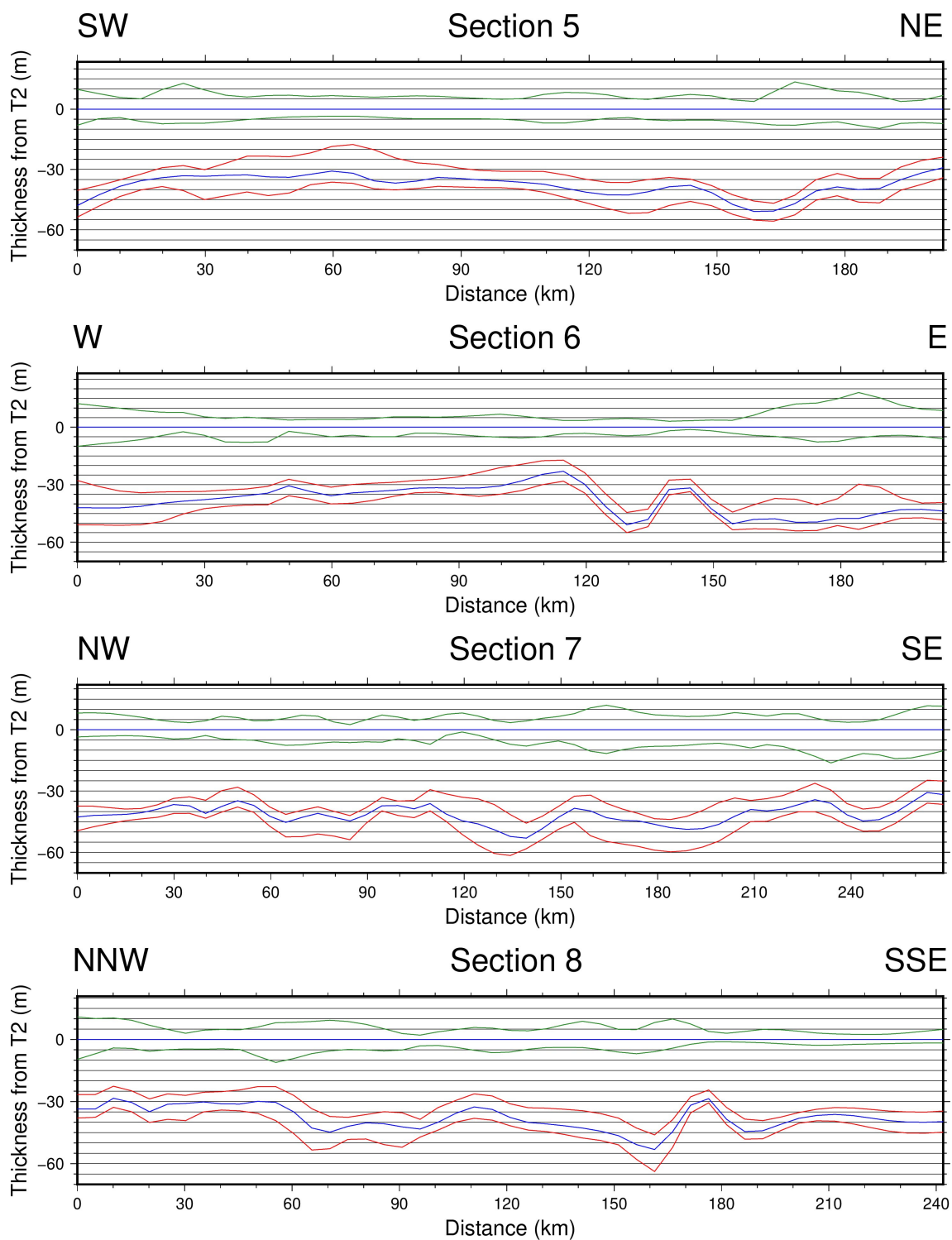


Figure 4.25: Cross-sections 5-8 over cumulative thickness 3D models represented with MFS of the upper tongue as datum (zero Y axis value).

The T-R sequences and geometric variations observed on cumulative thickness maps are evidenced by cross sections. Some slope breaks are more evident on the lower tongue surfaces than on the upper ones, as the S interval deposition generally flat-

tened out the previous geometries (figures 4.22 and 4.23). As an example, section 5 (figure 4.23) shows a regressive pattern (lower tongue, roughly at 60 km) which resembles the geometries often observed on seismic sections regarding the progradation of a coastline. Section 5 was in fact traced to cross one of the cuspidate geometries (described on the cumulative thickness maps, paragraph 4.3) that expand eastward after the deposition of succeeding intervals.

Cross sections 7 and 8 (represented in figures 4.23 and 4.25 with two different datum surfaces) were oriented parallel to the deformation front (NW - SE). These sections cross every major depositional system. The first depositional system crossed by section 7 is one of the two major systems described on cumulative thickness maps and in particular the one in the northern study area that became underfed. In fact, the upper tongue is represented by a thin drape on the underlying geometries up until almost 180-200 km from the start of section 7. At that point section 7 crosses the largest depositional system of the study area (in the central region) at the latitude of Edmonton. This system extends until around kilometer 60 of the adjacent (southern) section 8, where smaller scale cuspidate geometries (in plan view, figure 4.21) start to be crossed by its trace. The southern portion of section 8 represent a fully marine setting on gamma ray well logs. It is also worth noting that every normally oriented section presents a central region of variable extension (up to more than 100 km) with a flatter evolution than the proximal and distal areas. This trend is emphasized after the deposition of the S interval, which expanded these horizontal regions eastward (e.g. on section 1 between 50 and 80 km and on section 6 between 120 and 170 km). This behavior was emphasized shifting the datum to the upper tongue's MFS (figures 4.24 and 4.25). The top of the S interval appears flat on almost every section with that datum. In contrast, the lower tongue and the basal S interval appear as undulating surfaces, clearly influenced by the inherited geometry of the Belly River Group top that governed the deposition before being flattened out (exception made for the above-mentioned underfed system in the northern region) by the S interval accumulation, which developed with higher depositional rates in the central and southern study area. The upper tongue, then does not show significant variations and just drapes the S interval in the entire study area, exception made for the northern study area, where the upper regressive interval records a slight increase in distal accumulation.

4.5.2 Gamma ray expression and stacking patterns on cross sections

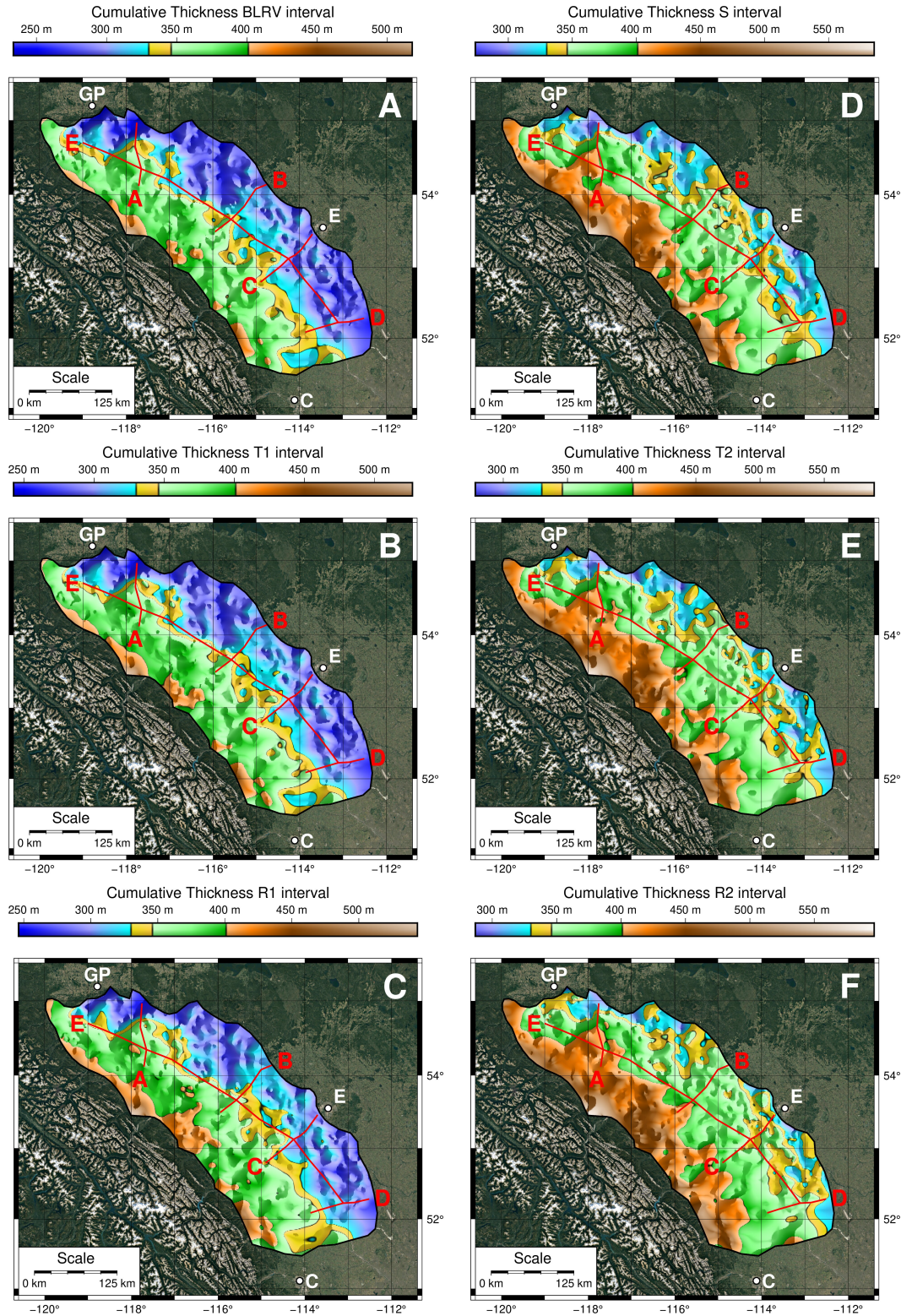


Figure 4.26: Location of section traces over cumulative thickness maps described in paragraph 4.3.

Five sections were used to refine interpretations in the transitional zone, on the eastern half of the study area (figure 4.26). The location of these sections was chosen to cover the full extension N-S of the study area crossing the most significant deposits and geometries found with the tridimensional analysis of the interpolated dataset. Each section thus crosses the transition (which bisect N-S the study area) between yellows and blues in figure 4.26. The schematic interpretation of the gamma ray expression is reported on every well log, specifically regarding channel bodies, sands and coal horizons. These interpretations and the main correlated surfaces summarize the paleoenvironmental eastward and southward variation of the stacking pattern throughout the Bearpaw succession. Sections A, B, C and D are respectively in the northern, central-northern, central-southern and southern study area (figure 4.26). Section E develop subparallel to the deformation front and crosses sections A, B, C and D. The pre-Bearpaw deposits of the Belly River Group contain channel bodies in sections A (figure 4.27) and C (figure 4.29). The top of the Belly River Group presents sand bodies alternated with shale horizons. Southwards, in section D (figure 4.30), sands disappear from pre-Bearpaw deposits and few coal horizons are found within fine sediments distributed in thin (<4 m) bodies. The T1 interval (lower Bearpaw tongue, transgressive and correlative strata) shows different accumulation patterns in each section. The T1 interval of section A (4.27) records minor accumulation northwards, and drapes some channel fills at its base. The lower tongue MFS expression in section A is widely referable to marine conditions in the northern well logs while it shifts southwards to shapes referable to emerged continental and transitional environments (see paragraph 3.3.2, 3.3.5 and 5.1). Section B (figure 4.28) shows an almost constant accumulation through its whole length during the lower transgressive phase, with some sandstone bodies located at the base of the southwestern well log. The lower MFS shape in section B suggest marine environments to the north east, gradually shifting southeastwards to continental deposits. Section C (4.29) does not follow the inferred direction of main sediment feeding system (as the other sections do, see paragraph 5.1) but instead crosses subsequent areas where sediments possibly cover inherited lows and highs as well as low accumulation areas (see figure 4.26). The T1 interval (and all of the others) in section C (4.29) thus shows variable thickness, depending on the position of the chosen well logs. The thicker zones are towards the south east, where the MFS shapes and the presence of channels and coal horizons suggest the persistence of alluvial environments. Section D (4.30) shows low accumulation during the T1 interval in coincidence with the finest granulometries. The MFS shape is typically marine in the last two well logs (towards ENE) which also record thicker transgressive deposits. The R1 interval shows two

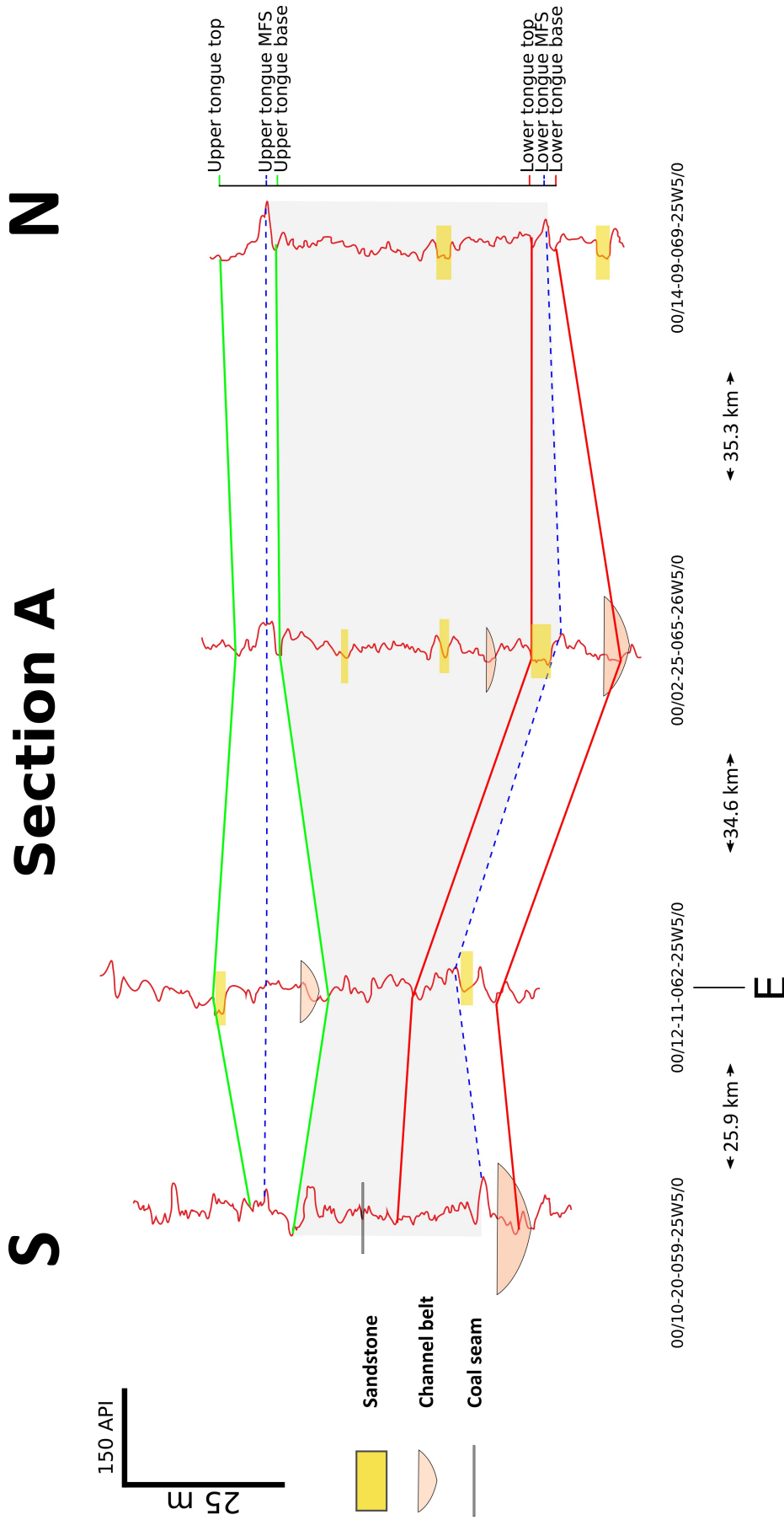


Figure 4.27: Cross section A in northern Alberta (Grande Prairie area, location map in figure 4.26). The correlated surfaces are traced in red (base and top of the lower Bearpaw tongue), green (base and top of the upper Bearpaw tongue) and blue (MFS of the respective T-R cycle). The grey area represents the sum of regressive Highstand and Falling Stage Systems Tract deposits (R1+S interval). Well-logs traces are all gamma ray ranging between 0 and 150 API.

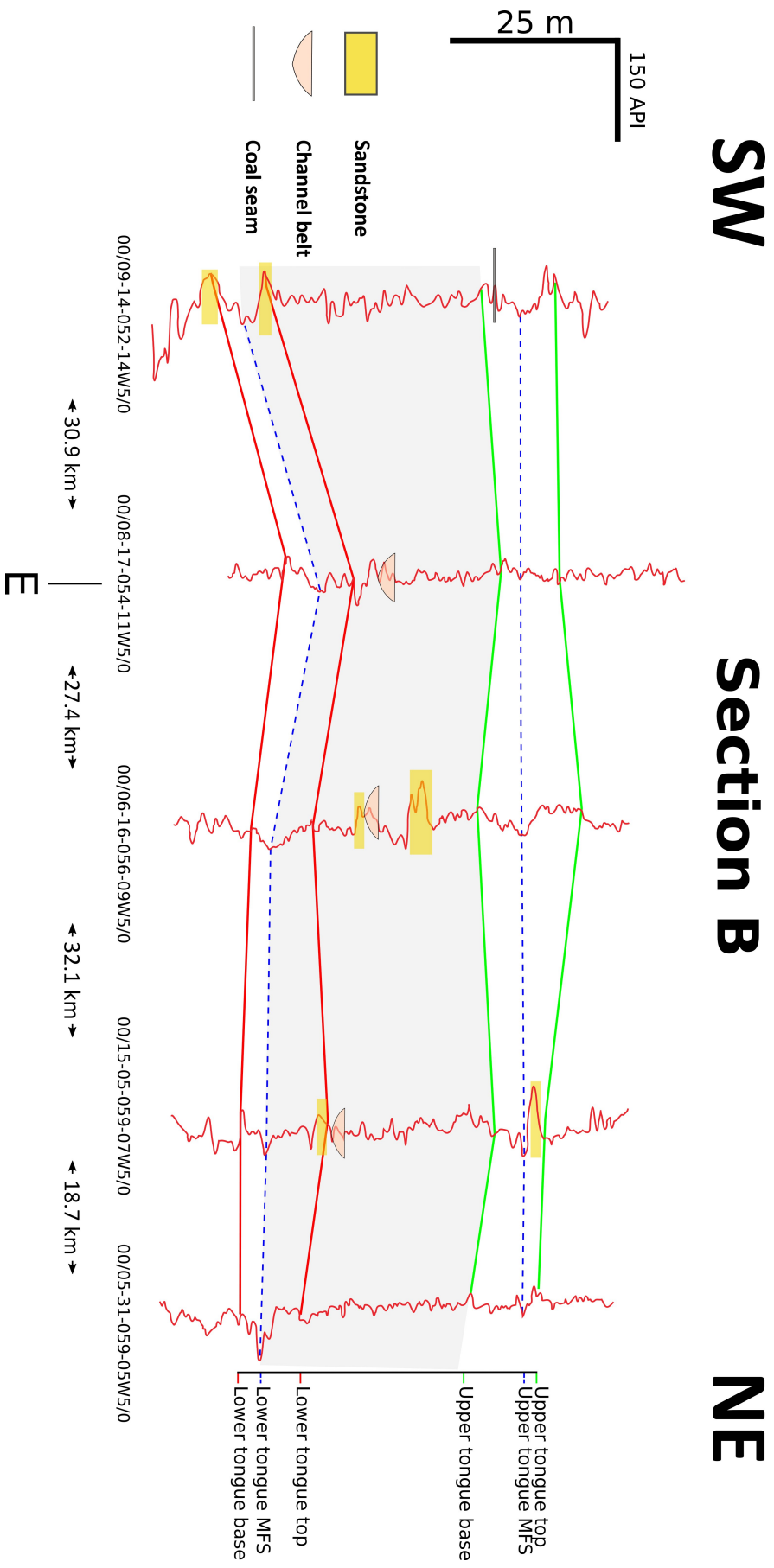


Figure 4.28: Cross section B in central northern Alberta (location map in figure 4.26). The correlated surfaces are traced in red (base and top of the lower Bearpaw tongue), green (base and top of the upper Bearpaw tongue) and blue (MFS of the respective T-R cycle). The grey area represents the sum of regressive Highstand and Falling Stage Systems Tract deposits (R1+S interval). Well-logs traces are all gamma ray ranging between 0 and 150 API.

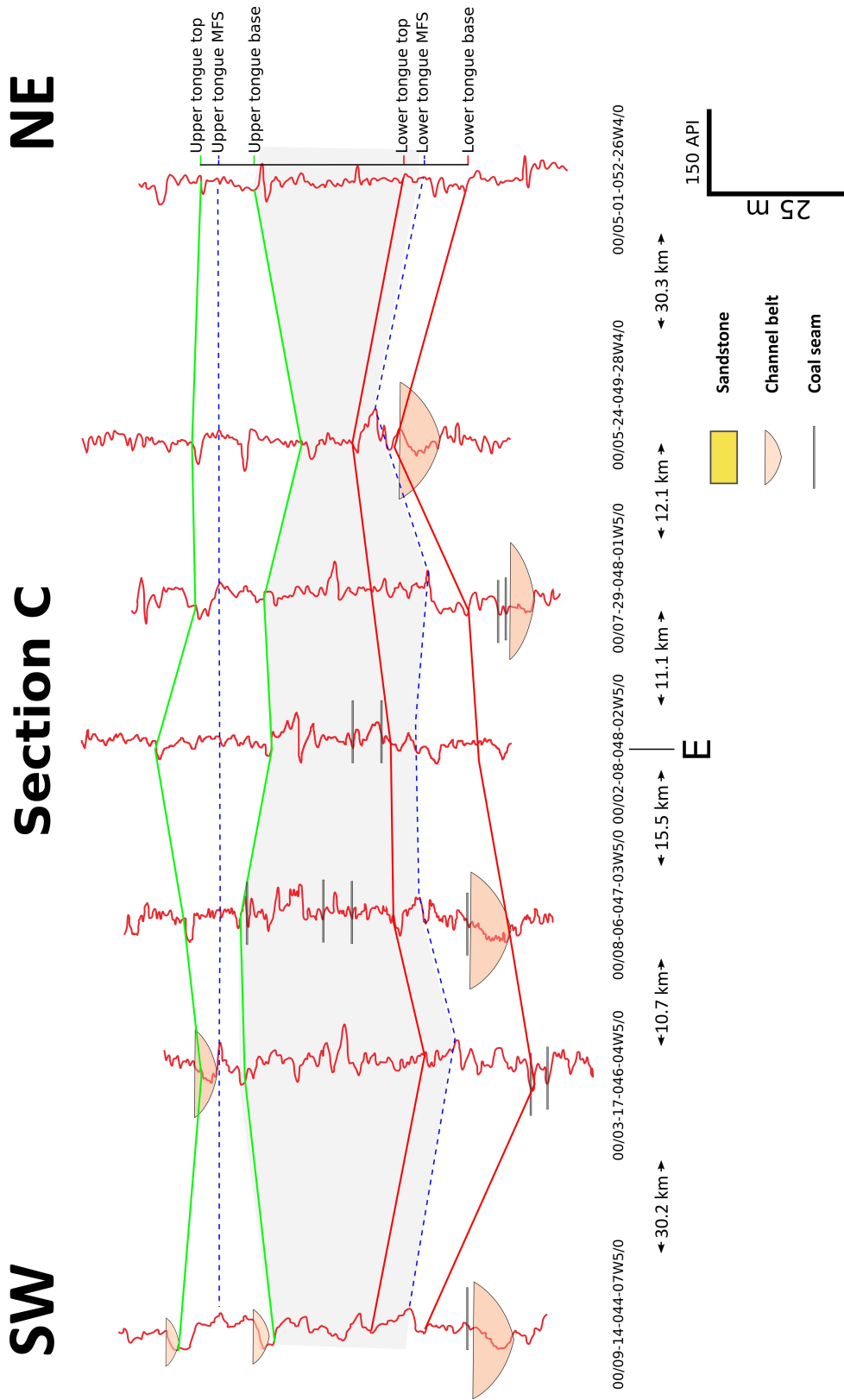


Figure 4.29: Cross section C in central southern Alberta (location map in figure 4.26). The correlated surfaces are traced in red (base and top of the lower Bearpaw tongue), green (base and top of the upper Bearpaw tongue) and blue (MFS of the respective T-R cycle). The grey area represents the sum of regressive Highstand and Falling Stage Systems Tract deposits (R1+S interval). Well-logs traces are all gamma ray ranging between 0 and 150 API.

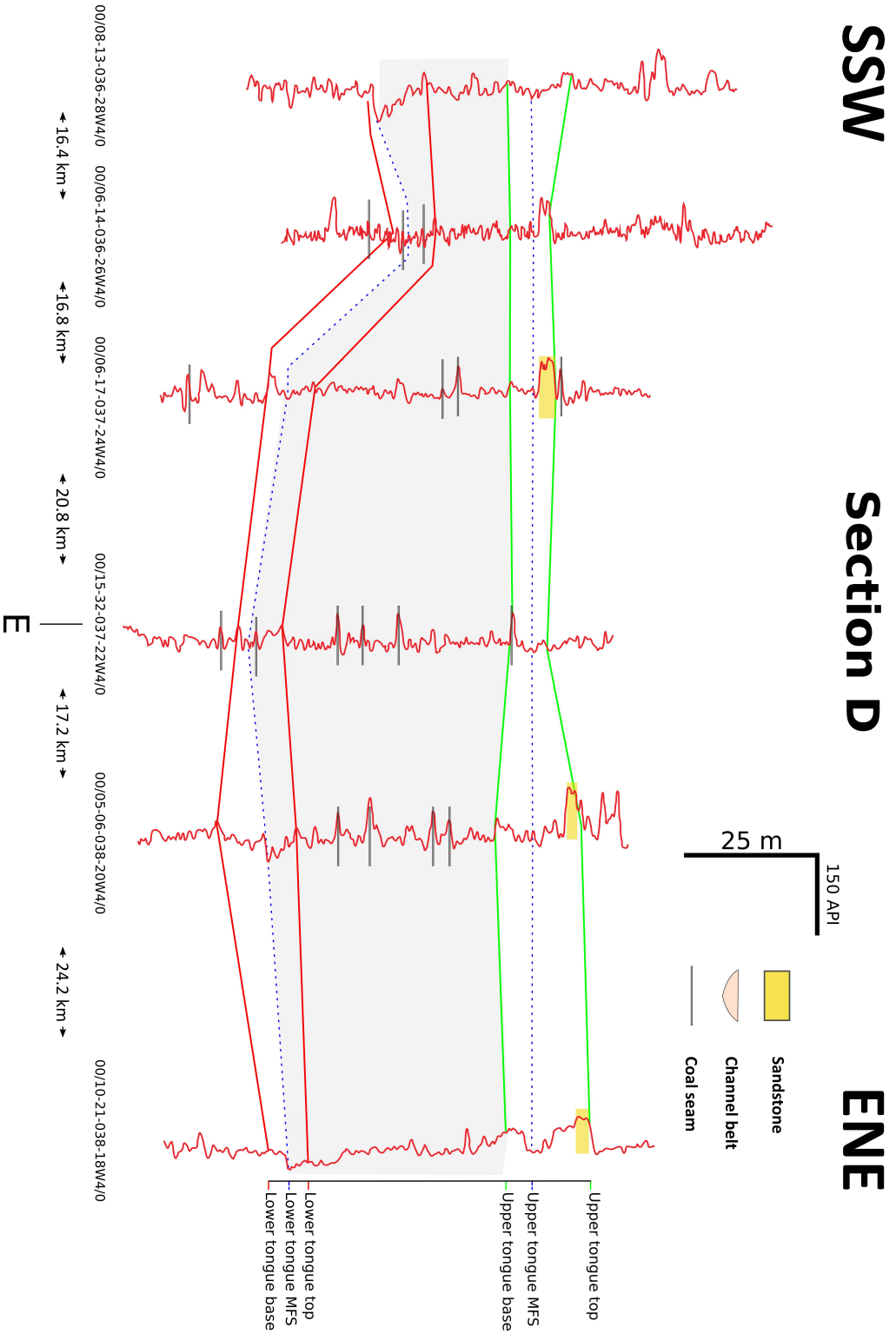


Figure 4.30: Cross section D in southern Alberta (location map in figure 4.26). The correlated surfaces are traced in red (base and top of the lower Bearpaw tongue), green (base and top of the upper Bearpaw tongue) and blue (MFS of the respective T-R cycle). The grey area represents the sum of regressive Highstand and Falling Stage Systems Tract deposits (R1+S interval). Well-logs traces are all gamma ray ranging between 0 and 150 API.

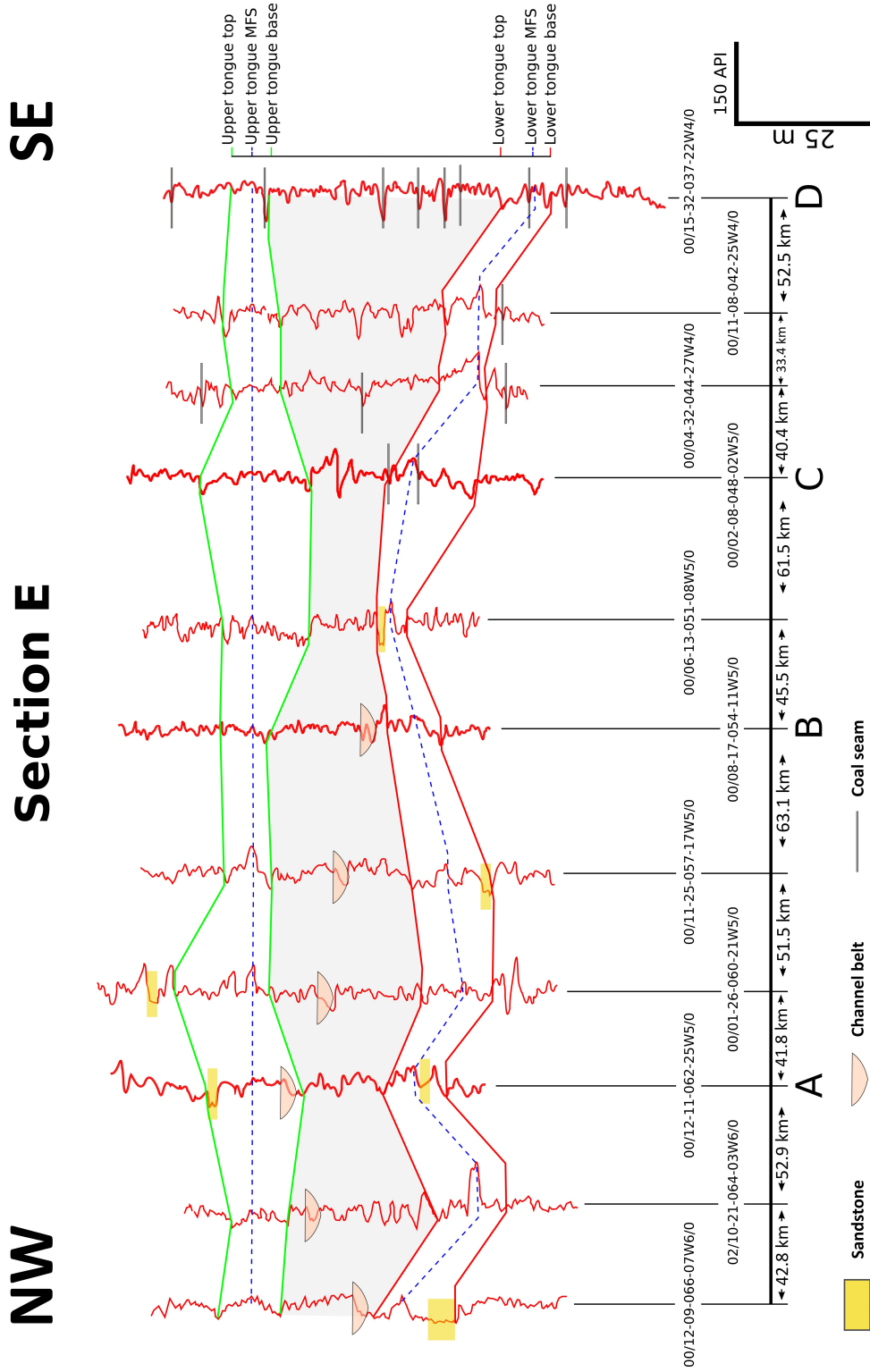


Figure 4.31: Cross section E in southern Alberta (location map in figure 4.26). The correlated surfaces are traced in red (base and top of the lower Bearpaw tongue), green (base and top of the upper Bearpaw tongue) and blue (MFS of the respective T-R cycle). The grey area represents the sum of regressive Highstand and Falling Stage Systems Tract deposits (RI+S interval). Well-logs traces are all gamma ray ranging between 0 and 150 API.

main thickness patterns. The first one is found in section A (4.27) where the R1 deposited more sediments southwards, hosts some sandstone in the central portion and almost pinches out toward the north. A similar trend, less accentuated, is found in section D (4.30), where coal horizons are present in the central and southwestern well logs. The southwestern well logs with coal horizons are referable to brackish, estuarine environments while the central portion shows transitional shapes, likely referable to prograding bodies (stacked coarsening upward trend). Sections B and C (central study area, respectively 4.28 and 4.29) show the second depositional pattern, where thicknesses are distributed almost uniformly along the section. Section C (4.29) in particular, shows a less uniform distribution of thicknesses probably due to the above-mentioned reason (section C does not follow the inferred direction of the main sediment feeding system in the area). The S interval presents, in the central sectors of the study area where a more uniform thickness on a SW - NE axis (section B, 4.28) or varies according to the section trace (section C). In section B (4.28) the S interval presents channel bodies and sandstones distributed in the central well logs. Section C (4.29), instead, presents finer deposits with sparse coal horizons in the central well logs. The second distribution pattern is found in both section A (4.27) and section D (4.30) and consists in rapidly basinward thickening deposits (toward the north for section A and toward east northeast for section D). The S interval in section A comprehends channel fill and sand bodies but almost completely lacks coal horizons (the only occurrence was found in its southern well log). Section D shows a complete lack of channel-related gamma-ray shapes while instead records abundant coal horizons within the S interval. These coal horizons in the southeastern study area were also recognized and mapped in other studies, the most recent is Hathway (2016). The T2 interval records generally thicker deposits in the central sections (B and C, figures 4.28 and 4.29) than in the northern and southern ones (respectively A and D, figures 4.27 and 4.30). The accumulation becomes thicker basinward in sections B, C and D, but in section A shows a clear pinch out trend. In section B and D, the basinward thickening trends correspond to well logs that present marine influence-related MFS gamma ray curve shape, while the thinner accumulation presents a typically continental MFS signature. Section C shows marine to coastal environments-related MFS shape in the northeastern well logs that gradually shift to more alluvial environments related MFS expression in the southwestern well logs. The T2 interval lacks coal horizons in the whole study area except for the southwestern section B where one occurrence was found. Section A shows a typically marine signature of the MFS in the northern well logs (corresponding to thinner accumulation) which shifts southwards towards alluvial

environments expression. The R2 interval shows two main accumulation patterns. In the central study area (section B and C, figures 4.28 and 4.29) the thickness of the R2 interval is uniform or slightly thinner towards the NE. In sections A and D (figures 4.27 and 4.30) instead the thickness increase basinwards, possibly in correspondence with prograding geometries and coarser deposits. The R2 interval completely lacks coal horizons. Channel fill bodies were found in the southwestern R2 interval of section C and sandstones are presents along sections A, B and D. The overall granulometry of the Bearpaw succession, inferred from the gamma ray API value, mostly presents coarse silt and pure shale. The succession is rarely interrupted by medium to fine sand deposits (≤ 6 m thick), mostly located within regressive upper tongue deposits (sections B,C,D) and the S interval (sections A, B). All of the above mentioned trends are clearly visible in section E (figure 4.31), in which the northern sector presents sand bodies within the Bearpaw T1 and R2 intervals as well as channel bodies within the S interval right where the section trace crosses the major distributional systems of the study area (see figure 4.26). The southern section E instead presents sparse coal horizons especially within the S interval, the lower Bearpaw tongue and the pre-Bearpaw deposits. Only one sand deposit was intercepted by section E, precisely within the R1 interval in the well log between section B and C. Section E doesn't intercept channel fill bodies in the southeastern well logs. The accumulation during the S interval gets thicker southeastwards, as the section trace crosses the area between yellows and blues in figure 4.26; the lack of channel fill bodies coincide with that southwards thickening trend.

4.5.3 Results comparison with published data

As described in the methods chapter (paragraph 3.3.3) the interpolated DEM surfaces were compared to the results obtained by Jerzykiewicz in his 1997 study. The sea-level referred surfaces were sampled on the same section traces of Jerzykiewicz (1997) for the comparison (location of section traces in figures 4.32, 4.33, 4.34 and 4.35). The distance between well logs (the resolution of the dataset in this study) is lower than the one in Jerzykiewicz's sections, thus some differences may depend on resolution biases (*e.g.* the sinuous trend of our surfaces with respect to the surfaces in Jerzykiewicz's background sections). The topography does not match perfectly with Jerzykiewicz (1997) although the sections were accurately aligned. That's primarily due to the differences in the topographic database (SRTM with 1 arc-sec resolution) that was used to sample Alberta elevations, which has a higher resolution than the database used in Jerzykiewicz (1997). Secondly, the differences may also be due to imprecisions in the georeferentiation process caused by section's line

thicknesses in the location maps found in Jerzykiewicz (1997), scarcity of usable georeferentiation points (river bends were used along with big Alberta cities appearing in the location maps) and also small geometrical deformations due to digitalization process of the published data.

The stratigraphic nomenclature was largely updated since the late 90s, the single wedge geometric model reported by Jerzykiewicz (and in numerous other studies from different authors) in section D-D' (figure 4.32) is no longer adopted since the recent discovery of the bipartition of the Bearpaw Fm. in at least two distinct major T-R events. In addition to that, some formations as the Dinosaur Park Fm. were established long after the publication of Jerzykiewicz (1997), thus are not even mentioned in the published sections, as noticeable in figures 4.32, 4.33, 4.34 and 4.35. Nonetheless each section presents the same trends and matches almost perfectly with Jerzykiewicz (1997). That similarity is expectable due to the fact that some of these published depths were used to calibrate the datum in this study, especially in the foothills area. The surfaces obtained in this study correspond, on the eastern part of the study area, to the Bearpaw Formation drawn by Jerzykiewicz (1997) and, in the foothills area, to the correlative stratigraphic intervals from the top of the Oldman Formation to the base of the Brazeau Formation. The higher temporal and spatial resolution of data from this study makes it easy to appreciate vertical oscillations of the surfaces across the contacts drawn in Jerzykiewicz (1997). The Belly River Group base (datum) matches almost perfectly the Lower Brazeau Fm. base. The greater difference is found in the deformed area under the foothills were Jerzykiewicz interpreted (especially in section E-E', figure 4.33) the faults system at the scale of the entire basin fill. Some of these structures - e.g. the fault that crosses the Bearpaw Fm. around km 50 of section E-E' (4.33) - were not recognized in this study. In the deformed area under the foothills, the methods used to interpolate the correlations in this study created the artifact of continuous lines which bends downward and then quickly shift direction to reach over 2000 m shallower depths on the western border of the study area. This was interpreted as the result of one or more major faults belonging to the same triangle zone depicted by Jerzykiewicz (1997) in section E-E' (figure 4.33). Although the fault dynamics observed in this study are the same found by Jerzykiewicz (1997), the position of the major deformation is significantly shifted westward (roughly 20 km) by our findings, thus the overlying and underlying units drawn in Jerzykiewicz (1997) are crossed by our dataset between 20 and 60 km in figure 4.33 (section E-E'). The interpretation of the fault system was just barely touched in this study not only because it was not the main purpose of this research but also because the surfaces appeared deformed only in the

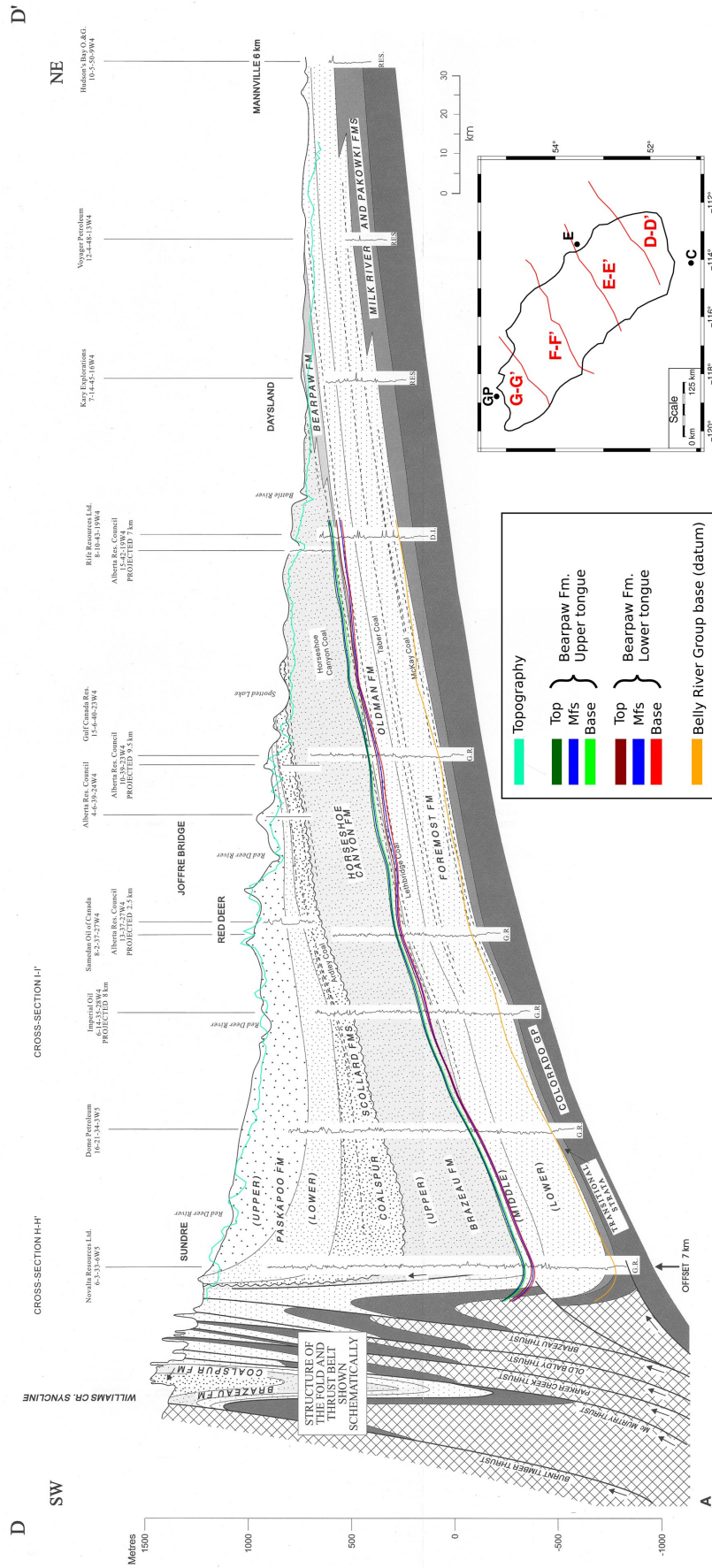


Figure 4.32: Section D-D' from Jerzykiewicz (1997) overlaid by surfaces from this study. The datum is sea level. Location of section trace in the inset. Modified after Jerzykiewicz (1997).

4.5. CROSS SECTIONS

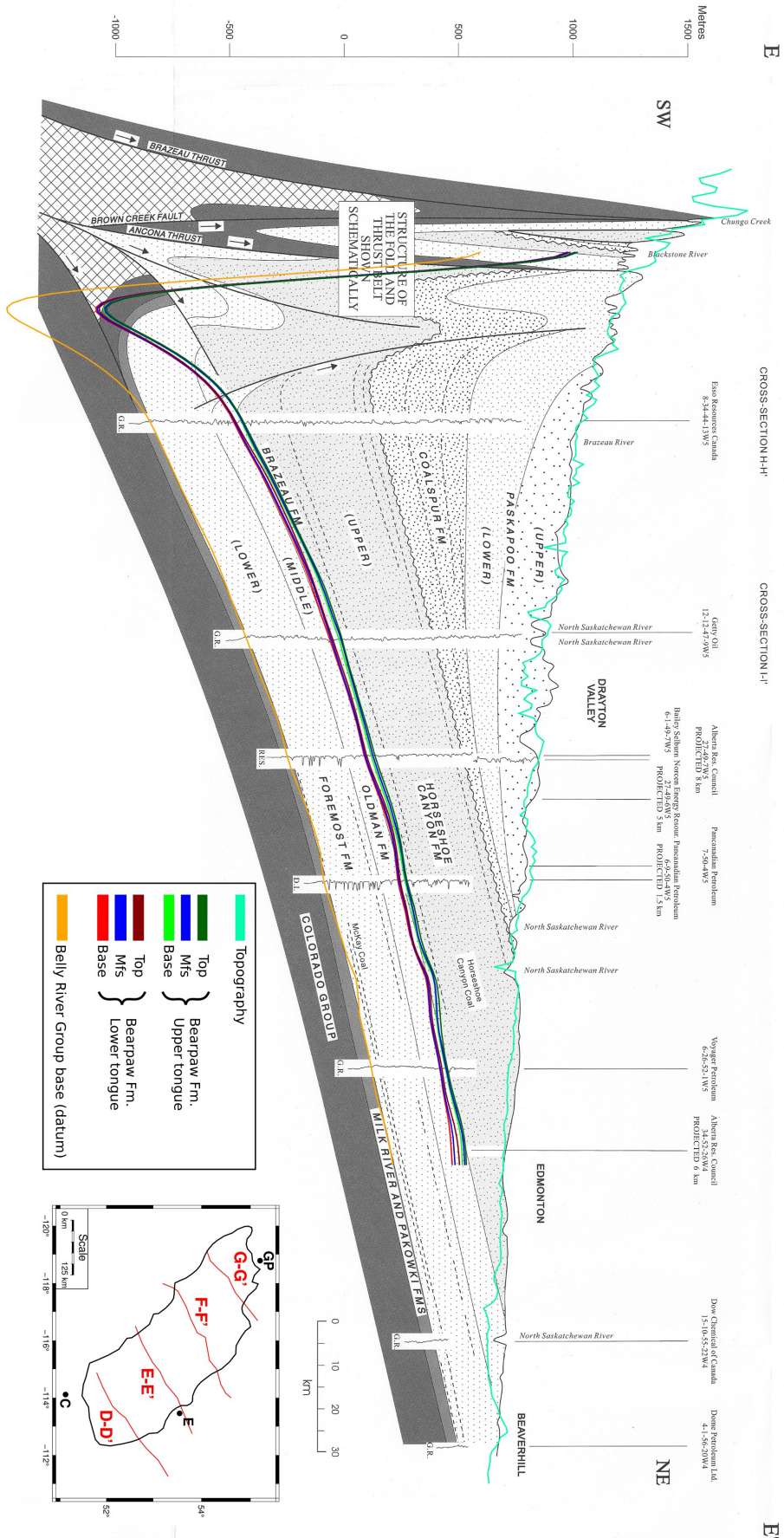


Figure 4.33: Section E-E' from Jerzykiewicz (1997) overlaid by surfaces from this study. The datum is sea level. Location of section trace in the inset. Modified after Jerzykiewicz (1997).

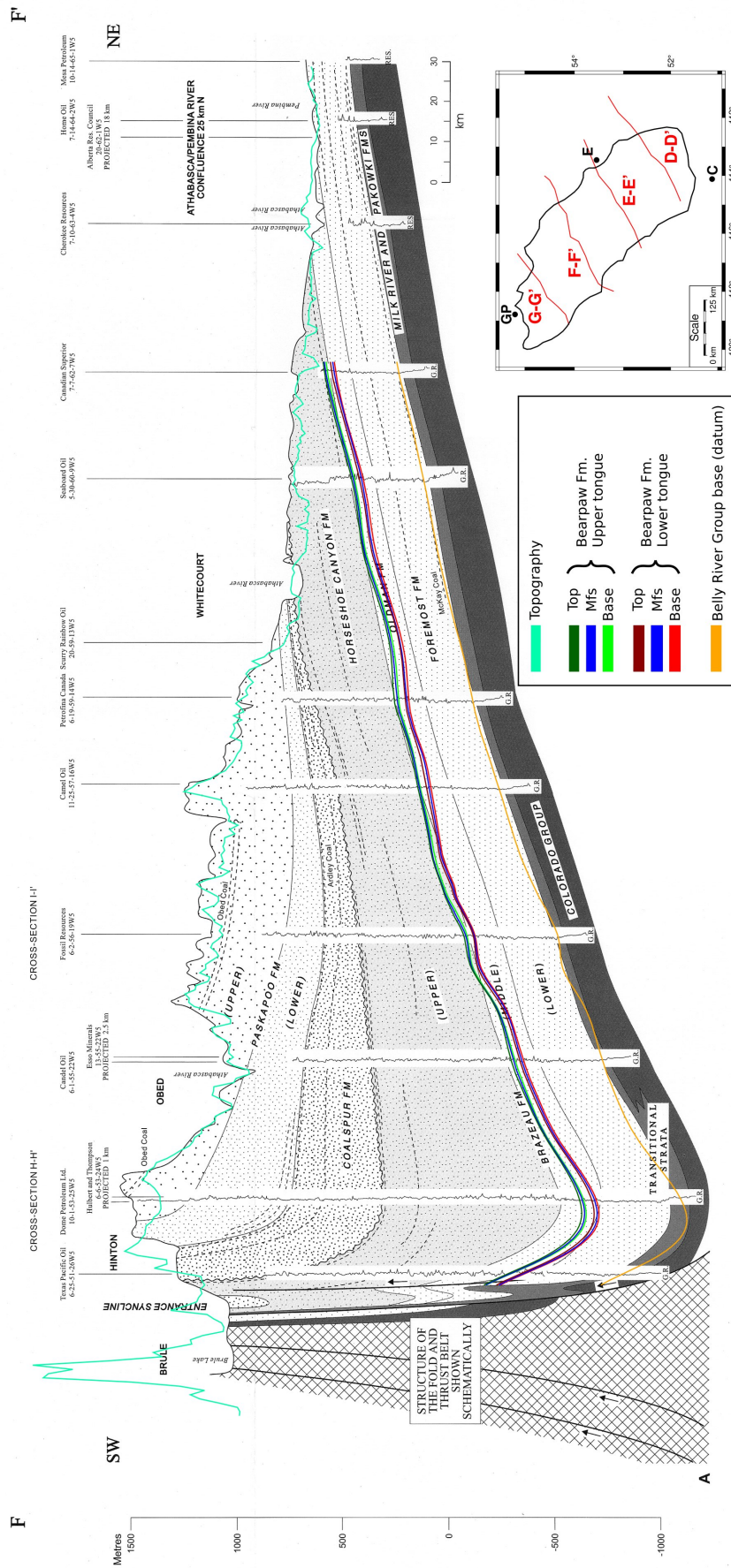


Figure 4.34: Section F-F' from Jerzykiewicz (1997) overlaid by surfaces from this study. The datum is sea level. Location of section trace in the inset. Modified after Jerzykiewicz (1997).

4.5. CROSS SECTIONS

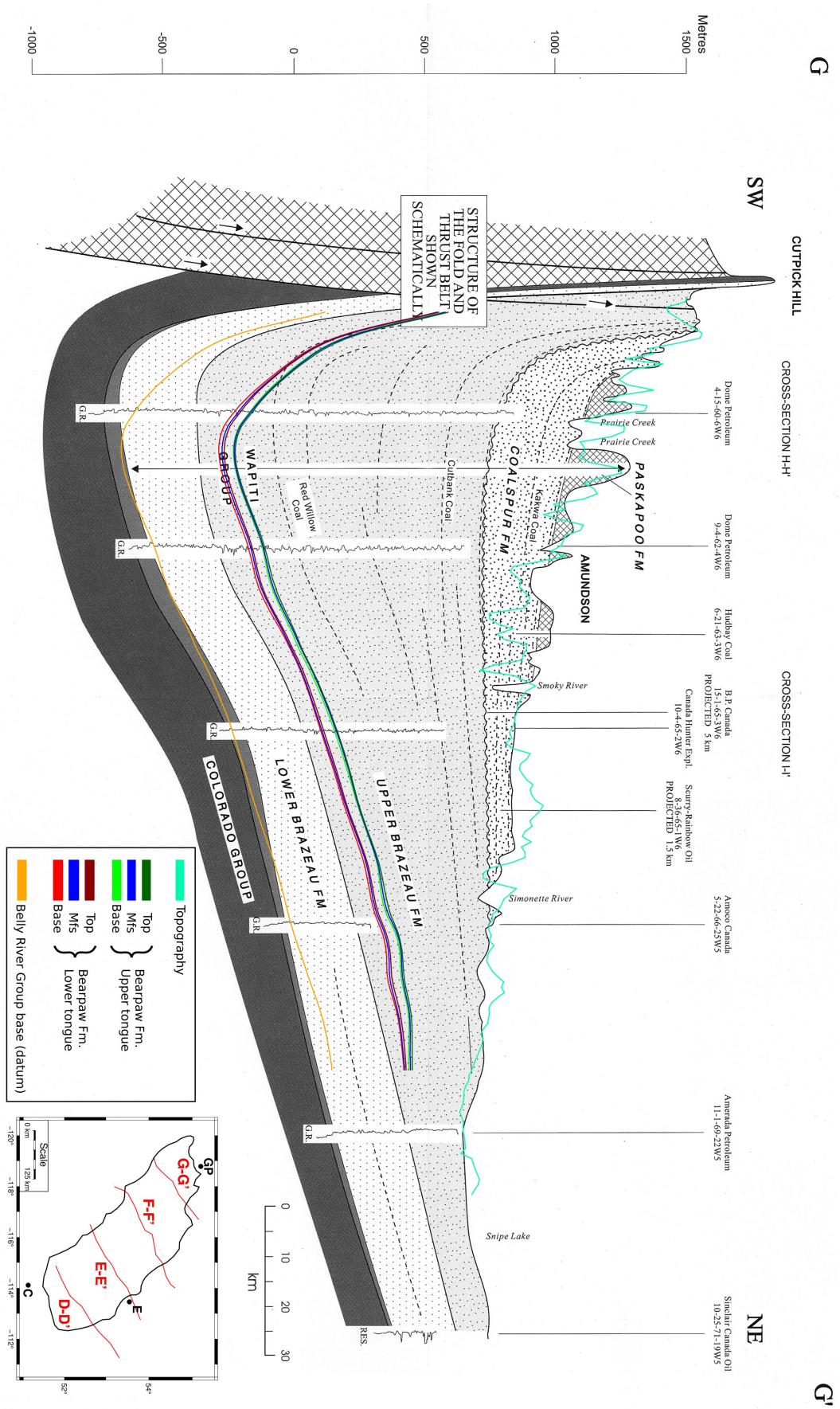


Figure 4.35: Section G-G' from Jerzykiewicz (1997) overlaid by surfaces from this study. The datum is sea level. Location of section trace in the inset. Modified after Jerzykiewicz (1997).

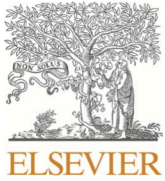
above described (paragraph 4.1) very small portion of the western study area which happened to be the most difficult and inaccurate to correlate, with low quality and quantity of data points. Overall, the sections highlight how the Bearpaw interval can be accurately used as a basin-wide marker for the Upper Cretaceous foreland strata correlations, as well as a reliable datum for shallower and deeper analysis, from the deformation front of the Rocky Mountains to the eastern Alberta plains, beyond the longitude of Edmonton.

4.6 Published article

The following pages include the [published article](#) titled "*Evolution of the Western Interior Seaway in west-central Alberta (late Campanian, Canada): implications for hydrocarbon exploration*" regarding the interpretation of most of the above reported results as well as their implications for the hydrocarbon system in Alberta. The article was authored by the same author, supervisor and co-supervisors of this thesis and was published in *Marine and Petroleum Geology* journal. Some of the images in this thesis are reported without explicit reference to this paper but nonetheless rightfully belong to it. The reader is kindly invited to cite the following paper for any reference regarding images, data or results contained both in other parts of this thesis and in Zubalich et Al. (2021).

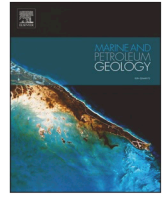
Sample reference:

Zubalich, R., Capozzi, R., Fanti, F., and Catuneanu, O. (2021). Evolution of the Western Interior Seaway in west-central Alberta (late Campanian, Canada): Implications for hydrocarbon exploration. *Marine and Petroleum Geology*, 124, 104779. doi: [10.1016/j.marpetgeo.2020.104779](https://doi.org/10.1016/j.marpetgeo.2020.104779)



Contents lists available at ScienceDirect

Marine and Petroleum Geology

journal homepage: www.elsevier.com/locate/marpetgeo

Research paper

Evolution of the Western Interior Seaway in west-central Alberta (late Campanian, Canada): Implications for hydrocarbon exploration

 Riccardo Zubalich^{a,*}, Rossella Capozzi^a, Federico Fanti^a, Octavian Catuneanu^b
^a Alma Mater Studiorum University of Bologna, Department of Biological, Geological and Environmental Sciences (BIGEA), via Zamboni 67, Bologna, Italy

^b Department of Earth and Atmospheric Sciences, University of Alberta, 1-26 Earth Sciences Building, Edmonton, Alberta, Canada, T6G 2E3

ARTICLE INFO

Keywords:

Western Interior Basin
 Western Interior Seaway
 Sequence stratigraphy
 West-central Alberta
 Late Campanian
 Hydrocarbon fields

ABSTRACT

This study presents the first integrated, high-resolution stratigraphic analysis of a large area of the Cretaceous Western Interior Basin in Alberta (western Canada), providing new tools to discriminate sedimentary processes and stratigraphic patterns of transgressive-regressive (T-R) cycles in correlative marine and non-marine domains. We integrate gamma ray well-log analysis, measured sections, and paleontological data to determine sediment accumulation and distribution during the second-order T-R cycle of the late Campanian Western Interior Seaway over a previously unstudied area encompassing approximately 97,000 km² of the Alberta foreland basin. The Bearpaw Formation, historically regarded as the product of a single transgression, is shown to include two T-R cycles, whose timing is constrained by new chronostratigraphic data that provides an unprecedented resolution (~200 kyr) for the Cretaceous of western North America. Seven reference stratigraphic markers were mapped across the study area from the marine deposits into the fluvial domains. 3D-modelled stratigraphic surfaces and stratigraphic intervals resulted in isopach maps for consecutive systems tracts, allowing detailed interpretations of their architecture and patterns of sediment accumulation. Our analysis provides paleogeographic maps for the Western Interior Seaway, focusing primarily on the evidence of the paleo-coastlines during the documented cycles. The distribution of fine-grained, primarily marine, sediments resulted in an effective seal for hydrocarbon accumulation in the Belly River Group. Further oil migration upsection, within the Edmonton group, was prevented by the occurrence of these sealing units. Data support the interpretation that eustasy provided the main control on the evolution of the Western Interior Seaway during the late Campanian.

1. Introduction

The Bearpaw Formation is a late Campanian age marine unit deposited in the Western Interior Basin (WIB) of Canada and United States between 74 and 73 Myr (Rogers et al., 2016; Eberth and Kamo, 2020). Exposures of this Formation extend over much of northern and central Montana (U.S.A.) as well as in the southern part of Alberta and Saskatchewan (Canada). The lithostratigraphic interval represented by the Bearpaw Formation separates two major clastic wedges: in ascending order the Belly River and Edmonton groups, both renowned for their remarkable fossil record and studies on the evolution of clastic systems (Russel and Chamney, 1967; Dodson, 1971, 1990; Currie and Koppelhus, 2005; Larson, 2010; Larson et al., 2013; Eberth et al., 2013; Cullen and Evans, 2016; Gilbert, 2019). As the Bearpaw Formation has a complex lateral relationship with the correlative non-marine units of the Belly River and Edmonton groups, previous sequence stratigraphic

studies investigated the possibility of defining mappable transgressive-regressive (T-R) sequences across Alberta, integrating exposures and geophysical well-log signatures. In the southern plains of Alberta, the Bearpaw Formation represents a second-order transgressive-regressive cycle, within which higher frequency (third-, fourth- and fifth-order) T-R sequences are nested (Hathway, 2016, and references therein). The time-transgressive geographic evolution of the Western Interior Seaway is reflected by the documented distribution of fine-grained, primarily marine, sediments that mark the Bearpaw Formation. This likely also resulted in a primary control on hydrocarbon accumulation as the Bearpaw Formation separates the Belly River and Edmonton groups, two major non-marine, clastic systems dominated by fluvial deposition. Oil fields have been discovered and exploited in the Belly River Formation: fluvial channel fills have formed traps in the western portions of the Alberta Basin, whereas to the east accumulation follows updip sandstone pinchouts (Creaney et al., 1994). The Belly

* Corresponding author.

E-mail address: riccardo.zubalich2@uniibo.it (R. Zubalich).

<https://doi.org/10.1016/j.marpetgeo.2020.104779>

Received 29 June 2020; Received in revised form 16 October 2020; Accepted 18 October 2020

Available online 21 October 2020

0264-8172/© 2020 Elsevier Ltd. All rights reserved.

River Group has been the subject of multiple oil-related investigations as it may form regionally prospective trends within the Alberta Basin. This Group was considered and explored as a further target with respect to the deeper Cardium Formation (Plint et al., 1986; Putnam, 1993). The hydrocarbon fields exploited in the Belly River Group are now believed to be bordered by updip faults that seal major channel fills (Putnam, 1993) and no information is provided on the sealing efficiency of those faults nor on the occurrence of overlying sealing stratigraphic units. Despite such premises, our comprehension of Bearpaw Formation sedimentary dynamics, extension of sequence boundaries in correlative non-marine deposits, and ultimately reciprocal stratigraphies (related to patterns of base-level change across the foreland system) remains limited as two critical lines of investigation have been only marginally addressed.

First, Bearpaw Formation and correlative deposits along the margin of the Canadian Cordillera remain largely understudied, although they provide critical information to decipher the paleogeography and depositional setting of a large sector of the WIB during the late Campanian. This interval includes the non-marine, correlative deposits of the Bearpaw Formation that occur in the fluvial beds of the Wapiti Formation, a clastic wedge that extends over much of the northernmost section of the Alberta foreland basin (Fanti and Catuneanu 2009, 2010 and references therein). Although several lines of investigation support the occurrence of Bearpaw deposits in western Alberta (Jerzykiewicz, 1996; Fanti and Catuneanu, 2010; Koppelhus and Fanti, 2019) a combination of limited exposures, lack of systematic coring and ambiguous well-log signatures precluded high-resolution studies in this area. Prior to this study, this area of transition from marine to non-marine domains was largely unknown and unmapped (Jerzykiewicz, 1997; Chen et al., 2005; Fanti and Catuneanu, 2009, 2010).

Second, the mode and tempo of both eustasy and tectonics on the evolution of the foreland system remains unsolved and debated, as most of available data refer exclusively to marine deposits and lack precise or high-resolution chronostratigraphic control. As western Alberta preserves a record of interbedded marine and non-marine facies related to the Western Interior Seaway, it offers a unique insight into the large-scale architecture of T-R cycles, making the Bearpaw events a remarkable case study. Our study aims to provide new data to discriminate, with unprecedented resolution, the dynamics of the Bearpaw T-R cycles with a sharp focus on how major stratigraphic and sequence stratigraphic surfaces define discrete units in primarily non-marine settings. In so doing, we combine well-log analyses, high-resolution GIS-based 3D reconstructions, and selected exposures in order to provide a robust stratigraphic framework within which more localized observation could be placed and rationalized. Results provided in this study allow discriminating previously unmapped depositional domains in west-central Alberta and their relative shifts during the Bearpaw time. Consequently, data presented here provide definitive information regarding the way in which the Bearpaw T-R cycles control hydrocarbon migration and accumulation in the late Campanian age successions of west-central and southern Alberta.

2. Geological setting

2.1. Study area, stratigraphic, and structural setting

The main deformation events recorded in the Alberta foreland basin took place during two orogenic periods: from Late Jurassic to Early Cretaceous and from Late Cretaceous to Paleocene (Bally et al., 1966; Price and Mountjoy, 1970; Price, 1981; Chamberlain et al., 1989; Underschultz, 1991; Jerzykiewicz and Norris, 1994; Jerzykiewicz, 1997). Compressive deformation from Jurassic to Paleocene transported the sedimentary units eastward towards the Alberta foreland basin (McMecham et al., 1993) forming a fold-and-thrust belt that propagated in the Alberta Foothills (Dawson et al., 1990, 1994). The foreland Mesozoic and Cenozoic strata dip to the SSW, although in the foothills

area they are folded on thrust anticlines and backthrusts (Stockmal et al., 2001), reversing their dip to the NNE and creating the western limb of the Alberta syncline (Pana and Van Der Pluijm, 2015). Shales of the Bearpaw Formation could have served as main detachment horizon of later thrust sheet formation in the foothills (Stockmal et al., 2001). The Western Interior Basin developed on the eastern side of the Canadian Rocky Mountains where successions from the Paleozoic to the Cenozoic ages, that overlie the crystalline basement, occur (Lee et al., 2018). This basin is dominated by western provenance siliciclastic successions produced by convergent tectonics along the western margin of the North American Craton (Monger, 1989).

Within this framework, our study area encompasses approximately 96,600 km² in west-central Alberta and extends N-S between the cities of Grande Prairie and Calgary and W-E between the deformation front of the Rocky Mountains and Edmonton (Fig. 1). The stratigraphic nomenclature and framework for the Upper Cretaceous strata in Alberta vary substantially with respect to the proximity to the foothills as well as from north to south. To the north and to the west of the city of Edmonton, the Wapiti Formation is time-equivalent to the Belly River Group (Foremost, Oldman, and Dinosaur Park formations), the Bearpaw Formation, and the Edmonton Group (Horseshoe Canyon and Battle formations) (Fig. 2). This clastic wedge is also correlative to the Brazeau Formation in the central foothills. The Wapiti Formation overlies the marine deposits of the Puskwaskau Formation, which is correlative with the Wapiabi Formation in the central foothills and the Lea Park Formation in the southern plains (see Fanti and Catuneanu, 2009; Eberth and Braman, 2012 for a detailed nomenclatural review) (Fig. 2).

2.2. The Bearpaw Formation and correlative deposits in Alberta

Numerous publications have dealt with the Bearpaw Formation providing valuable stratigraphic, structural and paleontological data (Wall and Singh, 1975; Dawson et al., 1990, 1994; Ainsworth, 1994; Wood, 1994; Cant, 1995; Catuneanu et al., 1997, 2000, 2011; Leckie et al., 1997; Catuneanu, 2006; Hathway, 2016; Gilbert and Bamforth, 2017; Gilbert et al., 2019). The Bearpaw Formation accumulated in an epeiric sea, which transgressed over non-marine deposits. The Bearpaw Formation includes a vast array of depositional facies representative of paralic settings, with lithologies ranging from marine shales to siltstones and sandstones. In western and central Alberta, deposition took place in coastal-to inner-shelf environments, whereas to the east Bearpaw deposits are representative of more offshore marine environments. The thickness of the Bearpaw Formation varies from the north, with a 'zero edge' placed near the city of Edmonton, to approximately 200 m to the south of Calgary and to ~400 m in southern Saskatchewan (Dawson et al., 1994; Hathway, 2016; and references therein). A combination of a series of bentonite beds and very fossiliferous layers allowed for a refined ammonite-based (primarily inoceramids) biozonation of the Western Interior Basin. In ascending order, the Bearpaw Formation in Alberta encompasses the *Didymoceras cheyennense*, *Baculites compressus*, and *Baculites cuneatus* ammonite zones (Kauffman et al., 1993; Tsujita and Westermann, 1998; Walaszczyk et al., 2001) (Fig. 2).

The complex, diachronous interval that characterizes the Bearpaw Formation with respect to the underlying Dinosaur Park Formation (Belly River Group) and overlying Horseshoe Canyon Formation (Edmonton Group) has been described in the literature for more than a century (the first study: Hatcher and Stanton, 1903). This led to the identification of mappable and stratigraphically constrained clastic wedges dominated by coal deposits, each bounded by marine shale and shallow-marine sandstones. This architecture has been interpreted as a combination of multiple factors, primarily sea-level change, orogenic phases, subsidence, and climate (Catuneanu et al., 1997, 1999; Eberth and Braman, 2012; Hathway, 2016). The stratigraphic revision of the Horseshoe Canyon Formation (HCFm) by Eberth and Braman (2012) provided a comprehensive column of the Bearpaw Formation with respect to underlying, overlying, and correlative non-marine deposits in

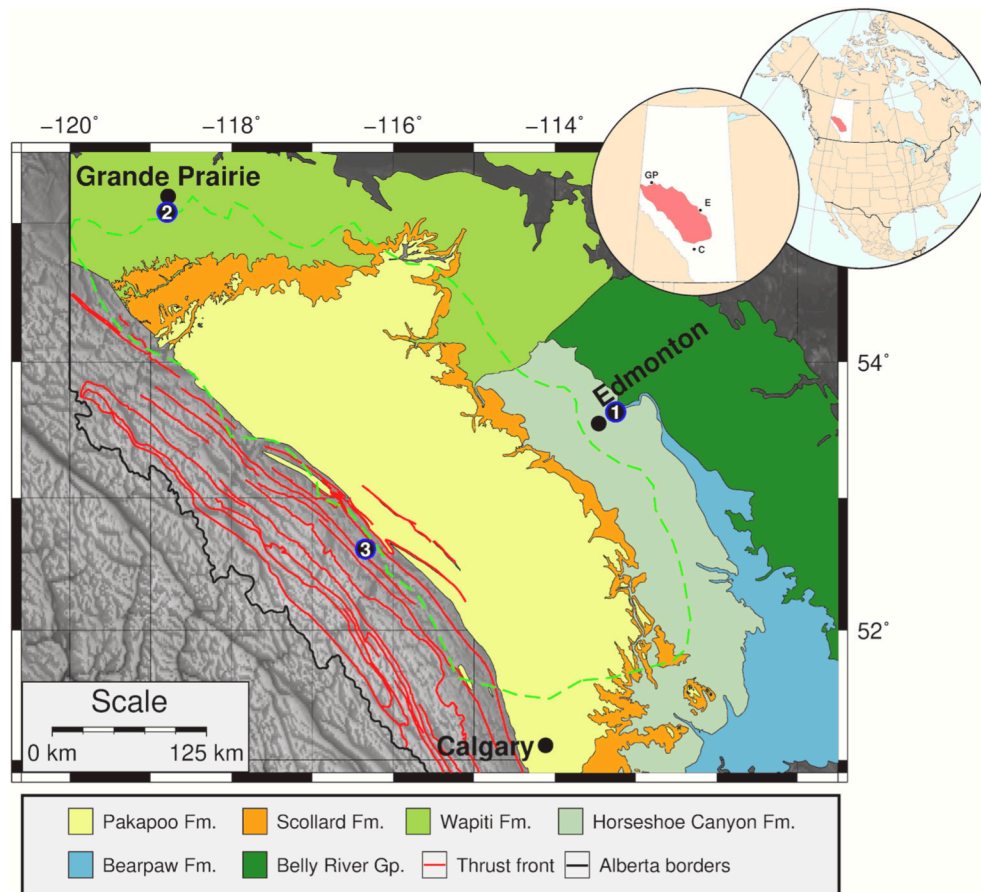


Fig. 1. Geological map of west-central Alberta with evidence of major external and foothills thrust fronts. Numbered circles indicate reference exposures for the studied interval (1 = Riverbend, 2 = Grande Prairie, 3 = Blackstone River; see Fig. 7). Green dashed line bounds the study area (located in the insets, red area). Background image and vector data: topography from ETOPO1 Global Relief Model (<https://www.ngdc.noaa.gov>) and vectors from the Alberta Geological Survey (modified after <https://www.ags.aer.ca>). (For interpretation of the references to color in this figure legend, the reader is referred to the Web version of this article.)

the province (Fig. 2). In ascending order, formally recognized units include Dinosaur Park Formation (top of the Belly River Group), lower Bearpaw tongue, Strathmore Member (the lower member within the HCFm), upper Bearpaw tongue, and Drumheller Member (HCFm). A third marine tongue introduced by Hamblin (2004) has been recognized by Eberth and Braman (2012) as the ‘Dorothy Tongue’, which occur to the south of our study area and is considered as correlative with the coaly deposits of the Drumheller Member. To the north and west, Wapiti Unit 3 is time equivalent to the maximum extension of the Western Interior Seaway based on sedimentological, radioisotopic, paleontological, and palynological data. Therefore, deposits that characterize Wapiti Unit 3 were interpreted to be correlative with the T-R cycles of the Bearpaw Formation (Fanti and Miyashita, 2009; Fanti and Catuneanu, 2009, 2010; Larson et al., 2018; Koppelhus and Fanti, 2019; Sullivan et al., 2019).

Eberth and Kamo (2020) provided a comprehensive, calibrated chronostratigraphy for the Horseshoe Canyon and Bearpaw formations based on samples acquired in the Red Deer River valley of southern Alberta. New U–Pb CA–ID–TIMS ages confine the Bearpaw–Strathmore interval between 74.308 ± 0.031 and 73.1 ± 0.1 Myr. The Dorothy Bentonite (described in Lerbekmo 2002), which occurs near the base of the upper Bearpaw tongue, resulted in an interpolated age of 73.7 ± 0.1 Myr, further constraining the age of the Strathmore–upper Bearpaw tongue transition (Fig. 2).

3. Data and methods

3.1. Subsurface dataset

To develop a robust stratigraphic scheme, 977 gamma-ray well logs were included in our analyses and arranged in a grid of 31 cross-sections

using IHS software Accumap and Acculog. The average distance between individual wells along the sections is ~10 km, although along reference sections it is often lower than 5 km. We included additional 141 reference wells located within main cross-sections to increase the resolution of our analyses (Fig. 3). Reference well logs available in the literature allowed for a more accurate discrimination of main stratigraphic surfaces. We included exposure-calibrated data available in the literature for the central plains of Alberta (Catuneanu et al., 1997; Eberth and Braman, 2012) as well as for the Grande Prairie and foothills regions (Jerzykiewicz, 1997; Fanti and Catuneanu, 2009, 2010) (Fig. 1). The sequence stratigraphic nomenclature and classification in this paper follow Catuneanu (2017, 2019a,b).

3.2. Criteria for well log correlations

As neither continuous nor large cores were available for the study area, the three-dimensional dataset presented here was created from the identification of major stratigraphic unconformities and marker beds. In ascending order, we identified the following stratigraphic markers: base of the Belly River Group (datum); base of the lower Bearpaw tongue on top of the Dinosaur Park Formation (and correlative deposits); maximum flooding surface (MFS) of the lower Bearpaw tongue; base of the Strathmore Member (Horseshoe Canyon Formation) on top of the lower Bearpaw tongue (and correlative deposits); base of the upper Bearpaw tongue on top of the Strathmore Member (and correlative deposits); MFS of the upper Bearpaw tongue; base of the Drumheller Member on top of the upper Bearpaw tongue (and correlative deposits).

A robust and unequivocal stratigraphic framework of non-marine successions based exclusively on geophysical data is commonly difficult to obtain given the limited lateral extent of fluvial depositional elements. As the Wapiti Formation deposits are primarily fluvial in origin,

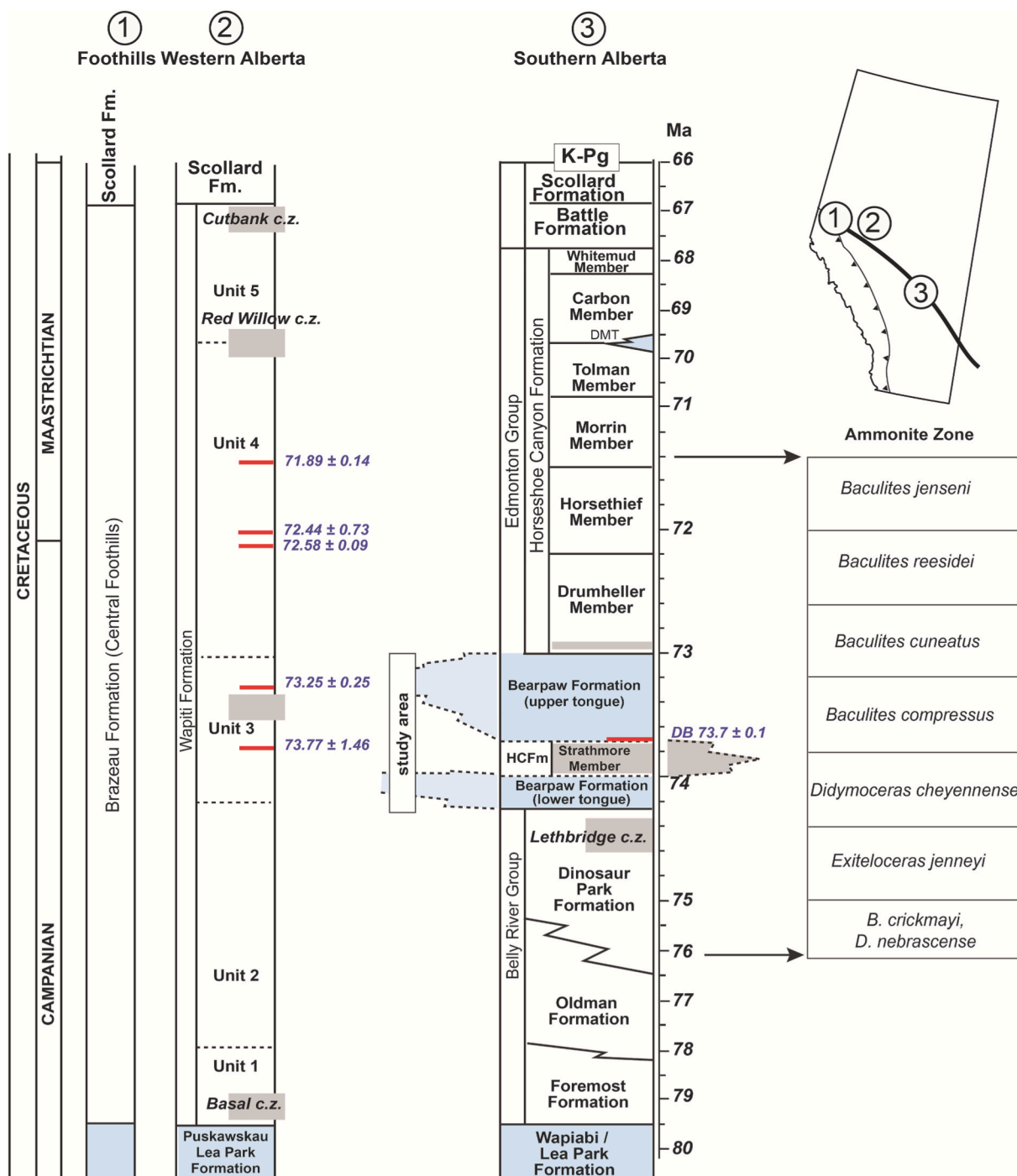


Fig. 2. Campanian to Paleogene lithostratigraphy and stratigraphic nomenclature for the study area (after Fanti and Catuneanu, 2009; Eberth and Braman, 2012), with indicated age constraints of the Bearpaw interval in southern Alberta. Red lines mark dated bentonites and grey squares indicate major coal zones (after Eberth, 2005; Currie et al., 2008; Fanti and Miyashita, 2009; Bell et al., 2014; Fanti et al., 2015; Eberth and Kamo, 2020). Marine reference formations in light blue. DB, Dorothy Bentonite. (For interpretation of the references to color in this figure legend, the reader is referred to the Web version of this article.)

their correlative deposits discussed here are based on the identification of stratigraphic markers, corroborated by the occurrence and lateral mappability of coal seams/zones, bentonites, distinctive lithological contacts, and proximity to exposures. The area located to the south of Edmonton is object of substantial literature that provide solid constraints for this study (Catuneanu et al., 1997; Jerzykiewicz, 1997; Eberth and Braman, 2012; Hathway, 2016). Following previous studies, beds exposed along the North Saskatchewan River valley north of Edmonton (WGS84: 53.675457, -113.294843) were examined for this study. The north-western limit of the study area is represented by the

Grande Prairie region (Fig. 3), roughly in correspondence with the Wapiti River valley. Critical stratigraphic, paleontological, and chronostratigraphic data for this area have been made available in recent publications (Fanti, 2009; Fanti and Miyashita, 2009; Fanti and Catuneanu, 2009, 2010; Bell et al., 2013, 2014; Fanti et al., 2015; Bell and Currie, 2016; Larson et al., 2018; Koppelhus and Fanti, 2019; Sullivan et al., 2019). To the south, previous studies in the foothills of southern Alberta documented the occurrence of upper shoreface and coastal marsh sediments related to the transgressive-regressive phases of the Bearpaw Formation at approximately 71 Myr (Jerzykiewicz et al.,

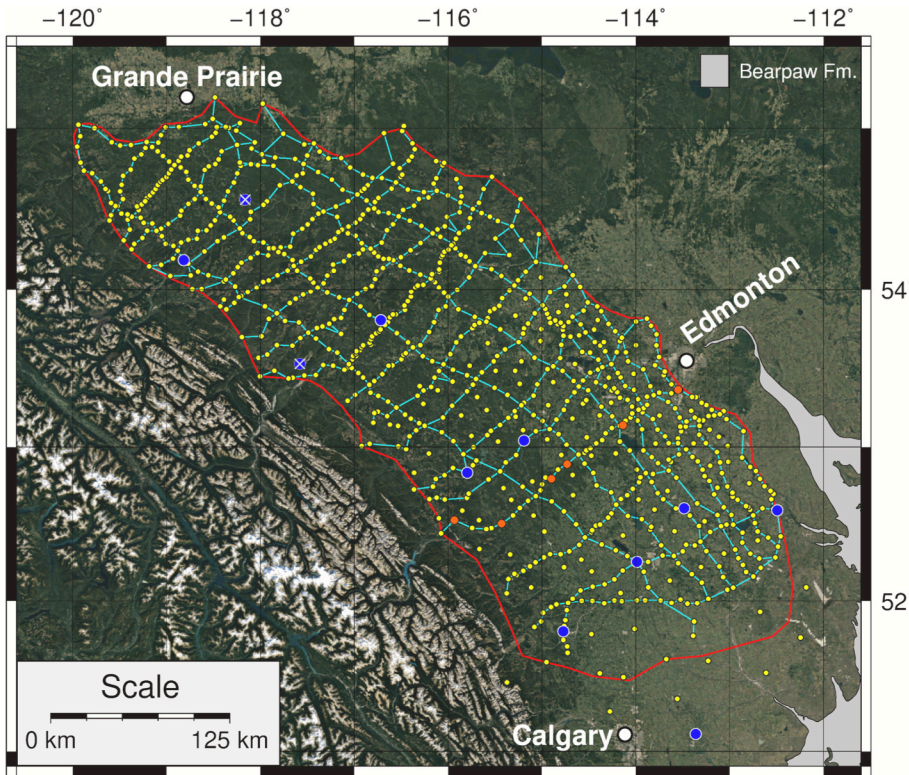


Fig. 3. Sections (light-blue) and well logs (yellow) used in this study, projected on a Google Earth satellite image. The area in grey represents the distribution of the Bearpaw Formation (see Fig. 1). Well logs indicated with blue dots have been used to compare depth correlations from this study and literature. Reference well logs are reported in Table 1 (crossed blue dots correspond to UWIs marked with an asterisk). Reference well logs shown in Fig. 4 are marked as orange dots. UWI = Unique Well Identifier. (For interpretation of the references to color in this figure legend, the reader is referred to the Web version of this article.)

1996). Correlative marginal marine sediments were reported farther north along the foothills in correspondence with major thrusts (i.e., Crowsnest Pass area, Tornado Mountain, Fording River, Blackstone River areas (see also Jerzykiewicz and Sweet 1986, 1988; Jerzykiewicz

1992, 1996, 2010; Dawson et al., 1994; Jerzykiewicz et al., 1996; Jerzykiewicz pers. comm. 2020).

Reference surfaces were marked on each well log to generate a dataset with georeferenced depths. The identification of each

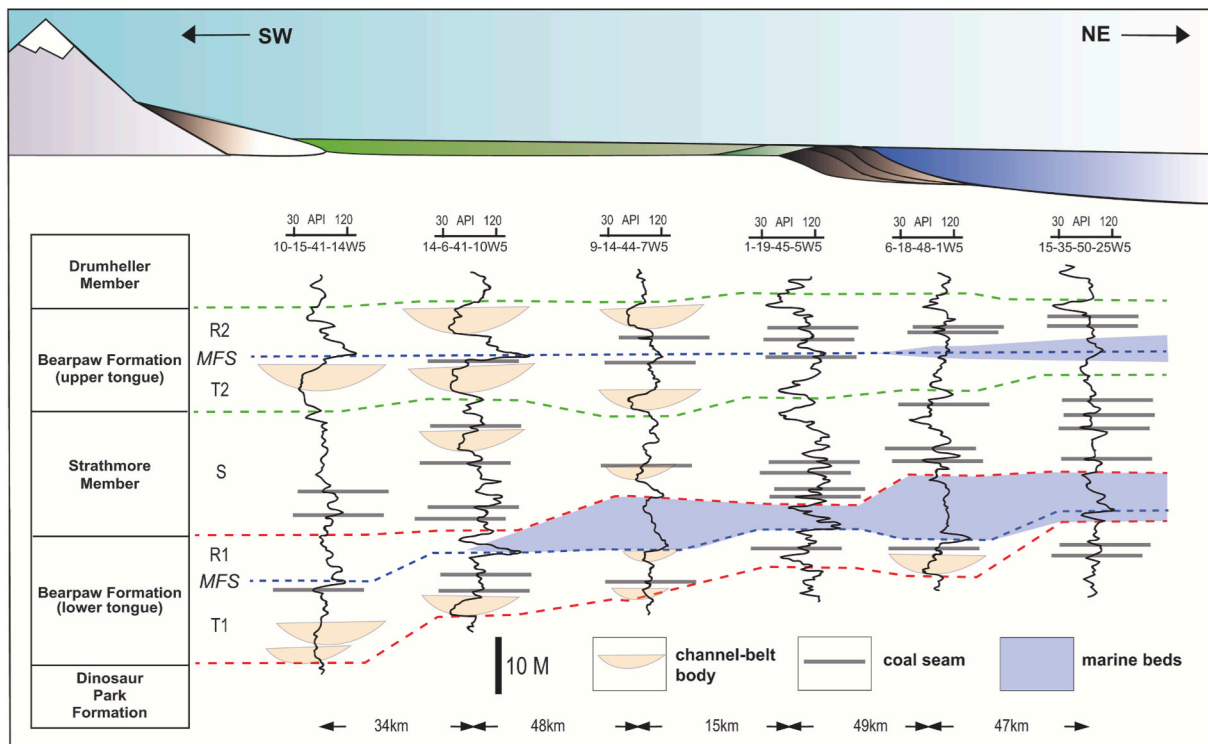


Fig. 4. Gamma-ray stratigraphic cross section illustrating the overall geometries, stacking patterns and stratigraphic surfaces (dashed lines) discussed in this paper. The stratigraphic datum is the Maximum Flooding Surface (MFS) of the Bearpaw Formation upper tongue. API = American Petroleum Institute units. See the reference map in Fig. 3 for the location of wells.

stratigraphic marker was the main tool used to infer non-marine sequence stratigraphic patterns related to the Bearpaw events in the study area. The stratigraphic relationships of such surfaces are shown in Figs. 4 and 5. For this study, the delineation of T-R sequences resulted the simplest approach to stratigraphic analysis. We used maximum flooding surface signatures within the Bearpaw Formation (lower and upper tongue) as primary reference surfaces. Although the identification of MFS signature across the study area allows for discussion of genetic stratigraphic sequences, this approach would limit observations to a fraction of the Bearpaw stratigraphic interval. Data collected for this study improved the resolution of observations by identifying the TS and RS surfaces for each cycle and the scheme of their expression is reported in Figs. 4 and 5. Consequently, for each tongue we discuss two juxtaposed systems tracts, transgressive (TST) and regressive (RST).

3.3. Tridimensional processing

Reference stratigraphic surfaces were identified and marked on each log using IHS softwares, exported and interpolated using GMT 5.4.5 (Generic Mapping Tools) scripts. The new dataset provided accurate Digital Elevation Models (DEM) with depths referred to modern sea level datum. Surfaces were reconstructed using a Green's function-based interpolation method (Wessel, 2009). We obtained a thickness map of six consecutive stratigraphic intervals with pixel-based subtractions of pairs of subsequent DEMs. 3D processing permitted to perform multiple analyses on acquired xyz coordinates, including cumulative thicknesses of selected stratigraphic intervals, variation in accumulation with respect to selected surfaces (isopachs) and volumetric measurements. This tridimensional reconstruction served as reference for the comparison with hydrocarbon fields distribution.

4. Results

4.1. Thickness distribution from the base of the Belly River group to the base of the Bearpaw lower tongue TST

The Puskwaskau-Wapiti contact (correlative of the Lea Park–Belly River contact) is used as datum. Fanti and Catuneanu (2009, 2010) discussed this transition from marine to continental deposits based on

multiple exposures and well-log signatures in west-central Alberta. The stratigraphic interval delimited by the datum and the base of the Bearpaw lower tongue, proved to be crucial in testing the occurrence of anomalies in the depositional setting of the study area, such as those related to tectonic deformation. In the study area, subsurface units develop at a very low angle and conformably with respect to the datum plane. Three-dimensional reconstruction of stratigraphic surfaces and thickness variations in this interval supports an overall homogenous setting for the Belly River and correlative Wapiti deposits in the study area. This preliminary test was necessary to trace the subsequent stratigraphic surfaces and unit thicknesses in the selected stratigraphic intervals (Fig. 6). From the base of the Belly River Group to the base of the Bearpaw lower tongue (Fig. 6-A) it is possible to recognize three major areas of thickness distribution that develop parallel to the modern Rocky Mountains deformation front: > 400 m (4% of the area), 300–400 m (67% of the area), and <300 m (29% of the study area). Overall thickness decreases rapidly from the SW towards NE. We observe higher accumulation in the internal areas that correspond to major modern sediment inputs, suggesting that major sediment inputs were perpendicular to the raising cordillera (e.g. Putnam, 1993). This pattern suggests that sediment inputs and transport were primarily oriented along a SW-NE direction during the Campanian. By examining the map of the Belly River Group (Fig. 6A) it appears that the thickest succession is in the central area of the basin that corresponds to the main location of the oil fields named Peco and Pembina East (Putnam, 1993).

4.2. Thickness distribution of the Bearpaw lower tongue TST (T1)

This interval includes deposits stratigraphically bounded by the base of the Bearpaw lower tongue and its MFS. Isopach map of T1 highlights a heterogeneous distribution of sediment, with values ranging from 1 m to a maximum of 20 m. Values < 5 m cover 41% of the study area, whereas 52% is covered by 5–10 m thick deposits, and 6% by deposits thicker than 10 m. The latter are primarily localized in the northern part of the study area (Fig. 6-B) and are organized in elongated belts, oriented SW-NE. To the south, lower accumulation (<5 m) characterizes most of the study area, where patches of thicker sedimentary bodies (5–20 m) are randomly distributed. This area with lower accumulation covers the central area of the Belly River clastic system entrapping oil migration

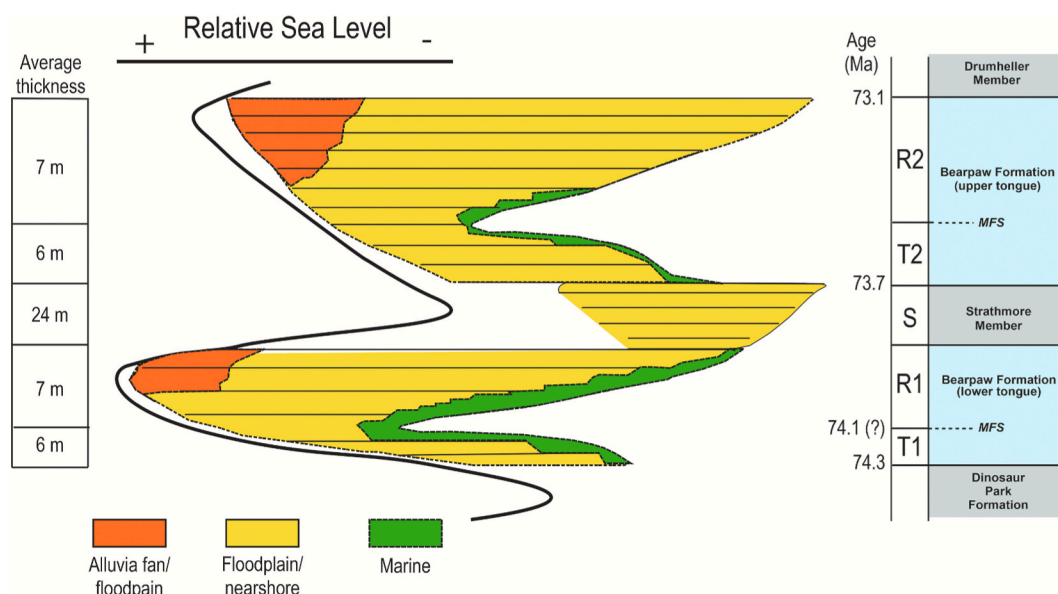
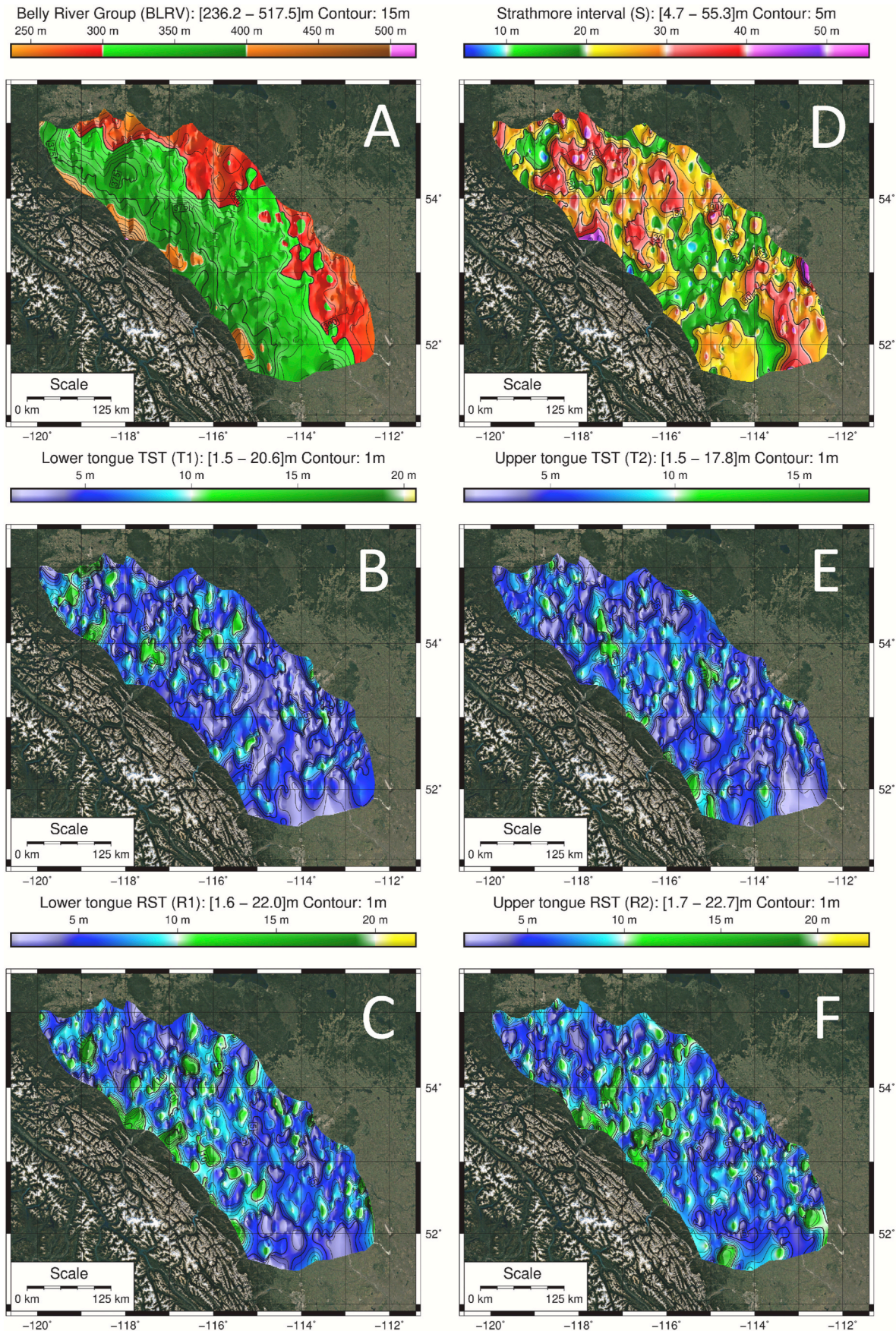


Fig. 5. Chronostratigraphic chart of the Bearpaw Formation stratigraphic interval. The TST and RST for the lower and upper Bearpaw tongues (and correlative deposits) are indicated as T1/R1 and T2/R2, respectively. Strathmore interval (S) is defined as accumulation between the top of R1 and the base of T2. Absolute dating and average thickness for each interval are indicated (Eberth and Kamo, 2020). The variation in lithologies, based on gamma ray logs, and the depositional architecture are interpreted as products of changes in relative sea level (see discussion in the text).



(caption on next page)

Fig. 6. Thickness distribution maps for the six analyzed intervals represented with different color scales. Shaded relief illumination is doubled to emphasize the geometry of deposits, light comes from northeast and from southeast. Thickness ranges [min-max] are indicated. The color palette is reported above each map. The color palettes of the T1-R1 and T2-R2 maps are the same. A) Belly River Formation shows the inherited substratum for the subsequent accumulation depicted by the described intervals forming the Bearpaw succession. The base of the Belly River Group has been used as datum for the correlations. B) Thickness of the Bearpaw lower tongue TST (T1) is on average 6 m. C) Thickness of the Bearpaw lower tongue RST (R1) is on average 7 m. D) Thickness of the Strathmore interval (S) up to the base of the Bearpaw upper tongue is on average 24 m. E) Thickness of the Bearpaw upper tongue TST (T2) is on average 6 m. F) Thickness of the Bearpaw upper tongue RST (R2) is on average 7 m. (For interpretation of the references to color in this figure, the reader is referred to the Web version of this article.)

(Fig. 6-B). Estimated volume of sediment accumulated during this interval is 565 km³, with an average thickness of 6 m (Fig. 5).

Geological samples representative of this interval were collected at Riverbend (North Saskatchewan River valley, north-east of Edmonton) and consist of dark grey shales rich in sponge spicules (Fig. 7-A). The MFS that bounds this interval has been locally used by previous authors to mark the Belly River (Dinosaur Provincial Park Formation) - Bearpaw transition, making it hard to document accumulation trends during the thin and geographically discontinuous TST of the lower Bearpaw tongue. Fanti and Catuneanu (2009, 2010) integrated subsurface, outcrop, and paleontological data to conclude that the non-marine deposits of Wapiti Unit 3 are correlative with the Bearpaw Formation of central Alberta. Wapiti Unit 3 includes fine-grained floodplain deposits, bentonitic paleosols, lenticular organic-rich mudstones, coal seams, and peat horizons deposited by high-sinuosity aggrading channels (Fig. 7-B). The diverse vertebrate fauna collected from this interval is typical of wet lowland environments dominated by high water table, with taxa referable not only to terrestrial conditions but also to brackish and marine ecosystems (Fanti and Miyashita 2009; Koppelhus and Fanti 2019; Fanti pers. obs, 2020).

4.3. Thickness distribution of the Bearpaw RST lower tongue (R1)

The Strathmore Member – and its correlative deposits across the study area – has been defined as genetically confined by the MFSs of the lower and upper Bearpaw tongues (see also Eberth and Braman, 2012; Hathway, 2016). The high-resolution dataset presented in this study discriminates more detailed accumulation trends within the Strathmore Member. Three discrete phases characterize this interval: R1, prograding S, and T2 (see description in paragraph 4.4 and 4.5). The lower part (R1) includes deposits that mark the transition from the marine Bearpaw shales to the sand and coal-dominated Strathmore beds (Fig. 6-C). The upper boundary of R1 is marked by the top of the coarsening up sequences (Fig. 4). The R1 interval involves sediment volumes comparable with those documented for the T1 interval and thickness from 5 to 20 m. The 68% of the study area is covered by deposits within the range 5–10 m and 12% with a thickness higher than 10 m. Thicker deposits (>10 m) are primarily documented on the western border of the study area. They occur in correspondence with modern sediment inputs, with an overall fan-like plan geometry, extending mainly toward E-NE in the central study area. Estimated volume of sediment accumulated during this interval is 691 km³ with an average thickness of 7 m (Fig. 5).

4.4. Thickness distribution of the Strathmore Member HCFm (S)

Much of the Strathmore Member accumulated between the end of the R1 and the base of T2 of the Bearpaw upper tongue. Isopachs of this stratigraphic interval record the maximum values, exceeding 50 m with an average value of 24 m (Fig. 5). Thicknesses under 20 m cover 29% of the study area, thicknesses between 20 and 30 m cover 49%, and over 30 m cover 22% of the study area. Although most of the thicker deposits (>40 m) are located close to the modern sediment inputs alluvial fans they appear also in the eastern margin of the study area, approximately 60 km to the SE of Edmonton. Isopachs between 20 and 40 m dominate the northwestern part of the study area (Fig. 6-D). Estimated volume of sediment accumulated during this interval is 2365 km³, with an increase of 88% with respect to the T1+R1 interval (entire Bearpaw lower tongue).

4.5. Thickness distribution of the Bearpaw upper tongue TST (T2)

The T2 interval includes deposits from the base of the upper tongue up to its MFS and encompasses sediment volumes similar to the T1 interval. However, the spatial distribution of the deposits changed compared to T1 (Fig. 6-E). Areas with less than 5 m of sediment accumulation cover 34% of the study area, 61% is covered by 5–10 m, and the 5% by deposits thicker than 10 m. The average sediment thickness for this interval is 6 m (Fig. 5). Deposits with less than 5 m in thickness develop roughly SW-NE and extend over larger areas in comparison with T1. Thicker deposits (>10 m) are localized on the western border of the study area and accumulated in the central and southern areas, rather than in northern ones. Lower sediment accumulation (<5 m) is documented in the more external south-eastern sectors of the study area, indicating a remarkable decrease in sediment supply when compared with the preceding S interval (Fig. 6-D). Estimated total volume of sediment accumulated during this interval is 579 km³, a value only 2% higher than T1.

4.6. Thickness distribution of the Bearpaw RST upper tongue (R2)

The R2 interval records sediment accumulation deposited between the Bearpaw upper tongue MFS and the base of the Drumheller Member (and correlative strata). A comparison with the underlying interval does not document a substantial increase in sediment accumulation. Thickness values less than 5 m characterize about the 16% of the study area, 5–10 m represent 72%, and higher values (>10 m) characterize 12%. The area covered with less than 5 m thick deposits is reduced and restricted to narrow patches mainly aligned along a SW-NE direction. During the R2 interval, thick deposits (>10 m) accumulated primarily in the north-central part of the study area. Estimated volume of sediments accumulated during this interval is 700 km³, a value only 1% higher than R1.

4.7. Rates of sedimentation

The stratigraphic interval discussed in this study is representative of approximately 1.2 ± 0.2 Myr, based on recent radioisotopic calibrations presented in Eberth and Kamo (2020). These chronostratigraphic constraints are used here to infer rates of sediment accumulation (RSA) for discrete stratigraphic intervals. The average cumulative not-decompacted thickness of the intervals from T1 to R2 is 51 ± 8 m. As this interval encompasses approximately 1.2 Myr, the averaged RSA is 4.2 ± 0.7 cm/kyr.

Eberth and Kamo (2020) provided the most recent estimations of RSA for the Late Cretaceous of Alberta. Such values are claimed by the authors to be consistent throughout the Dinosaur Park, Bearpaw, and lower Horseshoe Canyon formations; the provided RSA for this entire interval is 8.1 cm/kyr (196 m/2.425 Myr). Eberth and Kamo (2020) pointed out that 8.1 cm/kyr is a relatively high rate compared to southern Alberta Upper Cretaceous non-marine sections (cf. 3.5–4.8 cm/kyr reported by Eberth, 2005), and Lerbekmo et al., 2005). RSA documented in our study area are not comparable to those estimated by Eberth and Kamo (2020), or with those presented in Eberth (2005) and Lerbekmo et al. (2005) for the uppermost Belly River Group. Although the discrepancies in RSA values likely relate to different geographic areas, to the extension of Bearpaw marine tongues (i.e. southern vs central and western Alberta), and to a combination of multiple

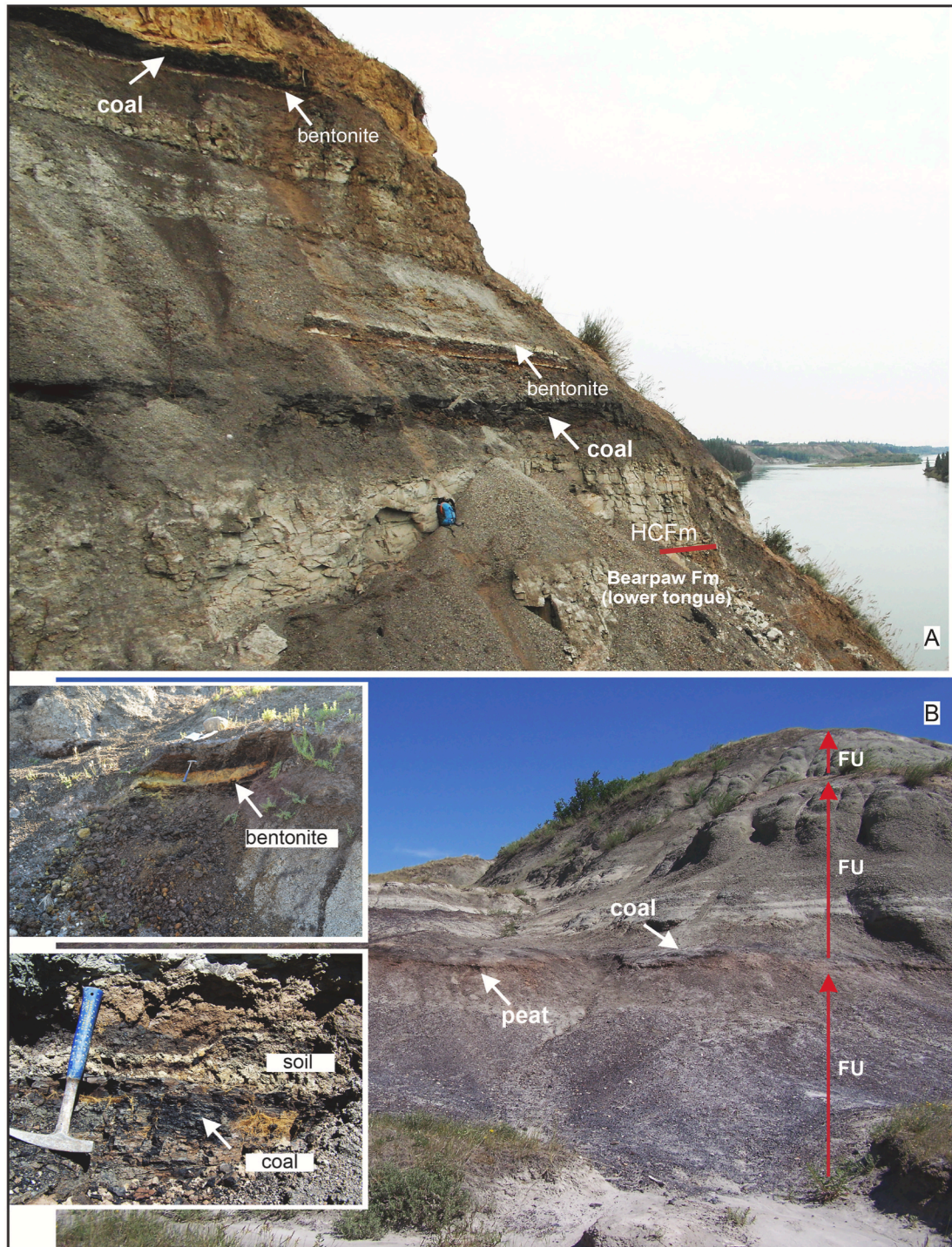


Fig. 7. A) Bearpaw Formation (BPFm) shale overlain by Horseshoe Canyon Formation (HCFm) basal sandstones near Riverbend (Edmonton). Base contact of the HCFm is marked by the red line, followed by 2.2 m thick grey sandstones. Upsection coal seams and bentonitic paleosols are indicated. In the lower part of the outcrop, the contact between Belly River Group fine sands and BPFm was found 6 m under the HCFm – BPFm contact. B) Non-marine deposits of the Wapiti Formation Unit 3 near Grande Prairie, Alberta. Fine-grained, silt-dominated channel deposits are interbedded with mudstones, tabular peat, coal seams, and bentonitic paleosols (see text for descriptions). FU, fining upward. (For interpretation of the references to color in this figure, the reader is referred to the Web version of this article.)

depositional settings (i.e., marine, paralic, fluvial, coal zones, etc.), the dataset presented in this study refines the RSA estimates for more discrete depositional intervals. The upper tongue of the Bearpaw Formation accumulated between 73.7 and 73.1 Myr (Eberth and Kamo, 2020) and in our study area includes on average 13 m of deposits. Therefore, the RSA for the upper Bearpaw Formation tongue would be

close to 2 cm/kyr. Radioisotopic ages indicate that the transgressive part of the lower Bearpaw Formation tongue accumulated between 74.3 and 74.1 Myr, with an average accumulation of 6 m, indicating a RSA value of 3 cm/kyr. The deposition of the prograding component of the Strathmore Member (R1+S) encompasses approximately 400 Ka (between 74.1 and 73.7 Myr), with an average accumulation of 32 m. The

RSA value for this interval is therefore close to 8 cm/kyr, although 80% of deposits accumulated during the progradation of the Strathmore lobes. RSA values for the Bearpaw Formation are therefore comparable with those estimated for southern Alberta (Eberth, 2005; Lerbekmo et al., 2005), although they change substantially when referred to specific transgressive or regressive phases.

5. Discussion

5.1. Cumulative maps and sediment distribution

Isopach and cumulative thickness maps of sediment accumulation (Figs. 6 and 8 respectively) derived from the 3D database allowed documenting the spatial distribution through time of sedimentary bodies during the Bearpaw T-R cycles. Changes in sediment accumulation are likely products of changes in relative sea level and the development of TST and RST systems tracts (Fig. 5).

T1. The distribution of sediments of the TST of the lower Bearpaw tongue shows a uniform deposition draping the uppermost Belly River Group and equivalent deposits (Fig. 8-A and B). Overall geometries show minor differences from the underlying unit arranged as large lobe/fan-like bodies measuring up to 100 km in width with more accumulation occurring in the northern sectors of the study area. The most distinctive alluvial fan systems are located along the present-day Smoky River. Thickness maps revealed multiple areas of major sediment accumulation in the foothills region near the present-day deformation front. From south to north, these areas are roughly located along the Tay and Panther rivers, North Saskatchewan River and Athabasca River. We identify two areas characterized by low accumulation in the eastern and northwestern margin of the study area. The basal deposits of the lower Bearpaw tongue are extensively documented for southern Alberta, Saskatchewan, and Montana where they are consistently characterized by a sharp and distinctive well-log signature, the juxtaposing of marine mudstone directly on top of coal-dominated beds, and a rapid transition into stacked coarsening upward marine, mud-dominated sequences (Catuneanu et al., 1997; Glombick, 2010; Rogers et al., 2016; Hathway, 2016; Street et al., 2019). Although this transition records a rapid change in the depositional settings (T1 represents approximately 200 kyr), no evidence of relevant disconformities has been reported in the literature nor observed in the study area, with the exception of a discontinuous ravinement surface (Catuneanu et al., 1997). In southern Alberta, the upper Dinosaur Park Formation records the transgression of the Bearpaw Formation and is dominated by tidally-influenced estuarine valley-fills associated with higher frequency changes in relative sea level (Eberth, 2002). The top of the Dinosaur Park Formation is represented by the Lethbridge coal zone, which developed as a result of rising water-table levels associated with the early transgressive phases of the Western Interior Seaway, and is characterized by laterally continuous coal seams. In southern Alberta and near the city of Edmonton, the basal contact of the lower Bearpaw tongue (Catuneanu et al., 1997; Glombick, 2010; Hathway, 2016; and references therein) is overlain by coarsening-upward intervals of silty mudstone with minor siltstone and sandstone (Eberth, 2005; Chen et al., 2005; Eberth and Braman, 2012; Hathway, 2016). This study indicates that during the TST of the lower Bearpaw tongue, west-central Alberta experienced higher sediment supply and accumulation compared to the historic study areas to the south.

R1. This interval represents the regressive stage (RST) of the Bearpaw lower tongue and correlative non-marine beds of the Strathmore Member of the Horseshoe Canyon Formation. Data support a more pronounced partitioning of the study area into northern, central and southern sectors. Cumulative map (Fig. 8-C) indicates overall accumulation trends, with a basinward shift of depositional systems located in the central foothills, primarily between the Brazeau and Athabasca rivers. In the north, low accumulation persists in the distal part with minor progradation. The central area marks high sedimentation in the

foothills that gradually decreases distally. In the southern sector we observed a progradation of the foothills system and a vast area of low accumulation located to the south of Edmonton, which is consistent with the occurrence of fine-grained, muddy sediments. At the time of writing, this interval has not been documented in outcrop. Eberth and Braman (2012) indicate that the lower deposits of the Strathmore Member in southern Alberta include mainly coal and non-marine carbonaceous shales, based on well-log signatures.

S. The isopach maps show a progradation of all depositional systems toward NE. In the foothills, high-accumulation areas extend up to a third of the study area and particularly along the Smoky, Athabasca, and Brazeau rivers and south of the North Saskatchewan River (Fig. 8-D). In the northern section, despite an overall progradational trend, an area of low-depositional rates persists east of the town of Grande Prairie. Major shifts in sediment accumulation are mapped in the central part of the area. The southern sector is less influenced by the overall prograding trend, including accumulation in the foothills area.

In the Edmonton area, the stratigraphic interval encompassing the lower Bearpaw tongue, Strathmore Member, and upper Bearpaw tongue has a thickness of approximately 50 m (Chen et al., 2005; Eberth and Braman, 2012; Hathway, 2016) and is dominated by alternating marine shales and coal-rich, paralic deposits. Published data about the depositional geometries of the Strathmore Member suggest progradation toward the south, where large (>130 km in diameter) lobes with an eastward pinch-out have been documented (Eberth and Braman, 2012). The position of the maximum regressive shoreline of the Strathmore Member identified from our dataset is consistent with data presented by Eberth and Braman (2012) for the Red Deer area, with a NW-SE orientation. Cross-sections available for the southern part of the study area support aggradation during the deposition of the Strathmore Member, although little has been discussed about its genetic interpretation. Based on our dataset, we conclude that this discrete interval corresponds to the highest accumulation rates of the Strathmore Member.

T2. This interval deposited during the transgressive component of the Bearpaw upper tongue. Isopachs indicate minor variation in sediment distribution across the study area, except for the central sector where a shift toward NE is apparent in both proximal and distal sections (Fig. 8-E). The northern sector still displays persistent areas of low sediment accumulation. Similar to the lower Bearpaw tongue, the onset of the second marine incursion in the study area is not represented by a sharp shift in lithologies and depositional settings. Basal sequences of this interval include a diverse array of deposits, including organic-rich mudstones, coal seams, and isolated channel bodies. The T2 interval differs from T1 in lacking a clear marine component, rather representing a widespread increase in the water table resulting in finer deposits and extensive coal zones. Such conditions persisted through the deposition of the Strathmore Member, although sediment accumulation increased remarkably during the S interval (see above). The lower Bearpaw tongue is characterized by tabular strata, whereas the upper tongue includes large clinoform geometries (Eberth and Braman, 2012; Hathway, 2016; this study). New paleogeographic and paleoecological reconstructions for the Campanian in Alberta provide new insights to understand the major faunal turnover in Alberta (Ryan and Evans, 2005; Mallon et al., 2012; Eberth et al., 2013).

R2. This interval records the final regressive stages of the Bearpaw Formation in the study area. Sedimentary input from the foothills became homogeneous, also documenting the final stage of the Bearpaw regression in the southern sector (Fig. 8-F). Areas of low accumulation persist near Grande Prairie and southeast of Edmonton, suggesting major sediment transport from the orogen without further supply from the foreland area. In central Alberta, the upper Bearpaw tongue T-R cycle encompasses approximately 600 kyr (Eberth and Kamo, 2020). Pending further chronostratigraphic controls on the Strathmore Member, data presented in Eberth and Kamo (2020) indicate that the upper tongue represents at least half of the entire time of deposition of the Bearpaw Formation and roughly twice the time of the lower tongue.

Fig. 8. Cumulative thickness maps of the Bearpaw succession highlighting the progressive variation of accumulation in the study area. Shaded relief illumination is doubled to emphasize the geometry of deposits, light comes from northeast and from southeast. Color palette shows same thickness intervals in each map. Black arrows indicate the relative magnitude and inferred shift of sediment accumulation. Red dashed lines bound the northwestern, central, and southwestern areas discussed in the text. A) Cumulative thickness map of the Belly River interval whose base is used as datum. B) Cumulative thickness map from the datum to the lower Bearpaw tongue MFS; higher accumulation areas are arranged as lobes. Low accumulation is recorded in the eastern margin of the area. C) Cumulative thickness map from the datum to the top of R1, showing a moderate basinward shift of the accumulation, mainly developing in the central sector. D) Cumulative thickness map from the datum to the top of the Strathmore interval. Northeastward progradation is strongly pronounced in the central sector. E) Cumulative thickness map from the datum to the upper tongue MFS. Minor accumulation leads to quite null geometric variations in sediment stacking pattern. F) Cumulative thickness map from the datum to the final regression (R2). Filling up of the southern sector is achieved, whereas low accumulation persists to the north. (For interpretation of the references to color in this figure, the reader is referred to the Web version of this article.)

5.2. Paleogeography of the Bearpaw Formation

The new dataset presented in this study, combined with detailed analyses of sediment distribution offers the opportunity to infer the paleogeographic evolution of the Alberta Basin during the Bearpaw time (Fig. 9). We recognize three adjoining areas characterized by distinctive trends. Near the foothills, the proximal (western) area deposits consist of coarse, lenticular or laterally interfingering and amalgamated bodies. Such beds represent multiple stacked and laterally amalgamated fluvial channel sandstones and lack coal horizons (Jerzykiewicz and McLean, 1980; Jerzykiewicz, 1992; Fanti, 2009; Fanti and Miyashita, 2009; Fanti and Catuneanu, 2009; Sullivan et al., 2019; Jerzykiewicz, pers. Comm. 2020).

To the east, in the central area, the depositional architecture of channel bodies displays less laterally-amalgamated sandstone bodies, with an increase in single, fining-upward bodies interbedded with finer floodplain deposits. Discontinuous coal seams, interbedded with organic-rich mudstone (crevasse-splay, overbank) suggest accumulation within alluvial plains with high-water table conditions (Fig. 9-A and B). Such alluvial deposits, encompassing the larger part of the study area, are distally delimited by a narrow area characterized by stacked and high-frequency coarsening upwards trends during regressive phases. Tabular and laterally continuous sand bodies, possibly linked to littoral sandbars, can be mapped in this area. Cross-sections indicate extensive coal zones interfingering with claystone and siltstone deposits, as documented in the southern plains for the Strathmore Member deposits. The gamma ray signatures in this area are consistent with transitional deposits typical of coastal environments such as backswamps, estuaries, and barrier-lagoons. As this interval is critical to our understanding of the geographic extent of the Bearpaw Formation during its two T-R cycles, 28 wells were combined to document the vertical characterization of deposits, and the along-dip variation in lithologies and depositional architecture (Fig. 9 and Table 1). Eastward of these wells, in the eastern distal area, the MFS expression on gamma ray logs is more consistent (even between distant logs), possibly due to the homogenization related to the increase in marine influence. Sediment distribution patterns suggest complex environmental transitions, strongly evocative of tidal embayment with vast submerged areas. We recognize a distal area with distinctive upward-coarsening then fining sequences (CU-FU), clear MFS signature and homogeneous finer sediments that likely pertained to a fully marine setting.

The paleogeographic maps presented in Fig. 9 allow the reconstruction of the geographic extent of the Bearpaw T-R events (Bustin and Smith, 1993; Dawson et al., 1990, 1994; Cobban et al., 1994; Roberts and Kirschbaum, 1995; Jerzykiewicz, 1997; Eberth and Braman, 2012; Slattery et al., 2015; Hathway, 2016; Blakey and Ranney, 2017) and highlight how they differ in terms of depositional environments in Alberta. The marine part of the lower Bearpaw tongue is widely distributed in the study area and its western boundary runs almost parallel to the deformation front. Coastal zones are narrowly elongated from the NW to the SE. On the contrary, marine deposits of the upper Bearpaw tongue are confined to most distal sectors of the study area. This paleogeography is inherited from the maximum extent of the prograding Strathmore Member and displays a complex geographic distribution of coastal-transitional environments. Possible shallow-marine

conditions persisted to the north-west of Edmonton during this interval. Although previous paleogeographic maps for this stratigraphic interval depicted our study area either as emerged or with a shoreline confined to the south of Edmonton (Dawson et al., 1990, 1994; Roberts and Kirschbaum, 1995; Eberth and Braman, 2012; Hathway, 2016), our analysis is consistent with the previous interpretation of Fanti and Catuneanu (2009, 2010) and further refine the correlation of the Wapiti Formation with the Bearpaw cycles. Thus, a combination of geological and paleontological data support that marine conditions related to the Bearpaw Seaway in the latest Campanian persisted not only in southern Alberta but also to the north-west, in the Grande Prairie region and possibly toward British Columbia. This interpretation is supported by data introduced in this study, which revise previous hypotheses on the geographic extension of the Western Interior Seaway (Dawson et al., 1990, 1994; Jerzykiewicz, 1997; Catuneanu et al., 1997; Hamblin, 2004; Hathway, 2016).

5.3. Inferences on hydrocarbon prospectivity

The base of the Belly River Group at approximately 80 Myr (Eberth and Deino, 1992; Eberth, 2005; Rogers et al., 2016; Freedman Fowler and Horner, 2015) marks the onset of continuous continental deposition in the Alberta foreland basin from the Campanian onward, with the Bearpaw Formation representing the sole and final exception of marine depositional systems. Data presented here provide reliable tools to discriminate the Bearpaw events and investigate the nature of consecutive T-R cycles in both marine and non-marine realms. The lower Bearpaw tongue is here interpreted as a rapid (almost 300 kyr long) marine incursion dominated by tabular geometries that originated in the shallow, epeiric Western Interior seaway. The transgression resulted in the widespread deposition of fine-grained sediments in marine to tidally-influenced coastal environments. The paleogeographic distribution of the lower Bearpaw tongue (Fig. 9) and its trends in gamma ray curves clearly indicate a rapid drowning of the channel-delta system of the uppermost Belly River units (i.e. Dinosaur Park Formation and lateral equivalents). This is particularly evident in the most oil-productive area corresponding to the Peco and Pembina East fields (Fig. 10A). Such geometries support the interpretation that deposits accumulated during the T1 interval of the Bearpaw Formation acted as effective seal of those fields (Fig. 10B). In post-Bearpaw units, almost exclusively coalbed methane and water have been found in drilled wells. This indicates that the Cardium oils that sourced the Belly River sands have been prevented to migrate upsection in the permeable Horseshoe Canyon units (including the Strathmore Member).

Continental conditions (i.e. fluvial and coastal marsh sediments) characterize the overlying Strathmore Member (S) that represents less than 400 kyr and includes about 50% of all deposits accumulated during the Bearpaw time (the value refers to our S interval, and rises to 75% if we consider the Strathmore Member as the interval delimited by the MFSs of the lower and upper Bearpaw tongues). A second rise of the base level resulted in the deposition of clinothems forming the upper Bearpaw tongue. Previous studies interpreted such changes in depositional style as the result of changes in flexural subsidence rate and continuous sedimentation across the basin within the range of variations of the rates of base-level rise (Catuneanu et al., 1997, 1999; Fanti and Catuneanu,

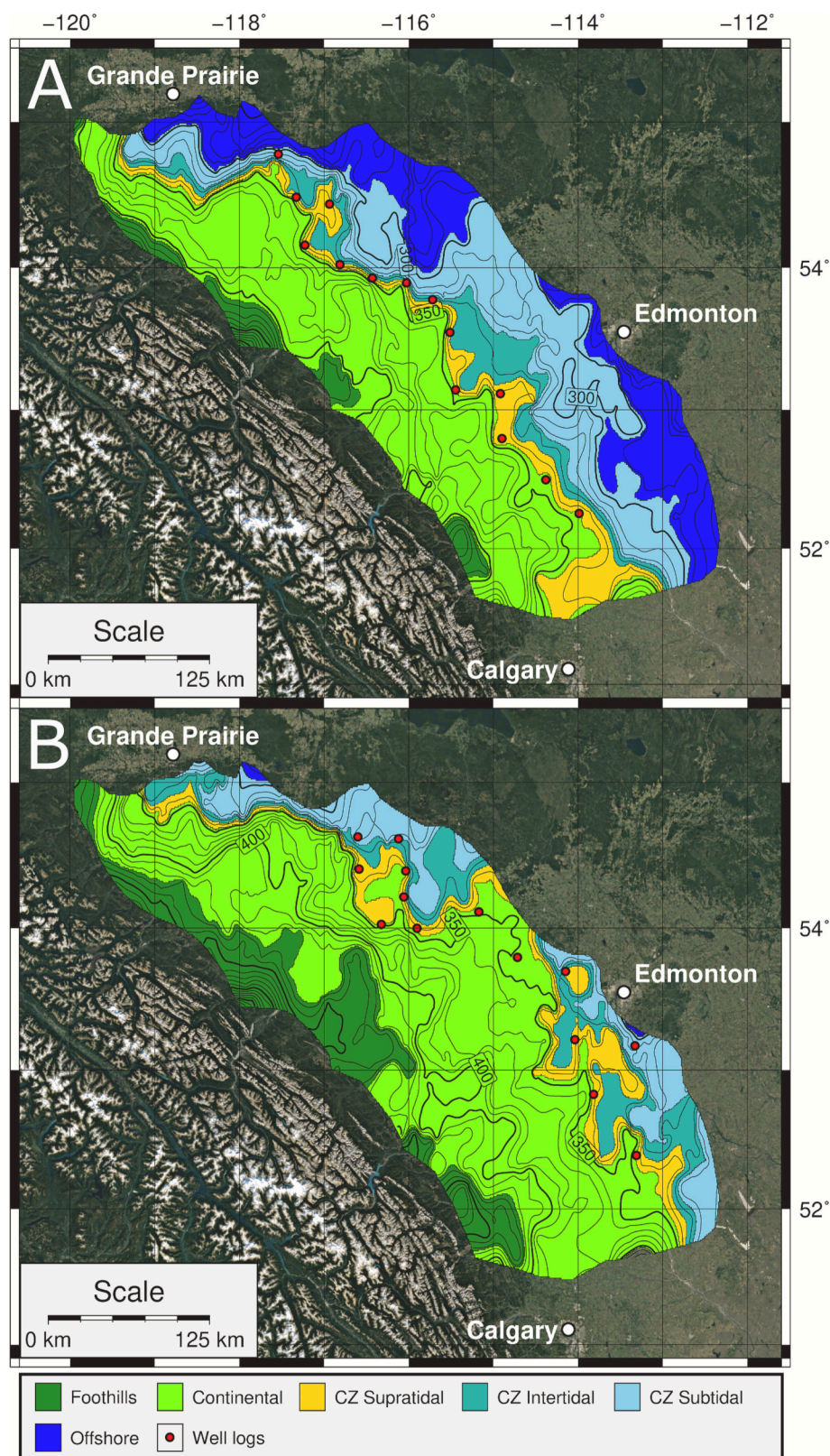


Fig. 9. Paleogeographic maps of the lower (A) and upper (B) tongue MFS surfaces. The isopachs are from the respective cumulative thickness maps T1 and T2 in Fig. 8. Sediment distribution patterns indicate three adjoining areas: 1 - near the foothills, deposits are dominated by coarse, lenticular or laterally interfingering bodies; 2 - typical alluvial deposits are widespread within continental plains; 3 - distal, flat transitional areas include widespread marine signature of the lower Bearpaw tongue (A). Nearshore environments are likely related to a complex development of tidal embayments with vast submerged areas (B). Well logs indicated by red dots (listed in Table 1) mark the eastward shift from subaerial to submerged deposition (in gamma ray trends, see text). CZ = Coastal Zone. (For interpretation of the references to color in this figure legend, the reader is referred to the Web version of this article.)

2010; Hathway, 2016). However, new data discussed in this study support that major eustatic control, combined with local factors, determined the location of depocenters. Three factors are consistent with the latter interpretation. First, new chronostratigraphic constraints document rapid (600 kyr or less) consecutive T-R cycles; second, no

depositional discontinuities have been documented in this interval that, instead, records a gradual shift of lithologies and facies; third, major feeding systems and distribution patterns of sediment remains unaltered throughout the stratigraphic interval. Recent multidisciplinary studies on eustatic sea-level changes during the Cretaceous document similar

Table 1

Reference well logs for this study and the ones used as markers for paleogeographic maps. Well logs marked with an asterisk are not present in our dataset and have been used to further calibrate the depths of the closest available data. Location of reference well logs are indicated with blue dots in Fig. 3. Location of all other reported well logs are indicated with red dots in Fig. 9.

UWI	Marker	Reference	Belly River Group base (m s.l. depth)	Bearpaw MFS Lower tongue (m s.l. depth)	Bearpaw MFS Upper tongue (m s.l. depth)
00/01-11-067-24W5/0	Lower coastal to continental	This study	61.5	364.8	415.8
00/16-30-063-22W5/0	Lower coastal to continental	This study	-144.2	192.7	238.1
00/10-10-063-20W5/0	Lower coastal to continental	This study	-117.6	232.3	267.7
00/08-02-060-22W5/0	Lower coastal to continental	This study	-390.1	-52.5	-9.4
00/16-19-058-19W5/0	Lower coastal to continental	This study	-415.7	-81.0	-36.7
00/09-15-057-17W5/0	Lower coastal to continental	This study	-299.0	38.8	75.8
00/06-04-057-14W5/0	Lower coastal to continental	This study	-226.7	111.5	157.6
00/02-28-055-12W5/0	Lower coastal to continental	This study	-192.0	148.0	181.5
00/06-02-053-11W5/0	Lower coastal to continental	This study	-272.5	65.0	111.8
00/09-18-048-10W5/0	Lower coastal to continental	This study	-485.9	-141.1	-116.0
00/11-02-048-07W5/0	Lower coastal to continental	This study	-285.5	56.2	85.3
00/09-14-044-07W5/0	Lower coastal to continental	This study	-432.9	-97.6	-64.8
00/05-04-041-03W5/0	Lower coastal to continental	This study	-327.3	21.3	52.6
00/10-07-038-28W4/0	Lower coastal to continental	This study	-194.5	153.4	177.2
00/09-14-065-18W5/0	Upper coastal to continental	This study	77.2	355.6	392.6
00/09-12-065-15W5/0	Upper coastal to continental	This study	166.0	462.6	493.0
00/10-35-062-18W5/0	Upper coastal to continental	This study	-45.4	241.4	287.5
00/10-28-062-14W5/0	Upper coastal to continental	This study	26.2	326.0	375.7
02/07-29-060-14W5/0	Upper coastal to continental	This study	-45.2	248.9	292.6
00/06-21-058-16W5/0	Upper coastal to continental	This study	-206.6	102.4	144.4
00/06-08-058-13W5/0	Upper coastal to continental	This study	-137.2	160.3	205.5
00/04-20-059-08W5/0	Upper coastal to continental	This study	119.3	423.6	466.9
02/12-32-055-05W5/0	Upper coastal to continental	This study	99.0	404.9	438.9
00/12-30-054-01W5/0	Upper coastal to continental	This study	172.7	474.1	509.5
00/10-11-049-01W5/0	Upper coastal to continental	This study	22.5	325.1	358.7
00/10-29-048-23W4/0	Upper coastal to continental	This study	153.8	428.7	466.2
02/14-26-044-27W4/0	Upper coastal to continental	This study	16.5	316.7	358.0
00/13-30-039-23W4/0	Upper coastal to continental	This study	63.6	356.8	408.1
00/07-12-025-25W4/0	Reference well log	Catuneanu et al. (1997)	No Data	437.1	482.5
00/10-04-065-02W6*	Reference well log	Jerzykiewicz (1997)	-194.4	No Data	No Data
00/06-02-056-19W5	Reference well log	Jerzykiewicz (1997)	-524.4	No Data	No Data
00/12-12-047-09W5	Reference well log	Jerzykiewicz (1997)	-436.5	No Data	No Data
00/04-15-060-06W6	Reference well log	Jerzykiewicz (1997)	-658.2	No Data	No Data
00/07-04-053-24W5*	Reference well log	Jerzykiewicz (1997)	-1068.5	No Data	No Data
00/08-34-044-13W5	Reference well log	Jerzykiewicz (1997)	-866.7	No Data	No Data
00/06-03-033-06W5	Reference well log	Jerzykiewicz (1997)	-759.3	No Data	No Data
00/14-02-042-18W4/0	Reference well log	Eberth and Braman (2012)	No Data	595.6	624.4
00/09-11-042-25W4/0	Reference well log	Eberth and Braman (2012)	No Data	351.1	397.1
00/10-07-038-28W4/0	Reference well log	Eberth and Braman (2012)	No Data	153.4	177.2

events (i.e. Schlanger et al., 1981; Miller et al., 2003; 2004, 2011; Haq, 2014 and references therein). Haq (2014) reports two globally documented transgressive-regressive cycles that appear to match with the age of the studied succession: the first roughly between 75.4 and 73.6 Myr (KCa6) and the second approximately between 73.6 and 72 Myr (KCa7; see also Miller et al., 2003; 2004). The paleogeographic evolution of the Alberta basin discussed in this study also raises hypothesis concerning the occurrence of mature hydrocarbons in post-Bearpaw units, as they may have bypassed the relatively thin Bearpaw seal and, thus, might be trapped in the Horseshoe Canyon Formation (including the Strathmore Member). However, to date, coalbed methane and water have been found in large quantities within the post-Bearpaw reservoirs while only small amounts of oil have been extracted from those units. This indicates that the Cardium Formation oils that sourced the Belly River sands have been prevented to migrate upsection in the permeable post-Bearpaw units.

During the Bearpaw T-R cycles, lower accumulation rates characterize the northwestern and southeastern margin of the study area (Fig. 8), suggesting locally persistent marine conditions throughout the studied time interval.

Given the occurrence of large channelized fluvial systems within the Belly River Group, such areas may represent a primary target for future prospective activities. The eustatic controls on the deposition of the Bearpaw cycles shed new light on how such controls can be discussed in foreland marine and non-marine successions as effective on hydrocarbon migration and accumulation.

6. Conclusions

Data presented in this study extend the available information on the nature and geographic extent of the Western Interior Seaway in west-central Alberta. This 3D analysis of transgressive-regressive (T-R) cycles documents the reciprocal architecture of marine and non-marine environments with an unprecedented resolution for the Cretaceous. The lower Bearpaw cycle records a rapid transgressive event that lasts ~200 kyr. The upper Bearpaw cycle shows a longer duration of approximately 600 kyr and records a minor rise of the base level. The inferred paleogeography for this interval remained relatively stable compared to the major evolution it underwent during the progradation of the Strathmore Member. During this T-R cycle residual marine conditions seem to persist only in southern Alberta and to the north-west in the Grande Prairie region. The rapid drowning associated with the lower Bearpaw cycle transgression above the channel and delta systems of the uppermost Belly River units, provided an efficient seal and thus played a key role in the formation of the most oil-productive reservoirs within the Belly River Group. In this setting, the Bearpaw Formation represented the sole and final event of marine sedimentation related to the Western Interior Seaway in Alberta, likely occurring because of a major eustatic control rather than tectonic deformation at the observed timescale. In fact, the documented Bearpaw T-R cycles do not show depositional discontinuities, but rather a record of a gradual, eastward shift of the shoreline.

The paleogeographic evolution and the inferred distribution of the

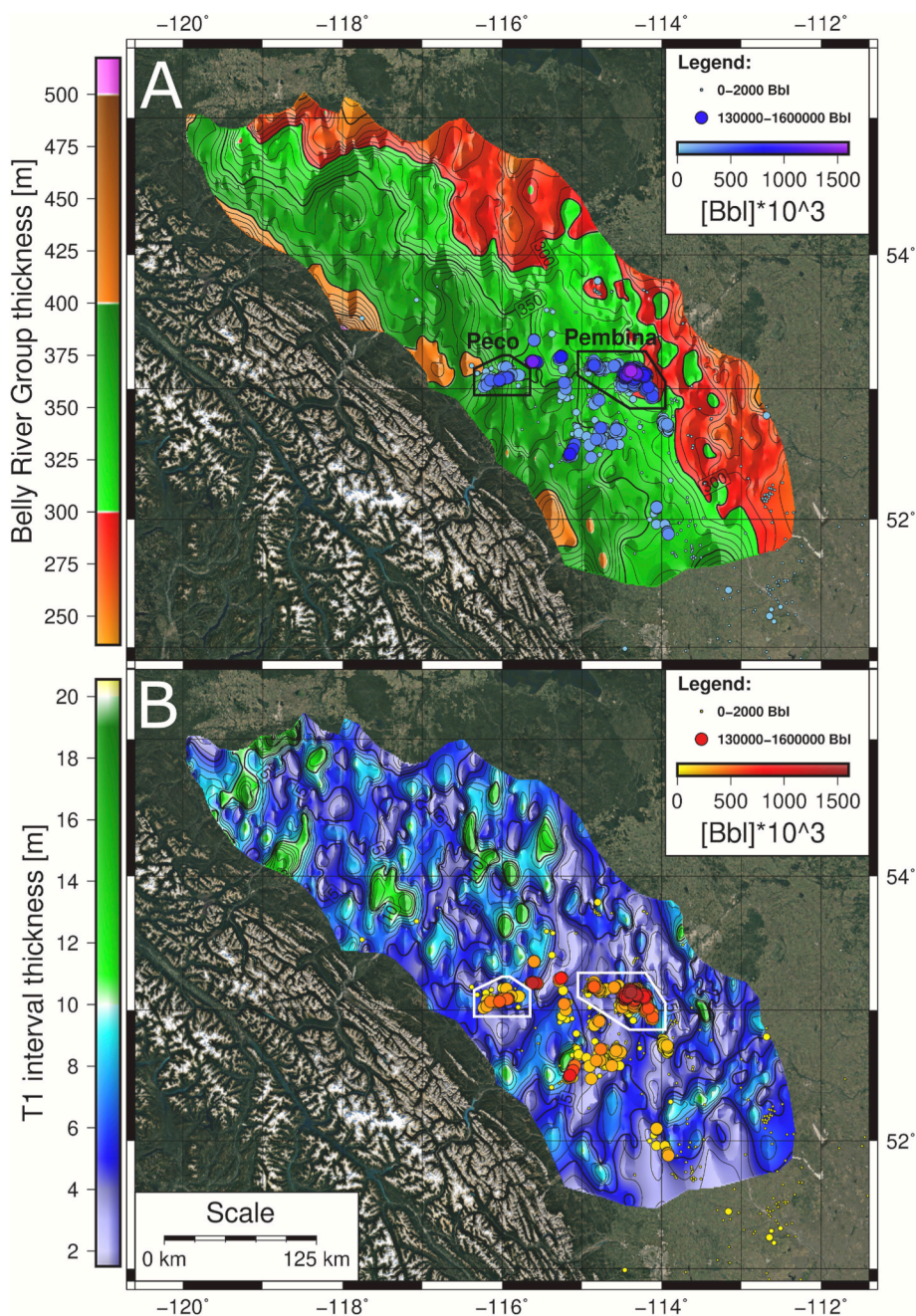


Fig. 10. Productive oil fields from the Belly River Group in Alberta. Shaded relief illumination is doubled to emphasize the geometry of deposits, light comes from northeast and from southeast. Wells are plotted on the isopach maps of (A) the Belly River group transgressive (T1) interval (see Fig. 6B). Color and size of dots (wells) are proportional to oil exploitation (see legend). Palette color-bars for respective thickness intervals are reported on the left in meters. Peco and Pembina East oil fields are indicated. The exploited area in A corresponds to channel-delta lobe systems and is overlain by 2–6 m of T1 interval’s fine-grained sediments (B) interpreted as the effective sealing for the oil that migrated from the Cardium Formation into the Belly River Group reservoirs. These Bearpaw transgressive fine-grained deposits prevented further upsection migration into basal channel systems of the Edmonton Group. (For interpretation of the references to color in this figure legend, the reader is referred to the Web version of this article.)

environments in the study area developed with a NW-SE oriented axis, external to the deformed foothills region of the Canadian Rocky Mountains fold and thrust-belt. The geometry of the foreland basin was inherited by flexural subsidence that provided the accommodation space for the deposition of mainly continental successions from the base of the Belly River Group (at approximately 80 Myr) up to the Tertiary. Sediment accumulation in the study area is linked to primary sources located in the rising cordillera throughout the entire studied interval. Major feeding systems and sediment distribution patterns remained almost unaltered throughout the studied stratigraphic interval, further supporting a gradual trend toward an overfilled foreland basin.

The methodologic approach presented in this study provides a useful tool to discriminate the interference of external eustatic controls in the evolution of a foreland basin.

CRedit authorship contribution statement

Riccardo Zubalich: Conceptualization, Data curation, Investigation, Methodology, Software, Visualization, Writing - original draft, Writing - review & editing. **Rossella Capozzi:** Supervision, Conceptualization, Project administration, Visualization, Writing - review & editing. **Federico Fanti:** Supervision, Conceptualization, Project administration, Visualization, Writing - review & editing. **Octavian Catuneanu:** Supervision, Visualization, Writing - review & editing.

Declaration of competing interest

The authors declare that they have no known competing financial interests or personal relationships that could have appeared to influence the work reported in this paper.

Acknowledgements

The authors wish to thank the reviewers Claudia Schröder-Adams, Fabiano Gamberi and Joshua Slattery for constructive comments that greatly improved this manuscript. We thank Benedikt Bayer (FRAGILE srl) for helping us with the code used for data processing, Tomasz Jerzykiewicz for providing background information and Dongqing Chen (Alberta Energy Regulator) for her suggestions and help in the field, Marco Venieri for the critical discussion and data on the hydrocarbon fields in Alberta. We thank University of Alberta for providing data access.

References

- Ainsworth, R.B., 1994. Marginal marine sedimentology and high-resolution sequence analysis; Bearpaw-Horseshoe Canyon transition, Drumheller, Alberta. *Bull. Can. Petrol. Geol.* 42 (1), 26–54. <https://doi.org/10.35767/gscpgbull.42.1.026>.
- Bally, A.W., Gordy, P.L., Stewart, G.A., 1966. Structure, seismic data, and orogenic evolution of southern Canadian Rocky Mountains. *Bull. Can. Petrol. Geol.* 14 (3), 337–381. <https://doi.org/10.35767/gscpgbull.14.3.337>.
- Bell, P.R., Currie, P.J., 2016. A high-latitude dromaeosaurid, *Boreonykus certekorum*, gen. et sp. nov. (Theropoda), from the upper Campanian Wapiti Formation, west-central Alberta. *J. Vertebr. Paleontol.* 36 (1) <https://doi.org/10.1080/02724634.2015.1034359>.
- Bell, P.R., Fanti, F., Mitchell, M.T., Currie, P.J., 2014. Marine reptiles (Plesiosauria and Mosasauridae) from the Puskwaskau Formation (Santonian–Campanian), west-central Alberta. *J. Paleontol.* 88 (1), 187–194. <https://doi.org/10.1666/13-043>.
- Bell, P.R., Fanti, F., Acorn, J., Sissons, R.S., 2013. Fossil mayfly larvae (Ephemeroptera, cf. Heptageniidae) from the late cretaceous Wapiti Formation, Alberta, Canada. *J. Paleontol.* 87 (1), 147–150. <https://doi.org/10.1666/12-058R.1>.
- Blakey, R.C., Ranney, W.D., 2017. Ancient Landscapes of Western North America: a Geologic History with Paleogeographic Maps. Springer. <https://doi.org/10.1007/978-3-319-59636-5>.
- Bustin, R.M., Smith, G.G., 1993. Coal deposits in the front ranges and foothills of the Canadian Rocky Mountains, southern Canadian Cordillera. *Int. J. Coal Geol.* 23 (1–4), 1–27. [https://doi.org/10.1016/0166-5162\(93\)90041-8](https://doi.org/10.1016/0166-5162(93)90041-8).
- Cant, D.J., 1995. Sequence stratigraphic analysis of individual depositional successions: effects of marine/nonmarine sediment partitioning and longitudinal sediment transport, Mannville Group, Alberta Foreland Basin, Canada. *AAPG Bull.* 79 (5), 749–762. <https://doi.org/10.1306/8D2B1B92-171E-11D7-8645000102C1865D>.
- Catuneanu, O., 2006. *Principles of Sequence Stratigraphy*. Elsevier.
- Catuneanu, O., 2017. Sequence stratigraphy: guidelines for a standard methodology. In: Montenari, M. (Ed.), *Stratigraphy and Timescales*, vol. 2. Academic Press, UK, pp. 1–57. <https://doi.org/10.1016/bs.sats.2017.07.003>.
- Catuneanu, O., 2019a. Model-independent sequence stratigraphy. *Earth Sci. Rev.* 188, 312–388. <https://doi.org/10.1016/j.earscirev.2018.09.017>.
- Catuneanu, O., 2019b. Scale in sequence stratigraphy. *Mar. Petrol. Geol.* 106, 128–159. <https://doi.org/10.1016/j.marpetgeo.2019.04.026>.
- Catuneanu, O., Galloway, W.E., Kendall, C.G.S.C., Miall, A.D., Posamentier, H.W., Strasser, A., Tucker, M.E., 2011. Sequence stratigraphy: methodology and nomenclature. *Newslett. Stratigr.* 44 (3), 173–245. <https://doi.org/10.1127/0078-0421/2011/0011>.
- Catuneanu, O., Sweet, A.R., Miall, A.D., 2000. Reciprocal stratigraphy of the Campanian–Paleocene Western Interior of North America. *Sediment. Geol.* 134 (3–4), 235–255. [https://doi.org/10.1016/S0037-0738\(00\)00045-2](https://doi.org/10.1016/S0037-0738(00)00045-2).
- Catuneanu, O., Sweet, A.R., Miall, A.D., 1999. Concept and styles of reciprocal stratigraphies: western Canada foreland system. *Terra Nova–Oxford* 11 (1), 1–8. <https://doi.org/10.1046/j.1365-3121.1999.00222.x>.
- Catuneanu, O., Sweet, A.R., Miall, A.D., 1997. Reciprocal architecture of Bearpaw TR sequences, uppermost Cretaceous, Western Canada Sedimentary Basin. *Bull. Can. Petrol. Geol.* 45 (1), 75–94. <https://doi.org/10.35767/gscpgbull.45.1.075>.
- Chamberlain, V.E., Lambert, R.S.J., McKerrow, W.S., 1989. Mesozoic sedimentation rates in the Western Canada Basin as indicators of the time and place of tectonic activity. *Basin Res.* 2 (3), 189–202. <https://doi.org/10.1111/j.1365-2117.1989.tb00034.x>.
- Chen, D., Langenberg, C.W., Beaton, A.P., 2005. Horseshoe Canyon–Bearpaw transition and correlation of associated coal zones across the Alberta Plains. Alberta Energy and Utilities Board.
- Cobban, W.A., Merewether, E.A., Fouch, T.D., Obradovich, J.D., 1994. Some Cretaceous Shorelines in the Western Interior of the United States. *Rocky Mountain Section (SEPM)*.
- Creaney, S., Allan, J., Cole, K.S., Fowler, M.G., Brooks, P.W., Osadetz, K.G., Macqueen, R., Snowdon, L., Riediger, C.L., 1994. *Petroleum Generation and Migration in the Western Canada Sedimentary Basin*. Geological Atlas of the Western Canada Sedimentary Basin, G.D. Mossop and I. Shetsen (comp.). Canadian Society of Petroleum Geologists and Alberta Research Council, pp. 455–468.
- Cullen, T.M., Evans, D.C., 2016. Palaeoenvironmental drivers of vertebrate community composition in the Belly River Group (Campanian) of Alberta, Canada, with implications for dinosaur biogeography. *BMC Ecol.* 16 (1), 52. <https://doi.org/10.1186/s12898-016-0106-8>.
- Currie, P.J., Koppelhus, E.B. (Eds.), 2005. *Dinosaur Provincial Park: a Spectacular Ancient Ecosystem Revealed*. Indiana University Press. <https://doi.org/10.1086/523131>.
- Currie, P.J., Langston Jr., W., Tanke, D.H., 2008. *New Horned Dinosaur from an Upper Cretaceous Bone Bed in Alberta*. NRC Research Press, p. 152.
- Dawson, F., Evans, C., Marsh, R., Richardson, R., Mossop, G.D., Shetsen, I., comp., 1994. *Uppermost Cretaceous and Tertiary strata of the Western Canada Sedimentary Basin*. In: *Geological Atlas of the Western Canada Sedimentary Basin*, vol. 4. Canadian Society of Petroleum Geologists and Alberta Research Council, Special Report, pp. 387–406.
- Dawson, F.M., Evans, C., Marsh, R., Power, B., 1990. Uppermost Cretaceous–Tertiary strata of the Western Canada Sedimentary Basin. *Bull. Can. Petrol. Geol.* 38 (1), 160–161.
- Dodson, P., 1990. Counting dinosaurs: how many kinds were there? *Proc. Natl. Acad. Sci. Unit. States Am.* 87 (19), 7608–7612. <https://doi.org/10.1073/pnas.87.19.7608>.
- Dodson, P., 1971. Sedimentology and taphonomy of the Oldman Formation (Campanian), Dinosaur Provincial Park, Alberta (Canada). *Palaeogeogr. Palaeoclimatol. Palaeoecol.* 10 (1), 21–74. [https://doi.org/10.1016/0031-0182\(71\)90044-7](https://doi.org/10.1016/0031-0182(71)90044-7).
- Eberth, D.A., Evans, D.C., Brinkman, D.B., Therrien, F., Tanke, D.H., Russell, L.S., 2013. Dinosaur biostratigraphy of the Edmonton Group (Upper Cretaceous), Alberta, Canada: evidence for climate influence. *Can. J. Earth Sci.* 50 (7), 701–726. <https://doi.org/10.1139/cjes-2012-0185>.
- Eberth, D.A., Braman, D.R., 2012. A revised stratigraphy and depositional history for the Horseshoe Canyon Formation (Upper Cretaceous), southern Alberta plains. *Can. J. Earth Sci.* 49 (9), 1053–1086. <https://doi.org/10.1139/e2012-035>.
- Eberth, D.A., 2005. 3. The geology. Dinosaur Provincial Park: a Spectacular Ancient Ecosystem Revealed, pp. 54–82.
- Eberth, D.A., 2002. Review and comparison of Belly River Group and Edmonton Group stratigraphy and stratigraphic architecture in the southern Alberta plains. In: 75th Anniversary Convention, Extended Abstracts, vol. 7. Canadian Society of Petroleum Geologist.
- Eberth, D.A., Deino, A.L., 1992. A geochronology of the non-marine Judith River Formation of southern Alberta. In: *Mesozoic of the Western Interior: Abstracts for the Society of Economic Paleontologists and Mineralogists Theme Meeting, Fort Collins, Colorado*. Society for Sedimentary Geology, Tulsa, Oklahoma, United States of America, pp. 24–25.
- Eberth, D.A., Kamo, S.L., 2020. High-precision U–Pb CA–ID–TIMS dating and chronostratigraphy of the dinosaur-rich Horseshoe Canyon Formation (Upper Cretaceous, Campanian–Maastrichtian), Red Deer River valley, Alberta, Canada. *Can. J. Earth Sci.* 57 (10), 1220–1237. <https://doi.org/10.1139/cjes-2019-0019>.
- Fanti, F., 2009. Bentonite chemical features as proxy of late Cretaceous provenance changes: a case study from the Western Interior Basin of Canada. *Sediment. Geol.* 217 (1–4), 112–127. <https://doi.org/10.1016/j.sedgeo.2009.03.015>.
- Fanti, F., Catuneanu, O., 2010. Fluvial sequence stratigraphy: the Wapiti Formation, west-central Alberta, Canada. *J. Sediment. Res.* 80 (4), 320–338. <https://doi.org/10.2110/jsr.2010.033>.
- Fanti, F., Catuneanu, O., 2009. Stratigraphy of the Upper Cretaceous Wapiti Formation, west-central Alberta, Canada. *Can. J. Earth Sci.* 46 (4), 263–286. <https://doi.org/10.1139/E09-020>.
- Fanti, F., Currie, P.J., Burns, M.E., 2015. Taphonomy, age, and paleoecological implication of a new Pachyrhinosaurus (dinosauria: ceratopsidae) bonebed from the Upper Cretaceous (Campanian) Wapiti Formation of Alberta, Canada. *Can. J. Earth Sci.* 52 (4), 250–260. <https://doi.org/10.1139/cjes-2014-0197>.
- Fanti, F., Miyashita, T., 2009. A high latitude vertebrate fossil assemblage from the Late Cretaceous of west-central Alberta, Canada: evidence for dinosaur nesting and vertebrate latitudinal gradient. *Palaeogeogr. Palaeoclimatol. Palaeoecol.* 275 (1–4), 37–53. <https://doi.org/10.1016/j.palaeo.2009.02.007>.
- Freedman Fowler, E.A., Horner, J.R., 2015. A new brachylophosaurin hadrosaur (Dinosauria: ornithischia) with an intermediate nasal crest from the Campanian Judith River Formation of northcentral Montana. *PLoS One* 10 (11). <https://doi.org/10.1371/journal.pone.0141304>.
- Gilbert, M., 2019. *Sedimentology, Ichnology, Sequence Stratigraphy and Vertebrate Paleontology of the Belly River Group, Southwestern Saskatchewan*. Canada (Doctoral dissertation, University of Saskatchewan).
- Gilbert, M.M., Buatois, L.A., Renaut, R.W., 2019. Ichnology and depositional environments of the Upper Cretaceous Dinosaur Park–Bearpaw Formation transition in the Cypress Hills region of southwestern Saskatchewan, Canada. *Cretac. Res.* 98, 189–210. <https://doi.org/10.1016/j.cretres.2018.12.017>.
- Gilbert, M., Bamforth, E.L., 2017. Paleocology of a Vertebrate Microfossil Assemblage from the Easternmost Dinosaur Park Formation (Upper Campanian) Saskatchewan, Canada: Reconstructing Diversity in a Coastal Ecosystem, vol. 23. Hosted by University of Alberta. <https://doi.org/10.1016/j.palaeo.2018.01.016>.
- Glombick, P.M., 2010. Top of the Belly River Group in the Alberta Plains: Subsurface Stratigraphic Picks and Modelled Surface. Alberta Geological Survey, Open file Report, 201010.
- Hamblin, A.P., 2004. The Horseshoe Canyon Formation in southern Alberta: surface and subsurface stratigraphic architecture, sedimentology, and resource potential. In: *Bulletin 578*, vol. 578. Geological Survey of Canada. <https://doi.org/10.4095/215068>.
- Hag, B.U., 2014. Cretaceous eustasy revisited. *Global Planet. Change* 113, 44–58. <https://doi.org/10.1016/j.gloplacha.2013.12.007>.
- Hathway, B., 2016. Regional T–R sequence stratigraphy and lithostratigraphy of the Bearpaw Formation (Upper Campanian), west-central and southwestern Alberta plains. *Bull. Can. Petrol. Geol.* 64 (3), 449–466. <https://doi.org/10.2113/gscpgbull.64.3.449>.
- Hatcher, J.B., Stanton, T.W., 1903. The stratigraphic position of the Judith River beds and their correlation with the Belly River Beds. *Science* 18, 211–212. <https://doi.org/10.1126/science.18.450.211>.

- Jerzykiewicz, T., 2010. Stratigraphic setting of the key bentonite layers in the nonmarine Saunders group – Upper Cretaceous to Paleocene strata of the Rocky Mountains in Alberta, Canada. A Guidebook to the Blackstone River Section Prepared for the GTS NEXT Project. Geoclastica Consulting Ltd. Calgary.
- Jerzykiewicz, T., 1997. Stratigraphic framework of the Upper Cretaceous to Paleocene strata of the Alberta basin. *Geol. Surv. Can. Bull.* 510, 121. <https://doi.org/10.4095/208902>.
- Jerzykiewicz, T., 1996. *Baculites Compressus Robinsoni* Cobban from the Crowsnest River Section at Lundbreck, Alberta: an Implication for the Timing of the Late Cretaceous Bearpaw Transgression into the Southern Foothills of Alberta. Geological Survey of Canada, Current Research, pp. 97–100, 1996.
- Jerzykiewicz, T., 1992. Controls on the distribution of coal in the Campanian to Paleocene post-Wapiabi strata of the Rocky Mountains. Controls on the Distribution and Quality of Cretaceous Coals 267, 139. <https://doi.org/10.1130/SPE267>.
- Jerzykiewicz, T., McLean, J.R., 1980. Lithostratigraphic and sedimentological framework of coal-bearing Upper Cretaceous-lower Tertiary strata, coal valley area, central Alberta foothills. Geological Survey of Canada. Paper 79-12.
- Jerzykiewicz, T., Norris, D.K., 1994. Stratigraphy, structure and syntectonic sedimentation of the Campanian 'Belly River' clastic wedge in the southern Canadian Cordillera. *Cretac. Res.* 15 (4), 367–399. <https://doi.org/10.1006/cres.1994.1022>.
- Jerzykiewicz, T., Sweet, A.R., McNeil, D.H., 1996. Shoreface of the Bearpaw sea in the footwall of the Lewis thrust, southern Canadian cordillera, Alberta. Geological Survey of Canada Current Research, pp. 155–163. <https://doi.org/10.4095/207421>, 1996.
- Jerzykiewicz, T., Sweet, A.R., 1988. Sedimentological and palynological evidence of regional climatic changes in the Campanian to Paleocene sediments of the Rocky Mountain Foothills, Canada. *Sediment. Geol.* 59 (1–2), 29–76. [https://doi.org/10.1016/0037-0738\(88\)90099-1](https://doi.org/10.1016/0037-0738(88)90099-1).
- Jerzykiewicz, T., Sweet, A.R., 1986. In: Caliche and Associated Impoverished Palynological Assemblages: an Innovative Line of Paleoclimatic Research into the Uppermost Cretaceous and Paleocene of Southern Alberta. Core Conference, Calgary, Alberta, pp. 1–19 (7).
- Kauffman, E.G., Sageman, B., Kirkland, J., Elder, W., Harries, P., Villamil, T., 1993. Molluscan biostratigraphy of the Cretaceous Western Interior Basin, North America. In: Caldwell, W., Kauffman, E. (Eds.), *Evolution of the Western Interior Basin. Special Paper, vol. 39. Geological Association of Canada*, pp. 397–434.
- Koppelhus, E.B., Fanti, F., 2019. Rare, non-marine deposits during the deposition of the Bearpaw Formation: interpreting the palaeoenvironment of the DC bonebed (Wapiti Formation) using palynology and palaeobotany. In: 7th Annual Meeting Canadian Society of Vertebrate Paleontology May 10-13, 2019 Grande Prairie, Alberta.
- Larson, D., Vavrek, M., Bell, P., Campione, N., Fanti, F., Sissons, R., Sullivan, C., 2018. A High-Latitude Assemblage of Fossil Turtles (Testudines) from the Late Campanian of Alberta, Canada. 78th SVP – Annual Meeting, Albuquerque (poster).
- Larson, N.L., Brezina, J., Landman, N.H., Garb, M.P., Handle, K.C., 2013. Hydrocarbon seeps: unique habitats that preserved the diversity of fauna in the Late Cretaceous Western Interior Seaway. Wyoming Geological Society Handbook. Wyoming Geological Society, Caspar, Wyo.
- Larson, N.L., 2010. Fossil coleoids from the Late Cretaceous (Campanian and Maastrichtian) of the Western Interior. *Ferrantia* 59, 78–113.
- Leckie, D.A., Vanbeselaere, N.A., James, D.P., 1997. Regional sedimentology, sequence stratigraphy and petroleum geology of the Mannville Group: Southwestern Saskatchewan. In: *Western Canada – Memoir 18. Petroleum Geology of the Mannville Group*, pp. 211–262.
- Lee, H., Jang, Y., Kwon, S., Park, M.H., Mitra, G., 2018. The role of mechanical stratigraphy in the lateral variations of thrust development along the central Alberta Foothills, Canada. *Geoscience Frontiers* 9 (5), 1451–1464. <https://doi.org/10.1016/j.gsf.2018.03.006>.
- Lerbekmo, J.F., Braman, D.R., Therrien, F., Koppelhus, E.B., Taylor, W., 2005. Paleomagnetostратigraphy. In: Currie, J., Koppelhus, E.B. (Eds.), *Dinosaur Provincial Park: a Spectacular Ancient Ecosystem Revealed*. Indiana University Press, Bloomington, pp. 83–87. <https://doi.org/10.1086/523131>.
- Lerbekmo, J.F., 2002. The Dorothy bentonite: an extraordinary case of secondary thickening in a Late Campanian volcanic ash fall in central Alberta. *Can. J. Earth Sci.* 39 (12), 1745–1754. <https://doi.org/10.1139/e02-079>.
- Mallon, J.C., Evans, D.C., Ryan, M.J., Anderson, J.S., 2012. Megaherbivorous dinosaur turnover in the Dinosaur Park Formation (upper Campanian) of Alberta, Canada. *Palaeogeogr. Palaeoclimatol. Palaeoecol.* 350, 124–138. <https://doi.org/10.1016/j.palaeo.2012.06.024>.
- McMechan, M.E., Thompson, R.I., Caldwell, W.G.E., Kauffman, E.G., 1993. The Canadian Cordilleran fold and thrust belt south of 66°N and its influence on the Western Interior Basin. In: Caldwell, W.G., Kauffman, E.G. (Eds.), *Evolution of the Western Interior Basin, vol. 39. Geological Association of Canada Special Paper*, pp. 73–90.
- Miller, K.G., Mountain, G.S., Wright, J.D., Browning, J.V., 2011. A 180-million-year record of sea level and ice volume variations from continental margin and deep-sea isotopic records. *Oceanography* 24 (2), 40–53. <https://doi.org/10.5670/oceanog.2011.26>.
- Miller, K.G., Sugarman, P.J., Browning, J.V., Komins, M.A., Olsson, R.K., Feigenson, M.D., Hernández, J.C., 2004. Upper Cretaceous sequences and sea-level history, New Jersey coastal plain. *GSA Bulletin* 116 (3–4), 368–393. <https://doi.org/10.1130/B25279.1>.
- Miller, K.G., Sugarman, P.J., Browning, J.V., Komins, M.A., Hernández, J.C., Olsson, R.K., Wright, J.D., Feigenson, M.D., Van Sickle, W., 2003. Late Cretaceous chronology of large, rapid sea-level changes: glacioeustasy during the greenhouse world. *Geology* 31 (7), 585–588. [https://doi.org/10.1130/0091-7613\(2003\)031<0585:LCCOLR>2.0.CO;2](https://doi.org/10.1130/0091-7613(2003)031<0585:LCCOLR>2.0.CO;2).
- Monger, J.W.H., 1989. Overview of cordilleran geology. In: Ricketts, B.D. (Ed.), *Western Canada Sedimentary Basin: A Case History. Canadian Society of Petroleum Geologists*, pp. 9–32.
- Paná, D.I., Van Der Pluijm, B.A., 2015. Orogenic pulses in the Alberta Rocky Mountains: radiometric dating of major faults and comparison with the regional tectono-stratigraphic record. *Bulletin* 127 (3–4), 480–502. <https://doi.org/10.1130/B31069.1>.
- Plint, A.G., Walker, R.G., Bergman, K.M., 1986. Cardium Formation 6. Stratigraphic framework of the Cardium in subsurface. *Bull. Can. Petrol. Geol.* 34 (2), 213–225.
- Price, R., 1981. The Cordilleran foreland thrust and fold belt in the southern Canadian Rocky Mountains. Geological Society, London, Special Publications 9 (1), 427–448. <https://doi.org/10.1144/GSL.SP.1981.009.01.39>.
- Price, R.A., Mountjoy, E.W., 1970. Geologic structure of the Canadian Rocky Mountains between Bow and Athabasca rivers - a progress report. In: Wheeler, J.O. (Ed.), *Structure of the Southern Canadian Cordillera. Geological Association of Canada Special Paper No. 6*.
- Putnam, P.E., 1993. A multidisciplinary analysis of Belly River-Brazeau (Campanian) fluvial channel reservoirs in west-central Alberta, Canada. *Bull. Can. Petrol. Geol.* 41 (2), 186–217. <https://doi.org/10.35767/gscpgbull.41.2.186>.
- Roberts, L.N.R., Kirschbaum, M.A., 1995. Paleogeography and the Late Cretaceous of the Western Interior of Middle North America; coal distribution and sediment accumulation. USGS. Professional paper 1561.
- Rogers, R.R., Kidwell, S.M., Deino, A.L., Mitchell, J.P., Nelson, K., Thole, J.T., 2016. Age, correlation, and lithostratigraphic revision of the Upper Cretaceous (Campanian) Judith River Formation in its type area (north-central Montana), with a comparison of low- and high-accommodation alluvial records. *J. Geol.* 124 (1), 99–135. <https://doi.org/10.1086/684289>.
- Russell, D.A., Chamney, T.P., 1967. Notes on the biostratigraphy of dinosaurian and microfossil faunas in the Edmonton Formation (Cretaceous) Alberta. *Natl. Mus. Can. Nat. Hist. Pap.* 35, 1–22.
- Ryan, M.J., Evans, D.C., 2005. 17. Ornithischian dinosaurs. In: Philip J Currie, P.J., Koppelhus, E.B. (Eds.), *Dinosaur Provincial Park: a Spectacular Ancient Ecosystem Revealed*, vol. 312. Indiana University Press. <https://doi.org/10.1086/523131>.
- Schlanger, S.O., Jenkyns, H.C., Premoli-Silva, I., 1981. Volcanism and vertical tectonics in the Pacific Basin related to global Cretaceous transgressions. *Earth Planet Sci. Lett.* 52 (2), 435–449. [https://doi.org/10.1016/0012-821X\(81\)90196-5](https://doi.org/10.1016/0012-821X(81)90196-5).
- Slattery, J.S., Cobban, W.A., McKinney, K.C., Harries, P.J., Sandness, A.L., 2015. Early Cretaceous to Paleocene Paleogeography of the Western Interior Seaway: the Interaction of Eustasy and Tectonism. Wyoming Geological Association Guidebook, pp. 22–60. <https://doi.org/10.13140/RG.2.1.4439.8801>, 2015.
- Stockmal, G.S., Lebel, D., McMechan, M.E., Mackay, P.A., 2001. Structural style and evolution of the triangle zone and external Foothills, southwestern Alberta: implications for thin-skinned thrust-and-fold belt mechanics. *Bull. Can. Petrol. Geol.* 49 (4), 472–496. <https://doi.org/10.2113/49.4.472>.
- Street, H.P., Bamforth, E.L., Gilbert, M.M., 2019. The formation of a marine bonebed at the Upper Cretaceous Dinosaur Park-Bearpaw transition of west-central Saskatchewan, Canada. *Front. Earth Sci.* 7, 209. <https://doi.org/10.3389/feart.2019.00209>.
- Sullivan, C., Fanti, F., Larson, D.W., Bell, P., Campione, N.E., Sissons, R., Vavrek, M., 2019. The Upper Cretaceous Wapiti Formation of northern Alberta, Canada as a unique window into the continental vertebrate fauna of boreal Laramidia during Bearpaw times. 79th Symposium of Vertebrate Paleontology. Annual Meeting, Brisbane.
- Tsujita, C., Westerman, G., 1998. Ammonoid habitats and habits in the Western Interior Seaway: a case study from the Upper Cretaceous Bearpaw Formation of southern Alberta, Canada. *Palaeogeogr. Palaeoclimatol. Palaeoecol.* 144, 135–160.
- Underschultz, J.R., 1991. Tectonic loading, sedimentation, and sea-level changes in the foreland basin of north-west Alberta and north-east British Columbia, Canada. *Basin Res.* 3 (3), 165–174. <https://doi.org/10.1111/j.1365-2117.1991.tb00125.x>.
- Walaszczyk, I., Cobban, W., Harries, P., 2001. Inoceramids and inoceramid biostratigraphy of the Campanian and Maastrichtian of the United States Western Interior Basin. *Revue Paleobiol. Geneve* 20, 117–234.
- Wall, J.H., Singh, C., 1975. A Late Cretaceous microfossil assemblage from the Buffalo Head Hills, north-central Alberta. *Can. J. Earth Sci.* 12 (7), 1157–1174. <https://doi.org/10.1139/e75-106>.
- Wessel, P., 2009. A general-purpose Green's function interpolator. *Computers & Geosciences* 35, 1247–1254. <https://doi.org/10.1016/j.cageo.2008.08.012>.
- Wood, J.M., 1994. Sequence stratigraphic and sedimentological model for estuarine reservoirs in the Lower Cretaceous Glauconitic member, southern Alberta. *Bull. Can. Petrol. Geol.* 42 (3), 332–351. <https://doi.org/10.35767/gscpgbull.42.3.332>.

Chapter 5

Discussion and conclusions

5.1 Reconstructed paleogeography of the Bearpaw Fm.

5.1.1 MFS paleogeography of the Bearpaw Fm. tongues

All the results presented herein led to the interpretation of two paleogeographic maps, both for the lower and for the upper Bearpaw tongue MFS. These maps could be traced following almost perfectly the cumulative thickness contour. This was expected after the observations about the overall “flatness” of west-central Alberta (i.e. sea level surfaces), it should not surprise that the paleotopography was almost preserved in the underground, being the only topographic re-shaping potential actors differential compaction (of a sediments column ranging from 300 to over 1000 m of sediment under the surface) and flexural tectonics (average less than 1° of flexuration, little to no fragile deformation). The shaly nature of sediments in the study area could led to interpret differential compaction as the sole agent modifying the shape of deposits but, to put this into scale, it could roughly account for centimetric effects because of the limited thickness of the Bearpaw intervals and the relative shallowness of the Campanian in the study area. The underlying morphologies over which the entire succession deposited (the paleotopography of the base of the Belly River Group) could be approximated as flat because normal topographic oscillations within an overall continental succession (mostly dominated by floodplains) are easily averaged by the mean thickness of about 330 m of sediment between the datum and the base of the Bearpaw succession. Thus, in the case of this study, representing the three-dimensional top surfaces of stacked stratigraphic intervals as subsequent cumulative thickness models referred to the same datum, is actually similar to representing paleotopographic variations, although it may not be

the case in other study areas.

The detailed analysis across the study area permitted to infer the paleogeographic evolution of west-central Alberta during the Bearpaw time. The reconstructions are reported in figures 5.1 and 5.2, respectively referred to the lower and to the upper Bearpaw tongue MFSs.

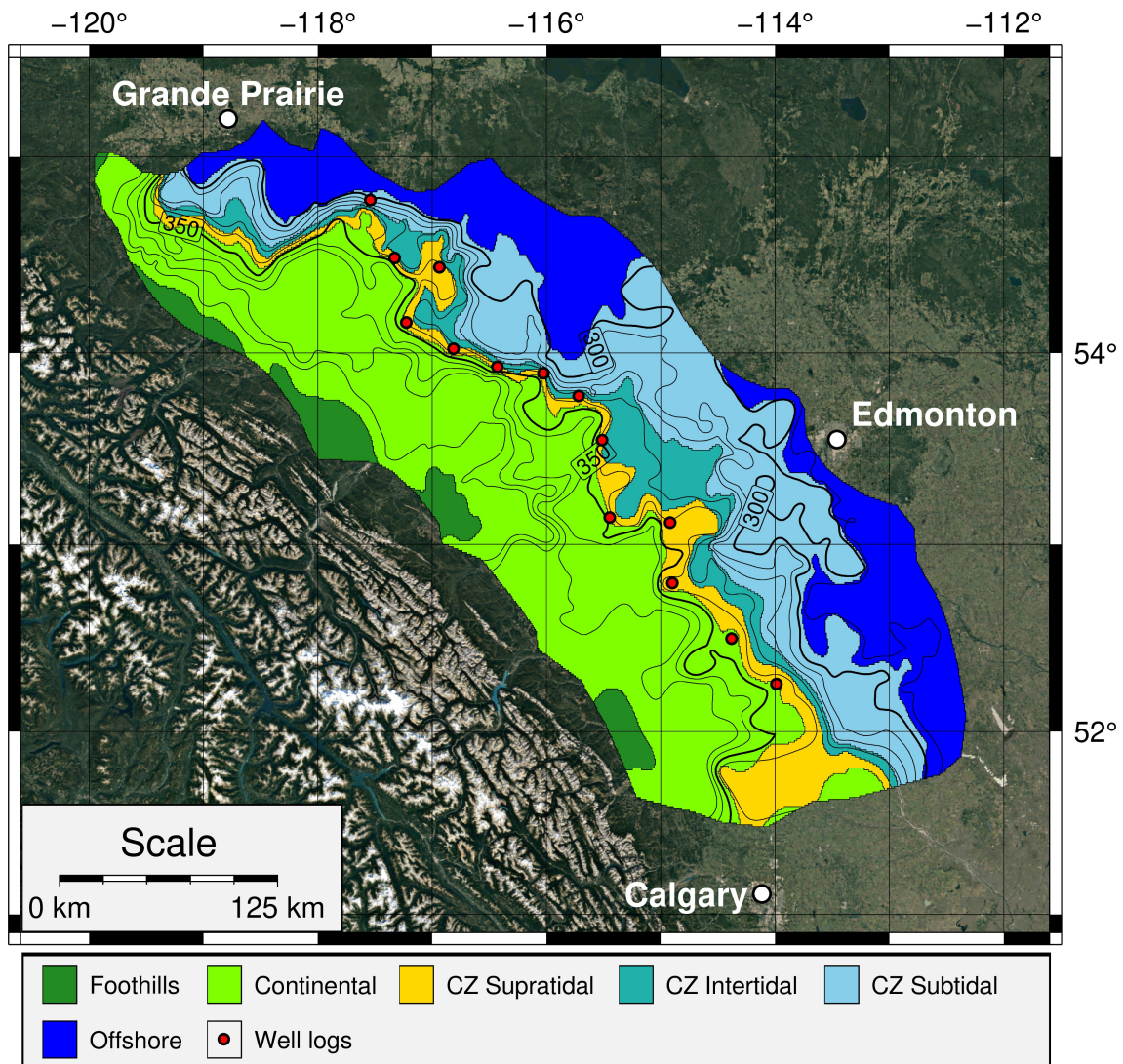


Figure 5.1: Paleogeography of the lower Bearpaw tongue MFS with location of the cross sections. Sediment distribution patterns indicate three adjoining areas: 1 - near the foothills, deposits are dominated by coarse, lenticular or laterally interfingered bodies; 2 - typical alluvial deposits are widespread within continental plains; 3 - distal, flat transitional areas include widespread marine signature of the lower Bearpaw tongue. Nearshore environments are likely related to a complex development of tidal embayments with vast submerged areas. Well logs indicated by red dots mark the eastward shift from subaerial to submerged deposition (in gamma ray trends). CZ = Coastal Zone.

Near the Foothills, gamma ray signatures represent coarse sand to fine gravel proximal deposits, multiple stacked and laterally amalgamated fluvial channel sandstones

5.1. RECONSTRUCTED PALEOGEOGRAPHY OF THE BEARPAW FM.

and systematically lack coal horizons (Jerzykiewicz and McLean, 1980; Jerzykiewicz, 1992; Fanti, 2009; Fanti and Miyashita, 2009; Fanti and Catuneanu, 2009; Sullivan et Al., 2019, Jerzykiewicz pers. Comm. 2020; this study; figures 5.1 and 5.2 dark green). Moving eastward in the central study area, the depositional architecture of channel sandstone bodies becomes less laterally-amalgamated and records an increase in single, fining-upward bodies interbedded with floodplain fine shales and coal seams.

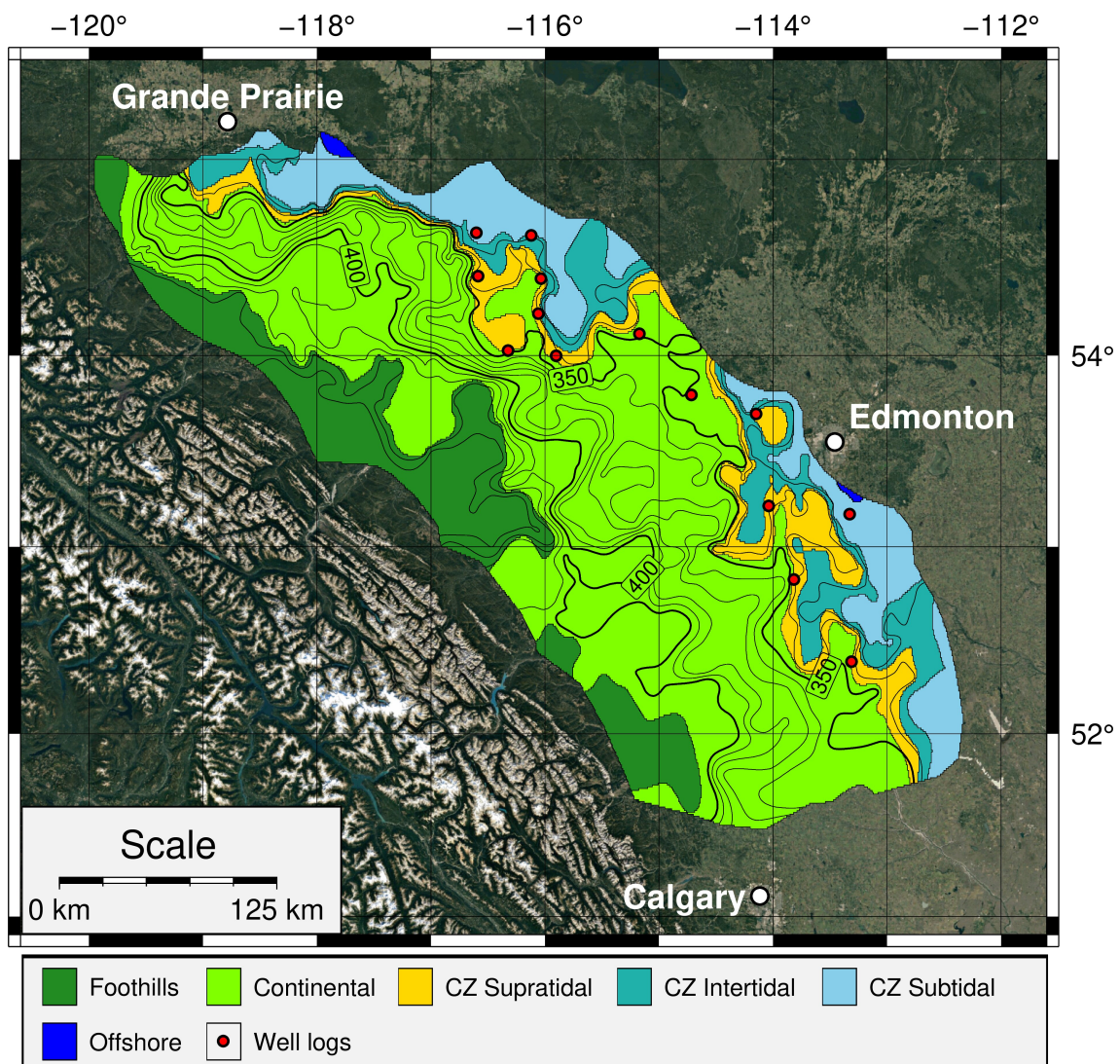


Figure 5.2: Paleogeography of the upper Bearpaw tongue MFS. Sediment distribution patterns indicate three adjoining areas: 1 - near the foothills, deposits are dominated by coarse, lenticular or laterally interfingered bodies; 2 - typical alluvial deposits are widespread within continental plains; 3 - distal, flat transitional areas include nearshore environments likely related to a complex development of tidal embayments with vast submerged areas. Well logs indicated by red dots mark the eastward shift from subaerial to submerged deposition (in gamma ray trends). CZ = Coastal Zone.

Coal seams appear discontinuous and interbedded with organic-rich mudstone, prob-

ably related to crevasse-splays, suggesting high-water table conditions within that alluvial plain (figures 5.1 and 5.2 green). These alluvial deposits cover most of the study area and are frequently bordered to the east by stacked coarsening upward regressive sequences. Adjacent to these coarsening-upward sequences, rare occurrences of tabular and laterally continuous fine sand bodies could be found, possibly linked to littoral sandbars and beaches (figure 5.1 and 5.2 yellow). Especially in the southern study area, cross sections indicate the presence of extensive coal zones, interfingering with claystone and siltstone deposits, in particular during the Strathmore Member. This area presents gamma ray signatures consistent with transitional deposits in coastal environments such as backswamps, estuaries or barrier-lagoons. The eastward transition to marine dominated environments is emphasized on gamma ray signatures (especially by the MFS surfaces) due to the homogenization effects related to the sudden increase in influence of marine processes (from subaerial to submerged environments) over the dispersion of sediments coming from river mouths. These processes act homogeneously over sediments that reach the submerged study area, mixing gamma ray emissions-responsible grains. Hence, they are able to affect the API value of coeval strata, shaping the GR curves with similar features related to the radioactivity of stacked sediments with different grain sizes during the T-R cycle (that's why FU-CU cycles are more uniform, regular and predictable in the submerged study area; see paragraph 3.3.2 and 3.3.5 for explanations about the MFS expression an FU-CU cycles on gamma ray well logs). Sediment distribution patterns in areas with higher distances between isopachs (almost flat surfaces) suggest the presence of tidal embayments and vast submerged areas (figure 5.1 and 5.2 shades of light-blue). In the most distal area of transition (eastern border of the study area) distinctive FU-CU sequences were also recognized. These sequences are traceable between different and distant (even hundreds of kilometers) well logs and mostly present fine sediments and lack of coal horizons, thus likely pertained to a fully marine setting (figure 5.1 and 5.2 in blue). The marine environments in the paleogeography of the lower Bearpaw tongue MFS are widespread across the eastern study area and the coastal zone develop subparallel to the deformation front from the southeastern study area up the Grande Prairie region. The paleontological record also supports the interpretation of marine environments in the northern study area, thanks to the diverse vertebrate fauna collected from the Wapiti Fm. Unit 3 (that correlates to the Bearpaw Fm., [Fanti and Miyashita, 2009](#); [Fanti and Catuneanu, 2009, 2010](#); [Larson et Al., 2018](#); [Koppelhus and Fanti, 2019](#); [Sullivan et Al., 2019](#)) in the Grande Prairie region, typical of wet lowland environments dominated by high water table, with taxa referable not only to terrestrial conditions but also to brack-

5.1. RECONSTRUCTED PALEOGEOGRAPHY OF THE BEARPAW FM.

ish and marine ecosystems (Fanti and Miyashita, 2009; Koppelhus and Fanti, 2019, Fanti pers. obs, 2020). The combination of published data, of the described gamma ray trends and of the interpreted MFS cumulative geometries thus allowed to trace a previously unnoticed geographic extent of Bearpaw T-R cycles and in particular the high-resolution shorelines derived from the MFS cumulative maps (figure 5.3).

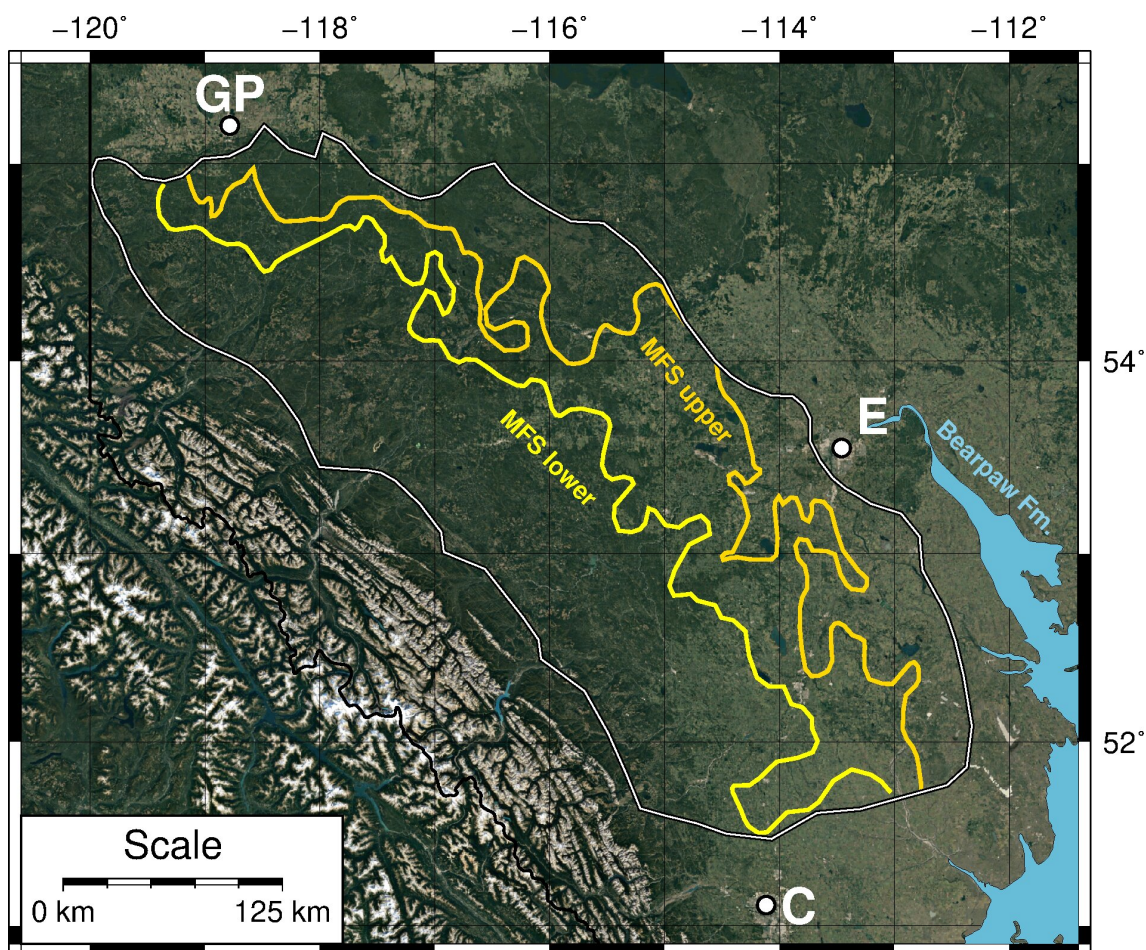


Figure 5.3: Bearpaw Fm. shorelines inferred from paleogeographic maps of both the lower Bearpaw tongue MFS and the upper Bearpaw tongue MFS. The Bearpaw Fm. marine extension (in outcrop) is reported from the geological map of Alberta.

The coastal zones of the lower Bearpaw tongue MFS paleogeography (figure 5.1)) appear either as narrowly elongated from NW to SE or aligned on a SW-NE axis (especially at the Edmonton latitude). The upper Bearpaw tongue MFS paleogeography (figure 5.2) instead represented an almost complete retreat of fully marine environment from the study area, and a clear sign of continental environments advancing eastward up to the eastern border of the study area (in the central region). The sediment distribution across intervals highlights that this paleogeography most likely established during the deposition of the S interval and was then inherited by

the upper Bearpaw tongue displaying a complex distribution of coastal-transitional environments. It is possible that in the northern region of the study area (NW of Edmonton), shallow marine conditions persisted during the upper tongue deposition, within rather underfed sub-basins mainly dominated by tidal influences, although previous studies depicted the Bearpaw succession in our study area either emerged or with a shoreline confined to the south of Edmonton (Dawson et Al., 1990, 1994; Roberts and Kirschbaum, 1995; Eberth and Braman, 2012; Hathway, 2016). The geologic map of Alberta depicts the Bearpaw Fm. outcropping marine deposits as confined by modern river valleys between Calgary and Edmonton (figure 5.3). This analysis showed instead that the geographic extent of the Bearpaw deposits spread over a much larger portion of the WIFB of west-central Alberta, up to the north and west of Edmonton and in the Grande Prairie area.

5.1.2 Paleogeographic context of west-central Alberta during late Campanian

The sections A, B, C, D and E (paragraph 4.5.2), cross the interpreted coastline reported in the paleogeographies (figures 5.1 and 5.2) and thus longshore currents, given a marine setting open to the east (open on the seaway), should have not permitted the deposition of very fine sediments (carried away in suspension) and should have deposited overall coarser sediments in the study area. The very fine sediments that can be seen through the entire study area (see figures from 4.27 to 4.31) thus imply a low energy depositional context (paleoenvironment). Coarse deposits are almost completely lacking in the study area and the used well logs (reported in paragraph 4.5.2) do not intercept sand bodies related to beach deposits. Outcropping sandstones were only found in the Riverbend outcrop (northeast of Edmonton, 30 km outside the study area) in the basal Horseshoe Canyon Fm., in contact with the top of the lower Bearpaw Fm. tongue (see paragraph 4.6 for a discussion on the outcropping sequence).

These observations led to interpret the study area as a narrow bay, elongated S-N, developing parallel to the deformation front and, thus, likely formed in response to flexural subsidence. The western side of the bay received all of the sediment from the source area (Rocky Mountains). There are few evidences supporting the hypothesis that the eastern side of the bay was actually the uplifted forebulge (the forebulge has not been studied as it is eroded). Nonetheless, this option seems reasonable given the depositional patterns observed to the east in the study area (discussed in chapter 4, paragraphs 4.2 and 4.3). Indeed, the uplifted and emerged forebulge may have also developed a small drainage system in its southern area, which could

explain the thickest deposit (>50 m) reported in the southeastern S interval thickness model (see figure 4.7) which is not in continuity with the prograding deposits clearly derived from the west (Rocky Mountains). Moreover, that small basin on the W side of the seaway was likely under a macrotidal regime, given the latitude and the narrow and elongated shape. In this scenario, the N-S oriented deposits (visible on 3D thickness models, figures 4.5, 4.6, 4.8 and 4.9) may be interpreted as muddy tidal bars, elongated in the direction of tides inflow and outflow as often seen in geomorphological modeling of tidal environments (Daidu et Al., 2013; Gensac et Al., 2015; Tang et Al., 2019). The bay received sediments from the W since pre-Bearpaw time. During the Bearpaw time a coincidence of lowering sea level (exception made for the transgressive intervals) and uplifting source area created high sediment flows in west-central Alberta, which oriented eastward and southeastward to follow the base-level change, as evidenced by the prograding western side of the study area. This re-arranging of sediment fluxes left underfed the northern distributary systems, favoring the ones developed in the central study area which prograded faster during the S interval (Falling Stage Systems Tract, FSST), after the T-R cycle of the lower Bearpaw tongue. The FSST in the study area is responsible for the production of the largest volumes of sediment deposited during the Bearpaw succession. This is consistent with the results obtained by numerous Authors regarding FSST deposits, including the recent study by Lobo and Ridente (2014). The progradation during the S interval almost closed the bay, acting as a barrier to the upper tongue transgression. Most of the bay was probably filled after the upper Bearpaw tongue deposition, leaving only a small portion of the southeastern study area covered by marine water after the upper tongue regressive phase. Nonetheless, a focus on the Bearpaw lower tongue intervals on section A (figure 4.27, located in the Grande Prairie area) reveals that the lower tongue shows southwards thickening deposits in the context of a pinch out pattern moving northwards. This indicates that only low sediment accumulation could reach northern areas during that T-R cycles. This depositional pattern was not found in the other sections, which instead show a more uniform thickness, with uniformly thinner (B, figure 4.28) or eastward thickening (D, figure 4.30) transgressive deposits covered by relatively thicker regressive deposits. The southern section (D, 4.30) shows instead an interesting basinwards thickening of the upper tongue regressive deposits which was not found in the central sections (B and C, 4.28 and 4.29), but was also found in section A (smaller in amplitude, figure 4.27). In section A in particular, this thickening trend appear in conjunction with a sharp, marine influence-related, MFS shape of the upper tongue in the northern well logs, which gradually turns blunter southwards (shifting through transitional

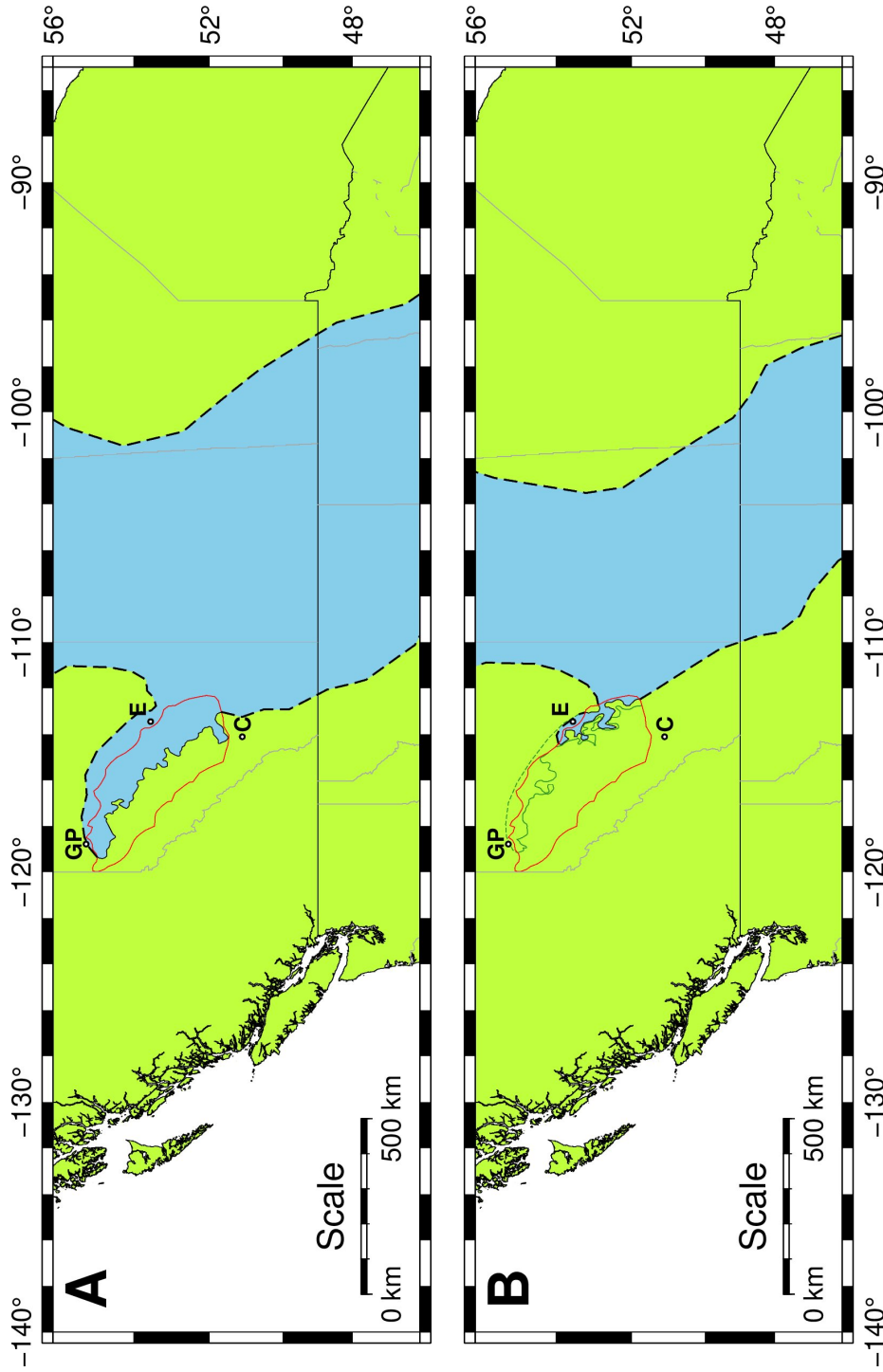


Figure 5.4: Schematic paleogeographies of the Bearpaw lower tongue MFS (A) and of the Bearpaw upper tongue top (basal Horseshoe Canyon Fm.). (B). Shorelines (black) inside the study area (red) are deducted by data from this study, lines in dark green (B) represents the shorelines reported in figure 5.3 for the upper Bearpaw tongue MFS. Shorelines next to the white background are modern shorelines of North America. Dashed lines (all colors) are indicative of the Western Interior Seaway shorelines. State boundaries and major Alberta cities are reported for geographic reference (GP = Grande Prairie, E = Edmonton, C = Calgary). Green color corresponds to land masses, light-blue corresponds to marine water.

and alluvial environments; see paragraphs 3.3.2, 3.3.5 and 5.1 for a discussion about MFS gamma ray expression). This is another evidence (along with those discussed in paragraph 5.1) which led to interpret that these areas were reached by the upper tongue transgression, as reported on the paleogeographic map in figure 5.2. Anyway, the thickening of deposits during the upper tongue regressive phase suggest that first, the underfed conditions that characterized the area during previous intervals were inverting trends and, second, that the area was likely rapidly abandoned by the shallow marine waters that reached it during the upper Bearpaw tongue transgression. For these reasons the schematic paleogeographic map for the top of the Bearpaw succession (lower Horseshoe Canyon Fm., figure 5.4) reports a small bay confined to the southeastern study area as well as the paleoshoreline of the upper tongue MFS (reported in figure 5.3). Given the geometries highlighted by the tridimensional analysis, it is nonetheless possible that a very narrow branch of that bay surrounded the bulk of deposits in the central study area (from outside the study area, east of Edmonton) and reached those zones (around 100 km southeast of Grande Prairie). The marine waters ingression could be facilitated by the relatively flat topography of the basin and by the macrotidal regime that should have developed at that latitude, in the context of such a narrow and elongated bay. In that case, the occurrence of shallow marine waters likely lasted for a short time before the final withdrawal of the seaway from Alberta. The existence of that narrow branch may also imply a practically inexistent sediment discharge from the eastern side of the discussed bay, otherwise such a narrow bay would have been easily closed by the progradation of both sides. As discussed in paragraph 4.6, recent paleontological studies found the occurrence of a diverse vertebrate fauna in the Grande Prairie Area including taxa referable to brackish and marine ecosystems (Fanti and Miyashita, 2009; Koppelhus and Fanti, 2019, Fanti pers. obs, 2020). Thus, future higher resolution paleontological studies might play a key role in confirming that the Upper Bearpaw transgression reached the Grande Prairie territories.

5.2 Paleogeographic interpretations of systems tracts

5.2.1 Chronostratigraphic resolutions

The paleogeographic reconstructions of the studied Bearpaw succession were carried out using the most recent published datings available at the time of writing (see paragraph 2.7). The dated units circumscribe the Bearpaw succession between 74.3 and 73.1 Myr and the Bearpaw upper tongue T-R cycle between 73.7 and 73.1 Myr (Eberth and Kamo, 2020). The succession was subdivided into five intervals based on

the correlated stratigraphic surfaces (see paragraphs 4.1 and 4.2): the two main T-R cycles belonging to the Bearpaw Fm. and correlative continental and coastal units in the western and central study area, namely T1, R1, T2, R2 and the S interval which comprehends most of the Strathmore Member (Horseshoe Canyon Fm.) deposits and the correlative coastal units in the eastern study area, i.e. lower hierarchy T-R cycle of the third tongue (introduced by Hamblin, 2004). The average thickness of each interval (figure 5.5) indicate that most of the accumulation happened during the S interval while the two T-R cycles averaged comparable sediment volumes. The paleogeographic interpretations here reported refer to the top of the T1 and T2 intervals (the maximum flooding surfaces of the respective T-R cycles, figures 5.1 and 5.2) and to the top of the Bearpaw succession (figure 5.4).

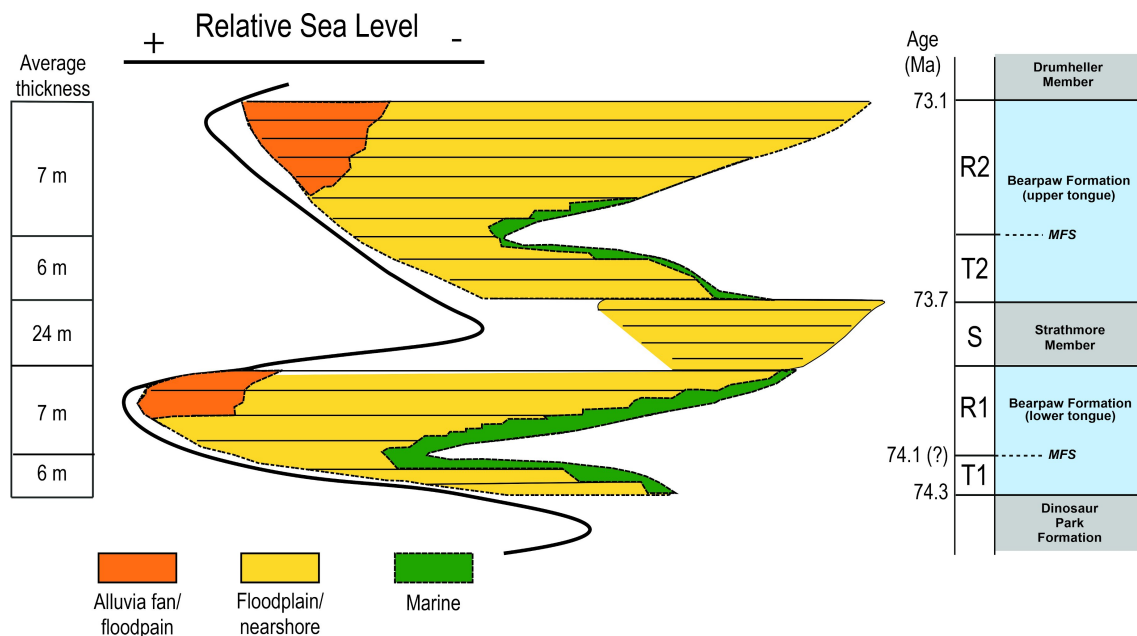


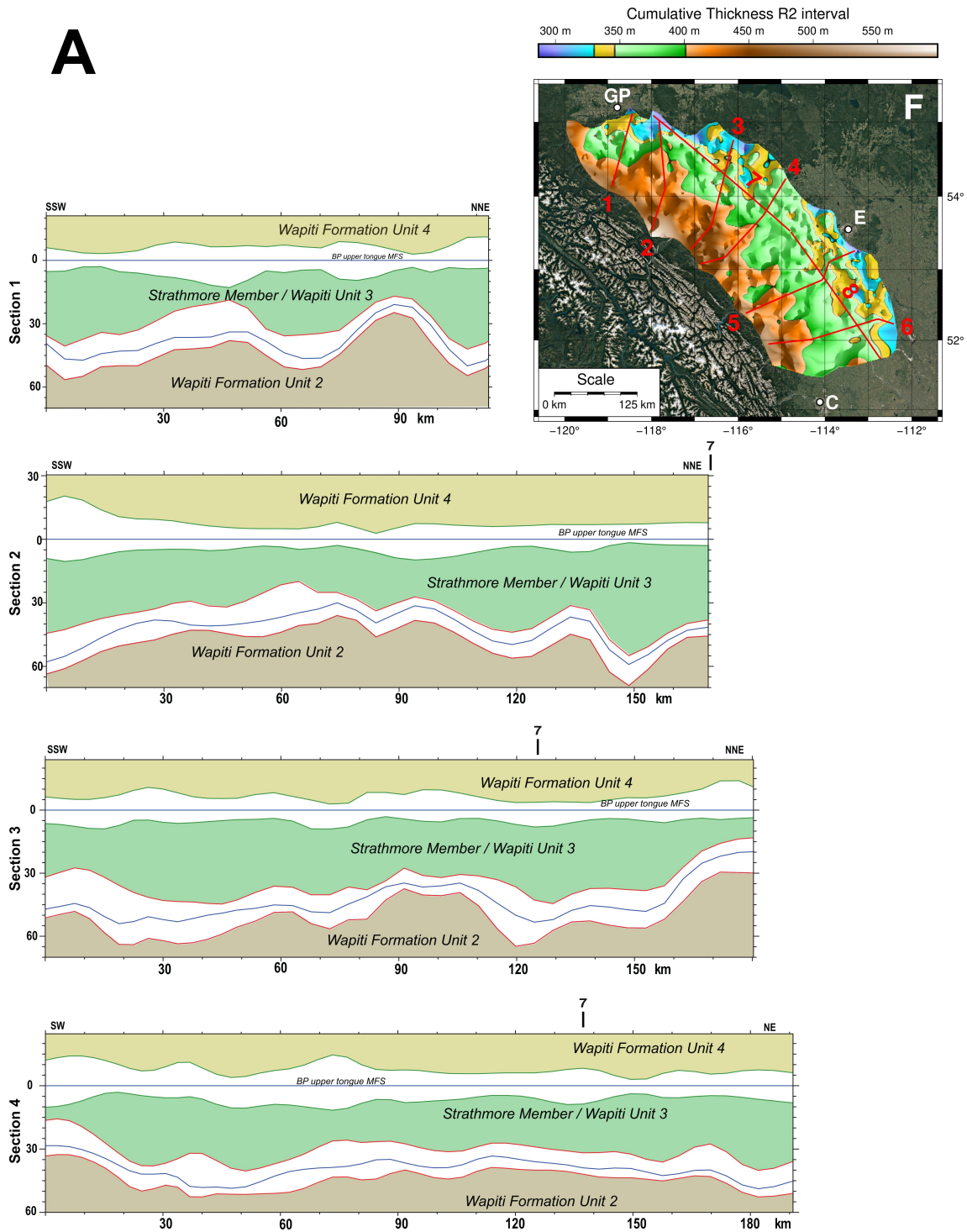
Figure 5.5: Chronostratigraphic chart of the Bearpaw Formation stratigraphic interval. The TST and RST for the lower and upper Bearpaw tongues (and correlative deposits) are indicated as T1/R1 and T2/R2, respectively. Strathmore interval (S) is defined as accumulation between the top of R1 and the base of T2. Absolute dating and average thickness for each interval are indicated (Eberth and Kamo, 2020, refer to paragraph 2.7). The environmental shifts based on gamma ray logs and the depositional architecture are interpreted as products of changes in relative sea level (see discussion in the text).

5.2.2 Geometric analysis of the Bearpaw-related systems tracts

The high-resolution GR analysis behind results presented in this study, showed that Belly River Group top physiography greatly influenced the deposition of the overlying Bearpaw interval. Most of the sedimentation during the lower tongue

5.2. PALEO GEOGRAPHIC INTERPRETATIONS OF SYSTEMS TRACTS

intervals indeed essentially draped the underlying geometries thus presenting only few cases (figure 5.6) where the lows of the Belly river Group top are almost flattened out by the T1 and R1 sedimentation.



This likely happened due to the distribution of the alluvial plain bodies (*e.g.* T1 basal channels in sections A and C discussed in paragraph 4.5.2, figures 4.27 and 4.28) in the context of the inherited articulations of highs and lows, with variations

up to 20-30 m (figure 5.6) in the Belly River Group top, which set the preferential paths that the lower tongue sedimentation followed. The sections represented with the upper tongue MFS as datum allow to clearly document how the sediment accumulation during the FSST (S interval, figure 5.6 in green) flattened the underlying geometries in the whole study area, setting a different physiography which the next T-R cycle, the upper Bearpaw tongue, inherited.

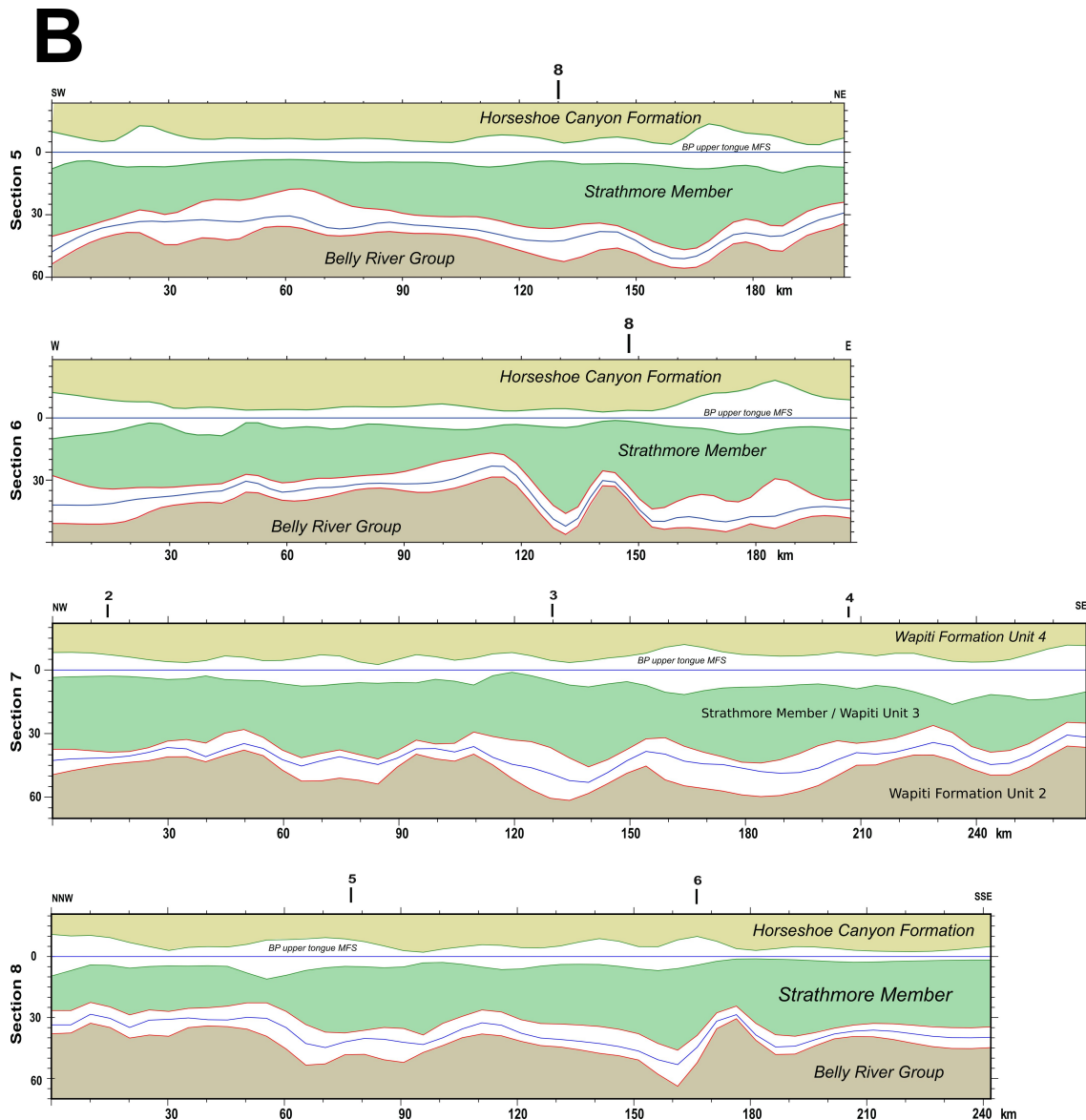


Figure 5.6: Simplified cross sections 1-4 (A, with location map on the cumulative thickness R2 interval map, see figure 4.21 for location maps over other intervals) and 5-8 (B) of the study area in west-central Alberta showing the stratigraphic distribution of intervals discussed in the text (in particular Bearpaw lower tongue, Strathmore Mbr. / Wapiti Unit 3, Bearpaw upper Tongue. Datum: upper tongue MFS). Horizontal scale in km, vertical scale in meters from the datum.

As described in paragraph 5.1.2 the upper Bearpaw tongue deposition took place

in almost three times more years and in a much different physiographic context than the wider, flexural bay in which the lower tongue deposited. Before the upper tongue transgression, the S interval accumulation had almost filled the bay, leaving only a very narrow and elongated area (mostly located outside the study area, to the E of Edmonton) covered by marine waters (figure 5.4). This residue of the original bay likely offered little accommodation space, but nonetheless acted as a new base level for the drainage system in the study area. During the upper transgression, marine waters reached the Grande Prairie area (as documented in figure 4.27) and on one side, shifted the base level, probably causing a slight readjustments of the drainage system. On the other side, that ingressions was "genetically" ephemeral. Indeed, shallow marine ingressions onto a flat physiography withdraw rapidly as they develop thanks to the close-to-flat angle of the flooded terrains. During the R2 interval, the northern, underfed, large lobe experienced a slight increase in sediment supply probably caused by the rapid pace at which that shallow marine ingressions was withdrawing from the Grande Prairie area, which induced the drainage system to follow the shifting base-level (note the evolving geometric features regarding the northern lobe from the S interval onwards, figure 4.26 in orange and green: during R2, these deposits re-started advancing basinwards). Figure 5.6 shows how the T2 interval presents an almost tabular trend toward NE, whereas toward the foothills, multiple, large, infilled areas resulted in the local accumulation of >10 meters of deposits, filling the lows of the inherited physiography of the S interval.

As represented in figure 5.7, cross sections plotted using the two MFSs as datum allow to emphasize depositional trends relative to both the upper and lower TST, from the marine environments to the coastal zone and to the correlative fluvial domain. Remarkably, the T1 interval (lower tongue transgression) clearly show accommodation space toward the marine-influenced areas (in blue), a bypass-area (in orange) where accommodation space is homogeneously low, and a vast area of high and localized accommodation (in green) that represent the alluvial domain. The same partition is observed in the T2 interval (upper tongue transgression) but with significant differences in the geographic extension of such areas (as well as in time of deposition, as the upper tongue lasted for 600 kyr, almost three times more than the lower tongue). Data presented in this study suggest that these differences can document two genetically different transgressive events. The lower tongue is a basin-wide, rapid transgression that is easily traced in correlative alluvial environments. The upper tongue represents high-water table conditions with the development of vast coaly/swamp/coastal lowlands on the whole eastern border of the study area.

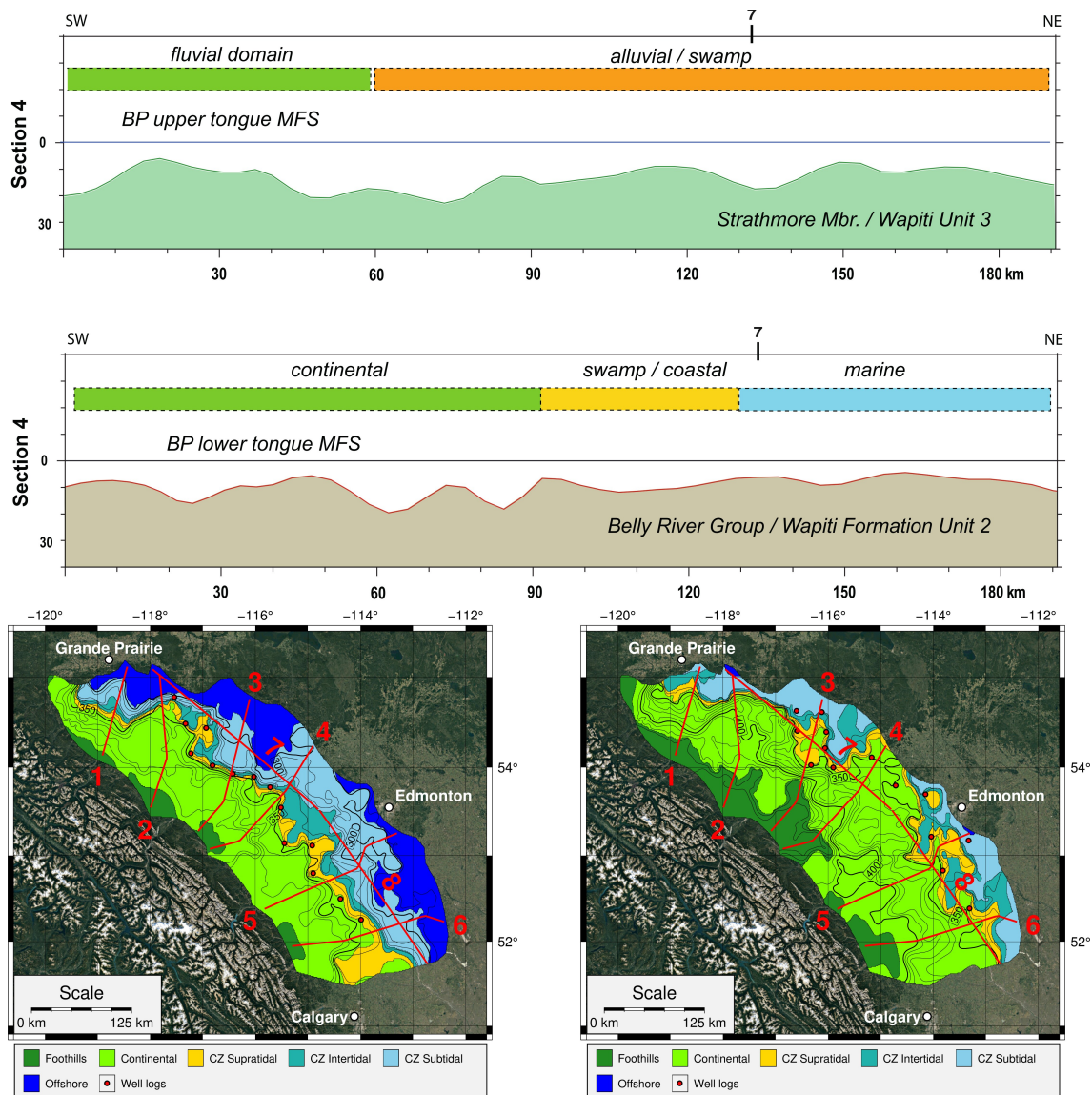


Figure 5.7: Paleogeographic map showing west-central Alberta during the lower and upper Bearpaw transgressive events, with section 4 plotted twice, using the MFS surfaces of both the lower and the upper Bearpaw tongues as datum.

Overall the continental sediments of the Belly River Group represent a subsidence-driven filling trend of the flexural basins which formed in west-central Alberta during the Upper Cretaceous. The Horseshoe Canyon Fm. also represents a filling up trend of continental sediments in the foredeep. The Bearpaw Fm. deposited between these two clastic wedges and represents the last, short discontinuity of continental sedimentation within the west-central Alberta foreland. In this work we found no evidence within the study area that links the deposition of the Bearpaw interval to tectonically driven sedimentation or suggests that the flexural subsidence was still active during the Bearpaw time. In the published article (reported in paragraph 4.6) instead, we discussed how the T-R cycles were eustatic in origin. At least three

factors were consistent with the latter interpretation. First, new chronostratigraphic constraints document rapid (600 kyr or less) consecutive T-R cycles and the presented thickness models and sedimentation rates clearly reports major accumulation during the FSST (S interval), as expectable in contexts of eustasy-driven base level variation (*e.g.* the recent study by [Lobo and Ridente, 2014](#)). Second, no depositional discontinuities have been documented within the Bearpaw succession that, instead, records a gradual eastward shift of lithologies and facies. Third, major feeding systems and sediment distribution patterns remained unaltered throughout the entire stratigraphic interval (and likely upsection until modern days, as most of them coincide geographically with modern superimposed valleys, still acting as sediments inputs to the foreland basin in Alberta). Finally, the Cretaceous sea level history in the study of [Haq \(2014\)](#), reports two global eustatic events (KCa6 and KCa7) likely related to the deposition of the Bearpaw Fm., although further investigations are needed as with the data available to this study these events could not be directly linked to the Bearpaw Fm. T-R cycles. In conclusion, the Bearpaw Fm. represents a short parenthesis (the last one in the study area) of eustasy-driven marine sedimentation within an overall continental filling up trend that interested the Late Cretaceous foreland basin of west-central Alberta. Therefore, this study provide a robust stratigraphic case study allowing to discriminate the genetic component of transgressive events in non-marine domains as well as crucial data to interpret the paleogeography of Alberta during the Campanian.

5.2.3 Implications for the petroleum system analysis

Following the conclusions about the petroleum system in west-central Alberta (reported in paragraph 4.6), as represented in figure 5.8, the Bearpaw lower tongue sediments sealed the top of the Belly River Group, juxtaposing marine shales to coarse, fluvial sandstones that characterize the mid-upper Belly River units (*i.e.* Oldman and Dinosaur Park formations). Thus, the Bearpaw Fm. and correlative deposits actually sealed some of the most productive oil resevoirs in Alberta. Nonetheless, as reported in paragraph 4.5.2, not only the lower Bearpaw tongue presents the requirements to act as an efficient seal, but the whole Bearpaw succession actually does. Infact, permeable sand bodies were almost completely lacking from the study area. In sections 4.28 and 4.29 (in the central study area, north and south of the Pembina zone), the analyzed strata (inferred from gamma ray logs) are mainly decametric intervals of silt and shales: fine to very fine sediments and, moreover, in continuity.

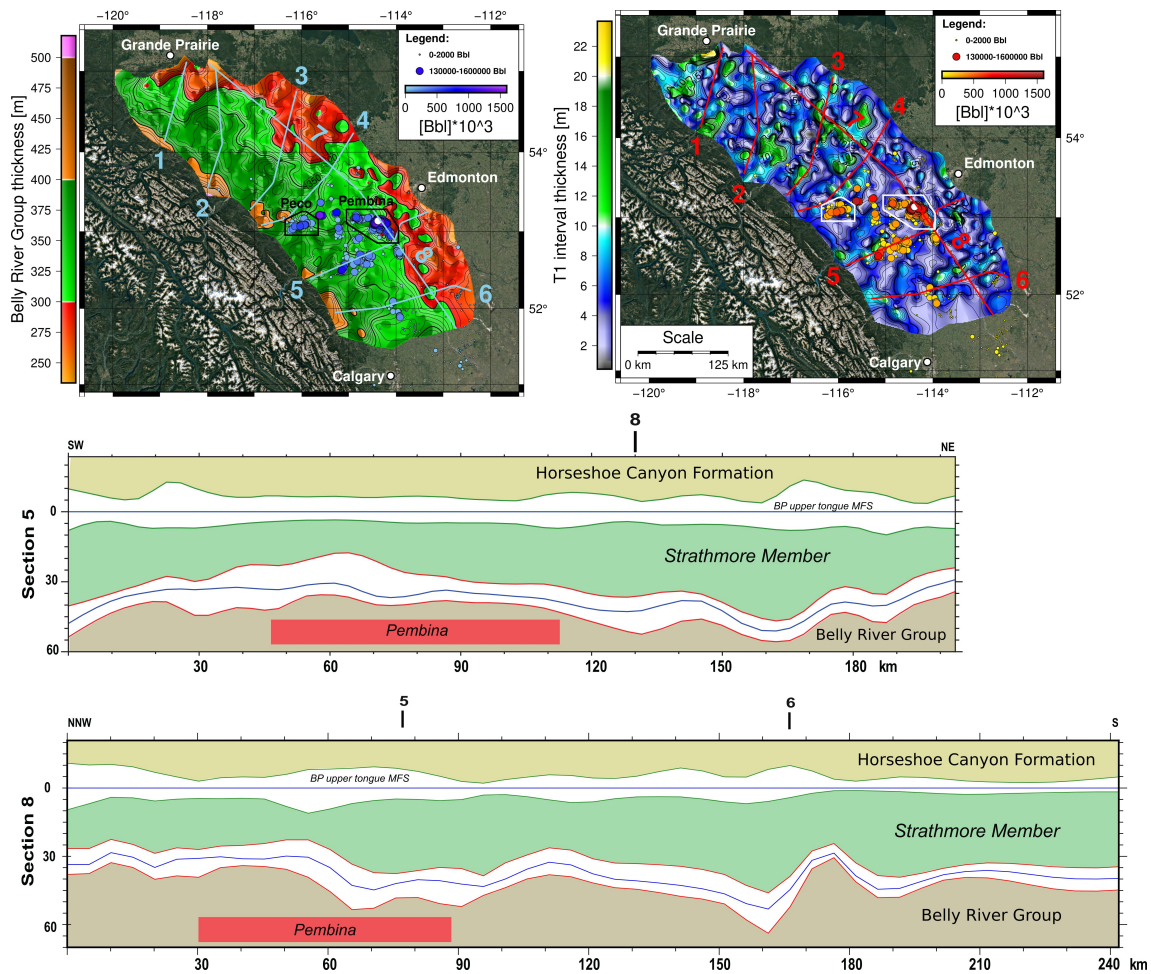


Figure 5.8: Simplified longitudinal cross sections 5 and 8 (upper tongue MFS as datum) showing the stratigraphic occurrence of the Pembina oil field and plan view of the location of section traces and exploited fields. Refer to figure 10 and relative text in paragraph 4.6 for a complete discussion about the maps under section traces. Wells are plotted on the isopach maps of (left) the Belly River Group and (right) Bearpaw lower tongue transgressive (T1) interval. Color and size of dots (productive wells) are proportional to oil exploitation (see the legend). Palette color-bars for respective thickness intervals are reported on the left in meters. Peco and Pembina East oil fields are indicated.

Especially in the S interval of section 4.28, sandstones and channel belts deposits were found, but they are rare, relatively thin (<10 m), sparse and surrounded by impermeable sediments. These observations lead to interpret the whole Bearpaw succession, including the S interval, as potential sealing units for the underlying productive reservoirs of the Belly River Group. Would the relatively thin T1 interval fail to seal the Belly River reservoirs, in places where fractures developed or simply permeability increased locally (*e.g.* in coastal zones of the paleogeographic maps), the overlying intervals could easily contain the leaked reserves, preventing upsection migration and eventually trapping them, likely within small reservoirs represented by coarser and isolated bodies in the studied succession. Further exploitation-aimed

exploration of these potential reservoirs within the Bearpaw succession will likely result non economically-interesting findings as no strong gamma ray hydrocarbon-related signature was observed in this study within the succession. Hence, further exploration for hydrocarbon resources within the Bearpaw succession is not suggested by our results.

5.3 Conclusions

This study deals in detail with a geological context that received a remarkable attention by the geologists of the last century and most of the times - if not always - past works tended to deal with it under a large scale perspective, on the basis of the available models and not using as detailed datasets as in this study. The major phases of structuring of the mountain range have been associated with flexural tectonics acting over the foreland system and interposed - or interplaying - with eustatic events of variable magnitude. On the base of the available models, all the phases of accommodation space creation during the Cretaceous in the foreland basin of west-central Alberta were associated to tectonic pulses active in the mountain range (which have very different temporal resolution than the one we discuss in this study). The Bearpaw interval deposited between the two continental clastic wedges which, as a whole, can be interpreted as in [Catuneanu et Al. \(1999\)](#), therefore as deposits that accumulated with minor variations during the late filling up phases, until the complete closure of the basin. This study significantly extended our understanding of the Bearpaw Formation and of the Western Interior Seaway (WIS) in west-central Alberta. Data here discussed include previously unveiled insights about the paleogeographic evolution and depositional dynamics on the western WIS shorelines. The spatial and temporal high-resolution analysis of the two main transgressive-regressive (T-R) cycles of the Bearpaw Formation presented and discussed in this study, lead to conclude the persistence of a significantly different scenario than the one described by previous literature. This research provide a strong case study documenting the reciprocal architecture of marine and non-marine environments, in continuity and on a previously unstudied vast area, within a well time-constrained succession for the late Campanian. Data provided here include the first 3D-modeled elaboration of the main stratigraphic surfaces concerning the T-R cycles, isopachs and cumulative maps for consecutive systems tracts and the first detailed mapping of the accumulation rates concerning each dated interval in the whole study area. Our results lead to interpret two paleogeographic scenarios for the MFS of the two T-R cycles with previously unmatched high-resolution, and to recognize the large scale

paleogeographic context of the study area relatively to the WIS. The large gamma ray well logs dataset upon which this study is based was accurately correlated with other surrounding areas from previous studies and a comparison was made between the results here presented and the results previously achieved by the Authors, contextualizing this study in the framework of other remarkable works and discoveries already published concerning such a long-studied and continuously evolving topic as the Bearpaw Formation. Moreover, the approach here presented permitted to identify the same T-R cycles already recognized outside our study area (historically regarded as a single, major T-R event) and the correlative deposits into the almost undocumented coastal and non-marine domains, finding depositional patterns and stratigraphic markers to follow into the continental succession of western Alberta which developed during the Bearpaw time. The events correlated in this study thus permit to trace coeval surfaces beyond the pure marine context, westward and northward toward the Rocky Mountains, that can be used by future studies not only to better understand the complex tectonic dynamics under the foothills but also as reference for stratigraphic well-log analysis of different time intervals in the area.

The paleogeographic evolution and the inferred distribution of the environments in the study area (figures 5.1 and 5.2) developed in the foreland basin on a NW-SE oriented axis, external to the deformed foothills region of the Canadian Rocky Mountains fold and thrust-belt. The geometry of the basin was inherited by flexural subsidence that provided the accommodation space for the deposition of mainly continental successions from the base of the Belly River Group (at approximately 80 Myr) up to the Tertiary. Sediment accumulation in the study area is linked to primary sources located in the rising cordillera throughout the entire studied interval. Major feeding systems and sediment distribution patterns remained unaltered throughout the studied stratigraphic interval. No strong evidence suggests a sediment source located to the east, signifying either a submerged forebulge, inexistent sediment discharge (no drainage system on the western forebulge) or a large distance from it. Within the S interval, a remarkably thick deposit was found in the southeastern study area, detached from the main sediment distribution trajectories and thus possibly linked to an eastern provenance. In this structural and depositional setting, the Bearpaw Formation represented the sole and final marine event in the Western Interior Seaway of Alberta. Data presented in this study permitted to interpret the Bearpaw T-R cycles as a response to a major eustatic control rather than tectonic deformation at the observed timescale. In fact, the documented Bearpaw T-R cycles do not show depositional discontinuities but rather a gradual eastward shift of the depositional systems in a relatively short time-span, thus can't be inter-

preted as a response to flexural subsidence increment induced by a tectonic pulse in the mountain range. The lower Bearpaw cycle include a radiometrically dated, rapid transgressive event (T1 interval) which lasted for 200 kyr. It is widely distributed in the foreland basin and formed in the context of a southwards-opening narrow and elongated bay on the western border of the WIS. That bay received, especially during the lower regressive event (R1 interval), moderate quantities of sediments from the west. These sediments deposited mainly in the central study area, forming a slope-break aligned N-S and subparallel to the Rocky Mountains deformation front which always prograded eastwards and southeastwards during the whole studied succession. The largest volume of sediment deposited during the Bearpaw time belongs to the S interval, interposed between the two Bearpaw T-R cycles, during which accumulation rates more than doubled, from mean values around 3 cm/kyr of the lower Bearpaw cycle up to 8 cm/kyr (with peak values over 17 cm/kyr). The S interval thus recorded the progradation of continental to paralic deposition through the entire study area. The deposition during the S interval was responsible for most of the environmental eastward shifts recorded during Bearpaw time, as well as for a consistent rearranging of the paleogeography of the foreland. In fact, during the S interval most of the accomodation space within the bay was consumed and only a very narrow branch to the east likely remained flooded by marine waters. Inferred coastal environments thus became more tidally influenced, developing large and flat geometries, easily flooded by daily tides as well as more susceptible to sea level changes. The upper Bearpaw T-R cycle developed in this context and lasted for at least 600 kyr (significantly more than the lower one) but nonetheless, deposited very similar volumes of sediment in west-central Alberta. The results of this study lead to conclude that the upper Bearpaw transgression has been actually able to reach the northern study area, as the lower T-R cycle did, anyway, the context in which the upper tongue sediment deposited was different. The lower Bearpaw tongue deposited in a wider bay, less influenced by the tides. The upper tongue represents instead high-water table conditions with the development of vast coaly swamps/-coastal lowlands on the whole central-eastern study area. Tidal flats covered the entire eastern border of the study area (implying a larger influence of tides, thus a narrower bay) and divided the northern area of Grande Prairie and the southern study area, both representing marine domain features on gamma ray well logs. The bipartition of the study area, given the paleogeographic context, the 3D geometries and the lithologies found, led to interpret the existence of the above cited narrow and elongated bay, which developed subparallel to deformation front and this shoreline conformation was never recognized before in Alberta. The inferred paleogeography

for the upper T-R cycle remained relatively stable compared to the major evolution it underwent during the S interval progradation, but at the end of it, its possible to infer that marine waters only flooded the bay in the southeastern portion of the study area, south of Edmonton, as the R2 interval deposition filled the bay following the lowering base level.

The rapid drowning that developed during the T1 interval overlapped the uppermost Belly River units (channels and delta systems) that act as reservoir of Peco and Pembina East oil fields. The paleogeography and lithology of the Bearpaw sea during the T1 interval (figure 5.1) paired to the distribution of productive oil fields in Alberta over the isopachs of the T1 interval and Belly River Group (figure 5.8), strongly suggested that this event provided an efficient seal and thus played a key role in the formation of the most oil-productive reservoirs of the Belly River Group. Nonetheless, further analysis highlighted how not only the lower transgressive interval but the whole Bearpaw succession presents fine to very fine impermeable sediments in continuity and thus has the potential to act as sealing unit for these reservoirs. In post-Bearpaw units, only coalbed methane and water have been found in drilled wells. This indicates that the Cardium oils that sourced the Belly River sands (Plint et Al., 1986; Putnam, 1993; Creaney et Al., 1994) have been prevented to migrate upsection in the permeable Horseshoe Canyon units (including the Strathmore Member). The eustatic events described in this study, then, have been very effective to provide an efficient seal for the exploited hydrocarbons fields in the late Cretaceous successions.

In conclusion, beyond the regional scientific interest, this study also documented (1) the level of resolution that can be obtained in any study area that presents a similar context and data availability, (2) the mappability of coeval surfaces and stratigraphic intervals that cross various continental, coastal and marine depositional settings and (3) the possibility to differentiate, in similar geological contexts, the accommodation space variability associated with tectonics or eustasy, clarifying which one controls the stratigraphic record over time.

5.4 Future developments

This research unveiled the real extension reached during the Campanian by the last marine ingressions in west-central Alberta. These events are responsible for the deposition of the Bearpaw Fm., a long-studied topic which continues to surprise for its complex genetic relation with eustatic and tectonic cycles. Nonetheless, the conclusions reached in this study need confirmation by future discoveries. Our gamma-ray

based approach almost totally exclude considerations about the climatic scenario in which the dynamics described by data here presented evolved. To understand and integrate the climatic scenario the only viable option is through high-resolution paleontological and palynological studies, which imply extended sampling campaigns and laboratory analysis. Southern Alberta outcrops of the Bearpaw Fm. near Calgary and northern Wapiti Fm. outcrops in Grande Prairie are now tridimensionally correlated on a vast area, hence these two locations may be the starting point for outcrop sampling campaigns. What was missing from this study indeed, is also direct data. All results here produced are derived from a detailed and accurate interpretation of both gamma ray well logs and literature data. An extensive facies analysis on cores can greatly improve the precision of the paleogeographic maps and the accuracy of our estimations, offering at the same time the opportunity to collect samples for paleontological and palynological analysis. Late Cretaceous was a notoriously "hot" period, understanding the climatic impact on the environments described in this study has the potential to lead to new discoveries which could significantly impact our understanding of modern climate change-related evolution of coastal areas and moreover, of their influence on the inland. Another interesting branch that this research could flow into is to replicate the same analysis in other areas and/or other time intervals, in order to further refine the methods here described and test their validity in different scenarios, thus implying not only different tectonic settings but also different time scales and resolutions. This study would have never been possible without the tools developed by the people contributing to the open-source community. Focusing on this second option could also mean contributing to that community with the publication of valuable open-source geomatic tools which could be useful (as well as lower the research costs and time) in any case study concerning spatial and multi-temporal data analysis with any kind of xyz dataset.

Bibliography

- Ainsworth, R. B. (1994). *Marginal marine sedimentology and high resolution sequence analysis; Bearpaw-Horseshoe Canyon transition, Drumheller, Alberta*. Bulletin of Canadian Petroleum Geology, 42(1), 26-54. [doi:10.35767/gscpgbull.42.1.026](https://doi.org/10.35767/gscpgbull.42.1.026)
- Alencaster, G. (1984). *Late Jurassic-Cretaceous molluscan paleogeography of the southern half of Mexico. Jurassic-Cretaceous Biochronology and Paleogeography of North America*. Geological Association of Canada Special Paper, 27, 77-88.
- Arthur, M. A., Kump, L. R., Dean, W. E., and Larson, R. L. (1991). *Superplume, supergreenhouse*. Eos, Transactions, American Geophysical Union, 72, 301.
- Arthur, M. A., Dean, W. E., and Schlanger, S. O. (1985). *Variations in the global carbon cycle during the Cretaceous related to climate, volcanism, and changes in atmospheric CO₂*. The carbon cycle and atmospheric CO₂: Natural variations Archean to present, 32, 504-529. [doi:10.1029/GM032p0504](https://doi.org/10.1029/GM032p0504)
- Bally, A. W., Gordy, P. L., and Stewart, G. A. (1966). *Structure, seismic data, and orogenic evolution of southern Canadian Rocky Mountains*. Bulletin of Canadian Petroleum Geology, 14(3), 337-381. [doi:10.35767/gscpgbull.14.3.337](https://doi.org/10.35767/gscpgbull.14.3.337)
- Bell, P. R., and Currie, P. J. (2016). *A high-latitude dromaeosaurid, Boreonykus certekorum, gen. et sp. nov.(Theropoda), from the upper Campanian Wapiti Formation, west-central Alberta*. Journal of Vertebrate Paleontology, 36(1). [doi:10.1080/02724634.2015.1034359](https://doi.org/10.1080/02724634.2015.1034359)
- Bell, P. R., Fanti, F., Mitchell, M. T., and Currie, P. J. (2014). *Marine Reptiles (Plesiosauria and Mosasauridae) from the Puskwaskau Formation (Santonian-Campanian), West-Central Alberta*. Plesiosaurs and Mosasaurs from the Puskwaskau Formation. Journal of Paleontology, 88(1), 187-194. [doi:10.1666/13-043](https://doi.org/10.1666/13-043)

- Bell, P. R., Fanti, F., Acorn, J., and Sissons, R. S. (2013). *Fossil mayfly larvae (Ephemeroptera, cf. Heptageniidae) from the Late Cretaceous Wapiti Formation, Alberta, Canada*. *Journal of Paleontology*, 87(1), 147-150. doi:10.1666/12-058R.1
- Blakey, R. C. (2013). *Key time slices of North American geologic history*. Colorado plateau Geosystems.
- Blakey, R. C., and Ranney, W. D. (2017). *Ancient landscapes of western North America: a geologic history with paleogeographic maps*. Springer. doi:10.1007/978-3-319-59636-5
- Bustin, R. M., and Smith, G. G. (1993). *Coal deposits in the front ranges and foothills of the Canadian Rocky Mountains, southern Canadian Cordillera*. *International Journal of Coal Geology*, 23(1-4), 1-27. doi:10.1016/0166-5162(93)90041-8
- Cant, D. J. (1995). *Sequence stratigraphic analysis of individual depositional successions: effects of marine/nonmarine sediment partitioning and longitudinal sediment transport, Mannville Group, Alberta Foreland Basin, Canada*. *AAPG bulletin*, 79(5), 749-762. doi:10.1306/8D2B1B92-171E-11D7-8645000102C1865D
- Catuneanu, O. (2006). *Principles of sequence stratigraphy*. Elsevier. ISBN: 9780080473987
- Catuneanu, O., 2017. *Sequence stratigraphy: Guidelines for a standard methodology*, In: M. Montenari (Ed.), *Stratigraphy and Timescales*, Academic Press, UK, 2, 1-57. doi:10.1016/bs.sats.2017.07.003
- Catuneanu, O., 2019a. *Model-independent sequence stratigraphy*. *Earth-Science Reviews*, 188, 312-388. doi:10.1016/j.earscirev.2018.09.017
- Catuneanu, O., 2019b. *Scale in sequence stratigraphy*. *Marine and Petroleum Geology*, 106, 128-159. doi:10.1016/j.marpetgeo.2019.04.026
- Catuneanu, O. (2004). *Retroarc foreland systems-evolution through time*. *Journal of African Earth Sciences*, 38(3), 225-242. doi:10.1016/j.jafrearsci.2004.01.004
- Catuneanu, O., Galloway, W. E., Kendall, C. G. S. C., Miall, A. D., Posamentier, H. W., Strasser, A., and Tucker, M. E. (2011). *Sequence stratigraphy: methodology and nomenclature*. *Newsletters on stratigraphy*, 44(3), 173-245. doi:10.1127/0078-0421/2011/0011

- Catuneanu, O., Sweet, A. R., and Miall, A. D. (2000). *Reciprocal stratigraphy of the Campanian-Paleocene western interior of North America*. *Sedimentary Geology*, 134(3-4), 235-255. doi:10.1016/S0037-0738(00)00045-2
- Catuneanu, O., Sweet, A. R., and Miall, A. D. (1999). *Concept and styles of reciprocal stratigraphies: Western Canada foreland system*. *Terra Nova-Oxford*, 11(1), 1-8. doi:10.1046/j.1365-3121.1999.00222.x
- Catuneanu, O., Sweet, A. R., and Miall, A. D. (1997). *Reciprocal architecture of Bearpaw TR sequences, uppermost Cretaceous, Western Canada sedimentary basin*. *Bulletin of Canadian Petroleum Geology*, 45(1), 75-94. doi:10.35767/gscpgbull.45.1.075
- Chamberlain, V. E., Lambert, R. S. J., and McKerrow, W. S. (1989). *Mesozoic sedimentation rates in the Western Canada Basin as indicators of the time and place of tectonic activity*. *Basin Research*, 2(3), 189-202. doi:10.1111/j.1365-2117.1989.tb00034.x
- Chen, D., Langenberg, C. W., and Beaton, A. P. (2005). *Horseshoe Canyon-Bearpaw transition and correlation of associated coal zones across the Alberta plains*. Alberta Energy and Utilities Board.
- Cochran, J. K., Landman, N. H., Turekian, K. K., Michard, A., and Schrag, D. P. (2003). *Paleoceanography of the late Cretaceous (Maastrichtian) Western Interior seaway of North America: evidence from Sr and O isotopes*. *Palaeogeography, Palaeoclimatology, Palaeoecology*, 191(1), 45-64. doi:10.1016/S0031-0182(02)00642-9
- Cobban, W. A., Merewether, E. A., Fouch, T. D., and Obradovich, J. D. (1994). *Some Cretaceous shorelines in the western interior of the United States*. Rocky Mountain Section (SEPM).
- Coney, P. J., Jones, D. L., and Monger, J. W. (1980). *Cordilleran suspect terranes*. *Nature*, 288(5789), 329-333. doi:10.1038/288329a0
- Creaney, S., Allan, J., Cole, K. S., Fowler, M. G., Brooks, P. W., Osadetz, K. G., Macqueen, R., Snowdon, L., and Riediger, C. L. (1994). *Petroleum generation and migration in the Western Canada Sedimentary Basin*, In: G.D. Mossop and I. Shetsen (Eds.), *Geological atlas of the Western Canada sedimentary basin*. Canadian Society of Petroleum Geologists and Alberta Research Council, 455-468.

- Cross, T.A. (1986), *Tectonic controls of foreland basin subsidence and Laramide style deformation, western United States*, In: Allen, P.A., and Homewood, P. (Eds.), *Foreland basins*. International Association of Sedimentologists Special Publications, 8, 15-39.
- Cullen, T. M., and Evans, D. C. (2016). *Palaeoenvironmental drivers of vertebrate community composition in the Belly River Group (Campanian) of Alberta, Canada, with implications for dinosaur biogeography*. BMC ecology, 16(1), 52. doi:10.1186/s12898-016-0106-8
- Currie, P. J., and Koppelhus, E. B. (2005). *Dinosaur Provincial Park: a spectacular ancient ecosystem revealed*. Indiana University Press. doi:10.1086/523131
- Currie, P. J., Langston, Jr, W., and Tanke, D. H. (2008). *New Horned Dinosaur from an Upper Cretaceous Bone Bed in Alberta*. NRC Research Press, pp. 152. doi:10.1139/9780660198194
- Daidu, F., Yuan, W., and Min, L. (2013). *Classifications, sedimentary features and facies associations of tidal flats*. Journal of Palaeogeography, 2(1), 66-80. doi:10.3724/SP.J.1261.2013.00018
- Dawson, F., Evans, C., Marsh, R. and Richardson, R. (1994). *Uppermost Cretaceous and Tertiary strata of the Western Canada Sedimentary Basin*, In: G.D. Mossop and I. Shetsen (Eds.), *Geological Atlas of the Western Canada Sedimentary Basin*. Canadian Society of Petroleum Geologists and Alberta Research Council, Special Report 4, 387-406.
- Dawson, F. M., Evans, C., Marsh, R., and Power, B. (1990). *Uppermost Cretaceous-Tertiary strata of the Western Canada Sedimentary Basin*. Bulletin of Canadian Petroleum Geology, 38(1), 160-161.
- DeCelles, P. G. (2004). *Late Jurassic to Eocene evolution of the Cordilleran thrust belt and foreland basin system, western USA*. American Journal of Science, 304(2), 105-168. doi:10.2475/ajs.304.2.105
- DeCelles, P. G., and Currie, B. S. (1996). *Long-term sediment accumulation in the Middle Jurassic-early Eocene Cordilleran retroarc foreland-basin system*. Geology, 24(7), 591-594. doi:10.1130/0091-7613(1996)024<0591:LTSAIT>2.3.CO;2
- DeCelles, P. G., and Giles, K. A. (1996). *Foreland basin systems*. Basin research, 8(2), 105-123. doi:10.1046/j.1365-2117.1996.01491.x

- de Cserna, Z. (1989). *An outline of the geology of Mexico*, In: Albert W. Bally, A.W., Palmer, A.R., *The Geology of North America-An overview*. Boulder, The Geological Society of America, A, 233-264.
- Dodson, P. (1990). *Counting dinosaurs: how many kinds were there?* Proceedings of the National Academy of Sciences, 87(19), 7608-7612. [doi:10.1073/pnas.87.19.7608](https://doi.org/10.1073/pnas.87.19.7608)
- Dodson, P. (1971). *Sedimentology and taphonomy of the Oldman formation (Campanian), dinosaur provincial park, Alberta (Canada)*. Palaeogeography, Palaeoclimatology, Palaeoecology, 10(1), 21-74. [doi:10.1016/0031-0182\(71\)90044-7](https://doi.org/10.1016/0031-0182(71)90044-7)
- Eberth, D. A., and Kamo, S. L. (2020). *High-precision U-Pb CA-ID-TIMS dating and chronostratigraphy of the dinosaur-rich Horseshoe Canyon Formation (Upper Cretaceous, Campanian-Maastrichtian), Red Deer River valley, Alberta, Canada*. Canadian Journal of Earth Sciences, 57(10), 1220-1237. [doi:10.1139/cjes-2019-0019](https://doi.org/10.1139/cjes-2019-0019)
- Eberth, D. A., Evans, D. C., Brinkman, D. B., Therrien, F., Tanke, D. H., and Russell, L. S. (2013). *Dinosaur biostratigraphy of the Edmonton Group (Upper Cretaceous), Alberta, Canada: evidence for climate influence*. Canadian Journal of Earth Sciences, 50(7), 701-726. [doi:10.1139/cjes-2012-0185](https://doi.org/10.1139/cjes-2012-0185)
- Eberth, D. A., and Braman, D. R. (2012). *A revised stratigraphy and depositional history for the Horseshoe Canyon Formation (Upper Cretaceous), southern Alberta plains*. Canadian Journal of Earth Sciences, 49(9), 1053-1086. [doi:10.1139/e2012-035](https://doi.org/10.1139/e2012-035)
- Eberth, D. A. (2005). *The Geology*, In: P.J. Currie and E.B. Koppelhus (Eds.), *Dinosaur Provincial Park: a spectacular ancient ecosystem revealed*, 54-82.
- Eberth, D. A. (2002). *Review and comparison of Belly River Group and Edmonton Group stratigraphy and stratigraphic architecture in the southern Alberta Plains*. Canadian Society of Petroleum Geologist, 75th Anniversary Convention, Extended Abstracts (Vol. 7).
- Eberth, D. A., and Deino, A. L. (1992). *A geochronology of the non-marine Judith River Formation of southern Alberta*, In: *Mesozoic of the Western Interior: Abstracts for the Society of Economic Paleontologists and Mineralogists Theme Meeting, Fort Collins, Colorado*. Society for Sedimentary Geology, Tulsa, Oklahoma, United States of America, 24-25.

- Elder, W. P., and Kirkland, J. I. (1994). *Cretaceous paleogeography of the southern Western Interior region*. Rocky Mountain Section (SEPM).
- Elder, W. P., Gustason, E. R., and Sageman, B. B. (1994). *Correlation of basinal carbonate cycles to nearshore parasequences in the Late Cretaceous Greenhorn seaway, Western Interior USA*. Geological Society of America Bulletin, 106(7), 892-902. doi:10.1130/0016-7606(1994)106<0892:COBCCT>2.3.CO;2
- Erickson, J. M. (1999). *The Dakota Isthmus - closing the late Cretaceous Western Interior Seaway*. Proceedings of the North Dakota Academy of Science, 53, 124-129.
- Fanti, F. (2009). *Bentonite chemical features as proxy of late Cretaceous provenance changes: A case study from the Western Interior Basin of Canada*. Sedimentary Geology, 217(1-4), 112-127. doi:10.1016/j.sedgeo.2009.03.015
- Fanti, F., and Catuneanu, O. (2010). *Fluvial sequence stratigraphy: the Wapiti Formation, west-central Alberta, Canada*. Journal of Sedimentary Research, 80(4), 320-338. doi:10.2110/jsr.2010.033
- Fanti, F., and Catuneanu, O. (2009). *Stratigraphy of the Upper Cretaceous Wapiti Formation, west-central Alberta, Canada*. Canadian Journal of Earth Sciences, 46(4), 263-286 . doi:10.1139/E09-020
- Fanti, F., Currie, P. J., and Burns, M. E. (2015). *Taphonomy, age, and paleoecological implication of a new Pachyrhinosaurus (Dinosauria: Ceratopsidae) bonebed from the Upper Cretaceous (Campanian) Wapiti Formation of Alberta, Canada*. Canadian Journal of Earth Sciences, 52(4), 250-260. doi:10.1139/cjes-2014-0197
- Fanti, F., and Miyashita, T. (2009). *A high latitude vertebrate fossil assemblage from the Late Cretaceous of west-central Alberta, Canada: evidence for dinosaur nesting and vertebrate latitudinal gradient*. Palaeogeography, Palaeoclimatology, Palaeoecology, 275(1-4), 37-53. doi:10.1016/j.palaeo.2009.02.007
- Frakes, L. A., Francis, J. E., and Syktus, J. I. (1992). *Climate Modes of the Phanerozoic*. Cambridge University Press. doi:10.1017/CBO9780511628948
- Freedman Fowler, E. A., and Horner, J. R. (2015). *A new brachylophosaurin hadrosaur (Dinosauria: Ornithischia) with an intermediate nasal crest from the Campanian Judith River Formation of northcentral Montana*. PloS one, 10(11). doi:10.1371/journal.pone.0141304

- Fuentes, F., DeCelles, P. G., and Gehrels, G. E. (2009). *Jurassic onset of foreland basin deposition in northwestern Montana, USA: Implications for along-strike synchronicity of Cordilleran orogenic activity*. *Geology*, 37(4), 379-382. doi:10.1130/G25557A.1
- Fuentes, F., DeCelles, P. G., Constenius, K. N., and Gehrels, G. E. (2011). *Evolution of the Cordilleran foreland basin system in northwestern Montana, USA*. *GSA Bulletin*, 123(3-4), 507-533. doi:10.1130/B30204.1
- Galloway, W. E. (1989). *Genetic stratigraphic sequences in basin analysis I: architecture and genesis of flooding-surface bounded depositional units*. *AAPG bulletin*, 73(2), 125-142. doi:10.1306/703C9AF5-1707-11D7-8645000102C1865D
- Gensac, E., Gardel, A., Lesourd, S., and Brutier, L. (2015). *Morphodynamic evolution of an intertidal mudflat under the influence of Amazon sediment supply-Kourou mud bank, French Guiana, South America*. *Estuarine, Coastal and Shelf Science*, 158, 53-62. doi:10.1016/j.ecss.2015.03.017
- Gilbert, M. (2019). *Sedimentology, Ichnology, Sequence Stratigraphy and Vertebrate Paleontology of the Belly River Group, southwestern Saskatchewan, Canada*. Doctoral dissertation, University of Saskatchewan. doi:10.13140/RG.2.2.12974.66885
- Gilbert, M. M., Buatois, L. A., and Renaut, R. W. (2019). *Ichnology and depositional environments of the Upper Cretaceous Dinosaur Park-Bearpaw formation transition in the Cypress Hills region of Southwestern Saskatchewan, Canada*. *Cretaceous Research*, 98, 189-210. doi:10.1016/j.cretres.2018.12.017
- Gilbert, M. M., Bamforth, E. L., Buatois, L. A., and Renaut, R. W. (2018). *Paleoecology and sedimentology of a vertebrate microfossil assemblage from the easternmost Dinosaur Park Formation (Late Cretaceous, Upper Campanian) Saskatchewan, Canada: Reconstructing diversity in a coastal ecosystem*. *Palaeogeography, Palaeoclimatology, Palaeoecology*, 495, 227-244. doi:10.1016/j.palaeo.2018.01.016
- Gill, J.R., and Cobban, W. A. (1973). *Stratigraphy and Geological History of the Montana Group and Equivalent rocks, Montana, Wyoming, and North and South Dakota*. U.S. Geological Survey Professional Paper, v, 776, 1-37.
- Glombick, P. M. (2010). *Top of the Belly River Group in the Alberta Plains: sub-surface stratigraphic picks and modelled surface*. Alberta Geological Survey, Open file Report, 10.

- Goldhammer, R. K., and Johnson, C. A. (1999). *Mesozoic sequence stratigraphy and paleogeographic evolution of northeast Mexico*. Geological Society of America Special Papers, 1-58. [doi:10.1130/0-8137-2340-X.1](https://doi.org/10.1130/0-8137-2340-X.1)
- Gradstein, F.M. (2012). *Introduction*, In: Gradstein, F.M., Ogg, J.G., Schmitz, M.D., and Ogg, G.M. (Eds.), *The Geological Time Scale 2012*, Elsevier, 1 -29. ISBN: 9780444594488
- Hamblin, A. P. (2004). *The Horseshoe Canyon Formation in southern Alberta: surface and subsurface stratigraphic architecture, sedimentology, and resource potential*. Bulletin 578: Geological Survey of Canada. [doi:10.4095/215068](https://doi.org/10.4095/215068)
- Haq, B. U. (2014). *Cretaceous eustasy revisited*. Global and Planetary change, 113, 44-58. [doi:10.1016/j.gloplacha.2013.12.007](https://doi.org/10.1016/j.gloplacha.2013.12.007)
- Hathway, B. (2016). *Regional T-R sequence stratigraphy and lithostratigraphy of the Bearpaw Formation (Upper Campanian), west-central and southwestern Alberta plains*. Bulletin of Canadian Petroleum Geology, 64(3), 449-466. [doi:10.2113/gscpgbull.64.3.449](https://doi.org/10.2113/gscpgbull.64.3.449)
- Hatcher, J.B. and Stanton, T.W. (1903). *The stratigraphic position of the Judith River beds and their correlation with the Belly River Beds*. Science, 18: 211-212. [doi:10.1126/science.18.450.211](https://doi.org/10.1126/science.18.450.211)
- Hay, W. W. (2008). *Evolving ideas about the Cretaceous climate and ocean circulation*. Cretaceous Research, 29(5-6), 725-753. [doi:10.1016/j.cretres.2008.05.025](https://doi.org/10.1016/j.cretres.2008.05.025)
- Hay, W. W., Eicher, D. L., and Diner, R. (1993). *Physical oceanography and water masses in the Cretaceous Western Interior Seaway*, In: *Evolution of the western interior basin*. St. John's: Geological Association of Canada, v. 39, 297-318
- Jeletzky, J.A. (1978). *Causes of Cretaceous oscillations of sea level in Western and Arctic Canada and some general geotectonic implications*. Geological Survey of Canada Bulletin, v. 77, 1- 44.
- Jeletzky, J. A. (1971). *Marine Cretaceous biotic province and paleogeography of western and arctic Canada: illustrated by a detailed study of ammonites*. Paper of the Geological Survey of Canada, 70, 1-92.
- Jerzykiewicz, T. (2010). *Stratigraphic setting of the key bentonite layers in the non-marine Saunders Group - Upper Cretaceous to Paleocene strata of the Rocky Mountains in Alberta, Canada*, In: *A guidebook to the Blackstone River section prepared for the GTS NEXT Project*, Calgary. Geoclastica Consulting Ltd.

- Jerzykiewicz, T. (1997). *Stratigraphic framework of the upper Cretaceous to Paleocene strata of the Alberta Basin*. Geological Survey of Canada Bulletin 510, 121 [doi:10.4095/208902](https://doi.org/10.4095/208902)
- Jerzykiewicz, T. (1996). *Baculites compressus robinsoni Cobban from the Crownsnest River section at Lundbreck, Alberta: an implication for the timing of the Late Cretaceous Bearpaw transgression into the southern foothills of Alberta*. Geological Survey of Canada, Current Research, 97-100. [doi:10.4095/207878](https://doi.org/10.4095/207878)
- Jerzykiewicz, T. (1992). *Controls on the distribution of coal in the Campanian to Paleocene post-Wapiabi strata of the Rocky Mountain*. Controls on the Distribution and Quality of Cretaceous Coals, 267, 139. [doi:10.1130/SPE267](https://doi.org/10.1130/SPE267)
- Jerzykiewicz, T. and McLean, J R. (1980). *Lithostratigraphic and sedimentological framework of coal-bearing Upper Cretaceous-Lower Tertiary strata, Coal Valley area, central Alberta Foothills*. Geological Survey of Canada, Paper 79-12. [doi:10.4095/102161](https://doi.org/10.4095/102161)
- Jerzykiewicz, T., and Norris, D. K. (1994). *Stratigraphy, structure and syntectonic sedimentation of the Campanian 'Belly River' clastic wedge in the southern Canadian Cordillera*. Cretaceous Research, 15(4), 367-399. [doi:10.1006/cres.1994.1022](https://doi.org/10.1006/cres.1994.1022)
- Jerzykiewicz, T., Sweet, A. R., and McNeil, D. H. (1996). *Shoreface of the Bearpaw Sea in the footwall of the Lewis Thrust, southern Canadian Cordillera, Alberta*. Geological Survey of Canada Current Research, 155-163. [doi:10.4095/207421](https://doi.org/10.4095/207421)
- Jerzykiewicz, T., and Sweet, A. R. (1988). *Sedimentological and palynological evidence of regional climatic changes in the Campanian to Paleocene sediments of the Rocky Mountain Foothills, Canada*. Sedimentary geology, 59(1-2), 29-76. [doi:10.1016/0037-0738\(88\)90099-1](https://doi.org/10.1016/0037-0738(88)90099-1)
- Jerzykiewicz, T., and Sweet, A. R. (1986). *Caliche and associated impoverished palynological assemblages: an innovative line of paleoclimatic research into the uppermost Cretaceous and Paleocene of southern Alberta*. Core Conference, Calgary, Alberta, (7)1-19
- Kauffman, E. G., and Caldwell, W. G. E. (1993). *The Western Interior Basin in space and time*, In: *Evolution of the western interior basin*. Geological Association of Canada, Special Paper 39, 1-30.
- Kauffman, E. G. (1984). *Paleobiogeography and evolutionary response dynamic in the Cretaceous Western Interior Seaway of North America*, In: *Jurassic-Cretaceous*

- biochronology and paleogeography of North America*. Geological Association of Canada, Special Paper 27, 273-306
- Kauffman, E. G. (1977). *Geological and biological overview: Western Interior Cretaceous basin*. *The Mountain Geologist*, 14, 75-99
- Kennedy, W. J., Landman, N. H., Christensen, W. K., Cobban, W. A., and Hancock, J. M. (1998). *Marine connections in North America during the late Maastrichtian: palaeogeographic and palaeobiogeographic significance of Jeletzkytes nebrascensis Zone cephalopod fauna from the Elk Butte Member of the Pierre Shale, SE South Dakota and NE Nebraska*. *Cretaceous Research*, 19(6), 745-775. [doi:10.1006/cres.1998.0129](https://doi.org/10.1006/cres.1998.0129)
- Koppelhus, E. B., and Fanti, F. (2019). *Rare, non-marine deposits during the deposition of the Bearpaw Formation: Interpreting the palaeoenvironment of the DC bonebed (Wapiti Formation) using palynology and palaeobotany*. 7th Annual Meeting Canadian Society of Vertebrate Palaeontology May 10-13, 2019 Grande Prairie, Alberta, pp. 25.
- Larson, D., Vavrek, M., Bell, P., Campione, N., Fanti, F., Sissons, R., Sullivan, C. (2018). *A high-latitude assemblage of fossil turtles (Testudines) from the Late Campanian of Alberta, Canada*. 78th SVP - Annual Meeting Albuquerque (poster).
- Larson, N. L., Brezina, J., Landman, N. H., Garb, M. P., and Handle, K. C. (2013). *Hydrocarbon seeps: unique habitats that preserved the diversity of fauna in the Late Cretaceous Western Interior Seaway*. Wyoming Geological Society Handbook. Wyoming Geological Society, Caspar, Wyo.
- Larson, N. L. (2010). *Fossil coleoids from the Late Cretaceous (Campanian and Maastrichtian) of the Western Interior*. *Ferrantia*, 59, 78-113.
- Leckie, D. A., Vanbeselaere, N. A., and James, D. P. (1997). *Regional sedimentology, sequence stratigraphy and petroleum geology of the Mannville Group: Southwestern Saskatchewan*. *Petroleum Geology of the Mannville Group, Western Canada - Memoir 18*, 211-262
- Lee, H., Jang, Y., Kwon, S., Park, M. H., and Mitra, G. (2018). *The role of mechanical stratigraphy in the lateral variations of thrust development along the central Alberta Foothills, Canada*. *Geoscience Frontiers*, 9(5), 1451-1464. [doi:10.1016/j.gsf.2018.03.006](https://doi.org/10.1016/j.gsf.2018.03.006)

- Lerbekmo, J. F., and Braman, D. R. (2005). *Magnetostratigraphic and palynostratigraphic correlation of late Campanian to early Maastrichtian strata of the Bearpaw and Horseshoe Canyon formations between the CPOG Strathmore corehole and the Red Deer Valley section, Alberta, Canada*. *Bulletin of Canadian Petroleum Geology*, 53(2), 154-164. doi:10.2113/53.2.154
- Lerbekmo, J. F., Braman, D. R., Therrien, F., Koppelhus, E. B., and Taylor, W. (2005). *Paleomagnetostratigraphy*, In: P.J. Currie and E.B. Koppelhus (Eds.), *Dinosaur Provincial Park: a spectacular ancient ecosystem revealed*. Indiana University Press, Bloomington, 83-87. doi:10.1086/523131
- Lerbekmo, J. F. (2002). *The Dorothy bentonite: an extraordinary case of secondary thickening in a Late Campanian volcanic ash fall in central Alberta*. *Canadian Journal of Earth Sciences*, 39(12), 1745-1754. doi:10.1139/e02-079
- Lillegraven, J.A., and Ostresh, L.M. (1990). *Late Cretaceous (earliest Campanian/-Maastrichtian) evolution of western shorelines of the North American Western Interior Seaway in relation to known mammalian faunas. Dawn of the age of mammals in the northern part of the Rocky Mountain Interior, North America*. *Geological Society of America Special Paper*, 243, 1-30. doi:10.1130/SPE243-p1
- Lobo, F. J., and Ridente, D. (2014). *Stratigraphic architecture and spatio-temporal variability of high-frequency (Milankovitch) depositional cycles on modern continental margins: an overview*. *Marine Geology*, 352, 215-247. doi:10.1016/j.margeo.2013.10.009
- Mallon, J. C., Evans, D. C., Ryan, M. J., and Anderson, J. S. (2012). *Mega-herbivorous dinosaur turnover in the Dinosaur Park Formation (upper Campanian) of Alberta, Canada*. *Palaeogeography, Palaeoclimatology, Palaeoecology*, 350, 124-138. doi:10.1016/j.palaeo.2012.06.024
- McFarlan Jr, E., and Menes, L. S. (1991). *Lower cretaceous*, In: Salvador, A. *The Gulf of Mexico Basin*. Boulder, Colorado, Geological Society of America, *The Geology of North America*, J, 181-204. doi:10.1130/DNAG-GNA-J.181
- McMechan, M. E., Thompson, R. I., Caldwell, W. G. E., and Kauffman, E. G. (1993). *The Canadian Cordilleran fold and thrust belt south of 66 N and its influence on the Western Interior Basin*, In: Caldwell, W.G., and Kauffman, E.G. (Eds), *Evolution of the Western Interior Basin*. Geological Association of Canada Special Paper, 39, 73-90.

- Miall, A. D., Catuneanu, O., Vakarelov, B. K., and Post, R. (2008). *The western interior basin*. *Sedimentary basins of the world*, 5, 329-362. doi:10.1016/S1874-5997(08)00009-9
- Miller, K. G., Mountain, G. S., Wright, J. D., and Browning, J. V. (2011). *A 180-million-year record of sea level and ice volume variations from continental margin and deep-sea isotopic records*. *Oceanography*, 24(2), 40-53. doi:10.5670/oceanog.2011.26
- Miller, K.G., Kominz, M.A., Browning, J.V., Wright, J.D., Gregory S. Mountain, Katz, M.E., Sugarman, P.J., Cramer, B.S., Christie-Blick, N., Pekar, S.F. (2005). *The Phanerozoic Record of Global Sea-Level Change*. *Science*, 310, 1293-1298. doi:10.1126/science.1116412
- Miller, K. G., Sugarman, P. J., Browning, J. V., Kominz, M. A., Olsson, R. K., Feigenson, M. D., and Hernández, J. C. (2004). *Upper Cretaceous sequences and sea-level history, New Jersey coastal plain*. *GSA Bulletin*, 116(3-4), 368-393. doi:10.1130/B25279.1
- Miller, K. G., Sugarman, P. J., Browning, J. V., Kominz, M. A., Hernández, J. C., Olsson, R. K., Wright, J.D., Feigenson, M.D. and Van Sickle, W. (2003). *Late Cretaceous chronology of large, rapid sea-level changes: Glacioeustasy during the greenhouse world*. *Geology*, 31(7), 585-588. doi:10.1130/0091-7613(2003)031;0585:LCCOLR;2.0.CO;2
- Monger, J.W.H. (1993). *Cretaceous tectonics of the North American Cordillera*, In: Caldwell, W.G.E., and Kauffman, E.G. (Eds.), *Evolution of the Western Interior Basin*. Geological Association of Canada Special Paper, 39, 31-47.
- Monger, J.W.H. (1989). *Overview of cordilleran geology*, In: Ricketts, B.D. (Ed.), *Western Canada Sedimentary Basin: A Case History*. Canadian Society of Petroleum Geologists, 9-32.
- Montgomery, E. B., Clark, D. A., Gibson, B. B., and Sheptycki, R. J. (1978). *The Canadian unique well identifier*. Canadian Petroleum Association and Canadian Association of Petroleum Producers.
- Owens, J.P., and Gohn, G.S. (1985). *Depositional history of the Cretaceous series in the US Atlantic Coastal Plain: Stratigraphy, paleoenvironments, and tectonic controls of sedimentation*, In: Van Nostrand, R., *Geologic Evolution of the United States Atlantic Margin: New York*. 25-86.

- Pană, D. I., and Van Der Pluijm, B. A. (2015). *Orogenic pulses in the Alberta Rocky Mountains: Radiometric dating of major faults and comparison with the regional tectono-stratigraphic record*. Bulletin, 127(3-4), 480-502. doi:10.1130/B31069.1
- Petersen, S. V., Tabor, C. R., Lohmann, K. C., Poulsen, C. J., Meyer, K. W., Carpenter, S. J., Erickson, J.M., Matsunaga, K.K.S., Smith, S.Y. and Sheldon, N. D. (2016). *Temperature and salinity of the Late Cretaceous western interior seaway*. Geology, 44(11), 903-906. doi:10.1130/G38311.1
- Pitman III, W. C. (1978). *Relationship between eustasy and stratigraphic sequences of passive margins*. Geological Society of America Bulletin, 89(9), 1389-1403. doi:10.1130/0016-7606(1978)89;1389:RBEASS;2.0.CO;2
- Pitman, W.C., III, and Golovchenko, X. (1983). *The effect of sea-level change on the shelf edge and slope of passive margins*. Society of Economic Paleontologists and Mineralogists Special Publication, 33, 41-58. doi:10.2110/pec.83.06.0041
- Plint, A. G., Walker, R. G., and Bergman, K. M. (1986). *Cardium Formation 6. Stratigraphic framework of the Cardium in subsurface*. Bulletin of Canadian Petroleum Geology, 34(2), 213-225. doi:10.35767/gscpgbull.34.2.213
- Price, R. (1981). *The Cordilleran foreland thrust and fold belt in the southern Canadian Rocky Mountains*. Geological Society, London, Special Publications, 9(1), 427-448. doi:10.1144/GSL.SP.1981.009.01.39
- Price, R. A., and Mountjoy, E. W. (1970). *Geologic structure of the Canadian Rocky Mountains between Bow and Athabasca Rivers - a progress report*, In: J. O. Wheeler, (Ed.) *Structure of the southern Canadian Cordillera*. Geological Association of Canada Special Paper No. 6.
- Putnam, P. E. (1993). *A multidisciplinary analysis of Belly River-Brazeau (Campanian) fluvial channel reservoirs in west-central Alberta, Canada*. Bulletin of Canadian Petroleum Geology, 41(2), 186-217. doi:10.35767/gscpgbull.41.2.186
- Rider, M. H. (1990). *Gamma-ray log shape used as a facies indicator: critical analysis of an oversimplified methodology*. Geological Society, London, Special Publications, 48(1), 27-37. doi:10.1144/GSL.SP.1990.048.01.04
- Ricketts, B.D. (2008), *Cordilleran Sedimentary Basins of Western Canada Record 180 Million Years of Terrane Accretion*, In: Miall, A.D. (Eds.), *Sedimentary basins of the world*. 5, 364-394. doi:10.1016/B978-0-444-63895-3.00010-3

- Roberts, L. N. R., and Kirschbaum, M. A. (1995). *Paleogeography and the Late Cretaceous of the Western Interior of middle North America; coal distribution and sediment accumulation*. USGS Professional paper 1561 [doi:10.3133/pp1561](https://doi.org/10.3133/pp1561)
- Rogers, R. R., Kidwell, S. M., Deino, A. L., Mitchell, J. P., Nelson, K., and Thole, J. T. (2016). *Age, correlation, and lithostratigraphic revision of the Upper Cretaceous (Campanian) Judith River Formation in its type area (north-central Montana), with a comparison of low-and high-accommodation alluvial records*. *The Journal of Geology*, 124(1), 99-135. [doi:10.1086/684289](https://doi.org/10.1086/684289)
- Ryan, M. J., and Evans, D. C. (2005). *Ornithischian Dinosaurs*, In: P.J. Currie and E.B. Koppelhus (Eds.), *Dinosaur Provincial Park: a spectacular ancient ecosystem revealed*, Indiana University Press 312. [doi:10.1086/523131](https://doi.org/10.1086/523131)
- Russell, D.A., Chamney, T.P., 1967. *Notes on the biostratigraphy of dinosaurian and microfossil faunas in the Edmonton Formation (Cretaceous) Alberta*. *Natl. Mus. Can. Nat. Hist. Pap.*, 35, 1-22.
- Sageman, B. B., Rich, J., Arthur, M. A., Birchfield, G. E., and Dean, W. E. (1997). *Evidence for Milankovitch periodicities in Cenomanian-Turonian lithologic and geochemical cycles, Western Interior USA*. *Journal of Sedimentary Research*, 67(2), 286-302. [doi:10.1306/D4268554-2B26-11D7-8648000102C1865D](https://doi.org/10.1306/D4268554-2B26-11D7-8648000102C1865D)
- Schlanger, S. O., Jenkyns, H. C., and Premoli-Silva, I. (1981). *Volcanism and vertical tectonics in the Pacific Basin related to global Cretaceous transgressions*. *Earth and Planetary Science Letters*, 52(2), 435-449. [doi:10.1016/0012-821X\(81\)90196-5](https://doi.org/10.1016/0012-821X(81)90196-5)
- Slattery, J. S., Cobban, W. A., McKinney, K. C., Harries, P. J., and Sandness, A. L. (2015). *Early Cretaceous to Paleocene paleogeography of the Western Interior Seaway: the interaction of eustasy and tectonism*. *Wyoming Geological Association Guidebook*, 22-60. [doi:10.13140/RG.2.1.4439.8801](https://doi.org/10.13140/RG.2.1.4439.8801)
- Sohl, N.F., Martinez, R., Salmeron-Urena, P., and Soto-Jaramillo, F. (1991). *Upper Cretaceous*, In: Salvador, A. (Ed.), *The Gulf of Mexico*. The Geological Society of America, The Geology of North America Series, J, 206-245.
- Stelck, C. R., Trollope, F. H., Norris, A. W., and Pemberton, S. G. (2007). *McMurray Formation foraminifera within the lower Albian (Lower Cretaceous) Loon River shales of northern Alberta*. *Canadian Journal of Earth Sciences*, 44(11), 1627-1651. [doi:10.1139/E07-033](https://doi.org/10.1139/E07-033)

- Stockmal, G. S., Lebel, D., Mcmechan, M. E., and Mackay, P. A. (2001). *Structural style and evolution of the triangle zone and external Foothills, southwestern Alberta: Implications for thin-skinned thrust-and-fold belt mechanics*. Bulletin of Canadian Petroleum Geology, 49(4), 472-496. doi:10.2113/49.4.472
- Stockmal, G.S., Cant, D.J., and Bell, J.S. (1992). *Relationship of the stratigraphy of the Western Canada foreland basin to Cordilleran tectonics: insights from geodynamic models*, In: Macqueen, R.W., and Leckie, D.A. (Eds.), *Foreland Basins and Fold Belts*. American Association of Petroleum Geologists Memoir, 55, 107-124. doi:10.1306/M55563C5
- Stott, D.F. (1993). *Evolution of Cretaceous foredeeps: a comparative analysis along the length of the Canadian Rocky Mountains*, In: Caldwell, W.G.E., and Kauffman, E.G. (Eds.), *Evolution of the Western Interior Basin*. Geological Association of Canada, Special Paper, 39, 131-150.
- Street, H. P., Bamforth, E. L., and Gilbert, M. M. (2019). *The formation of a marine bonebed at the Upper Cretaceous Dinosaur Park-Bearpaw transition of west-central Saskatchewan, Canada*. Frontiers in Earth Science, 7, 209. doi:10.3389/feart.2019.00209
- Sullivan, C., Fanti, F., Larson, D.W., Bell, P., Campione, N.E., Sissons, R., Vavrek, M. (2019). *The Upper Cretaceous Wapiti Formation of northern Alberta, Canada as a unique window into the continental vertebrate fauna of boreal Laramidia during Bearpaw times*. 79th Symposium of Vertebrate Paleontology, Annual Meeting, Brisbane
- Tang, M., Zhang, K., Huang, J., and Lu, S. (2019). *Facies and the architecture of estuarine tidal bar in the lower Cretaceous McMurray Formation, Central Athabasca Oil Sands, Alberta, Canada*. Energies, 12(9), 1769. doi:10.3390/en12091769
- Umhoefer, P.J. and Blakey, R.C. (2006). *Moderate (1600 km) northward translation of Baja British Columbia from southern California: An attempt at reconciliation of paleomagnetism and geology*, In: Haggart, J.W., Enkin, R.J. and Monger, J.W.H. (Eds.), *Paleogeography of the North American Cordillera: Evidence For and Against Large-Scale Displacements*. Geological Association of Canada, Special Paper, 46, 305-327.
- Underschultz, J. R. (1991). *Tectonic loading, sedimentation, and sea-level changes in the foreland basin of north-west Alberta and north-east British Columbia, Canada*. Basin Research, 3(3), 165-174. doi:10.1111/j.1365-2117.1991.tb00125.x

- Wall, J. H., and Singh, C. (1975). *A Late Cretaceous microfossil assemblage from the Buffalo Head Hills, north-central Alberta*. Canadian Journal of Earth Sciences, 12(7), 1157-1174. doi:10.1139/e75-106
- Weimer, R.J. (1984). *Relation of unconformities, tectonics, and sea-level changes, Cretaceous of Western Interior, USA*. AAPG Special volumes, M36, 7-35. doi:10.1306/M36440C2
- Weimer, R.J. (1978). *Influence of Transcontinental Arch on Cretaceous marine sedimentation, a preliminary report*, In: Pruit, J.D., and Coffin, P.E. (Eds.), *Energy resources of the Denver basin*. Rocky Mountain Association of Geologist Symposium, 211-22.
- Wessel, P., Luis, J. F., Uieda, L., Scharroo, R., Wobbe, F., Smith, W. H. F., and Tian, D. (2019). *The generic mapping tools version 6*. Geochemistry, Geophysics, Geosystems, 20(11), 5556-5564. doi:10.1029/2019GC008515
- Wessel, P., Smith, W. H. F., Scharroo, R., Luis, J. F., and Wobbe, F. (2013). *GMT 5: A major new release of the Generic Mapping Tools*. Eos Trans. AGU, 94(45), 409-410. doi:10.1002/2013EO450001
- Wessel, P. (2009). *A general-purpose Green's function-based interpolator*. Computers and geosciences, 35(6), 1247-1254. doi:10.1016/j.cageo.2008.08.012
- Wood, J. M. (1994). *Sequence stratigraphic and sedimentological model for estuarine reservoirs in the Lower Cretaceous Glauconitic member, southern Alberta*. Bulletin of Canadian petroleum geology, 42(3), 332-351. doi:10.35767/gscpgbull.42.3.332

Acknowledgements

I wish to thank the supervisor of this PhD project, Prof. Rossella Capozzi, for the guidance during my studies at University of Bologna, without which this study would have never been accomplished. Along with Prof. Capozzi, I also extend my acknowledgements to the co-supervisors, Prof. Federico Fanti and Prof. Octavian Catuneanu, for the great work and suggestions that remarkably improved this manuscript. I thank University of Alberta for providing data access, Benedikt Bayer (FRAGILE srl) for helping me with the code used for data processing, Tomasz Jerzykiewicz for providing background information, Dongqing Chen (Alberta Energy Regulator) for her suggestions and help in the field and Marco Venieri for the critical discussion and data on the hydrocarbon fields in Alberta. I also wish to thank the reviewers of this PhD thesis, Miriam Cobianchi and Giuseppe Rigo de Righi, for their suggestions that greatly improved this work.

Appendices

License and terms of use

The following code is reported in order to ensure transparency over raw data manipulation, data processing and representations reported in this study. The code is subdivided in different Bash scripts. Each script has a different purpose which is briefly explained in the header of the corresponding appendix and within the script itself by mean of the *comments* (texts preceded by a ”#” symbol and colored in green).

The reader is encouraged to use, copy or modify for any purpose
the whole - or parts of the - code reported below
under the following terms (*modified MIT-License*) of
free and open-source software distribution:

Copyright (c) 2021 Riccardo Zubalich

Permission is hereby granted, free of charge, to any person obtaining a copy of this software and associated documentation files (the ”Software”), to deal in the Software without restriction, including without limitation the rights to use, copy, modify, merge, publish, distribute, sublicense, and/or sell copies of the Software, and to permit persons to whom the Software is furnished to do so, subject to the following conditions:

The above copyright notice and this permission notice shall be included in all copies or substantial portions of the Software. Except as contained in this notice, the name(s) of the above copyright holders shall not be used in advertising or otherwise to promote the sale, use or other dealings in this Software without prior written authorization.

THE SOFTWARE IS PROVIDED ”AS IS”, WITHOUT WARRANTY OF ANY KIND, EXPRESS OR IMPLIED, INCLUDING BUT NOT LIMITED TO THE WARRANTIES OF MERCHANTABILITY, FITNESS FOR A PARTICULAR PURPOSE AND NONINFRINGEMENT. IN NO EVENT SHALL THE AUTHORS OR COPYRIGHT HOLDERS BE LIABLE FOR ANY CLAIM, DAMAGES OR OTHER LIABILITY, WHETHER IN AN ACTION OF CONTRACT, TORT OR OTHERWISE, ARISING FROM, OUT OF OR IN CONNECTION WITH THE SOFTWARE OR THE USE OR OTHER DEALINGS IN THE SOFTWARE.

Appendix 1 A

Format data tables, interpolate DEMs and calculate 3D models

Please note that the scripts reported in Appendix 1 (sections A to F) are hard-coded to work only with a very specific architecture and content of both the starting databases (input) and the mother directory in which the script is executed on a UNIX system. All scripts were tested and debugged only for the used operative system: Linux Ubuntu 18.04LTS (properly set up with the required packages). It is worth noting that the scripts are coded with accuracy and ease-of-use in mind rather than to be efficient and fast as they were specifically designed for this study and dataset structure and will therefore need some adaptation in order to run in other situations.

```
1 #!/bin/bash
2 IFS=$'\n'
3 echo "This script filters data within all .xls files in the present folder and
4     converts them to properly formatted .csv files"
5 #####
6 #                                     #
7 #             MAIN                     #
8 #                                     #
9 #####
10
11 mkdir csv 2>/dev/null
12 for f in *\ *; do mv "$f" "${f// /_}" 2>/dev/null; done
13
14     for xlsfile in $(ls *xls);do
15         csvfile=$(echo $xlsfile | awk -F'.' '{print $1}').csv
16         echo "uwi, lat, lon, kb_elevation, formation, tvd, sld"> csv/$csvfile
17         xls2csv -q1 $xlsfile | tail -n+36 | awk -F',' '{OFS = "," ; print $1,$2,$3,
18             $7,$10,$11,$7-$11}' >> csv/$csvfile
19     done
20 echo "I made the xls2csv conversion"
21
22 mkdir csv_sorted 2>/dev/null
```

```
23
24
25 # GET NAMES
26 cat csv/*csv | awk -F',' '{print $5}' | sort -u | tail -n+4 | head -n+7 >formations.
    txt
27
28 # GET UWIs and COORDINATES
29 cat csv/*csv | awk -F',' '{print $1}' | sort -u > holes.txt
30 sed -i '/uwi/d' ./holes.txt
31 tail -n +2 holes.txt > tmp.txt
32 mv tmp.txt holes.txt
33
34 #REMOVE BLANK SPACES AND ''' CHARACTERS FROM SURFACE NAME
35 for form in $(cat formations.txt)
36 do
37     form_nospace=${form//[[:blank:]]/}
38     form_nospace=${form_nospace%''*}
39     form_nospace=${form_nospace#*''}
40     #PRINT OUTPUT .csv FILES
41     cat csv/*csv | grep $form > csv_sorted/$form_nospace.csv
42 done
43
44 #CONVERT .shp OF THE STUDY AREA TO .gmt FORMAT
45 ogr2ogr -f "GMT" shapefiles/StudyArea_WGS.gmt shapefiles/SHP/StudyArea_WGS.shp
46
47 #CREATE DIRECTORIES AND SET UP FUNDAMENTAL VARIABLES
48 mkdir formations_grd 2>/dev/null
49 mkdir formations_grd/sea_level 2>/dev/null
50 mkdir formations_grd/sea_level/Filter_data 2>/dev/null
51 mkdir formations_grd/thickness 2>/dev/null
52 mkdir formations_grd/cumulative 2>/dev/null
53 increments=0.003
54 whole_extension=$(cat csv_sorted/*csv | awk -F',' '{print $3, $2}' | gmt gmtinfo -
    I$increments);
55 polygon=shapefiles/StudyArea_WGS.gmt
56
57 #INTERPOLATION AND CROPPING TO THE STUDY AREA EXTENSION
58 for form in $(cat formations.txt)
59 do
60     echo "==> Processing: $form"
61     form_nospace=${form//[[:blank:]]/}
62     form_nospace=${form_nospace%''*}
63     form_nospace=${form_nospace#*''}
64     echo "Greenspline: $form"
65     #GREENSPLINE INTERPOLATION
66     cat csv_sorted/$form_nospace.csv | awk -F',' '{print $3, $2, $7}' | gmt
    blockmedian -I$increments $whole_extension | gmt greenspline -I0.01
    $whole_extension -Gformations_grd/sea_level/GS_$form_nospace.grd -D5 -Sq
67     # THE MASK IS COMPOSED BY NaN VALUES OUTSIDE AND 1 INSIDE THE POLYGON
```

```
68  gmt grdmask $polygon -Rformations_grd/sea_level/GS_$form_nospace.grd -NNaN/1/1 -  
    Gmask.grd  
69  # MUL OPERATOR SETS TO NaN (MULTIPLICATION) THE AREA OUTSIDE THE MASK POLYGON  
70  gmt grdmath formations_grd/sea_level/GS_$form_nospace.grd mask.grd MUL = tmp.grd  
71  mv tmp.grd formations_grd/sea_level/GS_$form_nospace.grd  
72  done  
73  
74  #CALCULATE THICKNESS AND CUMULATIVE THICKNESS FROM SEA LEVEL DEMs  
75  echo "Doing the math..."  
76  
77  cd formations_grd/sea_level  
78  #SUBTRACTIONS FOR THICKNESS MODELS  
79  gmt grdmath GS_U-BRPW1BASE.grd GS_U-BLRVBase.grd SUB = ../thickness/GS_BLRV.grd  
80  gmt grdmath GS_U-BRPW1MFS.grd GS_U-BRPW1BASE.grd SUB = ../thickness/GS_T1.grd  
81  gmt grdmath GS_U-BRPW1TOP.grd GS_U-BRPW1MFS.grd SUB = ../thickness/GS_R1.grd  
82  gmt grdmath GS_U-BRPW2BASE.grd GS_U-BRPW1TOP.grd SUB = ../thickness/GS_STRATH.grd  
83  gmt grdmath GS_U-BRPW2MFS.grd GS_U-BRPW2BASE.grd SUB = ../thickness/GS_T2.grd  
84  gmt grdmath GS_U-BRPW2TOP.grd GS_U-BRPW2MFS.grd SUB = ../thickness/GS_R2.grd  
85  
86  cd ../thickness  
87  # ADDITIONS FOR CUMULATIVE THICKNESS MODELS  
88  gmt grdmath ../thickness/GS_BLRV.grd ../thickness/GS_T1.grd ADD = ../cumulative/  
    GS_BLRV_T1.grd  
89  gmt grdmath ../cumulative/GS_BLRV_T1.grd ../thickness/GS_R1.grd ADD = ../cumulative/  
    GS_BLRV_T1_R1.grd  
90  gmt grdmath ../cumulative/GS_BLRV_T1_R1.grd ../thickness/GS_STRATH.grd ADD = ../  
    cumulative/GS_BLRV_T1_R1_STRATH.grd  
91  gmt grdmath ../cumulative/GS_BLRV_T1_R1_STRATH.grd ../thickness/GS_T2.grd ADD = ../  
    cumulative/GS_BLRV_T1_R1_STRATH_T2.grd  
92  gmt grdmath ../cumulative/GS_BLRV_T1_R1_STRATH_T2.grd ../thickness/GS_R2.grd ADD =  
    ../cumulative/GS_BLRV_T1_R1_STRATH_T2_R2.grd  
93  
94  echo "> DONE!"
```

Appendix 1 B

Print maps of thickness and cumulative thickness 3D models

```
1 #!/bin/bash
2 IFS=$'\n'
3 echo " This script prints maps from input .grd file"
4
5 mkdir formations_grd/images 2>/dev/null
6
7 #SET UP FUNDAMENTAL VARIABLES, DIRECTORIES AND MAPS LAYOUT
8 cd formations_grd/sea_level
9 suffix="GS"
10 DPI=600
11 cpt="../../GMT_sealevel.cpt"
12 proj=JM15c
13 region=R-120.6/-111.4/50.9/55.5
14 lenght_colbar=w15c
15 label_spacing=500
16 lenght_scalebar=125
17 contour=50
18 A=${region%/*}
19 A=${A#*R}
20 B=${region##*/}
21 B=${B%/*}
22 C=${region%/*}
23 C=${C##*/}
24 D=${region##*/}
25 Xoff=-2.8
26 Yoff=0.7
27 TLY=$(echo "$C+$Yoff" | bc -l)
28 TRX=$(echo "scale=4;$A-($Xoff)" | bc -l)
29 TRY=$(echo "$C+$Yoff" | bc -l)
30 BRX=$(echo "scale=4;$A-($Xoff)" | bc -l)
31 echo $A $C > ../../quadrato.txt
32 echo $A $TLY >> ../../quadrato.txt
33 echo $TRX $TRY >> ../../quadrato.txt
```

```
34 echo $BRX $C >> ../../quadrato.txt
35 mkdir Gradient 2>/dev/null
36
37 #PRINT MAPS
38 echo "Working on sea level DEMs"
39 for grdfile in $(ls *.grd)
40 do
41     name=${grdfile%.*}
42     echo "processing: "$name".grd"
43     zmax=$(gmt grdinfo $name.grd -T)
44     zmax=${zmax#*/}
45     zmin=$(gmt grdinfo $name.grd -T)
46     zmin=${zmin%/*}
47     zmin=${zmin#*T}
48     #SET TITLE
49     case $name in
50         *BLRV*) longName="Belly River Gp. base";;
51         *1BASE*) longName="Lower Tongue base";;
52         *1MFS*) longName="Lower Tongue mfs";;
53         *1TOP*) longName="Lower Tongue top";;
54         *2BASE*) longName="Upper Tongue base";;
55         *2MFS*) longName="Upper Tongue mfs";;
56         *2TOP*) longName="Upper Tongue top";;
57         *) ;;
58     esac
59     #PRINT BACKGROUND IMAGE
60     gmt grdimage ../../GoogleEarth300.tif -$region -$proj -D -K -P > $name.ps
61     #CALCULATE GRADIENTS FOR SHADING
62     gmt grdgradient $name.grd -A60 -Ne0.6 -GGradient/gradient$name.nc
63     #PRINT INPUT GRID FILE
64     gmt grdimage $grdfile -$region -$proj -C$cpt -IGradient/gradient$name.nc -Q -K -O
65     -P >> $name.ps
66     #PRINT CONTOUR
67     gmt grdcontour $grdfile -$region -$proj -C$contour -A250+u+o+p0.4 -Q10000 -K -O -
68     P >> $name.ps
69     #PRINT MAP FRAME, TICKS, COORDINATES LABELS AND GRID
70     gmt pscoast -$region -$proj -Df -BwSnE -Ba2f1g1 -N1/1p,,-- -K -O -P >> $name.ps
71     #PRINT COLORS BAR
72     gmt psscale -DjTC+$lenght_colbar/0.5c+o0/-1.5+m+h -$region -$proj -C$cpt -I0.4 -
73     Ba$label_spacing+l"Depth s.l. $longName Contour: $contour\m"+u" m" -G$zmin/$zmax -
74     K -O -P >> $name.ps
75     #PRINT SCALE BAR
76     gmt psxy ../../quadrato.txt -$region -$proj -Gwhite -W0.75p,black -A -K -O -P >>
77     $name.ps
78     gmt psbasemap -$region -$proj -LjBL+c54+w$lenght_scalebar+o0.6/0.75c+l"Scale"+u+f
79     -O >> $name.ps
80     #CONVERT PS TO PNG AND TRIM TO IMAGE CONTENT
81     gmt psconvert $name.ps -Tg -E$DPI > $name.png
```

```
76     convert -trim $name.png $name.png
77 done
78
79 #ORGANIZE OUTPUT
80 mkdir ../images/postscript 2>/dev/null
81 mkdir ../images/sealevel 2>/dev/null
82     for grdfile in $(ls *.grd)
83     do
84         name=${grdfile%.*}
85         mv $name.ps ../images/postscript
86         mv $name.png ../images/sealevel
87     done
88
89 echo "Working on thickness distribution"
90 cd ../thickness
91 cpt="../../GMT_thickness.cpt"
92 lenght_colbar=w15c
93
94 mkdir Gradient 2>/dev/null
95 for grdfile in $(ls *.grd)
96 do
97     name=${grdfile%.*}
98     echo "processing: "$name".grd"
99     zmax=$(gmt grdinfo $name.grd -T)
100    zmax=${zmax#*/}
101    zmin=$(gmt grdinfo $name.grd -T)
102    zmin=${zmin%/*}
103    zmin=${zmin#*T}
104
105    export LC_NUMERIC="en_US.UTF-8"
106    zMIN=$(printf "%.1f\n" $zmin)
107    zMAX=$(printf "%.1f\n" $zmax)
108    export LC_NUMERIC="it_IT.UTF-8"
109
110    gmt grdimage ../../GoogleEarth300.tif -$region -$proj -D -K -P > $name.ps
111    gmt grdgradient $name.grd -A30/150 -Ne0.6 -GGradient/gradient$name.nc
112    gmt grdimage $grdfile -$region -$proj -C$cpt -IGradient/gradient$name.nc -Q -K -O
113    -P >> $name.ps
114
115    gmt pscoast -$region -$proj -Df -BwSnE -Ba2f1g1 -N1/1p,,-- -K -O -P >> $name.ps
114
115 #SET LABEL SPACING
116     if [[ $name == *"BLRV"* ]]
117     then
118         label_spacing=50
119     elif [[ $name == *"STRATH"* ]]
120     then
121         label_spacing=10
122     else
```

```
123         label_spacing=5
124     fi
125 #SET TITLE
126     case $name in
127         *BLRV*) longName="Belly River Group (BLRV)";;
128         *STRATH*) longName="Strathmore interval (S)";;
129         *T1*) longName="Lower tongue TST (T1)";;
130         *T2*) longName="Upper tongue TST (T2)";;
131         *R1*) longName="Lower tongue RST (R1)";;
132         *R2*) longName="Upper tongue RST (R2)";;
133         *) ;;
134     esac
135 #SET CONTOUR INTERVAL
136     case $name in
137         *BLRV*) interval=15
138                 aa=5;;
139         *STRATH*) interval=5
140                 aa=2;;
141         *) interval=1
142                 aa=5;;
143     esac
144     ann=$((($interval*$aa))
145     label="$longName: [$zMIN - $zMAX]m Contour: $interval\m"
146
147     gmt grdcontour $grdfile -$region -$proj -C$interval -A$ann+u+o+p0.4 -Q100 -K -O -
148     P >> $name.ps
149     gmt psscale -DjTC+$lenght_colbar/0.5c+o0/-1.5+m+h -$region -$proj -C$cpt -I0.4 -
150     Ba$label_spacing+l"$label"+u" m" -G$zmin/$zmax -K -O -P >> $name.ps
151     gmt psxy ../../quadrato.txt -$region -$proj -Gwhite -W0.75p,black -A -K -O -P >>
152     $name.ps
153     gmt psbasemap -$region -$proj -LjBL+c54+w$lenght_scalebar+o0.6/0.75c+l"Scale"+u+f
154     -O >> $name.ps
155     gmt psconvert $name.ps -Tg -E$DPI > $name.png
156     convert -trim $name.png $name.png
157 done
158
159 mkdir ../images/thickness 2>/dev/null
160 for grdfile in $(ls *.grd)
161 do
162     name=${grdfile%.*}
163     mv $name.ps ../images/postscript
164     mv $name.png ../images/thickness
165 done
166
167 echo "Let's work on cumulative thickness"
168 cd ../cumulative
169
170 cpt="../../mfsPalette.cpt"
171 lenght_colbar=w15c
```

```
168 label_spacing=50
169 contour=10
170 labCont=50
171 mkdir Gradient 2>/dev/null
172 for grdfile in $(ls *.grd)
173 do
174     name=${grdfile%.*}
175     echo "processing: "$name".grd"
176     zmax=$(gmt grdinfo $name.grd -T)
177     zmax=${zmax#*/}
178     zmin=$(gmt grdinfo $name.grd -T)
179     zmin=${zmin%/*}
180     zmin=${zmin#*T}
181
182 #SET MAP TITLE
183     case $name in
184         *BLRV) longName="from Datum to BLRV top";;
185         *STRATH) longName="from Datum to S";;
186         *T1) longName="from Datum to T1";;
187         *T2) longName="from Datum to T2";;
188         *R1) longName="from Datum to R1";;
189         *R2) longName="from Datum to R2";;
190         *) ;;
191     esac
192
193     gmt grdimage ../../GoogleEarth300.tif -$region -$proj -D -K -P > $name.ps
194     gmt grdgradient $name.grd -A30/150 -Ne0.6 -GGradient/gradient$name.nc
195     gmt grdimage $grdfile -$region -$proj -C$cpt -IGradient/gradient$name.nc -Q -K -O
196     -P >> $name.ps
197     gmt grdcontour $grdfile -$region -$proj -C$contour -A$labCont+u+o+p0.4 -Q500 -K -
198     O -P >> $name.ps
199     gmt pscoast -$region -$proj -Df -BwSnE -Ba2f1g1 -N1/1p,,- -K -O -P >> $name.ps
200
201     gmt psscale -DjTC+$length_colbar/0.5c+o0/-1.5+m+h -$region -$proj -C$cpt -I0.4 -
202     Ba$label_spacing+u" m" -G$zmin/$zmax -K -O -P >> $name.ps
203     gmt psxy ../../quadrato.txt -$region -$proj -Gwhite -W0.75p,black -A -K -O -P >>
204     $name.ps
205     gmt psbasemap -$region -$proj -LjBL+c54+w$length_scalebar+o0.6/0.75c+l"Scale"+u+f
206     -O >> $name.ps
207     gmt psconvert $name.ps -Tg -E$DPI > $name.png
208     convert -trim $name.png $name.png
209 done
210
211 #CUMULATIVE MAP FOR BELLY RIVER GROUP THICKNESS
212 cd ../thickness
213 for grdfile in $(ls *BLRV.grd)
214 do
215     name=${grdfile%.*}
216     echo "processing: "$name".grd"
```

```

211 zmax=$(gmt grdinfo $name.grd -T)
212 zmax=${zmax##*/}
213 zmin=$(gmt grdinfo $name.grd -T)
214 zmin=${zmin%%/*}
215 zmin=${zmin#*T}
216
217 #SET TITLE
218 longName="from Datum to BLRV top"
219
220 gmt grdimage ../../GoogleEarth300.tif -$region -$proj -D -K -P > ../cumulative/
$name "_cum".ps
221 gmt grdimage $grdfile -$region -$proj -C$cpt -IGradient/gradient$name.nc -Q -K -O
-P >> ../cumulative/$name "_cum".ps
222 gmt grdcontour $grdfile -$region -$proj -C$contour -A$labCont+u+o+p0.4 -Q500 -K -
O -P >> ../cumulative/$name "_cum".ps
223 gmt pscoast -$region -$proj -Df -BwSnE -Ba2f1g1 -N1/1p,,-- -K -O -P >> ../
cumulative/$name "_cum".ps
224 gmt psscale -DjTC+$lenght_colbar/0.5c+o0/-1.5+m+h -$region -$proj -C$cpt -IO.4 -
Ba$label_spacing+u" m" -G$zmin/$zmax -K -O -P >> ../cumulative/$name "_cum".ps
225 gmt psxy ../../quadrato.txt -$region -$proj -Gwhite -W0.75p,black -A -K -O -P >>
../cumulative/$name "_cum".ps
226 gmt psbasemap -$region -$proj -LjBL+c54+w$lenght_scalebar+o0.6/0.75c+l"Scale"+u+f
-O >> ../cumulative/$name "_cum".ps
227 gmt psconvert ../cumulative/$name "_cum".ps -Tg -E$DPI > ../cumulative/$name "_cum"
.png
228 convert -trim ../cumulative/$name "_cum".png ../cumulative/$name "_cum".png
229 done
230
231 cd ../cumulative
232 mkdir ../images/cumulative 2>/dev/null
233 for grdfile in $(ls *.grd)
234 do
235     name=${grdfile%.*}
236     echo "moving: "$name
237     mv $name.ps ../images/postscript
238     mv $name.png ../images/cumulative
239 done
240
241 for psfile in $(ls *.ps)
242 do
243     name=${psfile%.*}
244     echo "moving: "$name
245     mv $name.ps ../images/postscript
246     mv $name.png ../images/cumulative
247 done
248
249 echo "> DONE!"

```

Appendix 1 C

Calculate slope degrees and print maps

```
1 #!/bin/bash
2 IFS=$'\n'
3 echo "This script prints slope maps from different .grd file"
4
5 #####
6 #                                     #
7 #           FUNCTIONS                 #
8 #                                     #
9 #####
10
11 function print_slope_map {
12 # $1 = grid file
13 # $2 = output_name
14 # $3 = DPI output
15
16 #PLOT BACKGROUND IMAGE
17 gmt grdimage ../../GoogleEarth300.tif -$region -$proj -D -K -P > $2.ps
18 gmt grdgradient $1 -Ne0.6 -D -Sslope$2.nc -fg #CALCULATE GRADIENTS
19 #CONVERT SCALAR SLOPE VALUES TO DEGREES
20 gmt grdmath slope$2.nc ATAN PI DIV 180 MUL = slope2$2.nc
21
22     zmax=$(gmt grdinfo slope2$2.nc -T) #FIND EXTENT
23     zmax=${zmax#*/}
24     zmin=$(gmt grdinfo slope2$2.nc -T)
25     zmin=${zmin%/*}
26     zmin=${zmin#*T}
27
28     export LC_NUMERIC="en_US.UTF-8"
29     zMIN=$(printf "%.1f\n" $zmin) #ROUND VALUES TO 1 DECIMAL
30     zMAX=$(printf "%.1f\n" $zmax)
31     export LC_NUMERIC="it_IT.UTF-8"
32     echo "min: $zmin - $zMIN _____max: $zmax - $zMAX"
33 #MAKE SLOPE COLOR PALETTE
34 gmt grd2cpt slope2$2.nc -Cwhite,skyblue,forestgreen,yellow,red -S5 -Z > slope$2.cpt
35 cpt=slope$2.cpt
```

```

36 #PLOT SLOPE DATA EXCLUDING NaN (-Q)
37 gmt grdimage slope2$2.nc -$region -$proj -C$cpt -Q -K -O -P >> $2.ps
38 gmt grdcontour $1 -$region -$proj -C2 -A10+u+o+p0.4 -Q10000 -K -O -P -Wathinnest,
    black -Wcathinnest,darkgrey >> $2.ps #CALCULATE AND DRAW CONTOUR
39 #DRAW FRAME,GRID AND LABELS OF THE MAP
40 gmt pscoast -$region -$proj -Df -BwSnE -Ba2f1g1 -N1/1p,,- -K -O -P >> $2.ps
41 #PLOT COLORBAR
42 gmt psscale -DjTC+$lenght_colbar/0.5c+o0/-1.5+m+h -$region -$proj -C$cpt -I0.4 -Ba0
    .1+1"Slope $2 [$zMIN - $zMAX] degrees" -G$zmin/$zmax -K -O -P >> $2.ps
43 gmt psxy ../../quadrato.txt -$region -$proj -Gwhite -W0.75p,black -A -K -O -P >> $2.
    ps #PLOT WHITE SQUARE FOR THE SCALEBAR
44 gmt psbasemap -$region -$proj -LjBL+c54+w$lenght_scalebar+o0.6/0.75c+1"Scale"+u+f -O
    >> $2.ps #PLOT SCALEBAR
45
46 gmt psconvert $2.ps -Tg -E$3 > $2.png #CONVERT PS TO PNG
47 convert -trim $2.png $2.png #COMMAND FROM IMAGEMAGICK PACKAGE, CROPS TO IMAGE CONTENT
48
49 rm $2.ps slope$2.nc slope2$2.nc slope$2.cpt
50 }
51
52 #####
53 #                                     #
54 #             MAIN                     #
55 #                                     #
56 #####
57 #SET UP FUNDAMENTAL VARIABLES AND WORKING DIRECTORY
58 suffix="GS"
59
60 cd formations_grd/sea_level
61 mkdir Slope 2>/dev/null
62
63 proj=JM15c
64 region=R-120.6/-111.4/50.9/55.5
65 lenght_colbar=w15c
66 lenght_scalebar=125
67 freq_scale=70
68
69 #EXTRACT REGION VALUES FROM region VARIABLE
70 A=${region%%/*}
71 A=${A#*R}
72 B=${region##*/}
73 B=${B%%/*}
74 C=${region%/*}
75 C=${C##*/}
76 D=${region###*/}
77 #SET OFFSETS USED TO PRINT THE SCALE INSET ON MAPS
78 Xoff=-2.8
79 Yoff=0.7
80 #CALCULATE COORDINATES OF A SQUARE IN THE BOTTOM LEFT AREA TO PRINT THE SCALE INSET

```

```
    ONTO
81 TLY=$(echo "$C+$Yoff" | bc -l)
82 TRX=$(echo "scale=4;$A-($Xoff)" | bc -l)
83 TRY=$(echo "$C+$Yoff" | bc -l)
84 BRX=$(echo "scale=4;$A-($Xoff)" | bc -l)
85 echo $A $C > ../../quadrato.txt
86 echo $A $TLY >> ../../quadrato.txt
87 echo $TRX $TRY >> ../../quadrato.txt
88 echo $BRX $C >> ../../quadrato.txt
89
90 #CALCULATE AND PRINT SLOPE FOR EACH .grd IN THESE DIRECTORIES
91 cd ../sea_level #SEA LEVEL DEMS DIRECTORY
92 for grdfile in $(ls *.grd)
93 do
94     name=${grdfile%.*}
95     echo "> Processing: $name..."
96     print_slope_map $grdfile $name 300
97 done
98
99 cd ../thickness #THICKNESS 3D MODELS DIRECTORY
100 for grdfile in $(ls *.grd)
101 do
102     name=${grdfile%.*}
103     echo "> Processing: $name..."
104     print_slope_map $grdfile $name 300
105 done
106
107 cd ../cumulative #CUMULATIVE THICKNESS 3D MODELS DIRECTORY
108 for grdfile in $(ls *.grd)
109 do
110     name=${grdfile%.*}
111     echo "> Processing: $name..."
112     print_slope_map $grdfile $name 300
113 done
114
115 echo "> DONE!"
```

Appendix 1 D

Calculate rates of sediment accumulation and print maps

```
1 #!/bin/bash
2 clear
3 echo "This script calculates rates of sediment accumulation (in cm/kyr) based upon
4     previously processed thickness intervals, then prints relative maps"
5 echo
6 #####
7 #                                     #
8 #             FUNCTIONS               #
9 #                                     #
10 #####
11
12 function printRSA {
13 # $1 = INPUT GRIDFILE
14 local name=$(basename $1)
15 name=${name%.*}
16
17 #SET UP FUNDAMENTAL VARIABLES
18 lenght_colbar=w15c
19 label_spacing=1
20 lenght_scalebar=125
21 CITY_SIZE=0.25c
22 CITY_PEN=1p,black
23 CITY_FILL=white
24 CITY_LABEL+=f14p,Helvetica-Bold,white+j
25 CITY_LABEL_OFFSET=0.2c/0.2c
26 #PARSING OF Z RANGES AND MEAN Z FROM grdinfo COMMAND
27     zmax=$(gmt grdinfo $1 -T)
28     zmax=${zmax##*/}
29     zmin=$(gmt grdinfo $1 -T)
30     zmin=${zmin%/*}
31     zmin=${zmin#*T}
32 MIN=$(echo "$zmin" | awk '{printf "%.1f\n", $1}')
```

```
33 MAX=$(echo "$zmax" | awk '{printf "%.1f\n", $1}')
34 MEAN=$(gmt grdinfo -L2 $1 | tail -n 2 | head -n 1 | awk -F' ' '{printf "%.1f\n", $3}'
   )
35
36 echo "> Calculating palette: $name [$zmin - $zmax]..."
37 gmt grd2cpt $1 -Cblue,skyblue,green,yellow,red -Fr -E6 -Z > $cpt
38
39 #SET UP MAP'S LABELS, CONTOUR SPACING AND ANNOTATION
40 case $name in
41     rsa_T1_R1_STRATH_T2_R2) contour=0.5
42                             longName="from T1 to R2 (contour: $contour cm/kyr)"
43                             min_cont_lenght=50
44                             labCont=2.5
45                             lettera="";;
46     rsa_R1_STRATH_T2_R2) contour=0.5
47                             longName="from R1 to R2 (contour: $contour cm/kyr)"
48                             min_cont_lenght=50
49                             labCont=2.5 ;;
50     rsa_T2_R2) contour=0.5
51                 longName="from T2 to R2 (contour: $contour cm/kyr)"
52                 min_cont_lenght=50
53                 labCont=2.5
54                 lettera="D";;
55     rsa_R1_STRATH) contour=1
56                 longName="from R1 to S (contour: $contour cm/kyr)"
57                 min_cont_lenght=50
58                 labCont=5
59                 lettera="C";;
60     rsa_BLRV_T1_R1_STRATH_T2_R2) contour=0.5
61                 longName="from Datum to R2 (contour: $contour cm/kyr)"
62
63                 min_cont_lenght=50
64                 labCont=2.5
65                 lettera="A";;
66     rsa_BLRV) contour=0.5
67                 longName="of the Belly River Group (contour: $contour cm/kyr)"
68                 min_cont_lenght=50
69                 labCont=2.5
70                 lettera="";;
71     rsa_T1) contour=0.5
72             longName="of T1 (contour: $contour cm/kyr)"
73             min_cont_lenght=50
74             labCont=2.5
75             lettera="B";;
76 *) ;;
77 esac
78 #PRINT MAP FOR INPUT GRIDFILE ($1)
79 echo "> Printing $name..."
```

```
80 file="images/RSA/$name.ps"
81 gmt grdimage ../GoogleEarth300.tif -$region -$proj -D -K -P > $file
82 gmt grdimage $1 -$region -$proj -C$cpt -Q -K -O -P >> $file
83 gmt grdcontour $1 -$region -$proj -C$contour -A$labCont+o+p0.3 -Q$min_cont_lenght -K
  -O -P >> $file
84 gmt pscoast -$region -$proj -Df -BwSnE -Ba2f1g1 -N1/1p,,- -K -O -P >> $file
85 gmt psscale -DjTC+$lenght_colbar/0.5c+o0/-1.5+m+h -$region -$proj -C$cpt -I0.4 -
  Ba$label_spacing+l"RSA $longName" -G$zmin/$zmax -K -O -P >> $file
86 gmt psxy ../quadrato.txt -$region -$proj -Gwhite -W0.75p,black -A -K -O -P >> $file
87 gmt psxy ../shapefiles/Cities_WGS.gmt -$region -$proj -Sc$CITY_SIZE -G$CITY_FILL -
  W$CITY_PEN -K -O -P >> $file
88 gmt pstext ../shapefiles/Cities_labels2.txt -$region -$proj -F$CITY_LABEL -
  Dj$CITY_LABEL_OFFSET -K -O -P >> $file
89   echo "-113 55.3 MIN = $MIN" | gmt pstext -$region -$proj -F+f12p,Helvetica-Bold,
  white+jML -K -O -P >> $file
90   echo "-113 55.1 MAX = $MAX" | gmt pstext -$region -$proj -F+f12p,Helvetica-Bold,
  white+jML -K -O -P >> $file
91   echo "-113 54.9 MEAN = $MEAN" | gmt pstext -$region -$proj -F+f12p,Helvetica-Bold
  ,white+jML -K -O -P >> $file
92   echo "-120.5 55.3 $lettera" | gmt pstext -$region -$proj -F+f32p,Helvetica-Bold,
  white+jML -K -O -P >> $file
93 gmt psbasemap -$region -$proj -LjBL+c54+w$lenght_scalebar+o0.6/0.75c+l"Scale"+u+f -O
  >> $file
94 gmt psconvert $file -Tg
95 rm $file
96 }
97
98 #####
99 #                                     #
100 #          MAIN                       #
101 #                                     #
102 #####
103
104 export LC_NUMERIC="en_US.UTF-8"
105 cd formations_grd
106 rm -r RSA 2>/dev/null
107 mkdir RSA
108
109 #AGE IN YEARS TO BASE CALCULATIONS UPON
110 t_baseT1=74300000
111 t_baseR1=74100000
112 t_baseT2=73700000
113 t_topR2=73100000
114 t_datum=80000000
115
116 #CALCULATING INTERVALS R1+S T2+R2 R1+S+T2+R2 T1+R1+S+T2+R2
117 echo "> Doing the math..."
118 gmt grdmath thickness/GS_R1.grd thickness/GS_STRATH.grd ADD = RSA/R1_STRATH.grd
119
```

```
120 gmt grdmath thickness/GS_T2.grd thickness/GS_R2.grd ADD = RSA/T2_R2.grd
121
122 gmt grdmath thickness/GS_R1.grd thickness/GS_STRATH.grd ADD = RSA/tmp.grd
123 gmt grdmath RSA/tmp.grd thickness/GS_T2.grd ADD = RSA/tmp2.grd
124 gmt grdmath RSA/tmp2.grd thickness/GS_R2.grd ADD = RSA/R1_STRATH_T2_R2.grd
125 rm RSA/tmp.grd RSA/tmp2.grd
126
127 gmt grdmath RSA/R1_STRATH_T2_R2.grd thickness/GS_T1.grd ADD = RSA/T1_R1_STRATH_T2_R2
    .grd
128
129 gmt grdmath RSA/T1_R1_STRATH_T2_R2.grd thickness/GS_BLRV.grd ADD = RSA/
    BLRV_T1_R1_STRATH_T2_R2.grd
130
131 #RSA IS REPRESENTED IN cm/Kyr
132 unit=100
133 time=1000
134
135 #CALCULATE TIMESPANS
136 T1_R1_STRATH_T2_R2=$(( $t_baseT1 - $t_topR2 ))
137 R1_STRATH_T2_R2=$(( $t_baseR1 - $t_topR2 ))
138 T2_R2=$(( $t_baseT2 - $t_topR2 ))
139 R1_STRATH=$(( $t_baseR1 - $t_baseT2 ))
140 BLRV_T1_R1_STRATH_T2_R2=$(( $t_datum - $t_topR2 ))
141 BLRV=$(( $t_datum - $t_baseT1 ))
142 T1=$(( $t_baseT1 - $t_baseR1 ))
143
144 #CALCULATE RSA VALUES
145 echo "> Calculating RSA..."
146 #DIVIDE BY YEARS AND MULTIPLY 100 TO GET cm OUT OF meters
147 gmt grdmath RSA/T1_R1_STRATH_T2_R2.grd $unit MUL = RSA/tmp.grd #CONVERSION m TO cm
148 gmt grdmath RSA/tmp.grd $T1_R1_STRATH_T2_R2 DIV = RSA/tmp2.grd #CALCULATE RSA IN cm/
    yr
149 gmt grdmath RSA/tmp2.grd $time MUL = RSA/rsa_T1_R1_STRATH_T2_R2.grd #CONVERT cm/yr TO
    cm/kyr
150 rm RSA/tmp.grd RSA/tmp2.grd
151
152 #OUTPUT ZMIN AND ZMAX FROM THE OBTAINED .grd FILES
153 echo "[zmin-zmax] T1_R1_STRATH_T2_R2.grd: $(gmt grdinfo RSA/T1_R1_STRATH_T2_R2.grd -T
    )"
154 echo "[zmin-zmax] RSA($T1_R1_STRATH_T2_R2): $(gmt grdinfo RSA/rsa_T1_R1_STRATH_T2_R2.
    grd -T)"
155
156 gmt grdmath RSA/R1_STRATH_T2_R2.grd $unit MUL = RSA/tmp.grd
157 gmt grdmath RSA/tmp.grd $R1_STRATH_T2_R2 DIV = RSA/tmp2.grd
158 gmt grdmath RSA/tmp2.grd $time MUL = RSA/rsa_R1_STRATH_T2_R2.grd
159 rm RSA/tmp.grd RSA/tmp2.grd
160 echo "[zmin-zmax] R1_STRATH_T2_R2.grd: $(gmt grdinfo RSA/R1_STRATH_T2_R2.grd -T)"
161 echo "[zmin-zmax] RSA($R1_STRATH_T2_R2): $(gmt grdinfo RSA/rsa_R1_STRATH_T2_R2.grd -T
    )"
```

```

162
163 gmt grdmath RSA/T2_R2.grd $unit MUL = RSA/tmp.grd
164 gmt grdmath RSA/tmp.grd $T2_R2 DIV = RSA/tmp2.grd
165 gmt grdmath RSA/tmp2.grd $time MUL = RSA/rsa_T2_R2.grd
166 rm RSA/tmp.grd RSA/tmp2.grd
167 echo "[zmin-zmax] T2_R2.grd: $(gmt grdinfo RSA/T2_R2.grd -T)"
168 echo "[zmin-zmax] RSA($T2_R2): $(gmt grdinfo RSA/rsa_T2_R2.grd -T)"
169
170 gmt grdmath RSA/R1_STRATH.grd $unit MUL = RSA/tmp.grd
171 gmt grdmath RSA/tmp.grd $R1_STRATH DIV = RSA/tmp2.grd
172 gmt grdmath RSA/tmp2.grd $time MUL = RSA/rsa_R1_STRATH.grd
173 rm RSA/tmp.grd RSA/tmp2.grd
174 echo "[zmin-zmax] R1_STRATH.grd: $(gmt grdinfo RSA/R1_STRATH.grd -T)"
175 echo "[zmin-zmax] RSA($R1_STRATH): $(gmt grdinfo RSA/rsa_R1_STRATH.grd -T)"
176
177 gmt grdmath RSA/BLRV_T1_R1_STRATH_T2_R2.grd $unit MUL = RSA/tmp.grd
178 gmt grdmath RSA/tmp.grd $BLRV_T1_R1_STRATH_T2_R2 DIV = RSA/tmp2.grd
179 gmt grdmath RSA/tmp2.grd $time MUL = RSA/rsa_BLRV_T1_R1_STRATH_T2_R2.grd
180 rm RSA/tmp.grd RSA/tmp2.grd
181 echo "[zmin-zmax] BLRV_T1_R1_STRATH_T2_R2.grd: $(gmt grdinfo RSA/
    BLRV_T1_R1_STRATH_T2_R2.grd -T)"
182 echo "[zmin-zmax] RSA($BLRV_T1_R1_STRATH_T2_R2): $(gmt grdinfo RSA/
    rsa_BLRV_T1_R1_STRATH_T2_R2.grd -T)"
183
184 gmt grdmath thickness/GS_BLRV.grd $unit MUL = RSA/tmp.grd
185 gmt grdmath RSA/tmp.grd $BLRV_T1_R1_STRATH_T2_R2 DIV = RSA/tmp2.grd
186 gmt grdmath RSA/tmp2.grd $time MUL = RSA/rsa_BLRV.grd
187 rm RSA/tmp.grd RSA/tmp2.grd
188 echo "[zmin-zmax] BLRV.grd: $(gmt grdinfo thickness/GS_BLRV.grd -T)"
189 echo "[zmin-zmax] RSA($BLRV): $(gmt grdinfo RSA/rsa_BLRV.grd -T)"
190
191 gmt grdmath thickness/GS_T1.grd $unit MUL = RSA/tmp.grd
192 gmt grdmath RSA/tmp.grd $T1 DIV = RSA/tmp2.grd
193 gmt grdmath RSA/tmp2.grd $time MUL = RSA/rsa_T1.grd
194 rm RSA/tmp.grd RSA/tmp2.grd
195 echo "[zmin-zmax] T1.grd: $(gmt grdinfo thickness/GS_T1.grd -T)"
196 echo "[zmin-zmax] RSA($T1): $(gmt grdinfo RSA/rsa_T1.grd -T)"
197
198 #SET UP FUNDAMENTAL VARIABLES, DIRECTORIES AND MAP LAYOUT
199 rm -r images/RSA 2>/dev/null
200 mkdir images/RSA
201
202 proj=JM15c
203 region=R-120.6/-111.4/50.9/55.5
204 cpt="RSA/rsa_cpt.cpt"
205 A=${region%/*}
206 A=${A#*R}
207 B=${region#*/}
208 B=${B%/*}

```

```
209 C=${region%/*}
210 C=${C##*/}
211 D=${region###*/}
212 Xoff=-2.8
213 Yoff=0.7
214 TLY=$(echo "$C+$Yoff" | bc -l)
215 TRX=$(echo "scale=4;$A-($Xoff)" | bc -l)
216 TRY=$(echo "$C+$Yoff" | bc -l)
217 BRX=$(echo "scale=4;$A-($Xoff)" | bc -l)
218 echo $A $C > ../quadrato.txt
219 echo $A $TLY >> ../quadrato.txt
220 echo $TRX $TRY >> ../quadrato.txt
221 echo $BRX $C >> ../quadrato.txt
222
223 #PRINT RESULTING MAPS
224 printRSA RSA/rsa_BLRV_T1_R1_STRATH_T2_R2.grd
225 printRSA RSA/rsa_T1_R1_STRATH_T2_R2.grd
226 printRSA RSA/rsa_R1_STRATH_T2_R2.grd
227 printRSA RSA/rsa_T2_R2.grd
228 printRSA RSA/rsa_R1_STRATH.grd
229 printRSA RSA/rsa_BLRV.grd
230 printRSA RSA/rsa_T1.grd
231
232 #CONVERSIONS
233 for f in $(ls images/RSA/*.png)
234 do
235 echo "> Trimming $(basename $f)"
236 convert $f -trim $f
237 done
238
239 export LC_NUMERIC="it_IT.UTF-8"
```

Appendix 1 E

Calculate volumes

```
1 #!/bin/bash
2 IFS=$'\n'
3
4 echo "This script calculates the volume and 5m & 10m contour covered area of
   thickness grids"
5
6 #####
7 #
8 #     FUNCTIONS
9 #
10 #####
11
12 function volumeBetween {
13 # calcola volume fra due contour
14 # $1 = grid file
15 # $2 = out txt title
16 # $3 = contour low
17 # $4 = contour high
18 # $5 = contour step
19
20 case $1 in
21   *STRATH*) gmt grdvolume $1 -C$3/$4/$5 -Sk -fg | awk -F '\t' '{if ($1 ==0 || $1 ==
22     20 || $1 == 30) print $1,$3,$2}' >> $2.txt;;
23   *BLRV*) gmt grdvolume $1 -C$3/$4/$5 -Sk -fg | awk -F '\t' '{if ($1 ==0 || $1 ==
24     300 || $1 == 400) print $1,$3,$2}' >> $2.txt;;
25   *)gmt grdvolume $1 -C$3/$4/$5 -Sk -fg | awk -F '\t' '{if ($1 ==0 || $1 == 5 || $1
26     == 10) print $1,$3,$2}' >> $2.txt;;
27 esac
28
29 # grdvolume -Sk CALCULATES VOLUME IN km^2*z_unit (z_unit is m)
30 totVol=$(gmt grdvolume $1 -Sk -fg | awk -F ' ' '{printf "%.0f\n", $3}' )
31 # DIVISION BY 1000 GIVES THE RESULT IN km^3
32 totVol=$(echo "$totVol/1000" | bc -l | awk '{printf "%.1f\n", $1}')
33 # "%.0f\n" FORMAT THE OUTPUT WITH ZERO DECIMALS, USE "%.5f\n" TO KEEP FIVE DECIMALS
34 totArea=$(gmt grdvolume $1 -Sk -fg | awk -F '\t' '{printf "%.0f\n", $2}')
```

```

32
33 mean_z=$(gmt grdinfo -L2 $1 | tail -n 2 | head -n 1 | awk -F' ' '{printf "%.3f\n", $3}')
34 z_stdev=$(gmt grdinfo -L2 $1 | tail -n 2 | head -n 1 | awk '{print $5}')
35 totArea=$(gmt grdvolume $1 -Sk -fg | awk -F '\t' '{printf "%.0f\n", $2}')
36 totVol=$(echo "scale=7; ($mean_z/1000)*$totArea" | bc | awk '{printf "%.1f\n", $1 }')
37 echo $mean_z
38
39 tmp=$(awk -F ' ' '{printf "%.0f\n", $3}' $2.txt | head -n 2 | tail -n 1)
40 thin=$(echo "scale=3; $totArea-$tmp" | bc -l)
41 thick=$(awk -F ' ' '{printf "%.0f\n", $3}' $2.txt | head -n 2 | tail -n 1)
42 thicker=$(awk -F ' ' '{printf "%.0f\n", $3}' $2.txt | tail -n 1)
43 tmp=$(echo $thick-$thicker | bc -l)
44 if [ $k -eq 1 ]; then
45     echo -e "grd_file\tttot_k3\ttot_k2\tkm2<5m\tkm2>5m\t5>km2<10m\tkm2>10m" >>
46     formations_grd/measures/volume/table.txt
47 fi
48
49 #SAVE % OF COVERED AREA
50 thin=$(echo "scale=4; ($thin/$totArea)*100" | bc -l | awk -F ' ' '{printf "%.1f\n", $1}')
51 thick=$(echo "scale=4; ($thick/$totArea)*100" | bc -l | awk -F ' ' '{printf "%.1f\n", $1}')
52 tmp=$(echo "scale=4; ($tmp/$totArea)*100" | bc -l | awk -F ' ' '{printf "%.1f\n", $1 }')
53 thicker=$(echo "scale=4; ($thicker/$totArea)*100" | bc -l | awk -F ' ' '{printf "%.1f\n", $1}')
54 if [ $k -eq 1 ]; then
55     echo -e "grd_file\tttot_k3\ttot_k2\t%<5m\t%>5m\t5>%<10m\t%>10m" >>
56     formations_grd/measures/volume/percent_table.txt
57 fi
58 echo -e "$2\t$totVol\t100%\t$thin\t$thick\t$tmp\t$thicker" >> formations_grd/measures/volume/percent_table.txt
59 }
60 #####
61 #
62 # MAIN #
63 #
64 #####
65
66 rm -r formations_grd/measures
67 mkdir formations_grd/measures
68 mkdir formations_grd/measures/volume
69 k=1 #COUNTER VARIABLE TO KNOW WHICH IS THE FIRST CYCLE WITHIN THE FUNCTIONS
70

```

```
71 #MEASURE VOLUME BETWEEN TWO .grd FILES
72 for file in $(ls formations_grd/thickness/*.grd)
73 do
74     name=$(gmt grdinfo $file -C | awk -F '\t' '{print $1}')
75     name=${name##*/}
76     name=${name%.*}
77     from=0
78     to=$(gmt grdinfo $file -C | awk -F '\t' '{print $7}') #is grd Zmax
79     step=5
80     volumeBetween $file $name $from $to $step $region
81     k+=1
82     mv $name.txt formations_grd/measures/volume
83 done
84
85 #PRINT AND FORMAT OUTPUT ON SCREEN
86 column -t formations_grd/measures/volume/table.txt
87 column -t formations_grd/measures/volume/percent_table.txt
```

Appendix 1 F

Measure and print cross sections

```
1 #!/bin/bash
2 IFS=$'\n'
3 echo " This script exports 2D profiles sampled on cumulative thickness .grd files in
   locations specified by coordinates in the .csv input files"
4
5 #####
6 #
7 #     FUNCTIONS
8 #
9 #####
10
11 function sample {
12 for filename in ../Sezioni/csv/*.csv # INPUT csv FILES MUST BE PLACED IN THIS FOLDER
13 do
14     name=${filename%.*}
15     name=${name#*/}
16     name=${name#*/}
17     name=${name#*/}
18
19     # CSV FIELD SEPARATOR MUST BE A COMMA
20     cat $filename | sed -e 's/,/ /g' >> ../Sezioni/merge/mergeXY.txt
21     cat $filename | sed -e 's/,/ /g' > ../Sezioni/XY$name.txt
22
23     echo "> Sampling cumulative thickness gridfiles with coordinates from $filename"
24     gmt grdtrack ../Sezioni/XY$name.txt -Gthickness/GS_BLRV.grd -nl -Af > ../Sezioni/
25     $name\_xyz_BLRV.txt
26     gmt grdtrack ../Sezioni/XY$name.txt -Gcumulative/GS_BLRV_T1.grd -nl -Af > ../
27     Sezioni/$name\_xyz_BLRV_T1.txt
28     gmt grdtrack ../Sezioni/XY$name.txt -Gcumulative/GS_BLRV_T1_R1.grd -nl -Af > ../
29     Sezioni/$name\_xyz_BLRV_T1_R1.txt
30     gmt grdtrack ../Sezioni/XY$name.txt -Gcumulative/GS_BLRV_T1_R1_STRATH.grd -nl -Af
31     > ../Sezioni/$name\_xyz_BLRV_T1_R1_STRATH.txt
32     gmt grdtrack ../Sezioni/XY$name.txt -Gcumulative/GS_BLRV_T1_R1_STRATH_T2.grd -nl
33     -Af > ../Sezioni/$name\_xyz_BLRV_T1_R1_STRATH_T2.txt
34     gmt grdtrack ../Sezioni/XY$name.txt -Gcumulative/GS_BLRV_T1_R1_STRATH_T2_R2.grd -
```

```

nl -Af > ../Sezioni/$name\_xyz_BLRV_T1_R1_STRATH_T2_R2.txt
30 done
31
32 gmt grdtrack ../Sezioni/merge/mergeXY.txt -Gthickness/GS_BLRV.grd -nl -Af > ../
Sezioni/merge/xyz_BLRV.txt
33 gmt grdtrack ../Sezioni/merge/mergeXY.txt -Gcumulative/GS_BLRV_T1.grd -nl -Af >
../Sezioni/merge/xyz_BLRV_T1.txt
34 gmt grdtrack ../Sezioni/merge/mergeXY.txt -Gcumulative/GS_BLRV_T1_R1.grd -nl -Af >
../Sezioni/merge/xyz_BLRV_T1_R1.txt
35 gmt grdtrack ../Sezioni/merge/mergeXY.txt -Gcumulative/GS_BLRV_T1_R1_STRATH.grd -
nl -Af > ../Sezioni/merge/xyz_BLRV_T1_R1_STRATH.txt
36 gmt grdtrack ../Sezioni/merge/mergeXY.txt -Gcumulative/GS_BLRV_T1_R1_STRATH_T2.grd
-nl -Af > ../Sezioni/merge/xyz_BLRV_T1_R1_STRATH_T2.txt
37 gmt grdtrack ../Sezioni/merge/mergeXY.txt -Gcumulative/GS_BLRV_T1_R1_STRATH_T2_R2.
grd -nl -Af > ../Sezioni/merge/xyz_BLRV_T1_R1_STRATH_T2_R2.txt
38
39 }
40
41 function multiSegment {
42 echo "> Creating multisegment file for: $1"
43 for table in $(ls $1*xyz*.txt)
44 do
45 name=${table%.*}
46 name=${name#*/}
47 gmt mapproject $table -$region -Gk-to | awk '{print $4,$3}' > 2D/distances$name.
txt
48 awk 'BEGIN{OFS=FS=" "}{$1=sprintf("%5.2f",$1)}1 {$2=sprintf("%4.1f",$2)}1' 2D/
distances$name.txt > 2D/tmp_distances$name.txt
49 awk '{print $1,$2}' 2D/tmp_distances$name.txt > 2D/distances$name.txt
50 rm 2D/tmp_distances$name.txt
51 echo "> Made: $name"
52 done
53
54 for dist in $(ls 2D/distances$1*.txt)
55 do
56 case $dist in
57 *R2.txt) color=3;;
58 *T2.txt) color=2;;
59 *STRATH.txt) color=3;;
60 *R1.txt) color=1;;
61 *T1.txt) color=2;;
62 *BLRV.txt) color=1;;
63 *););
64 esac
65 echo ">-Z$color" >> 2D/$1_DIST_multiseg.txt
66 awk '{print $1,$2}' $dist >> 2D/$1_DIST_multiseg.txt
67 done
68 echo "> Made: $1_DIST_multiseg.txt"
69 }

```

```

70
71 function getInfo {
72 Xmax=$(awk '{print $1}' 2D/distances$1_xyz_BLRV.txt | tail -1)
73 Ymax=$(awk '{print $2}' 2D/distances$1_xyz_BLRV_T1_R1_STRATH_T2_R2.txt | sort -nr |
    head -1)
74 Xmin=0
75 Ymin=$(awk '$2 > 0 {print $2}' 2D/distances$1_xyz_BLRV.txt | sort -nr | tail -1)
76
77 #FOR BETTER APPEARANCE SLIGHTLY ENLARGE THE REPRESENTED REGION
78 Ymin=$(echo "$Ymin-10" | bc -l) # 10 m LOWER THAN Ymin
79 Ymax=$(echo "$Ymax+10" | bc -l) # 10 m HIGHER THAN Ymax
80
81 range="R$Xmin/$Xmax/$Ymin/$Ymax" #SET THE NEW RANGE
82 echo $range > 2D/$1_range.txt
83 echo $range
84 }
85
86 function printa {
87 echo "> Drawing: $1"
88 #SET ORIENTATION LABELS
89 case $1 in
90     1*) TL="SSW"
91         TR="NNE";;
92     2*) TL="SSW"
93         TR="NNE";;
94     3*) TL="SSW"
95         TR="NNE";;
96     4*) TL="SW  "
97         TR="  NE";;
98     5*) TL="SW  "
99         TR="  NE";;
100    6*) TL="W    "
101        TR="    E";;
102    7*) TL="NNW"
103        TR="SSE";;
104    8*) TL="NW  "
105        TR="  SE";;
106    *) ;;
107 esac
108
109 # WHITE SPACES ARE IMPORTANT SINCE LABELS ARE IN THE TITLE OF THE SECTION
110 lab_title=$(echo -e "$TL
    Section $1
    $TR")
111
112 gmt psxy 2D/$1_DIST_multiseg.txt -$2 -$pro -BWSne+t$lab_title -Bxa30f10+1"Distance (
    km)" -Bya30f10g30+1"Cumulative Thickness (m)" -C2D/cpt.cpt -W0.5p $create > 2D/
    out/$1.ps
113 gmt psxy -$2 -$pro -T $finalize >> 2D/out/$1.ps
114

```

```

115 echo "> Converting: $1"
116 gmt psconvert -Te 2D/out/$1.ps > 2D/out/$1.eps
117 gmt psconvert -Tg 2D/out/$1.ps > 2D/out/$1.png
118 rm 2D/out/$1.ps
119 }
120
121 function datumSelect { #RECALCULATE VALUES OF INPUT CROSS SECTION REFERRED TO A
    SPECIFIC SURFACE WHICH IS THEN REPRESENTED BY Y = 0
122 # $1=section
123 # $2=datum surface
124 mkdir datumSelect datumSelect/out datumSelect/$1 datumSelect/$1/$2 2>/dev/null
125
126 #CALCULATE SURFACES REFERRED TO INPUT DATUM
127 awk -F' ' '{print $2}' 2D/distances$1_xyz_$2.txt > datumSelect/$1/$2/datum_$2.txt
128 for distanceFile in $(ls 2D/distances$1*.txt)
129 do
130     title=$(basename $distanceFile)
131     title=${title%.*}
132     echo -e "> DS_Working on $(basename distanceFile) section=$1 datum=$2"
133     awk -F' ' -v OFS="\t" '{print $1,$2}' $distanceFile > datumSelect/tmp.txt
134     paste datumSelect/tmp.txt datumSelect/$1/$2/datum_$2.txt | awk -F'\t' '{ $4 = $2
        - $3}1' | awk '{print $1,$4}' > datumSelect/$1/$2/XY_$2_$title.txt
135 done
136 rm datumSelect/tmp.txt
137
138 if [ $2 = "BLRV_T1" ];
139 then
140     Ymin=$(awk '$2 > 0 {print $2}' datumSelect/$1/$2/XY_$2_distances$1_xyz_BLRV.txt |
        sort -nr | tail -1)
141     Ymax=$(awk '{print $2}' datumSelect/$1/$2/
        XY_$2_distances$1_xyz_BLRV_T1_R1_STRATH_T2_R2.txt | sort -nr | head -1)
142 else
143     Ymin=-50
144     Ymax=$(awk '{print $2}' datumSelect/$1/$2/
        XY_$2_distances$1_xyz_BLRV_T1_R1_STRATH_T2_R2.txt | sort -nr | head -1)
145 fi
146
147 Xmin=0
148 Xmax=$(awk '{print $1}' datumSelect/$1/$2/XY_$2_distances$1_xyz_BLRV.txt | tail -1)
149
150 #FOR BETTER APPEARANCE
151 Ymin=$(echo "$Ymin-20" | bc -l)
152 Ymax=$(echo "$Ymax+10" | bc -l)
153 range="R$Xmin/$Xmax/$Ymin/$Ymax"
154 echo $range > datumSelect/$1/$2/$1_range.txt
155
156 echo "> DS_Creating multisegment file for: $1 - $2"
157 for dist in $(ls datumSelect/$1/$2/XY_$2_*.txt)
158 do

```

```

159     case $dist in
160         *R2.txt) color=3;;
161         *T2.txt) color=2;;
162         *STRATH.txt) color=3;;
163         *R1.txt) color=1;;
164         *T1.txt) color=2;;
165         *BLRV.txt) color=1;;
166         *););
167     esac
168     echo ">-Z$color" >> datumSelect/$1/$2/$1_$2_DIST_multiseg.txt
169     awk '{print $1,$2}' $dist >> datumSelect/$1/$2/$1_$2_DIST_multiseg.txt
170 done
171 echo "> DS_Drawing: $1"
172 labX=$2
173 labX=${labX##*_}
174 gmt psxy datumSelect/$1/$2/$1_$2_DIST_multiseg.txt -$range -$pro -BWSne+t$lab_title -
    Bxa30f10+l"Distance (km)" -Bya30f5g5+l"Thickness from $labX (m)" -C2D/cpt.cpt -W0
    .50p >> datumSelect/out/$1_$2.ps
175
176 echo "> DS_Converting: $1"
177 gmt psconvert -Tg datumSelect/out/$1_$2.ps
178 gmt psconvert -Te datumSelect/out/$1_$2.ps
179 mv datumSelect/out/$1_$2.eps datumSelect/out/$1_datum$labX.eps
180 rm datumSelect/out/$1_$2.ps
181 }
182
183 #####
184 #                                     #
185 #             MAIN                     #
186 #                                     #
187 #####
188
189 export LC_NUMERIC="en_US.UTF-8" #SET PERIOD AS DECIMAL SEPARATOR INSTEAD OF COMMA
190
191 cd formations_grd
192 mkdir ../images/profiles 2>/dev/null
193 mkdir ../Sezioni/merge 2>/dev/null
194 rm ../Sezioni/merge/mergeXY.txt
195
196 sample #SAMPLE GRD FILES BASED ON COORDINATES IN INPUT .csv FILES
197
198 #SET UP FUNDAMENTAL VARIABLES
199 create="-K"
200 continue="-K -0"
201 finalize="-0"
202 pro=JX23c/5c
203 proj=JM15c
204 south=50.9
205 north=55.5

```

```
206 east=-111.4
207 west=-120.6
208 region=R$west/$east/$south/$north
209
210 cd ../Sezioni
211 rm -r 2D 2>/dev/null
212 rm -r datumSelect 2>/dev/null
213 mkdir 2D 2>/dev/null
214 mkdir 2D/out 2>/dev/null
215
216 #CALCULATE A COLOR PALETTE
217 gmt makecpt -Cred,blue,forestgreen -T1/4/1 -N > 2D/cpt.cpt
218
219 n_Sezioni=8
220 for ((z=1;z<=$n_Sezioni;z++)); #PRINT EVERY SECTION
221 do
222     multiSegment $z
223     range=$(getInfo $z)
224     printa $z $range
225     datumSelect $z BLRV_T1 #ALSO WITH DATUM MFS1
226     datumSelect $z BLRV_T1_R1_STRATH_T2 #AND WITH DATUM MFS2
227 done
228
229 cd 2D/out
230 for file in *.png #EDIT IMAGES
231 do
232     echo "> Rotating and trimming $file"
233     convert $file -rotate 90 -trim $file
234 done
235 for f in $(ls ../../datumSelect/out/*.png)
236 do
237     echo "> Rotating and trimming $(basename $f)"
238     convert $f -rotate 90 -trim $f
239 done
240
241 echo "All sections are DONE"
242 export LC_NUMERIC="it_IT.UTF-8" #SET COMMA AS DECIMAL SEPARATOR
```

